The composition of coarse sediment in basal Upper Old Red Sandstone alluvial fan conglomerates of the northwest Midland Valley, Scotland : A provenance study.

David K. Goold

Submitted for the Degree of M.Sc.
University of Glasgow
October 1986

CONTENTS

LIST OF FIGURES

SUMMARY

A provenance investigation of coarse detritus (sand to boulder size) associated with basal Upper Old Red Sandstone (Upper Devonian) alluvial fans has been carried out in the northwest Midland Valley of Scotland.

Detailed Petrographic, XRD and SEM studies of sandstones (lithic arenites) interbedded with conglomerate units confirm previously suspected compositional differences for three localities, Portencross, Wemyss Bay and Roseneath along the Firth of Clyde Upper ORS dispersal system. Much of this detritus is interpreted as first cycle and reflects abrupt compositional changes in essentially metamorphic basement lithologies beneath the northwest Midland Valley. These changes may be summarised as increasing metamorphic grade towards the north/northwest ranging from low greenschist facies in the southeast to garnet grade in the northwest. This is combined with a trend from a significant basic plutonic/volcanic input to a more acid igneous component in a similar direction. A substantial amount of reworking of older sediment is also implied for the entire region; characteristic lithic fragments suggest sediment of at least Silurian to early Devonian age contributed detritus to the developing Upper ORS basin.

Textural investigation of sand sized material indicates immaturity, and no significant decrease in grain size for these alluvial sediments in the direction of supposed palaeoflow (S/SW-N/NE). This has also been detected in the cobble-boulder size conglomerate material. This, together with the unique compositional assemblages, reinforces the view that the Upper ORS basin in the Firth of Clyde subsided diachronously with earlier deposits overlain by younger sediments as the basin margins receeded towards the south/southwest.

Major oxide and trace element analysis of *southerly* derived intermediate and acid igneous boulders at Roseneath, the most northerly of the localities investigated, reveals that they have clear affinities with Lower Devonian (c410 Ma) granitoids intruded into the SW Highlands Dalradian metamorphic terrain some 30-40+km to the *north*. Many granodiorite clasts also display evidence of incipient Cu mineralization, a feature also recognised in

the SW Highlands igneous suite. Preliminary geochemical and petrographical analysis of the metamorphic clasts at Roseneath also reveals many significant similarities with lithologies of similar metamorphic grade in the SW Highlands 30-40km to the north.

In contrast, however, Rb-Sr isotopic data obtained from co-magmatic granodioritic boulders suggests an emplacement age of at least 516±5Ma for an intrusion whose initial $^{87}Sr/^{86}Sr$ ratio was of the order of 0.704. This significantly predates the SW Highlands granites although the initial strontium ratio together with trace element features implies that the 'Roseneath pluton' and many SW Highlands granites must have shared a common origin in the deep crust or mantle; the latter being preferred on account of a large (?) Grenville inherited zircon component as detected by U-Pb isotopic analysis.

The paradoxical nature of much of the evidence obtained in this study makes conclusions regarding provenance of the basal Upper ORS difficult to draw. The simplest based model for the northwest Midland Valley may have parallels in westward extension of the Midland Valley in Ireland (Connemara) where Dalradian and largely undeformed Cambro-Ordovician plutonic lithologies are combined in a complex thrust related mixed terrain.

ACKNOWLEDGEMENTS

I particularly wish to thank my supervisor Brian J. Bluck for his thoughtful enthusiasm, patience and encouragement. Technical facilities were generously provided at the Department of Geology, University of Glasgow, by Professor B. E. Leake. Much of the isotopic work was carried out by the staff at the Scottish Universities Research and Reactor Centre at East Kilbride and special thanks go to Alan P. Dickin who interpreted the data. The assistance of the staff at Scotpet Ltd, where the typescript was prepared, is also gratefully acknowledged. Finally I would like to thank my parents for their generosity and support throughout the course of my studies.

CHAPTER 1
INTRODUCTION

1.1 Old Red Sandstone Deposition - Tectonic Models

It has been established for several years that sediments of Devonian age were deposited in Britain within two distinct palaeo-environments. A northern region stretching from Southern Ireland, south central Wales through central and northern England and Ireland to central and northern Scotland is typified by terrigenous, desert-like deposits of clastic red-beds. To the south, carbonates, interstratified with terrigenous sediment have been interpreted as a zone of fluctuating coastline, migrating northwards during the Devonian. Recently, Simon and Bluck (1982) have envisaged a major southerly flowing dispersal system linking the two areas lying in the region of the present day North Channel and Irish Sea in order to explain observed palaeodrainage patterns in central Scotland/north east Ireland and Wales (but see also Allen and Crowley 1983).

Within Scotland itself, the Old Red Sandstone (ORS) appears to have been deposited in two contrasting provinces. In the extreme northeast Lower, Middle and Upper ORS sediments were predominantly laid down under placid lacustrine conditions. This Orcadian Basin extended northeastwards from just south of the Moray Firth at least into the region presently occupied by the Orkney and Shetland Isles. To the south, in the Midland Valley, an area which is presently no more than 100 km from the Southern margin of the Orcadian Basin, higher energy conditions existed in what was probably a rapidly subsiding fault controlled basin dominated by fluvial sediments with minor lacustrine and caliche deposits. Major tectonic influence for the southern (Midland Valley) province is indicated by the complete absence there of Middle ORS. In this region, thick Lower ORS is unconformably overlain by a thinner succession of dominantly Upper Devonian age.

Between the two major basins, thin and scattered pockets of Lower, Middle and possibly Upper ORS are found resting unconformably on Dalradian and Moine metamorphic rocks at Lorne, Crieff, Blairgowrie, Rhynie, Elgin and in the northwest Highlands (see Bluck 1984).

The contrasting nature of the juxtaposed Scottish provinces, together with the occurrence of the intervening outliers has provided serious difficulties for palaeogeographic reconstructions.

The first large scale attempts at synthesising ORS deposition within a tectonic framework were made by George (1960, 1965). Despite the fact that the greatest thickness and extent of ORS rocks in central Scotland are now contained within two major NE-SW trending fractures [the Highland Boundary Fault (HBF) in the north and the Southern Uplands Fault (SUF) in the south (Fig 1.1)], deposition of the ORS was not considered to have been controlled by movement of these structures, at least not during the Lower Devonian. In the north it was observed that the HBF outcrop is clearly transgressed by Lower ORS sediments which rest unconformably upon Dalradian metamorphics north of this line. Lack of marginal deposits developed along the fault line was also cited as evidence against a fault bounded rift basin. It was postulated that rifting, initiated during the Middle Devonian was largely responsible for erosion of Lower ORS sediments north of the HBF and preservation of 8 to 9km (maximum) of sandstone in the Midland Valley. The uniformity of Upper ORS development across its presently exposed extent suggested deposition in a non-tectonically controlled basin where sediment was laid down over the Mid-Devonian eroded Lower ORS including the rift fault system. Thus Upper ORS was seen to transgress the HBF and a large part of now eroded Lower ORS north of the fault where in places it rested unconformably on Dalradian schists. Poor exposure limited estimations of the extent to which Upper ORS of the southern basin developed across into the Southern Highlands but George (1965) saw clear signs that the northern and southern provinces could be correlated only during late Devonian times and proposed that a Mid-Devonian barrier located between the most southerly exposures of Middle ORS and the Midland Valley basin was breeched by transgressive Upper ORS sediments of the southern province. George also envisaged waters of the southern province spilling into the Orcadian basin at times during the Lower Devonian.

Until the late sixties, detailed lithological and provenance investigations of Devonian sediments for the Midland Valley were sparse, due to the unfossiliferous nature of the rocks (Bluck 1967). Prior to this time, published accounts are restricted to a brief report on the Upper ORS between Inverkip and Largs by Kennedy (in Richey et al 1937) and slightly more detailed

Fig 1.1 (next page). Simplified pre-Carboniferous geological map of Scotland. Study area enclosed by box. BNV - Ben Nevis granite; BSH - Ballachulish granite; CFL - Criffel granite; CGM - Cairngorm granite; DST - Distinkhorn granite; ETV - Etive granite; GBH - Garabal Hill granite; GCO - Glen Coe granite.

Post-Devonian
Devonian sediments and volcanics
Plutonic intrusives (predominantly Lower Devonian)
Silurian-Ordovician of the Southern Uplands
Cambro-Ordovician of the northwest Highlands
Dalradian metasediments of the southern Highlands
Pre-Dalradian lithologies (Moine, Torridonian and Lewisian) of the north and northwest Highlands.

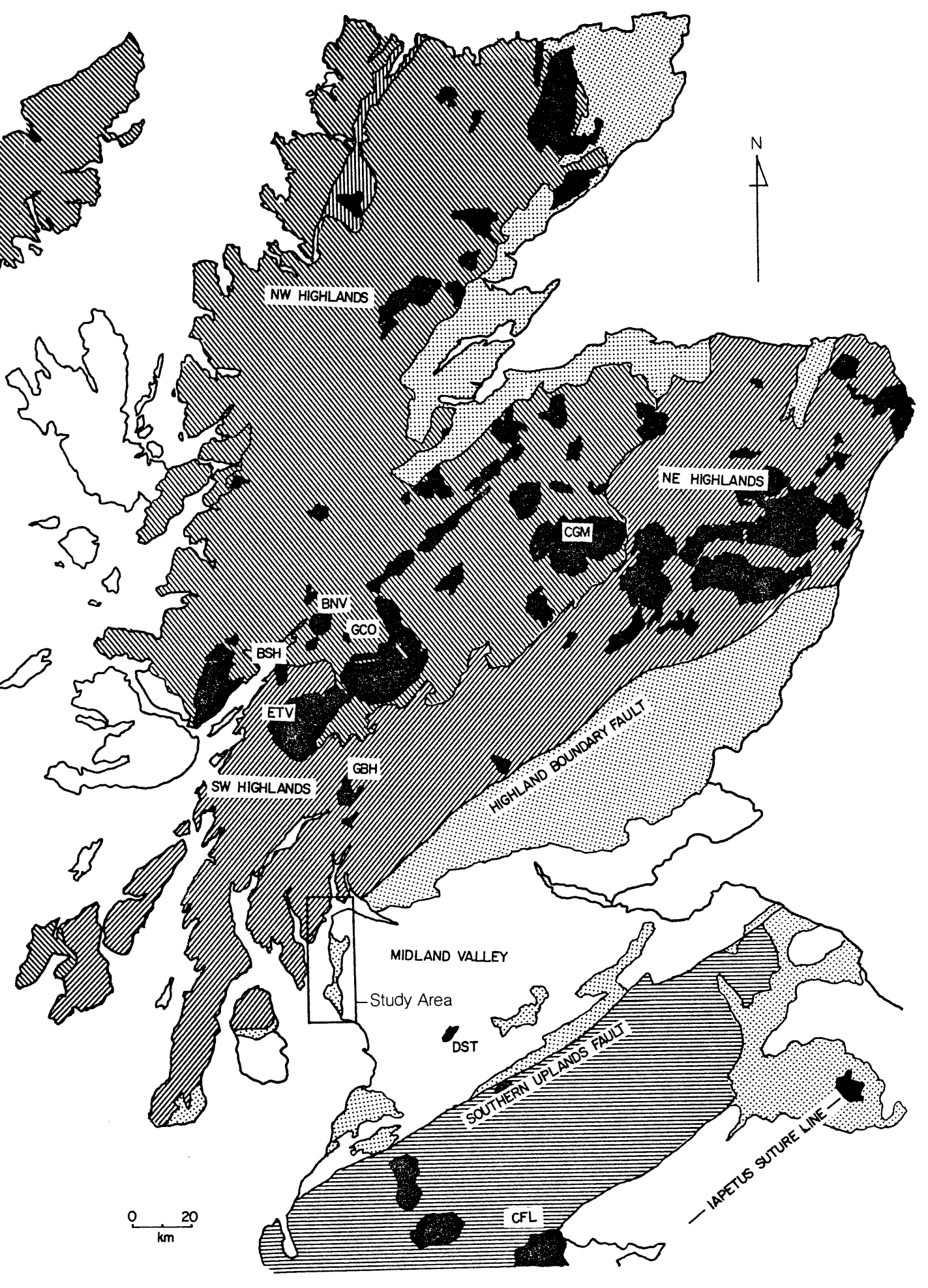
N
NW HIGHLANDS
NE HIGHLANDS
CGM
BNV
GCO
BSH
ETV
GBH
SW HIGHLANDS
HIGHLAND BOUNDARY FAULT
MIDLAND VALLEY
Study Area
DST
SOUTHERN UPLANDS FAULT
IAPETUS SUTURE LINE
CFL
0 20
km

reports by MacGregor and MacGregor (1948) on the ORS of the Midland Valley, the nature of the ORS in the West Kilbride - Largs district by Patterson (1951) and the relationship between the ORS and the Highland Boundary in Arran (Friend et al 1963).

For the Midland Valley basin as a whole, the results of this early work provided a very general picture of cylcical sedimentation of fluvial and lacustrine sequences in a periodically flooded and desiccated slowly subsiding basin. Sediment derived from uplifted mountain areas in the Highlands and Southern Uplands was interbedded particularly during the Lower Devonian by lava flows of variable composition. More specifically, in the Firth of Clyde area, the Southwest Highlands were seen as the principle souce of detritus to the basin on the basis of similarities observed between metamorphic clasts contained in the frequent conglomerates and exposed **in situ** rocks of the Dalradian metamorphic terrain immediately to the north (Fig. 1.2).

Lithofacies analysis initiated in the Upper ORS in the Firth of Clyde by Bluck (1967) has resulted in a wealth of information concerning the stratigraphy, provenance and depositional environment for these sediments. For the eastern Firth of Clyde, the area under investigation in the present study, Fig. 1.3 provides a composite summary of currently available lithostratigraphic, environmental, compositional and dispersal pattern data for Lower and Upper ORS collated from the work of Bluck (1967, 1978, 1980a, 1980b), Downie and Lister (1969), Francis et al (1970), Morton (1976, 1979), Read and Johnson (1967) and Wilson (1971, 1980).

Lower ORS in the NW Midland Valley

Direct information concerning sediments of Lower Devonian age in this area is scarce due to relatively thick cover of Upper ORS and younger rocks. Elsewhere in the northern Midland Valley (east of Loch Lomond) Lower ORS are disposed in a broad NE-SW trending structure, the Strathmore syncline (Fig 1.2). Correlation of the Lower ORS section at Ardmore/Balmaha (Fig. 1.3) with those described for the northeastern limb of the Strathmore Syncline was recognised by Morton (1976, 1979). Here, as elsewhere in the northern Midland Valley, deposition is considered to have taken place near to the northern margins of a fault controlled basin which during middle and top $\overset{U}{/\!\backslash}$ORS was infilled with detritus derived from

Fig 1.2 (next page). Simplified pre-Carboniferous geological map of the northwest Midland Valley and adjoining areas showing localities mentioned in the text.

Post-Devonian

Upper ORS sandstones and conglomerates

Lower ORS sandstones and conglomerates

Lower Devonian intrusive

DEVONIAN

Schistose grit, greywacke, slate and phyllite

Undifferentiated mica schist

Epidote/chloritic schists and schistose grits

Quartzite and quartz schist

DALRADIAN

Epidiorite and hornblende schist

Undifferentiated mica schist

MOINIAN

Fault

Documented location of Cu mineralization

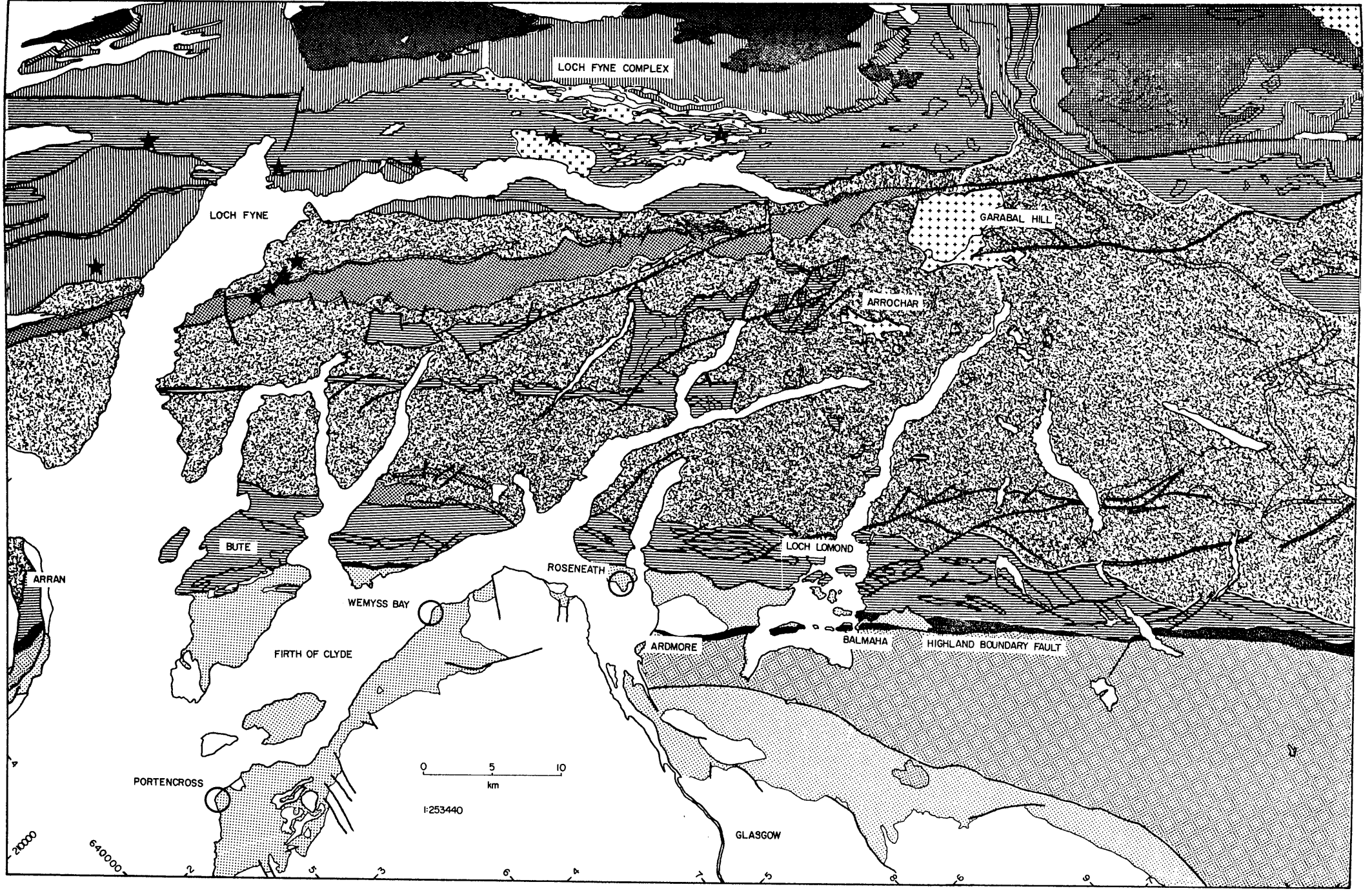
LOCH FYNE COMPLEX
LOCH FYNE
GARABAL HILL
ARROCHAR
BUTE
ARRAN
LOCH LOMOND
ROSENEATH
WEMYSS BAY
FIRTH OF CLYDE
ARDMORE
BALMAHA
HIGHLAND BOUNDARY FAULT
PORTENCROSS
GLASGOW
0 5 10
km
1:253440
20000
640000

Fig 1.3 (next page). Generalized log sections of Devonian sequences in the reviewed area showing: lithology; palaeoflow direction; conglomerate clast composition; proposed stratigraphy and; interpreted environments of deposition. See Fig 1.2 for locations.

Lithology:

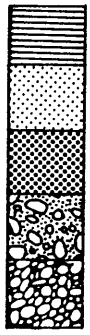

Mudstone, siltstone

Sandstone

Pebble conglomerate

Boulder conglomerate (matrix supported)

Boulder conglomerate (clast supported)

Clast Composition:

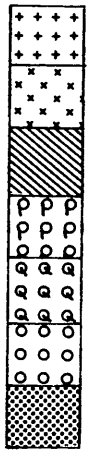

Igneous (plutonic/hypabyssal)

Igneous (volcanic)

Metamorphic (biotite-garnet schist)

Metamorphic (phyllite etc)

Quartzite

Vein quartz

Greywacke

After Bluck (1967, 1978, 1980a, 1980b), Downie and Lister (1969), Francis et al (1970), Morton (1976, 1979), Read and Johnson (1967) and Wilson (1971, 1980).

AC Ardmore Conglomerate; BC Balmaha Conglomerate; BS Balloch Sandstone; CC Cardross Conglomerate; GS Geilston Sandstone; HF Hunterston Formation; HM Haupland Muir Formation; KB Kelly Burn Formation; LM Leap Moor Formation; PB Portencross Beds; RC Roseneath Conglomerate; SC Sandy's Creek Beds; SF Skermorlie Formation; SM Seamill Formation; W Wemyss Bay Formation.

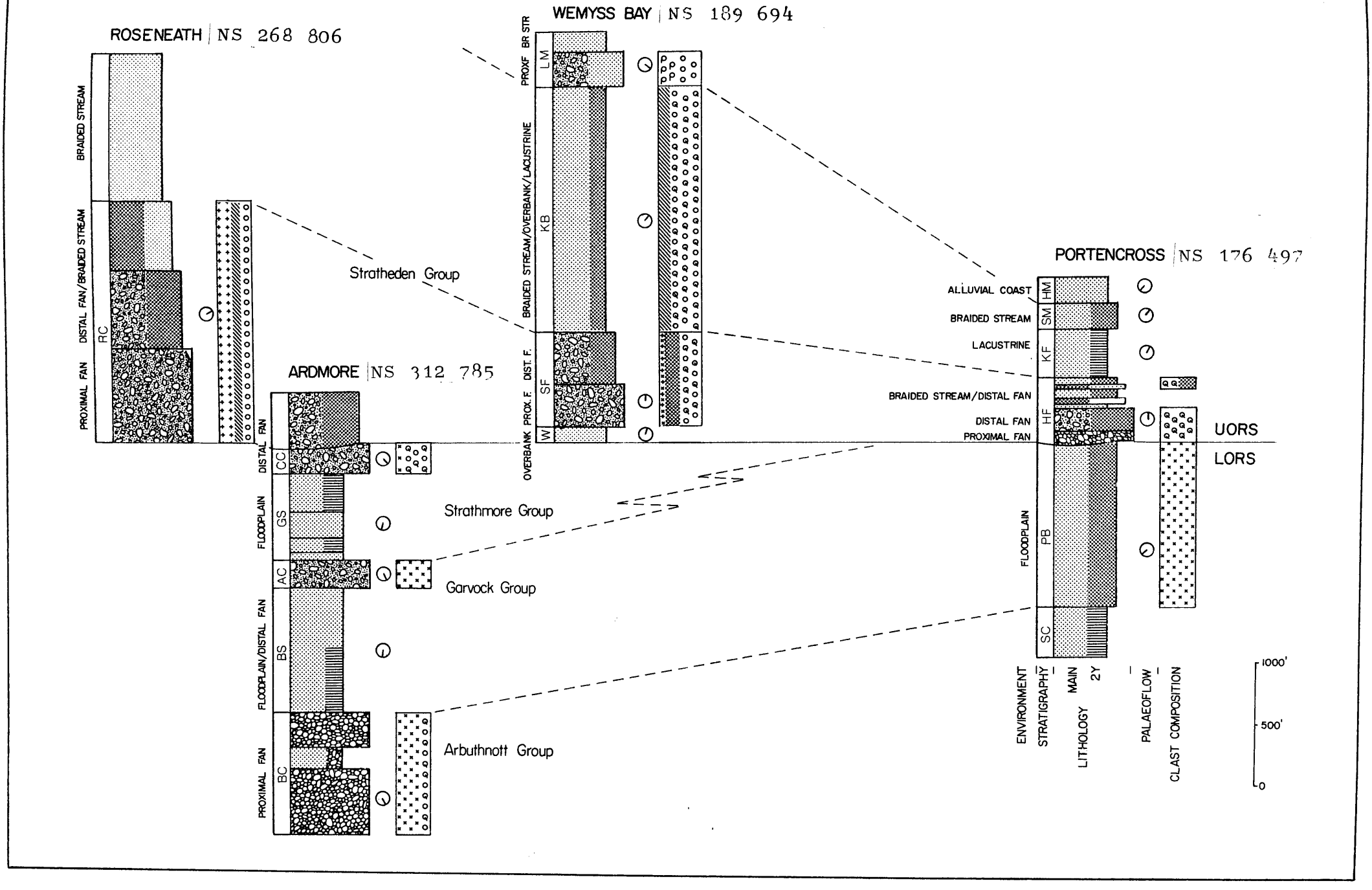
ROSENEATH NS 268 806
WEMYSS BAY NS 189 694
PORTENCROSS NS 176 497
ARDMORE NS 312 785
Stratheden Group
Strathmore Group
Garvock Group
Arbuthnott Group
UORS
LORS
BRAIDED STREAM
DISTAL FAN/BRAIDED STREAM
PROXIMAL FAN
RC
PROXF
BR STR
LM
BRAIDED STREAM/OVERBANK/LACUSTRINE
KB
DIST. F.
SF
PROX. F
OVERBANK
W
ALLUVIAL COAST
BRAIDED STREAM
LACUSTRINE
BRAIDED STREAM/DISTAL FAN
DISTAL FAN
PROXIMAL FAN
HM
SM
KF
HF
DISTAL FAN
FLOODPLAIN
CC
GS
AC
FLOODPLAIN/DISTAL FAN
BS
PROXIMAL FAN
BC
FLOODPLAIN
PB
SC
ENVIRONMENT
STRATIGRAPHY
LITHOLOGY
MAIN
2Y
PALAEOFLOW
CLAST COMPOSITION
1000'
500'
0

overlies an apparently locally developed lower sandstone (the Wemyss Bay Formation) whose base is not seen. The conglomerates display an upward fining interpreted as transitions from proximal fan through distal fan and braided stream facies to overstepping pebbly sandstones and siltstones of floodplain and lacustrine facies (Black 1967). Dispersal patterns determined by Bluck (1978, 1980a) suggest that this essentially fluviatile sequence was derived from the south or southwest. Further to the southwest in Kintyre, dispersal directions for the basal conglomerate indicate flow from the north and northeast, opposite to those for comparable sections in the Firth of Clyde. This led Bluck (1980a) to invoke an upland area separating the main Midland Valley basin from another embayment at Kintyre.

In the north and west Firth of Clyde the fining upward sequence described above is overlain by breccias and conglomerates of proximal fan and debris flow facies and ends with possibly bioturbated soil profiles with minor conglomerates. These late Upper ORS sediments have dispersal trends towards the southeast, draining an area which must correspond to the presently exposed Southwest Highlands. At Portencross in the south, sandstones with calcrete in an interpreted alluvial coast environment are viewed as precursors to Lower Carboniferous marine sedimentation.

The Upper ORS basin in the Firth of Clyde, like its Lower ORS equivalent, seems to have deepened towards the north east and is presently truncated against a structure approximately located along the trend of the HBF. The uniform development and northward thickening of the basal conglomerate consistently derived from the south/south west across the whole length of the basin, almost certainly requires a fault controlled and southerly receeding basin margin similar to that invoked for the Lower ORS basin. At least three fault controlled sub-basins have been identified by Bluck (1978) in the northwest Midland Valley to explain conglomerate wedges present at Roseneath Point, Wemyss Bay and Portencross (Fig. 1.4). It has also been suggested that the overstepping floodplain deposits may represent distal equivalents of the proximal fan developing in the younger sub-basin to the south as the basin margin receeded. In fact, evidence for diachronous fault control, together with similarities with present day fault controlled basins is such that alluvial deposition in a pull-apart basin has been proposed for the Upper ORS (Bluck 1980a; but see also Leeder

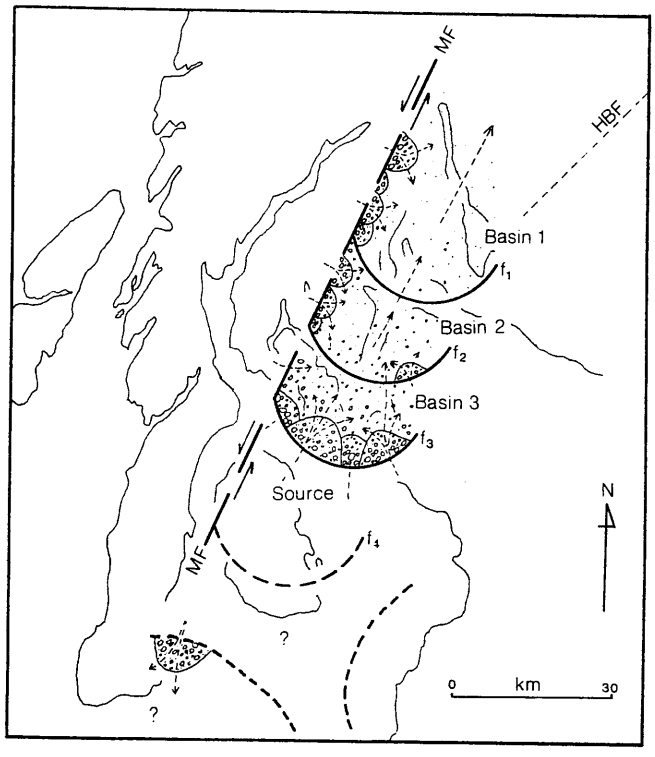

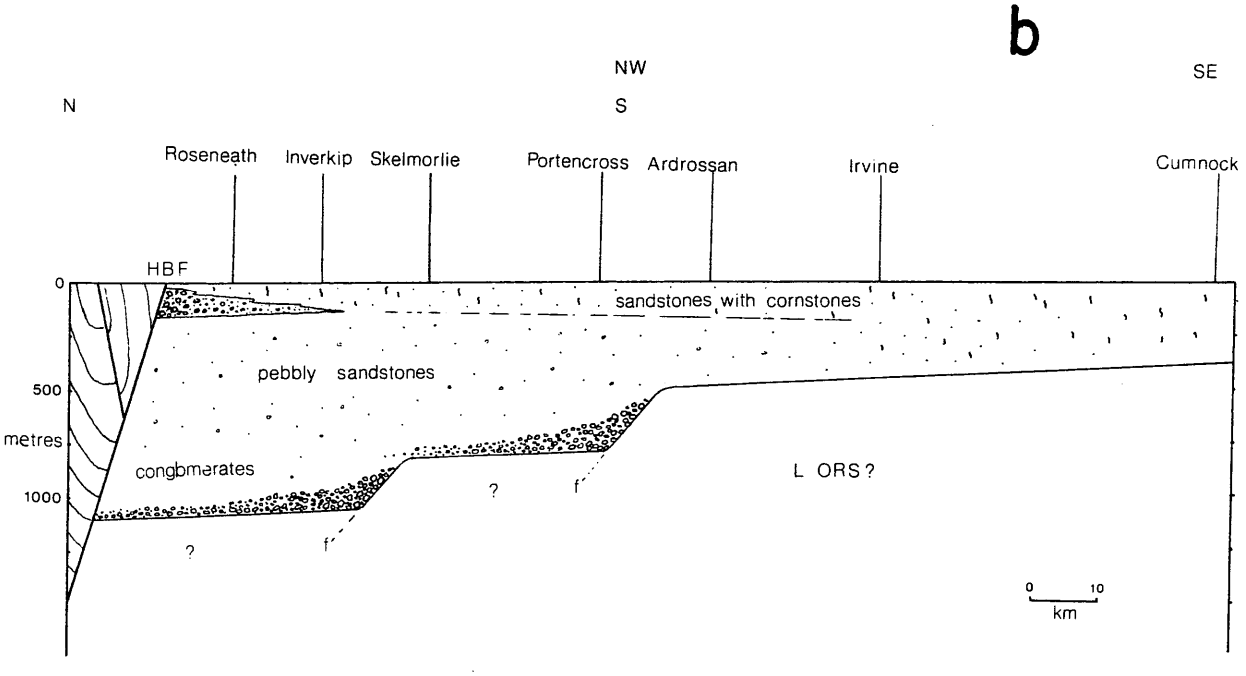

ig 1.4. a) Map of the northwest Midland Valley showing conjectural locations of faults controlling the evolution of the Upper ORS basin. b) Section through the Upper ORS in the northwest Midland Valley showing lithological divisions. Both modified from Bluck (1980a). See Fig 1.2 for locations.

1982). Thus the basin may have been initiated by strike-slip movement (sinistral) along a major fracture approximately corresponding to the present trend of the HBF, although it is clear that deposition extended northwards beyond this. Within the Midland Valley basin, movement along the major fracture would result in progressive development of extension related lobate faults approximately at right angles to the main fracture producing diachronously developing sub-basins with a progressively south/southwesterly receeding sediment source. Clast size reduction is not observed in a 'downflow' direction and this, together with a lack of clast type mixing within the basin is cited as further evidence against a unified dispersal system. Gradually, however, as the basin evolved, a trend towards homogenisation is considered to have resulted in a single dispersal system in the middle Upper ORS as described by Simon and Bluck (1982).

1.2 ORS Conglomerate Compositions

Detailed examination of clast types in the Firth of Clyde ORS conglomerates was first made by Friend et al (1963). In their study of the Devonian sediments in Arran, evidence was presented for a compositional distinction between Upper and Lower parts of the succession in addition to obvious lateral variations. Equally significant was their observation that the vast input of metamorphic material into the Upper ORS (the Lower ORS is dominated by volcanic detritus) includes a significant proportion of higher grade schist than is presently exposed in the Dalradian metamorphic terrain immediately to the north. At the same time a higher schist content for the Upper ORS relative to Lower ORS was recognised geochemically for sandstones at Ardmore Point in the extreme north of the present basin (Bowes 1963)

Clast compositions for both Lower and Upper ORS conglomerates in the study area are now well documented (Bluck 1978, 1980a; Morton 1976, 1979) and have been summarised in Fig. 1.3. Vertical variations in composition are generally attributable to an upward decline in less stable lithic components. This produces an upward maturing assemblage eventually dominated by vein quartz and quartzite. However, there is no observed maturation in a downflow direction for conglomerates in the basal Upper ORS. Indeed it would appear that clast compositions become increasingly immature in the direction of supposed dispersal.

At least three compositionally discrete clast assemblages are recognised in a northwards traverse of the Upper ORS basin:

i) At **Portencross** (NS 176497) the basal conglomerate of the Hunterston Formation is dominated by large boulders of quartzite and smaller clasts of vein quartz and red sandstone. The quartzite boulders display rounding textures attributed to reworking, and their presence in conglomerates of Silurian and Ordovician age in the Highland Border Complex and Southern Midland Valley suggests a complex history of recycling (see Bluck 1984). The quartzite conglomerate at Portencross is overlain by a thinner conglomerate consisting chiefly of greywacke pebbles which are distinctly similar to Silurian greywackes which presently outcrop in southern Scotland.

ii) Approximately 20km to the north, the basal conglomerate at **Wemyss Bay** (NS 189694) also contains a considerable quartzite component but is characterised by volcanic detritus of both basic/intermediate and acidic compositions (although the former probably predominate). Pebbles of porphyritic granite (s.l.) are occassionally present here, as are pebbles of metagreywacke similar to greywacke detritus at Portencross but which now display the development of deformational cleavages.

iii) **At Roseneath** (NS 268806) in the extreme north of the present Upper ORS basin, the ubiquitous quartzite clasts are accompanied by mixed hypabyssal and acid plutonic detritus together with cobbles of high greenschist facies (biotite-garnet grade) grits and semi-pelitic material.

Clasts in the northern portions of the basin especially are of uncertain provenance since they do not reflect lithologies presently exposed in the Dalradian metamorphic terrain *immediately* to the north. Only in conglomerates and breccias of late Upper ORS age (for example the southwesterly dispersed Leap Moor Formation at Wemyss Bay) are clasts of unequivocal local Dalradian type (i.e. low greenschist facies slates and phyllites) to be found.

The first cycle nature of the debris in the Upper ORS basal conglomerates is suggested primarily by the large size of sub-rounded lithic detritus (occasionally exceeding 1m diameter) and by a condition in which clast size has a positive correlation with bed thickness (Bluck 1967). The northerly/northeasterly dispersal, combined with the Dalradian source mismatch, led Bluck (1984) to suggest a local derivation for the basal conglomerate from the south outwith the Dalradian and, within the Midland Valley basement itself, a view supported by Dickin (1984) with the observation that the ORS sediments in Arran have common Pb characteristics more typical of Torridonian sediments than of the juxtaposed Dalradian terrain to the north.

1.3 Aims

The single objective of this study is to extend previous investigations into the provenance of basal Upper Old Red Sandstone detritus in the northwest Midland Valley. This will be attempted in two ways :

1) by analysing and comparing the composition, texture and diagenesis of sand size detritus in the basal Upper Old Red Sandstone at three localities in the Firth of Clyde and;

2) using proven geochronological and geochemical techniques, to classify and place constraints on the affinities of igneous and metamorphic cobble-boulder size detritus in the southerly derived basal Upper Old Red Sandstone at Roseneath Point.

CHAPTER 2

SANDSTONE PETROLOGY

2.1 Introduction

Petrologic analysis, investigating modal and heavy mineral composition, texture, and diagenesis, has been performed on sandstone samples from each of the three areas of basal UORS conglomerate of this study (Portencross, Wemyss Bay and Roseneath). From these data it is possible to i) determine compositional variations for the basal UORS across the NW Midland Valley basin, ii) assess if, as implied by differing clast populations in the conglomerates, there is a difference in sandstone petrography at each of the three areas and iii) compare variations in sandstone petrography with variations in conglomerate composition.

2.2 Petrofacies Analysis

Table 2.1 records the results of point count analysis of 24 thin sections of sandstones from the base of the UORS at three localities in the Firth of Clyde area.

2.2.1 Method

For this study, thin sections were cut perpendicular to bedding (Textoris 1971), this being especially important for grain size analysis (Turner and Whitaker 1976). Sections were not stained for plagioclase or K-feldspar since identification of these minerals is easily made using optical properties alone. Point count measurements were made using a mechanical stage and a semi-automated totaliser. A grid spacing was chosen which enables c. 200 grains to be counted on each section without individual grains being counted more than once. A minimum grain size cut-off is normally employed, approximately corresponding to 0.625mm (4 phi) as described by Dickinson (1970). Grains smaller than 4 phi are difficult to identify optically and may result in a false impression of composition. For this study, however, compositional variations with grain size are particularly apparent when distinctions are made between mono- and polycrystalline quartz, and use of a 2 phi (0.25mm) cut-off has been employed for all grain compositions.

Table 2.1 (next page). Modal point counts of selected basal conglomerate sandstones from the Firth of Clyde Upper ORS. Values shown are based on 200 total rock points per section; see Table 2.2 for parameters.

Values recalculated to include only clastic grains.

LOCATION	SAMPLE	Qm	Qp	K	P	Lv	Lm	Ls	Q	F	L	Qm	F	Lt	Qm	Qp	L	Qp	Lv	Ls	Lm	Lv	Ls
Roseneath	DGD01	48	22	06	06	03	15	00	70	12	18	48	12	40	55	25	20	88	12	00	83	17	00
	DGD02	47	22	08	07	01	15	00	69	15	16	47	15	38	55	26	19	96	04	00	94	06	00
	D GD03	41	28	10	05	00	16	00	69	15	16	41	15	44	48	33	19	100	00	00	100	00	00
	DGD04	46	24	07	04	09	19	00	70	11	19	46	11	43	52	27	21	100	00	00	100	00	00
	DGD05	49	24	08	02	01	16	00	73	10	17	49	10	41	54	27	19	96	04	00	94	06	00
	DGD06	44	26	07	06	03	14	00	70	13	17	44	13	43	51	30	17	90	10	00	82	18	00
	DGD07	48	31	04	03	01	13	00	79	07	14	48	07	45	52	33	15	97	03	00	93	07	00
	DGD08	38	30	07	08	09	08	00	68	15	17	38	15	47	45	35	20	77	23	00	47	53	00
	DGD09	39	32	06	00	05	18	00	71	06	23	39	06	55	42	34	24	86	14	00	78	22	00
	DGD10	45	40	01	04	01	08	01	85	05	10	45	05	50	47	42	11	96	02	02	80	10	10
	DGD11	40	29	06	07	06	14	00	69	11	20	40	11	49	45	33	22	83	17	00	70	30	00
	DGD12	40	32	08	01	07	11	01	72	09	19	40	09	51	44	35	21	80	18	02	58	37	05
Wemyss Bay	WBS01	31	30	06	01	18	09	05	61	07	32	31	07	62	33	32	34	57	34	09	28	56	16
	WBS02	26	30	04	02	23	00	15	56	06	38	26	06	68	28	32	40	44	34	22	00	60	40
	WBS03	25	28	03	02	26	04	12	53	05	42	25	05	70	26	30	44	43	39	18	10	62	28
	WBS04	20	23	04	04	31	03	15	43	08	49	20	08	72	22	25	53	33	45	22	06	63	31
	WBS05	17	23	05	06	35	00	14	40	11	49	17	11	72	19	26	55	32	49	19	00	71	29
	WBS06	20	29	04	03	27	04	13	49	07	44	20	07	44	20	07	73	22	31	47	42	39	19
	WBS07	31	31	03	01	19	02	13	62	04	34	31	04	65	32	32	35	49	30	21	06	56	38
	WBS08	27	35	04	08	21	00	05	62	12	26	27	12	61	31	40	29	57	34	09	00	81	19
	WBS09	28	27	06	05	30	00	04	55	11	34	28	11	61	31	30	38	44	49	07	00	88	12
	WBS10	23	35	05	04	21	03	09	58	09	33	23	09	68	25	38	36	54	32	14	09	64	27
	WBS11	15	23	09	04	31	01	17	38	13	49	15	13	72	17	26	56	32	44	24	02	63	35
	WBS12	27	28	09	05	20	01	10	55	14	31	27	14	59	31	33	36	48	34	17	03	65	32
Portencross	DGP01	15	36	01	04	00	00	44	51	05	44	15	05	80	16	38	46	45	00	55	00	00	100
	DGP02	07	30	06	10	00	00	48	37	16	48	07	16	78	09	35	56	38	00	62	00	00	100
	DGP03	15	52	00	04	00	00	29	67	04	29	15	04	81	16	54	30	64	00	36	00	00	100
	DGP04	08	41	02	02	00	00	47	49	04	47	08	04	88	08	43	49	47	00	53	00	00	100
	DGP05	13	36	10	12	00	00	29	49	22	29	13	22	65	17	46	37	55	00	45	00	00	100
	DGP06	28	42	02	05	00	00	23	70	07	23	28	07	65	30	45	25	65	00	35	00	00	100
	DGP07	18	33	00	02	01	00	46	51	02	47	18	02	80	18	34	48	41	01	58	00	02	98
	DGP08	12	32	17	10	01	00	28	44	27	29	12	27	61	16	44	40	53	02	45	00	03	97
	DGP09	18	47	04	06	00	00	25	65	10	25	18	10	72	20	52	28	65	00	35	00	00	100
	DGP10	07	30	04	10	00	00	39	37	24	39	07	24	69	09	40	51	53	00	57	00	00	100
	DGP11	15	34	02	05	00	00	44	49	07	44	15	07	78	16	37	47	44	00	56	00	00	100
	DGP12	04	25	07	10	00	00	54	29	17	54	04	17	79	05	30	65	32	00	68	00	00	100

2.2.2 Presentation of data

Variations in framework mode for clastic sediments have conventionally been represented using ternary plots on a standard QFL diagram, the three apices being:

Q - Total quartzose grains of both poly- and monocrystalline varieties. Chert, orthoquartzite and metaquartzite lithic fragments are included.

F - Monocrystalline feldspar grains (plagioclase and K-feldspar).

L - Lithic fragments of igneous, metamorphic or sedimentary varieties. Mica flakes are grouped into this category.

A QFL diagram for the basal UORS rocks is shown in Fig. 2.1a. Nomenclature fields devised by McBride (1963) are also displayed (Fig 2.1b).

Compositional variations for the three conglomerates are immediately obvious from this plot. Despite considerable overlap between Wemyss Bay and Portencross, there are generally less lithic fragments in the sediments when traced northwards from Portencross to Roseneath. The Portencross sediments are the most compositionally variable with representatives from feldspathic litharenite, litharenite, sublitharenite and lithic sub-arkose. Roseneath sediments are compositionally restricted, being mainly litharenites or sub-litharenites. Feldspar is a surprisingly minor component in all areas.

Fig. 2.1c combines data for the whole UORS (top, middle and base) determined by Bluck (1978). Comparison of the data from the entire UORS basin in the western Midland Valley with those obtained from this more extensive study shows a wide variety of sandstone types in the Clyde area, but the general immaturity of the basal UORS rocks is emphasised.

Dickinson (1970), along with many other workers, have observed that concentrations towards the Q apex usually indicate maturity. However, the occurrence of highly quartzose sediments in all areas (especially Roseneath) plotting close to the Q apex, and therefore defined as mature, are clearly quite immature on textural grounds (see section 2.5). This ambiguous facet of the standard QFL diagram has already been noted by Graham et al (1976), especially where categorization of polycrystalline quartzose lithic fragments of chert, orthoquartzite and metaquartzite are concerned.

Fig 2.1 (next page). a) Modal QFL compositions for the basal Upper ORS (this study). b) QFL nomenclature fields devised by McBride (1963): 1 quartz arenite; 2 sub-arkose; 3 sub-litharenite; 4 lithic sub-arkose; 5 arkose; 6 lithic arkose; 7 feldspathic litharenite; 8 litharenite. c) Modal QFL compositions for the top, middle and base Upper ORS (from Bluck 1978). d) Provenance fields for the QFL diagram (from Dickinson and Suczek 1979): 1 Craton Interior; 2 Transitional Continental; 3 Basement Uplift; 4 Recycled Orogenic; 5 Dissected Arc; 6 Transitional Arc; 7 Undissected Arc.

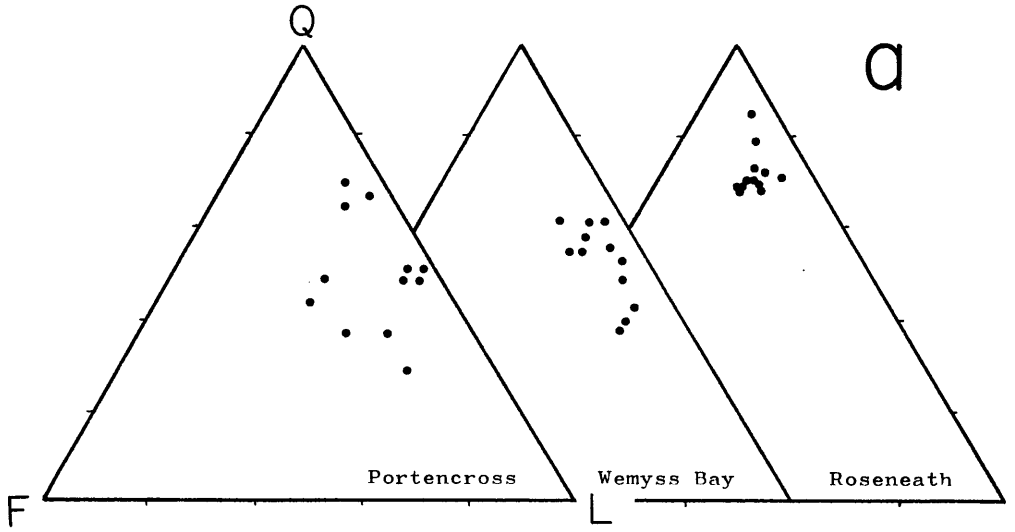
Q
a
F
L
Portencross
Wemyss Bay
Roseneath

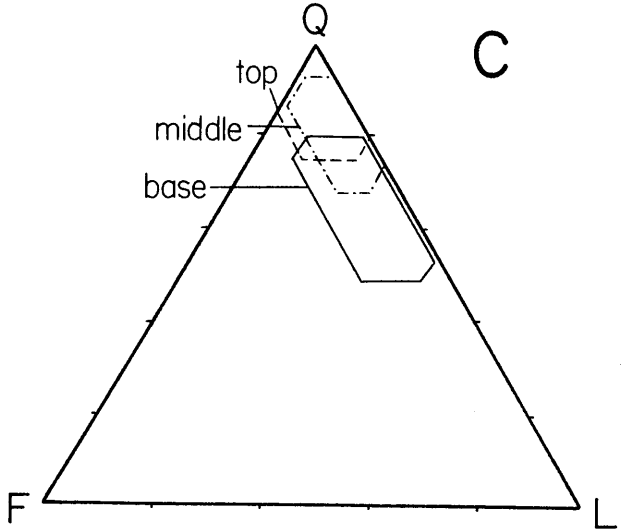
Q
c
top
middle
base
F
L

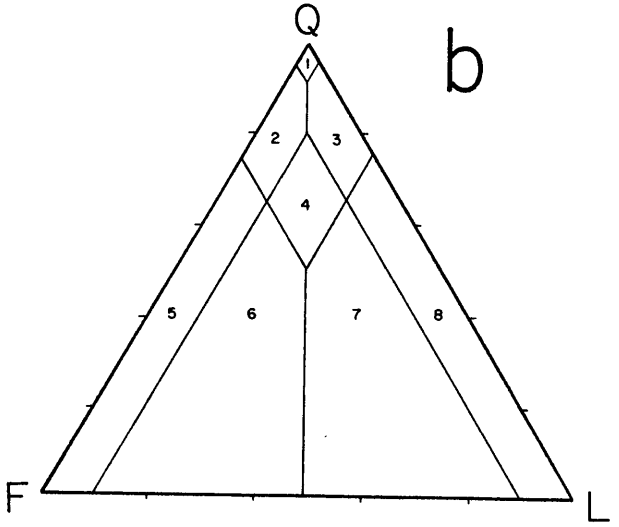
Q
b
1
2
3
4
5
6
7
8
F
L

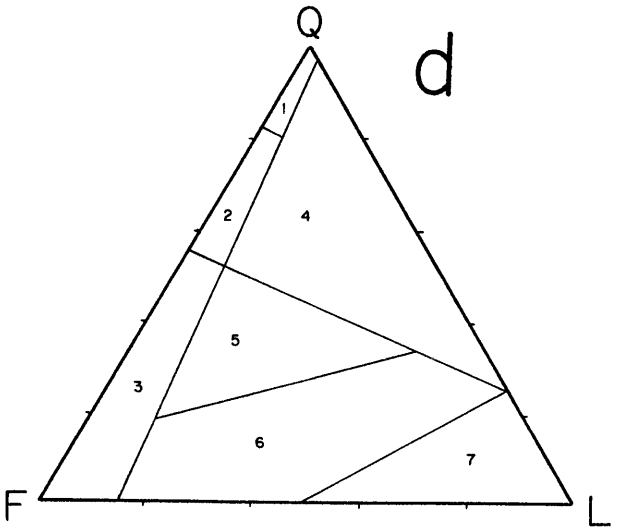
Q
d
1
2
3
4
5
6
7
F
L

In order to determine provenance, it has become fasionable in recent years to undertake compositional investigations using an expanded scheme of parameters based on the traditional three-fold Q, F and L groupings. Table 2.2 summarises the petrographic parameters recognised in this classification, and the abbreviations which occur in the following account are found in this table. Various parameter combinations have been used in provenance studies and has led to the development of QmFLt, QpLvLs, QmQpL (Graham et al 1976), QmPK (Dickinson and Suczek 1979), QpLvmLsm and LmLvLs (Ingersoll 1983) diagrams. In addition, provenance studies based on the new ternary diagrams have resulted in a reappraisal of the QFL diagram with the determination of provanance fields (Dickinson and Suczek 1979 and Dickinson et al 1983). It should be pointed out, however, that inferences based upon the distinction between poly- and mono crystalline quartz are tentative.

In this investigation, for example, polycrystallinity is highly variable within sandstone units where it is essentially dependent upon grain size (section 2.3.1). No grain size control has been exercised in any of the above mentioned provenance studies other than employing Dickinson's (1970) 4 phi cut-off. It may be that in investigations where large numbers of samples are examined (e.g. 500 points for not less than 200 samples as in Ingersoll 1983) grain size control is not important. However, for this relatively limited survey, a coarser cut-off at 2 phi (0.25mm) was considered necessary for the study of mono- and polycrystalline quartz where only medium and coarse sized sands (Wentworth size class) are recorded.

To display the data for the UORS the three complimentary diagrams of Graham et al (1976) have been chosen in addition to the standard QFL plot. These are QmFLt, QmQpL and QpLvLs (Figs. 2.2a, b and c respectively). The LmLvLs diagram of Ingersoll (1983) is also particularly relevant (Fig. 2.2d). Provenance fields for QFL and QmFLt plots accompany the appropriate diagrams.

The majority of samples analysed fall into the field of 'Recycled Orogenic' (Dickinson et al 1983) on both QFL and QmFLt diagrams. The Roseneath sandstones are dominantly 'Quartzose Recycled', whereas Wemyss Bay and Portencross sandstones are mostly 'Transitional Recycled' with a few Portencross rocks being 'Lithic Recycled' and 'Mixed'. This is primarily

Q = Qm + Qp	where	Q	=	total quartzose grains
		Qm	=	monocrystalline quartz grains
		Qp	=	polycrystalline quartz grains
F = P + K	where	F	=	total feldspar grains
		P	=	plagioclase feldspar grains
		K	=	potassium feldspar grains
Lt = L + Qp	where	Lt	=	total aphanitic lithic grains
		L	=	total unstable aphanitic lithic grains
L = Lm + Lv + Ls	where	Lm	=	metamorphic aphanitic lithic grains
		Lv	=	volcanic-hypabyssal aphanitic lithic grains
		Ls	=	sedimentary aphanitic lithic grains

TABLE 2.2 Explanation of grain parameters used in this study.

Fig 2.2 (next page) a) QmFLt diagrams for the basal Upper ORS with provenance fields from Graham et al (1976): 1 Craton Interior; 2 Transitional Continental; 3 Basement Uplift; 4 Quartzose recycled; 5 Transitional Recycled; 6 Lithic Recycled; 7 Mixed; 8 Dissected Arc; 9 Transitional Arc; 10 Undissected Arc. b) QmQpL diagram for the basal Upper ORS. c) QpLvLs diagram for the basal Upper ORS. d) LmLvLs diagram for the basal Upper ORS.

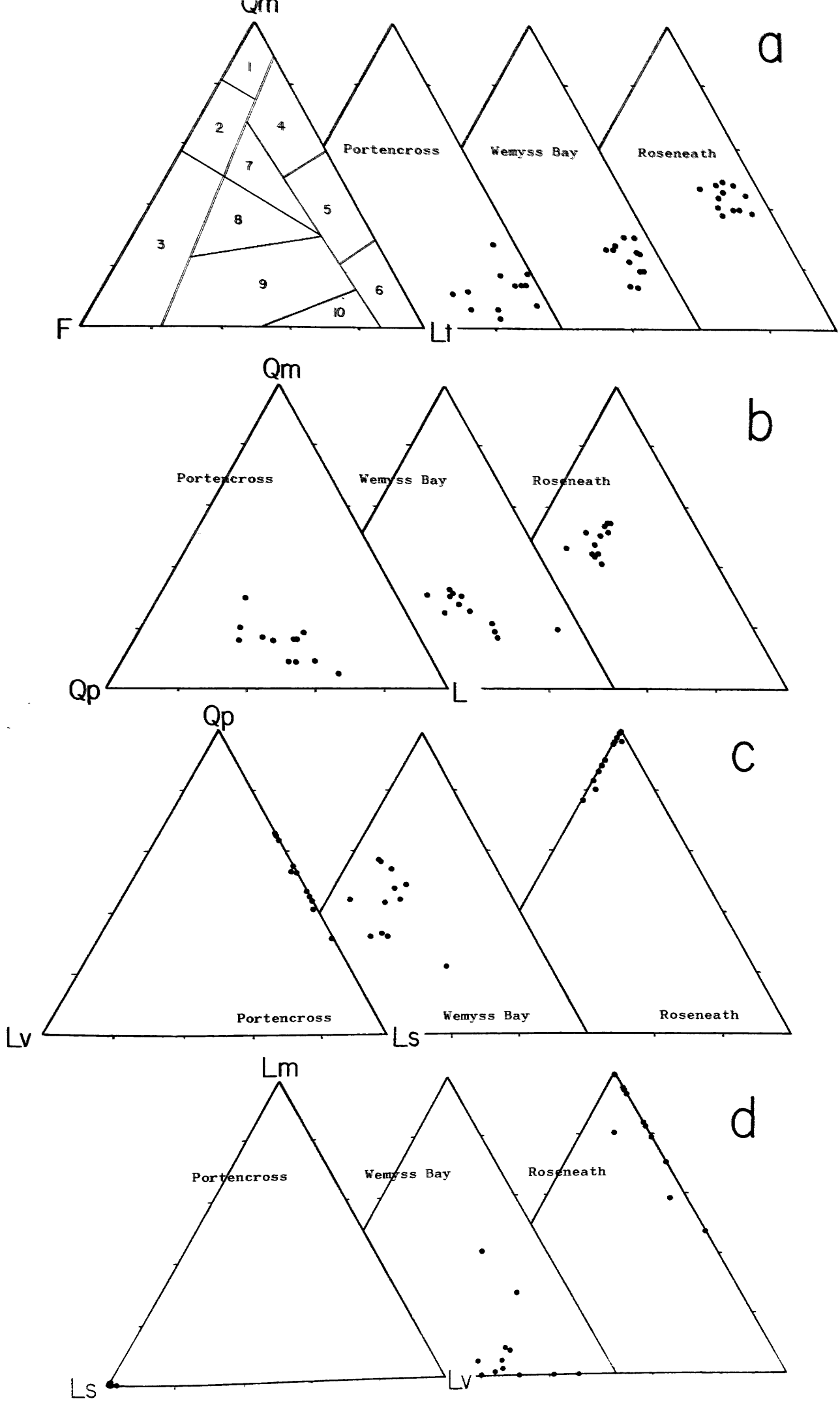
Qm
a
1
2
4
7
5
8
3
9
6
10
F
Portencross
Wemyss Bay
Roseneath
Lt
Qm
b
Portencross
Wemyss Bay
Roseneath
Qp
L
Qp
c
Lv
Portencross
Wemyss Bay
Roseneath
Ls
Lm
d
Portencross
Wemyss Bay
Roseneath
Ls
Lv

indicative of a sedimentary source with subordinate volcanic rocks. These source rocks may be partly metamorphosed and are eroded during orogenic uplift of fold belts or thrust sheets.

Such a provenance for these UORS rocks is not consistent with the view that the ORS was a post-orogenic (Caledonian) subsiding basin which, in the terminology of Dickinson et al (1983) would represent one of the Continental Block categories (craton interior, transitional continental and basement uplift). Dickinson and Suczek (1979) do, however, admit that fields for Continental Block and Recycled Orogens merge where stable frameworks of high maturity are involved. The anomalously high maturity of these UORS rocks due to quartz content has already been noted.

2.3 Description of the Mineralogy

2.3.1 Quartz

Quartz is the largest single component in these UORS sediments, where it occurs as mono- and polycrystalline grains. It is also present in authigenic form as quartz overgrowths and microcrystalline pore-fills and grain coatings.

Monocrystalline quartz varies from even and slightly undulose to highly undulose extinguishing. Much of this quartz is interpreted as being of volcanic origin due to frequently observed B-type grains (Hatch et al 1972, p93 and 236), displaying rounded or corroded surfaces with embayments often associated with heavy mineral inclusions (Fig. 2.3 and 2.4 See also section 3.2). These volcanic types are present in all three areas but particularly at Wemyss Bay and are subordinate at Roseneath Point. Polycrystalline quartz is also a major component and includes both orthoquartzite grains and grains typical of metamorphic rocks, showing both sutured and polygonised intercrystal boundaries (Fig. 2.4). Occassionally, fragments of quartz-rich rocks may be observed which have undergone particularly high grade metamorphism, where individual grains become highly elongate and crystal boundaries are indistinct (Young 1976).

Inclusions in quartz are common and include: tourmaline [usually green-brown (Fig.2 14)]; zircon (colourless); apatite; rutile; and chlorite/muscovite.

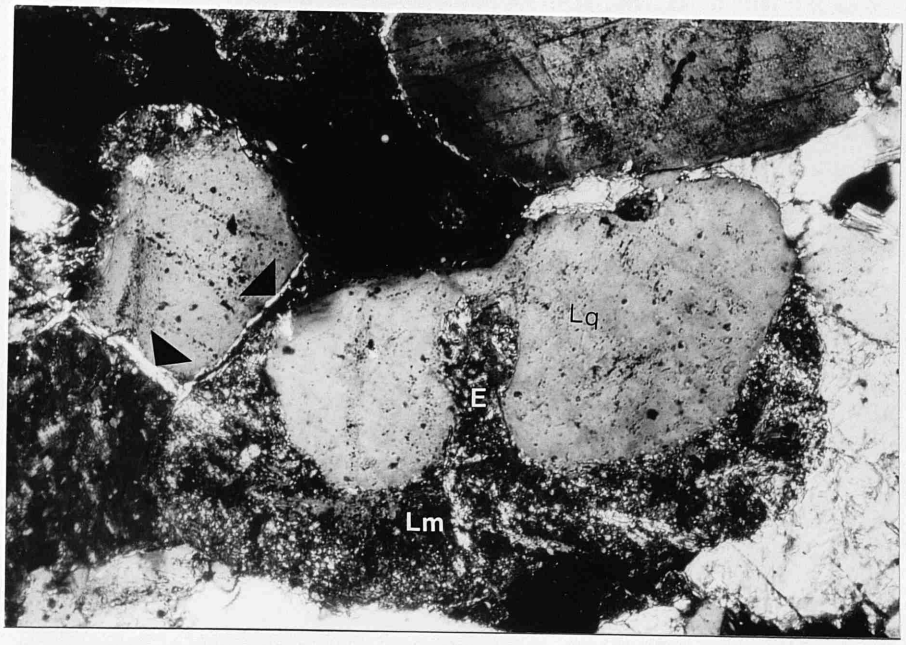

Fig 2.3 TS photomic, XPL, X40. Upper ORS sandstone, Wemyss Bay. Acid volcanic/hypabyssal lithic grain displaying silicified matrix (Lm) and quartz crystal (Lq) with embayment (E). Stage 2 detrital illite (arrows) coats detrital grains and preserved in contact zones after compaction.

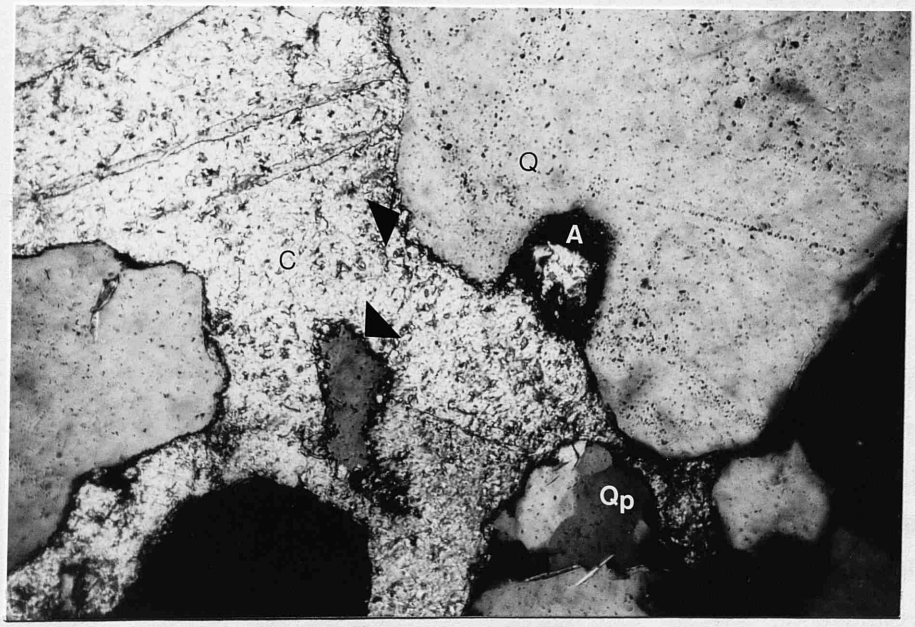

Fig 2.4 TS photomic, XPL, X40. Sandstone, Roseneath. Volcanic/hypabyssal monocrystalline quartz grain (Q) with embayment containing apatite crystal (A). Corroded margins of detrital quartz (arrows indicates instability of this phase relative to carbonate (C). Metamorphic polycrystalline quartz grain (Qp) containing mica inclusions.

Detrital quartz as a provenance indicator

The usefulness of quartz as an indicator of provenance has been much professed in the literature. The most recent studies have made use of two fundamental properties of detrital quartz: the presence or absence of undulatory extinction; and the polycrystallinity of the detrital grains (Blatt and Christie 1963, Basu et al 1975, Basu 1976, Young 1976, Mack 1981, Mack et al 1981 and Mack et al 1983). Morton (1976) identified the abundance of polygonised quartz (semi composite grains with straight boundaries meeting at 120°) over polycrystalline quartz displaying sutured contacts for the Lower ORS in the Firth of Clyde. The dominance of polygonised quartz over sutured polycrystalline grains for the Upper ORS of this study suggests a similar provenance, which Morton located within the Dalradian of the southwest Highlands using the classification of Voll (1960).

An investigation of UORS rocks was carried out following the successes of Granmayeh (1978) in obtaining good linear relationships between polycrystallinity and undulatory extinction, polycrystallinity and size, and undulatory extinction and size, and the application of the results to an interpretation of the provenance of Torridonian sediments. Figs. 2.5a-e display the results of this type of analysis to the UORS sediments. Polycrystallinity (Qp/Q) is seen to have a tenuous positive correlation with grain size within areas (Fig. 2.5c). This relationship is not unexpected and has been observed by other workers. However, this study failed to obtain linear relationships with sufficiently high correlation coefficients for plots of polycrystalline abundance versus size, polycrystallinity versus undulatory extinction, polycrystalline abundance versus undulatory extinction, and undulatory extinction versus grain size, although the latter may display an unconvincing positive correlation.

Young (1976) devised a polycrystalline quartz provenance diagram in which, it was claimed, quartz populations with different provenances occupy different zones. Mack et al (1981) revised the classification but retained the three original stability fields: low grade metamorphic; high grade metamorphic; and plutonic polycrystalline quartz. This scheme was considered particularly applicable to the sandstones interbedded with the UORS conglomerates since known clast populations within the conglomerates indicate an increasing grade of metamorphic fragments northwards and an increase in plutonic fragments in the same direction. It should therefore be possible to compare the compositions of the interbedded sandstones with the composition of the conglomerates.

Fig 2.5 (next 2 pages). a) Polycrystallinity : % undulatory plot for the basal Upper ORS sediments. b) Polycrystalline abundance : % undulatory plot for the basal Upper ORS sediments. c) Polycrystallinity : size plot for basal Upper ORS sediments. d) Polycrystalline abundance : size plot for basal Upper ORS sediments. e) % undulatory : size plot for basal Upper ORS sediments. (*) Portencross sandstones; (□) Wemyss Bay sandstones; (●) Roseneath sandstones.

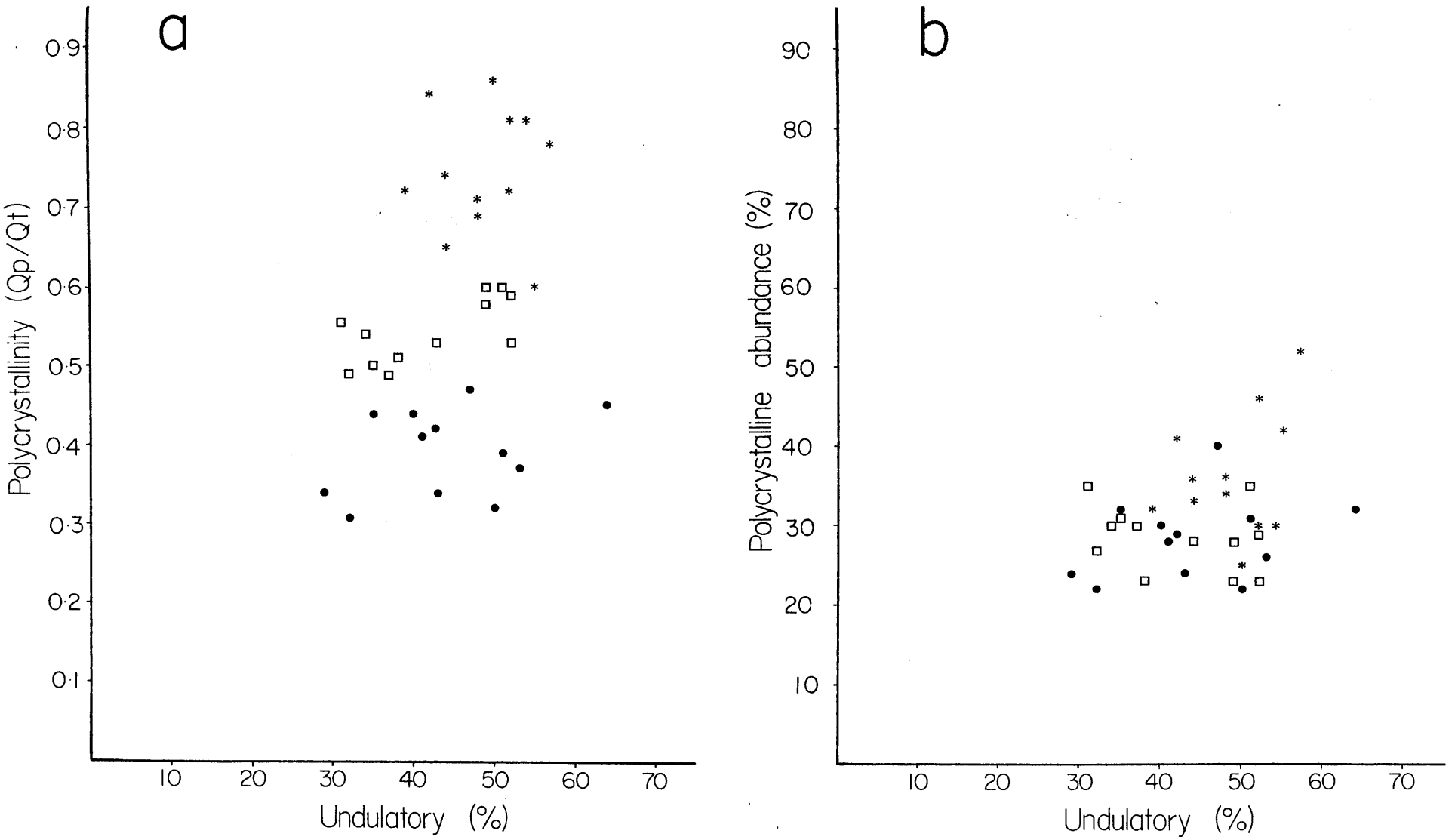
a
Polycrystallinity (Qp/Qt)
0·9
0·8
0·7
0·6
0·5
0·4
0·3
0·2
0·1
10
20
30
40
50
60
70
Undulatory (%)
b
Polycrystalline abundance (%)
90
80
70
60
50
40
30
20
10
10
20
30
40
50
60
70
Undulatory (%)

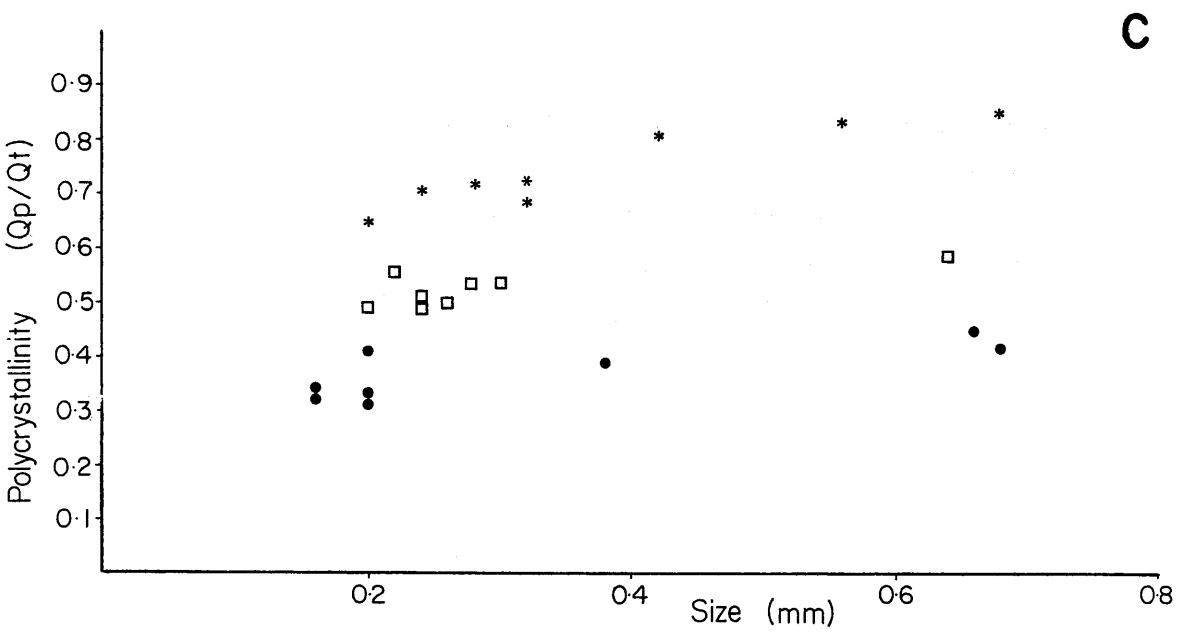
c
Polycrystallinity (Qp/Qt)
0·9
0·8
0·7
0·6
0·5
0·4
0·3
0·2
0·1
0·2
0·4
0·6
0·8
Size (mm)

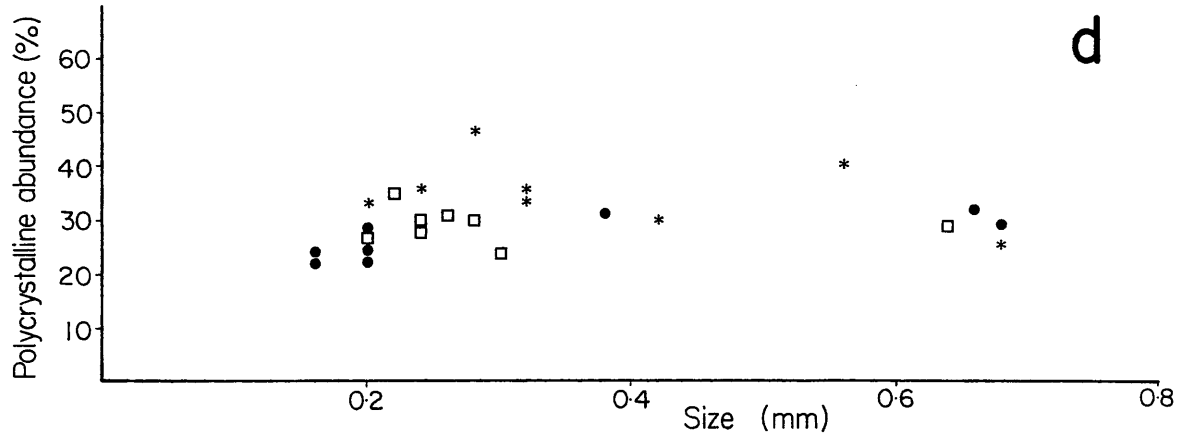
d
Polycrystalline abundance (%)
60
50
40
30
20
10
0·2
0·4
0·6
0·8
Size (mm)

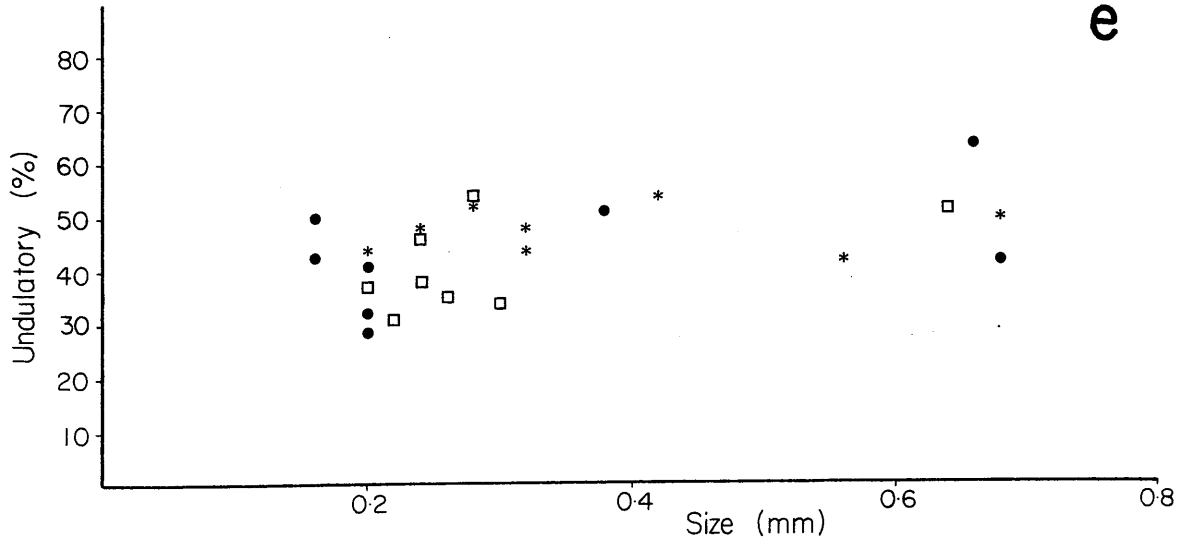
e
Undulatory (%)
80
70
60
50
40
30
20
10
0·2
0·4
0·6
0·8
Size (mm)

The modified scheme employed by Mack et al (1981) involves a plot of polycrystallinity index versus instability index. The polycrystallinity index is the ratio of polycrystalline quartz to total quartz. The instability index is the ratio of unstable to total polycrystalline quartz. The classification of quartz grains into unstable and stable varieties was made using the methods of Young (1976), and summarised as a flow diagram in Fig. 2.6. Fig. 2.7 shows the polycrystalline quartz provenance diagram for the three UORS conglomerate units in the Firth of Clyde. What is immediately obvious is that all three units share high polycrystallinity index values which are considerably in excess of all the stability fields shown by Mack et al (1981) but are within the fields published by Mack et al (1983). These fields were determined by Young (1976) by examination of the quartz fraction in 65 metamorphic rocks from low grade (chlorite and biotite), medium grade (cordierite) and high grade (sillimanite) zones. Additionally, a heavy weighting may be observed in the diagram towards high grade and/or plutonic species. This is clearly contradictory to the evidence from conglomerate clasts, in which metamorphic rocks nowhere exceed garnet grade and plutonic clasts are only found in significant numbers at Roseneath Point.

Four explanations are possible for the anomalous results:

i) High grade metamorphic and plutonic igneous rocks formed a distal source for the basal UORS fine sediment. The sandstones thus derived were then mixed with the conglomerate clasts of local origin.

ii) The source of UORS fine and coarse sediment included pre-existing sedimentary rocks (sandstone) the provenance of which is not determined (?LORS). These sandstones, when subjected to weathering, broke down into a major sand source and combined with a primary source for the conglomerate.

iii) Vein quartz clasts, associated with low grade metamorphics are pervasive in all three conglomerates, especially at Wemyss Bay and Roseneath. Thin sections of these pebbles indicate that they must contribute large quantities of poly-crystalline material to the sandstone of a highly stable nature (unsutured grain boundaries and relatively non-undulose extinction).

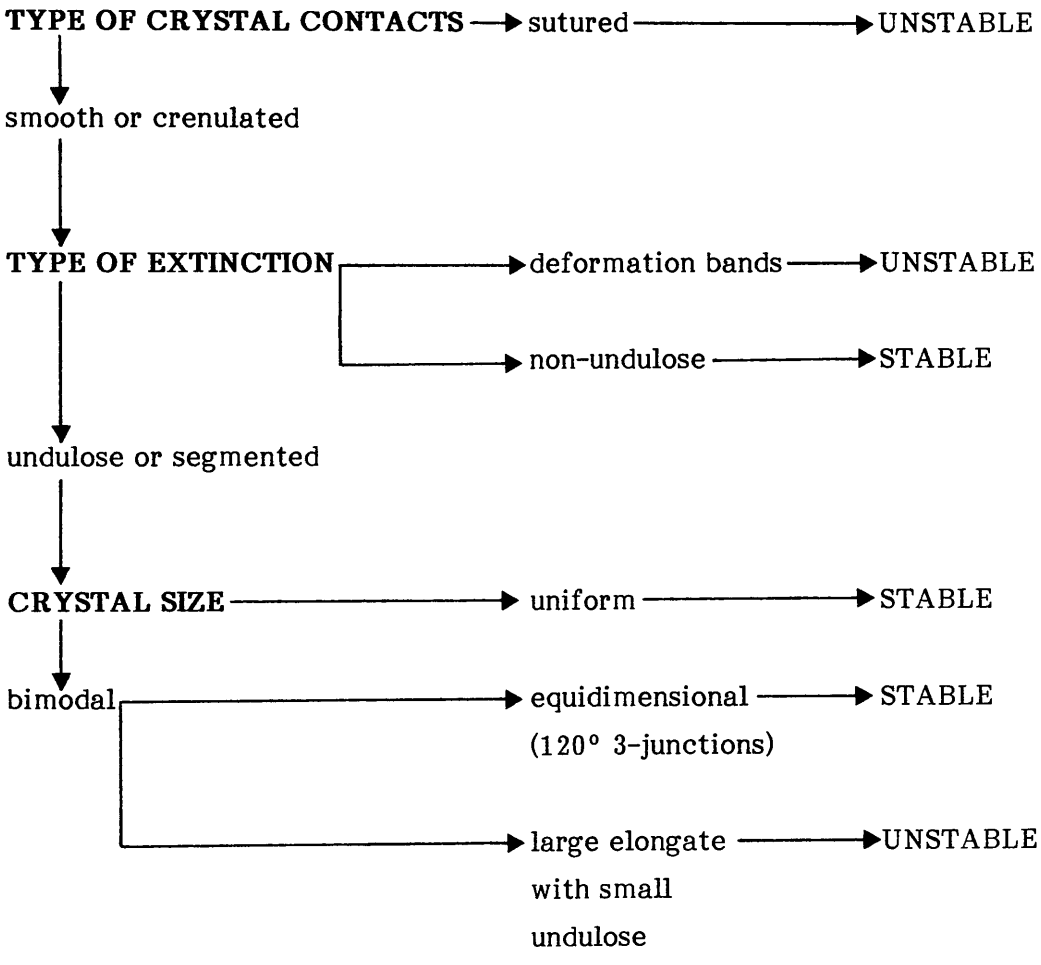

Fig 2.6. Flow diagram for determination of stable and unstable quartz grains. Adapted from Young (1976).

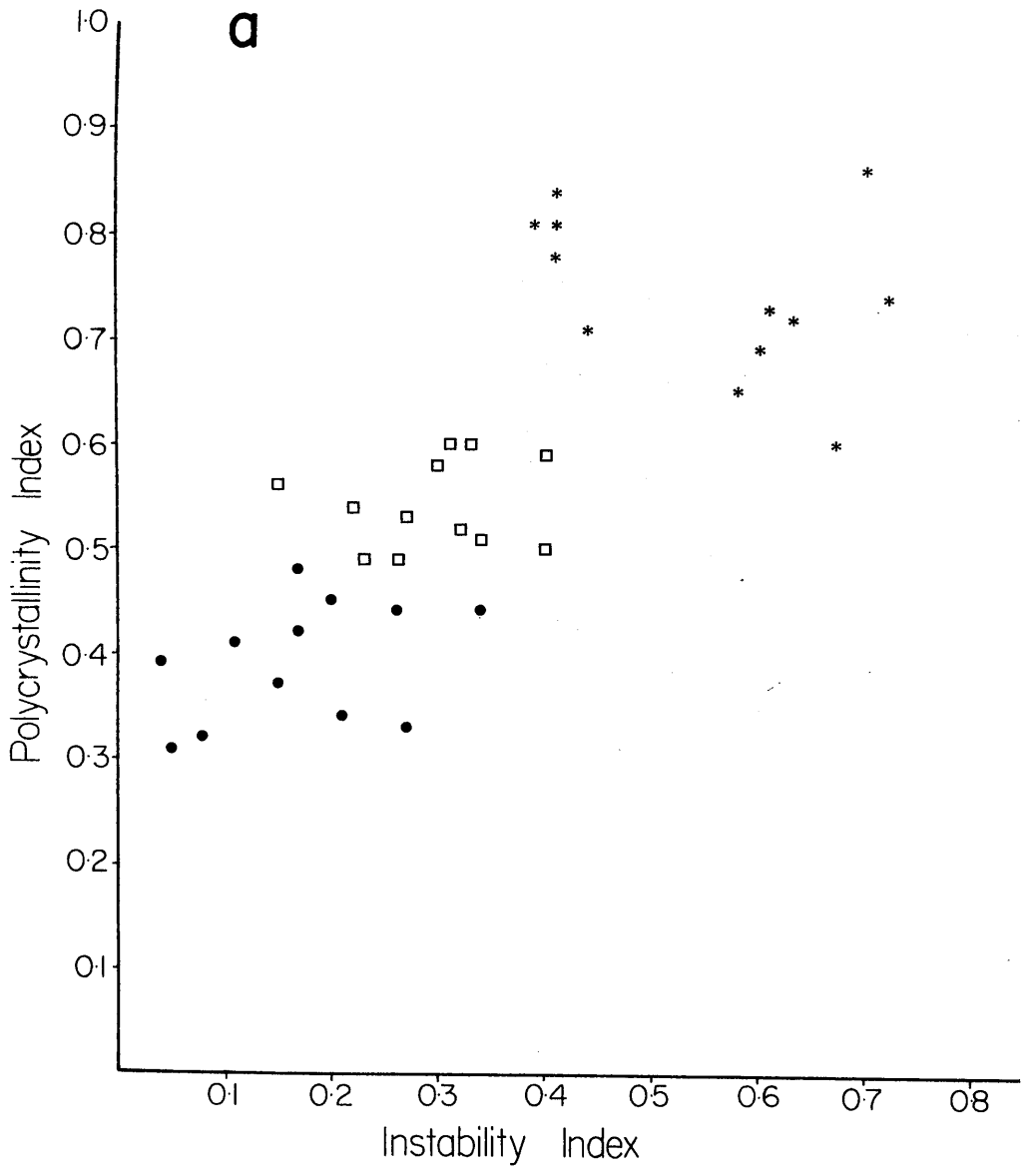

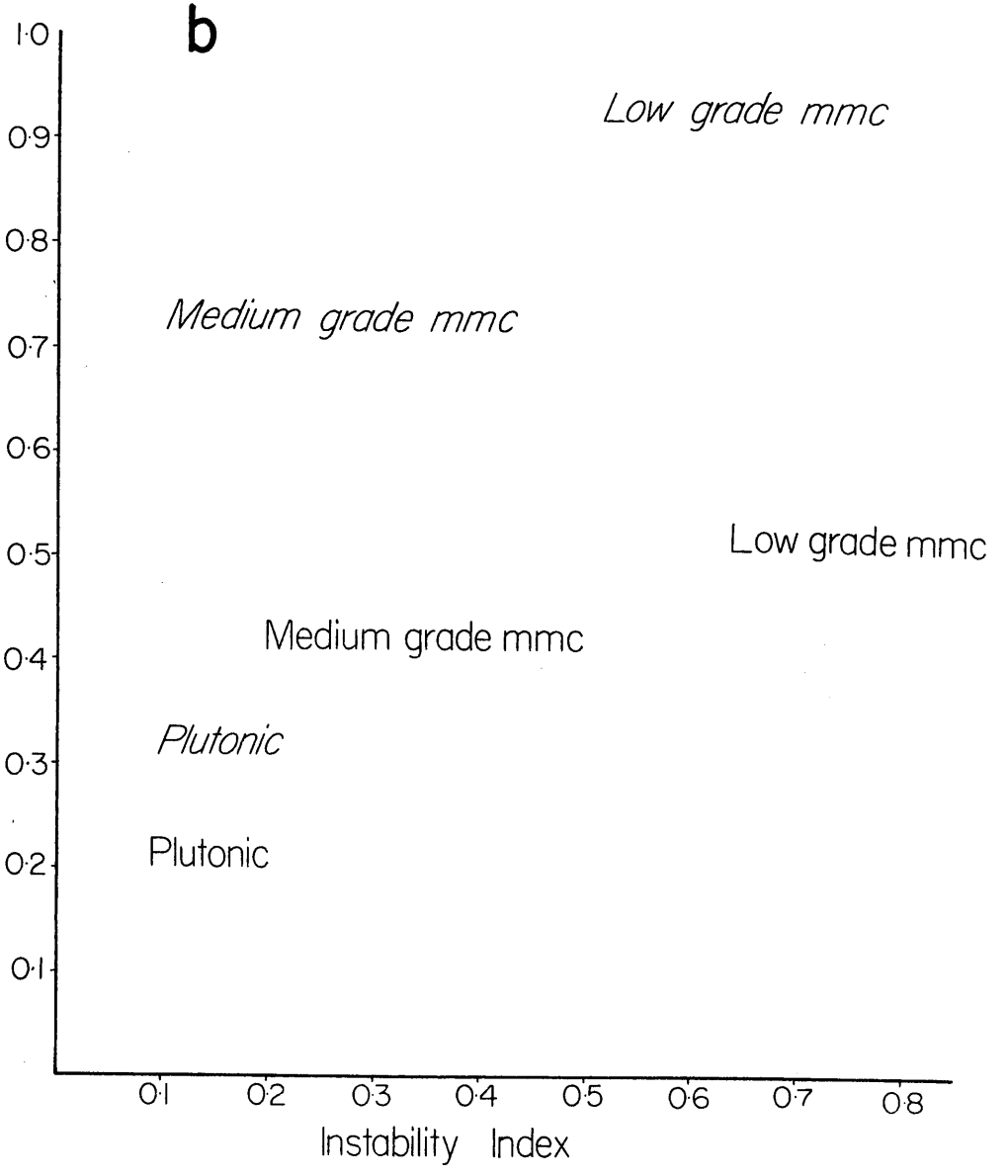

Fig 2.7 a) Polycrystallinity Index : Instability Index for basal Upper ORS. See Fig 2.5 for key. b) Provenance fields for Fig 2.7a from Mack et al 1981 (normal print) and Mack et al 1983 (itallics).

The first explanation is considered unlikely since the angularity and immature nature of the sandstone grains suggests that they have not travelled far, although the rate of rounding of quartz grains is admittedly very slow. A combination of explanations ii) and iii) seems most plausible. Highly rounded clasts in the conglomerates together with evidence from heavy mineral studies suggests a significant amount of reworked material entered the UORS dispersal system(s). However, if vein quartz was a large contributor, the coarse crystalled nature of this polycrystalline medium sized grains, which in the diagram would dilute the sediment and subsequently reduce the polycrystallinity index. This is not observed to any great degree in the sandstones. If vein quartz is partly responsible it must cast serious doubt on the usefulness of this diagram, especially in sandstones derived from areas of low-medium grade metamorphics. Vein quartz appears to be prolific in such terrains.

2.3.2 Feldspar

Plagioclase and K-feldspar together rarely form more than 15% of the detrital constituents and average c. 10%. The P/F ratio (plagioclase/total feldspar) is exceedingly variable, but averages for Roseneath, Wemyss Bay and Portencross are 0.44 (σ = 0.18), 0.40 (σ = 0.13) and 0.66 (σ = 0.19) respectively. This probably indicates the relative importance of plagioclase at Portencross.

Large, subhedral detrital feldspars displaying myrmekitic texture (intergrowth of quartz and plagioclase) are particularly common in the Wemyss Bay sediments, and such textures are often observed in granite clasts in the Roseneath conglomerates (Fig. 3.10).

K-feldspars generally do not display cross-hatched twinning (indicative of microcline) in the UORS despite evidence from XRD analysis indicating that approximately equal proportions of orthoclase and microcline are present. Microcline which does not display cross-hatched twinning is rare in any rock (Deer et al 1977) but is considered to have resulted from plagioclase-microcline convertion (Martin 1974). At Portencross, on the other hand, larger quantities of crosshatched twinned microcline in the greywacke clasts (Fig. 2.10c) must contribute to the feldspar in the UORS in that area.

Alkali feldspar structural state determination by X-ray diffraction

Wright (1968) developed an efficient method for the rapid determination of compositions and structural states of single crystals of alkali feldspar using Xray diffraction. This scheme was based on, and tested by, a more complex system using computer refined unit-cell parameters also using X-ray diffraction data (Wright and Stewart 1968).

With this method, numerous investigations of alkali feldspars in igneous rocks have been published but only a limited number of workers have applied this technique to provenance studies of sedimentary rocks (e.g. Stablein and Dapples 1977, Suttner and Basu 1977). Certainly, the main problem with the application of this technique is that most clastic rocks will contain a non-equilibrium assemblage of alkali feldspars from multiple sources. Thus, use of a single grain analysis system might not be applicable to other grains in the same rock.

The failure in this study to isolate single K-feldspar grains of a sufficiently large size (0 phi) from the sandstones in the UORS conglomerates led to the development of an aggregate-grain method of analysis (see Appendix I.3). This has also recently been attempted with different objectives and with very limited success by Plymate and Suttner (1983).

Data interpretation

The major problem with the aggregate grain system employed here is that a heterogeneous assemblage of alkali feldspar crystals is separated from the sandstones reflecting a multi-source provenance. For example, a diffractogram for the Roseneath sandstone displays four distinct peaks for each of the $\bar{2}04$ and 060 reflections. This indicates that there are four distinct populations of K-feldspar present with unique structural states. In order to determine the state of a particular population it is vital to know exactly which 060 peak corresponds to which $\bar{2}04$ peak so that its position may be plotted on the diagram. Since the sandstones are interbedded with coarse conglomerates it was assumed that the parent rocks providing K-feldspar to the sands would probably be represented by clasts in the conglomerates. Peak positions for K-feldspars separated from these clasts could then be

used to eliminate corresponding peaks in the sandstone trace. Tables 2.3 and 2.4 respectively display the peak positions for the main K-feldspar bearing clasts and aggregate grain peak positions for the three areas of UORS.

The main K-feldspar bearing clasts at each area are as follows:

i) Roseneath: granite (s.l.), porphyritic microgranite and biotite schist.

ii) Wemyss Bay: granite (s.l.), rhyolite and low grade metagreywacke.

iii) Portencross: greywacke and metagreywacke.

A typical diffractogram for a K-feldspar separate from the Roseneath sandstones is shown in Fig. 2.8. Four feldspar populations appear to be present. The four peaks for the 060 and $\bar{2}04$ reflections have been assigned a, b, c and d in order of decreasing intensity. The most intense peaks might be expected to represent feldspars derived from the schists and acid igneous clasts, being the most abundant K-feldspar bearing rocks in the Roseneath conglomerate. Positions for averaged values of the 060 and $\bar{2}04$ peaks for igneous and schist separates (from Table 2.3) are also indicated in Fig. 2.8. It is obvious that the most intense peak in this sandstone (peak a) correlates closely with the averaged peak position for the acid igneous rocks. Also, the schists appear to be responsible for the second most intense peaks (peak b). Two of the four peaks can therefore be accounted for in this manner. If the remaining peaks for all the sandstones are paired off according to their relative intensities (c with c, d with d) and plotted on Wright's graph, the d peaks fall in the region of high sanidine, while the c peaks define a field intermediate between orthoclase and high sanidine (Fig. 2.9b).

Interpretation of the c and d peaks is therefore somewhat uncertain. However, an intensity related pairing is favoured for the following reasons:

i) Intensity pairing held for the most intense peaks a and b.

ii) DGD03 is the only sandstone separate from Roseneath to show only three peaks. The most intense peaks correspond to the igneous and metamorphic feldspars as usual. The third peaks define a point within the intermediate orthoclase/sanidine field already proposed for the c peaks, and is of possible authigenic origin (see iv below).

LOCATION	SAMPLE	$\bar{2}01$ 2θ	002 2θ	$\bar{1}13$ 2θ	060 2θ	$\bar{2}04$ 2θ
Roseneath	DGA03 (qtz porphyry)				41.68	50.71
	DGA04 (qtz porphyry)				41.66	50.71
	DGA 10 (microgranite)	c. 21.18	27.55	36.67 - 38.77	41.71	50.69
	DGA 11 (qtz porphyry)		27.50	38.60 - 38.72	41.73	50.70
	DGB02 (phenocryst)	c. 20.94	27.60	38.75 - 38.83	41.64	50.71
	DGB03 (qtz porphyry)		27.57	38.62-38.73	41.69	50.67
	DGB05 (microgranite)		27.58		41.68	50.70
	DGB07 (microgranite)				41.69	50.70
	DGB09 (qtz porphyry)		27.59	38.65 - 38.74	41.66	50.70
	DGB10 (granodiorite)		27.54		41.67	50.68
	DGB11 (granodiorite)				41.68	50.68
	DGB12 (granodiorite)		27.58		41.70	50.71
	DGB15 (granodiorite)				41.69	50.69
	DGB16 (qtz porphyry)				41.67	50.71
Roseneath	DGS02 (bte schist)				41.86	50.58
	DGS03 (bte schist)	21.33		38.65	41.89	50.60
	DGS04 (bte schist)	21.33		38.62	41.86	50.57
	DGS05 (bte schist)				41.85	50.58
	DGS06 (bte schist)				41.84	50.57
	DGS07 (bte schist)	21.30		38.64	41.92	50.60
Wemyss Bay	WBG01 (granite)				41.70	50.57
	WBG02 (granite)				41.68	50.59
	WBG03 (granite)	c.20.90		c. 38.60	41.69	50.57
	WBG04 (granite)				41.66	50.57
	WBG05 (granite)				41.67	50.59
	WBG06 (greywacke)				41.78	50.55
	WBG07 (metagreywacke)	20.87		38.59	41.77	50.54
	WBG08 (metagreywacke)				41.80	50.55
Portencross	DGP20 (greywacke)	20.91		38.62	41.73	50.58
	DGP21 (greywacke)				41.75	50.57
	DGP22 (greywacke)				41.70	50.58
	DGP23 (metagreywacke)	20.97		c. 38.60	41.75	50.55
	DGP24 (metagreywacke)				41.75	50.54
	DGP25 (greywacke)				41.74	50.55
	DGP26 (metagreywacke)				41.76	50.55

Table 2.3. Diffractogram peak positions for K-feldspar separates from selected conglomerate clasts, Firth of Clyde basal Upper ORS.

LOCATION	SAMPLE	060 2θ	$\bar{2}04$ 2θ	PEAK TYPE
Roseneath	DGDO1	41.66	50.66	a
		41.87	50.58	b
		41.75	50.78	c
		41.60	50.84	d
	DGD02	41.74	50.68	a
		41.86	50.60	b
		41.68	50.79	c
		41.54	50.85	d
	DGD03	41.67	50.70	a
		41.83	50.57	b
		41.62	50.76	c
	DGDO4	41.76	50.69	a
		41.83	50.55	b
		41.70	50.76	c
		41.59	50.84	d
	DGDO7	41.70	50.67	a
		41.82	50.60	b
		41.65	50.75	c
		41.56	50.83	d
Wemyss Bay	WBS01	41.69	50.58	a
	WBS02	41.66	50.56	a
		41.72	50.74	b
	WBS03	41.68	50.56	a
		41.73	50.75	b
	WBS04	41.71	50.59	a
	WBS05	41.73	50.58	a
		41.68	50.75	b
Portencross	DGP02	41.73	50.55	a
	DGP03	41.71	50.58	a
		41.81	50.69	b
	DGP04	41.75	50.56	a
	DGP05	41.75	50.54	a
	DGP06	41.74	50.58	a
		41.80	50.74	b

Table 2.4. Diffractogram peak positions for aggregate grain K-fs separates from UORS.

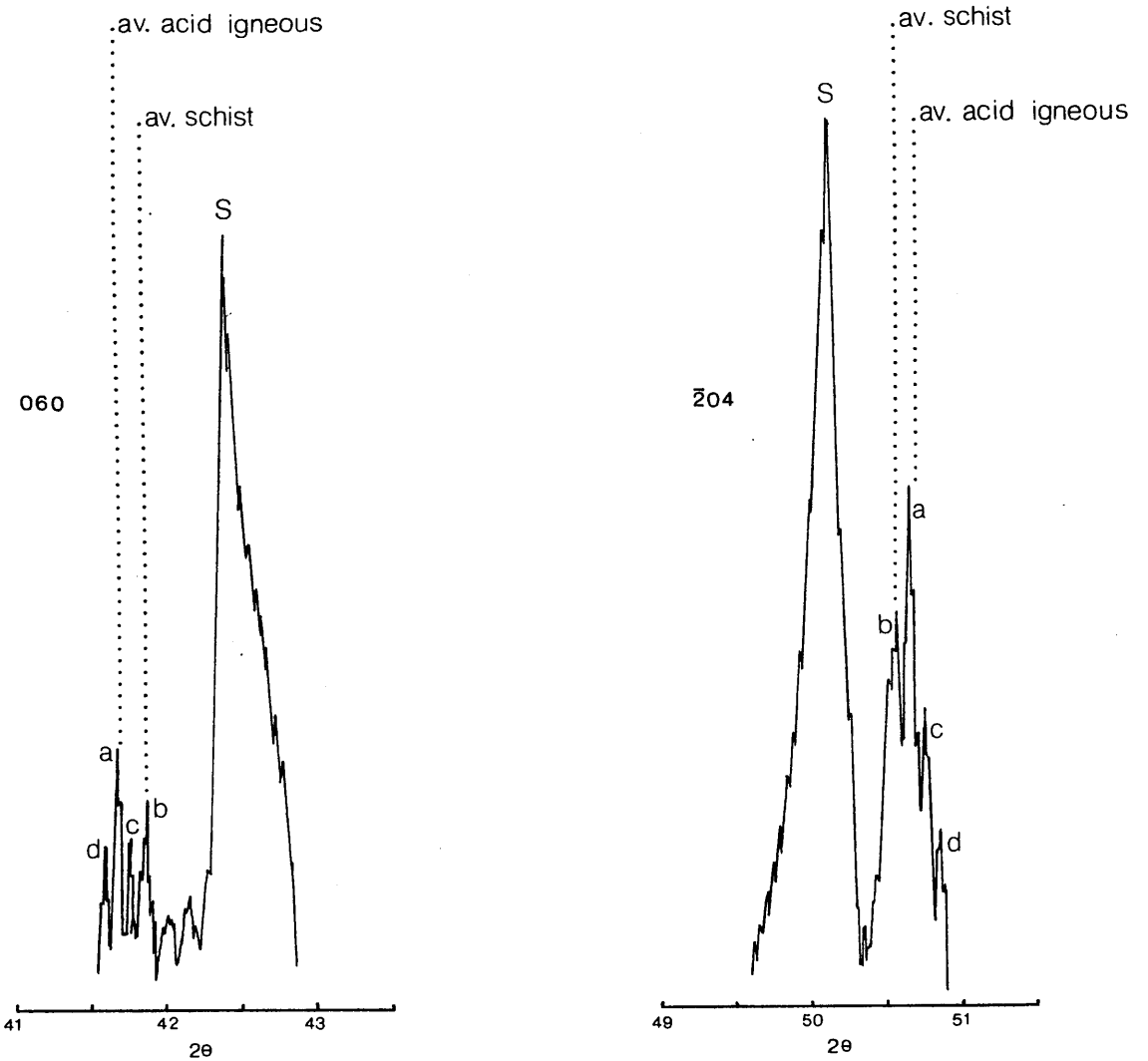

Fig 2.8. Sections of a typical XRD diffractogram of K-feldspar separate from the Roseneath sands showing positions of 060 and $\bar{2}04$ reflections. S peaks-silica standard reflections.

Fig 2.9 (next page). Plots of 2θ (060) against 2θ($\bar{2}$04) reflections for: K-feldspar separates from clasts in basal Upper ORS conglomerates at Roseneath, Wemyss Bay and Portencross (a,c and e respectively) and; K-feldspar separates of sandstones from basal Upper ORS at Roseneath, Wemyss Bay and Portencross (b,d and f respectively).

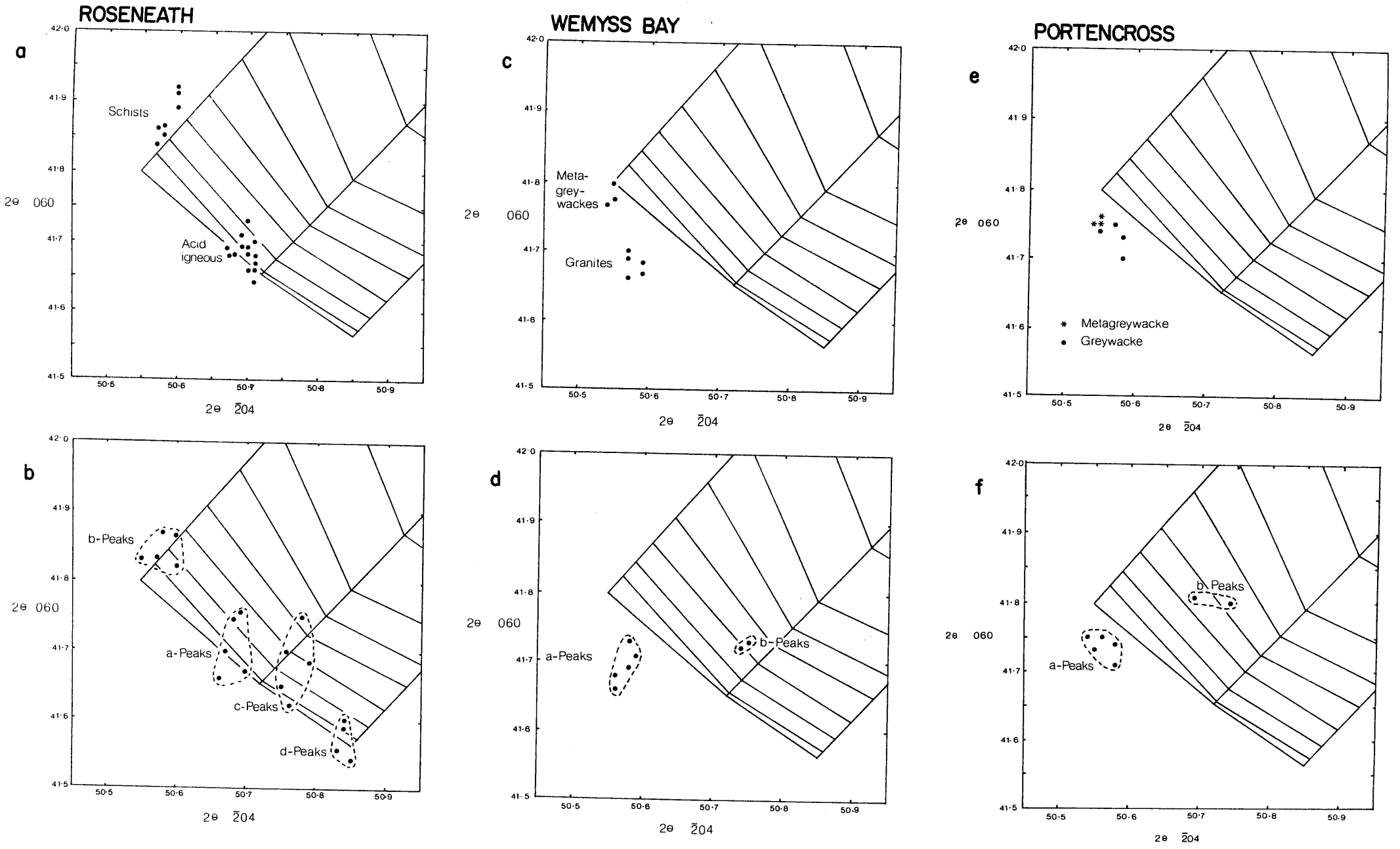
ROSENEATH
a
Schists
Acid igneous
2θ 060
2θ 204
b
b-Peaks
a-Peaks
c-Peaks
d-Peaks
WEMYSS BAY
c
Meta-grey-wackes
Granites
d
a-Peaks
b-Peaks
PORTENCROSS
e
Metagreywacke
Greywacke
f
a-Peaks
b-Peaks

iii) Volcanic fragments are present in small quantities in the conglomerates and, although their feldspars were not analysed by XRD in this study, they would be expected to approach disordered sanidine (approximate field for d peaks Fig. 2.9b).

iv) In an intensity pairing, c peaks for all the sandstones define a field which is broadly similar to that shown for authigenic feldspars in the St. Peters Sandstone (Woodard 1972). These might well be interpreted as authigenic overgrowths developed during diagenesis.

Fig. 2.9a shows the stability fields for K-feldspar separated from the Roseneath conglomerate clasts. K-feldspar in the schists cluster tightly with a composition closely approximating maximum microcline. This ordered state would be expected for feldspars of this metamorphic grade. Another tight cluster is observed at a composition close to orthoclase. These grains were separated from the acid igneous rocks and it is important to notice that it is not possible to differentiate between hypabyssal and plutonic types on this basis. The chemical similarities between these igneous rocks are discussed further in Chapter 3.

Interpretation of diffraction patterns for detrital alkali feldspar at Wemyss Bay is comparatively simple. At most only two populations are present. Fig. 2.9c shows the stability fields for K-feldspar obtained from granite and greywacke pebbles in the conglomerates. When the peak positions of detrital K-feldspar from sandstones with only one population are considered (WBS01 and WBS04) the compositions and structural states are identical to those for the granites. In the sandstones which contain two K-feldspar populations, one set obviously belongs to the granite field and can be eliminated. The remaining peaks fall consistently into the greywacke field. This pairing is also seen to be intensity related. Fig. 2.9d displays the population fields for the Wemyss Bay detrital K-feldspar. It should be noted that no authigenic feldspar is detected here. It is also particularly interesting to observe that the granite clasts have a significantly different cluster position to the granodiorites and associated porphyries at Roseneath. The difference in position of the fields is probably greater than that expected for variations within a single pluton.

At Portencross, DGP02, DGP04 and DGP05 contain only one detrital feldspar population. Comparison of these values with those determined for greywacke clasts (Fig.2.9e) indicates close similarities. DGP03 and DGP06 display two feldspar populations. The most intense peaks are like those for the greywackes (Fig. 2.9f). The remaining peaks define compositions which are of unknown origin but plot close to the authigenic feldspars of the St. Peter Sandstone.

2.3.3 Lithic Fragments

In all three areas quartzites are the most abundant fragments, although it is difficult to differentiate between ortho- and metaquartzite grains. Polycrystalline grains with reasonably abundant muscovite and biotite, and with tourmaline inclusions have been interpreted as metaquartzites. Petrologically, these metaquartzites are similar to polycyclic quartzite boulders and pebbles which are ubiquitous in the LORS and UORS conglomerates, and for which no certain origin has presently been found (see Bluck 1984). The fragments are pink in colour, fine to coarse grained and, apart from quartz, contain little else than a few flakes of mica. Where crystal boundaries are distinct and unsutured, a sedimentary origin is preferred (probably micro-fragments of red-stained sandstone pebbles occurring in the conglomerates of presumed LORS affinity - Fig. 2.10a,b). A distinction can also be made between metaquartzites (pervasive in all areas but particularly abundant at Portencross) and quartz-mica schists (restricted in occurrence to the Roseneath area), on the basis of mica content and occassionally by the presence of metamorphic garnets (Figs. 2.11 and 2.12).

At Portencross the most characteristic lithic type is a fine grained shaley mudstone which has a gritty appearance due to relatively large rounded quartzes within the matrix (Fig. 2.13).

Fine grained sedimentary material also occurs at Wemyss Bay but is subordinate to low grade metagreywacke (Fig. 2.10c). The most characteristic lithic component here is volcanic material of both andesitic and more acid compositions (Figs. 2.14 and 2.15). Intermediate types probably dominate over acid types, although both are highly altered and stained by iron oxide. Many of the acid fragments show evidence of hydrothermal alteration (silicification) described for the acid porphyry clasts in the Roseneath

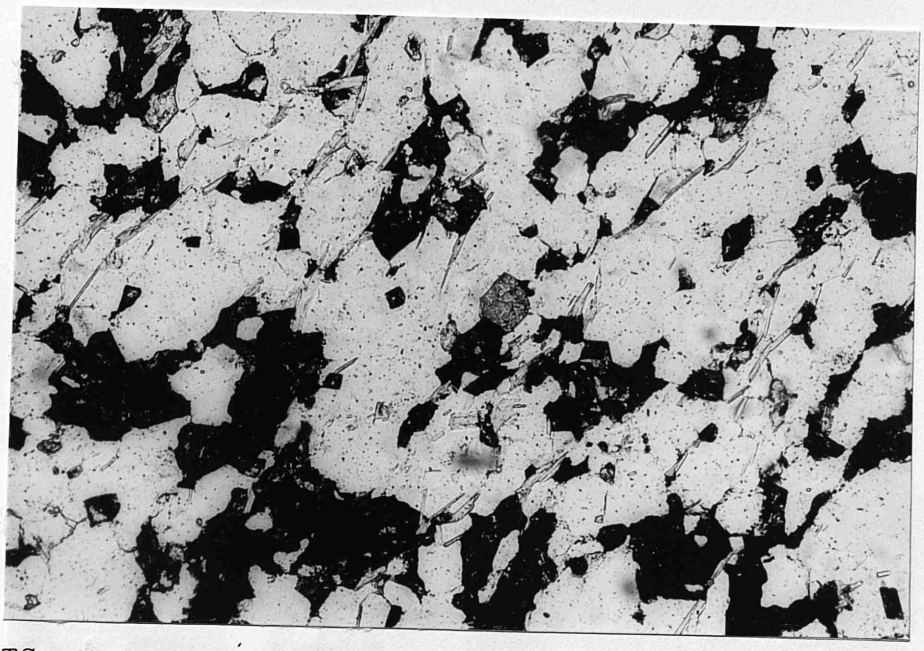

Fig 2.10a. TS photomic, PPL, X10. ?Lower ORS sandstone pebble, Portencross. See also Fig 2.10b . Tightly compacted quartz arenite showing nearly complete occlusion of porosity. Note early development of fabric (top right to bottom left) as depicted by preferred orientation of micas (chlorite and muscovite) and elongation of quartz grains.

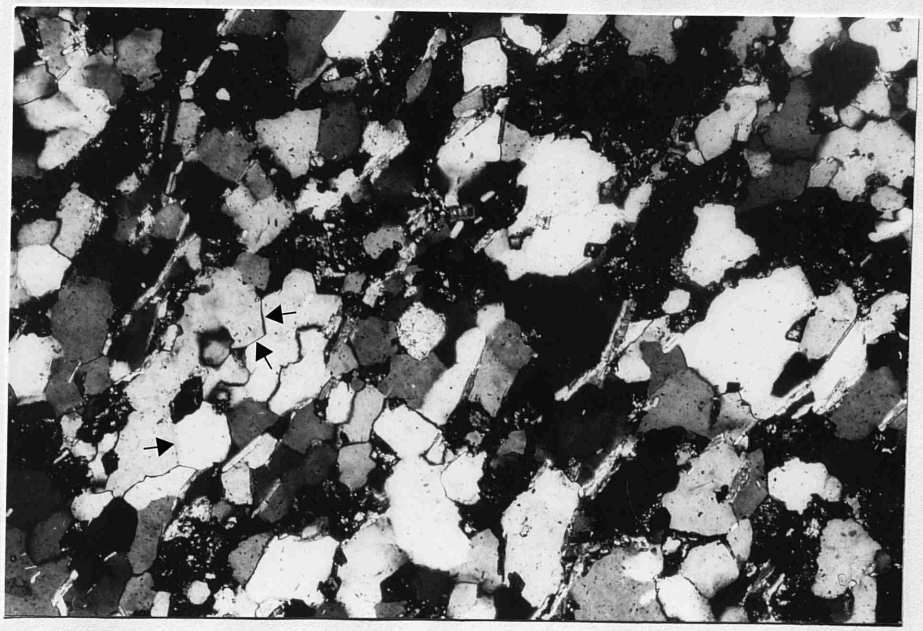

Fig 2.10b. TS photomic, XPL, X10. ?Lower ORS sandstone pebble, Portencross. See also Fig 2.10a. Dominance of straight grain/grain contacts with triple junctions (arrows) over sutured contacts (pressure solution) illustrates the importance of silica precipitation by quartz overgrowth during induration of the sediment. Original grain boundaries are no longer distinguishable.

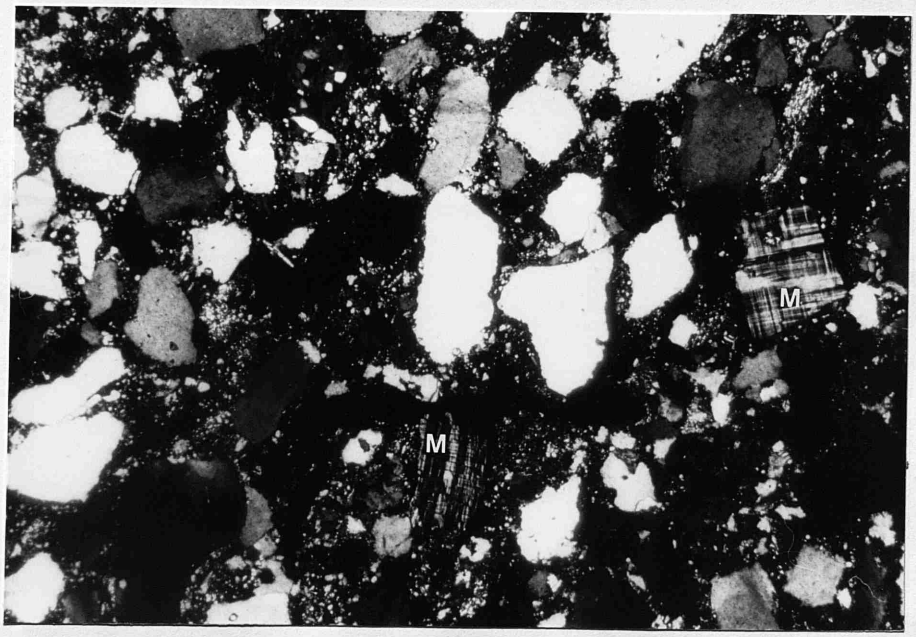

Fig 2.10c. TS photomic, XPL, X25.2. Metagreywacke pebble, Portencross. Note abundance of microcline grains (M), and occurrence of both rounded and angular surfaces.

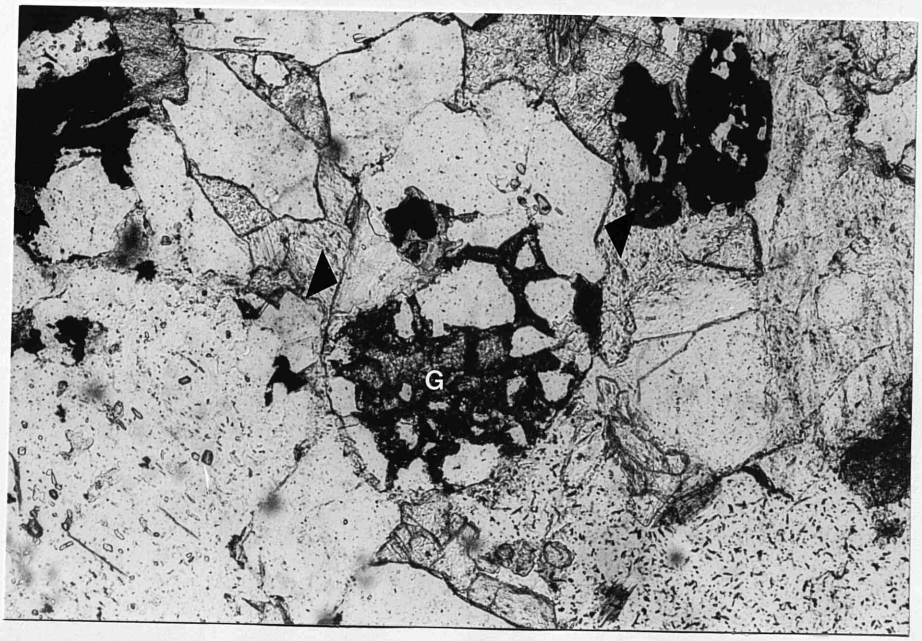

Fig 2.11a. TS photomic, PPL, X25.2. Sandstone, Roseneath. Garnet (G) bearing schist fragment displaying stage 1 iron oxide grain coating (arrows). See Fig 2.11b.

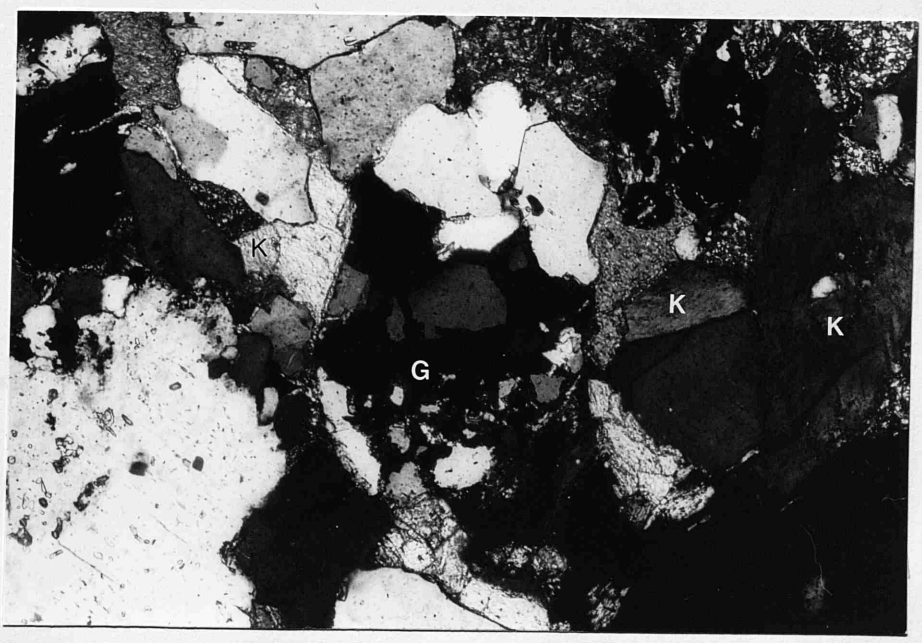

Fig 2.11b. TS photomic, XPL, X25.2. Sandstone, Roseneath. See Fig 2.11a. Note high content of detrital K-feldspar.

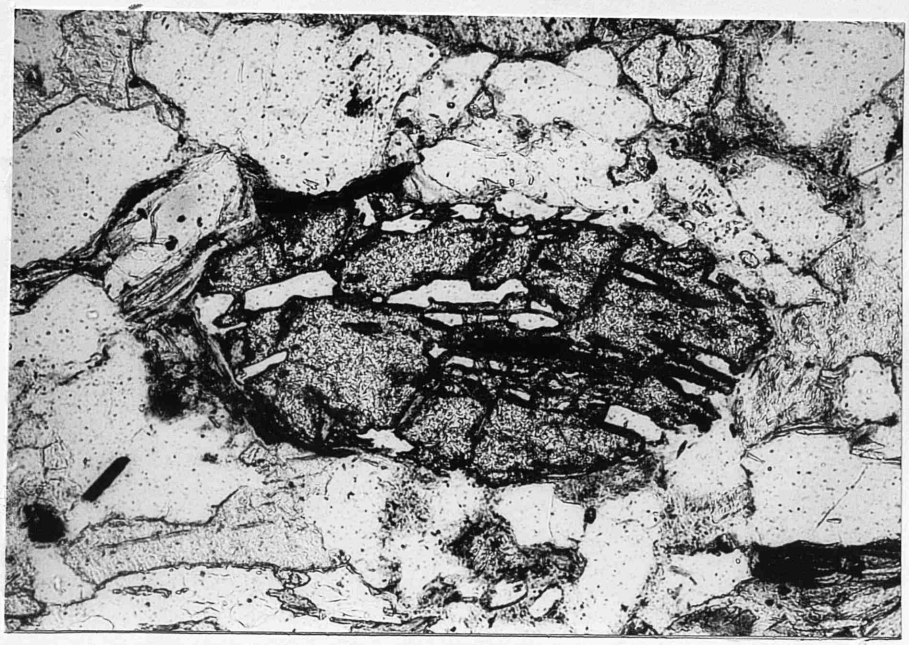

Fig 2.12. TS photomic, PPL, X25.2. Sandstone, Roseneath. Large detrital garnet grain displaying elongate and rotated quartz inclusion trails. Note stage 1 iron oxide coating on all detrital grains.

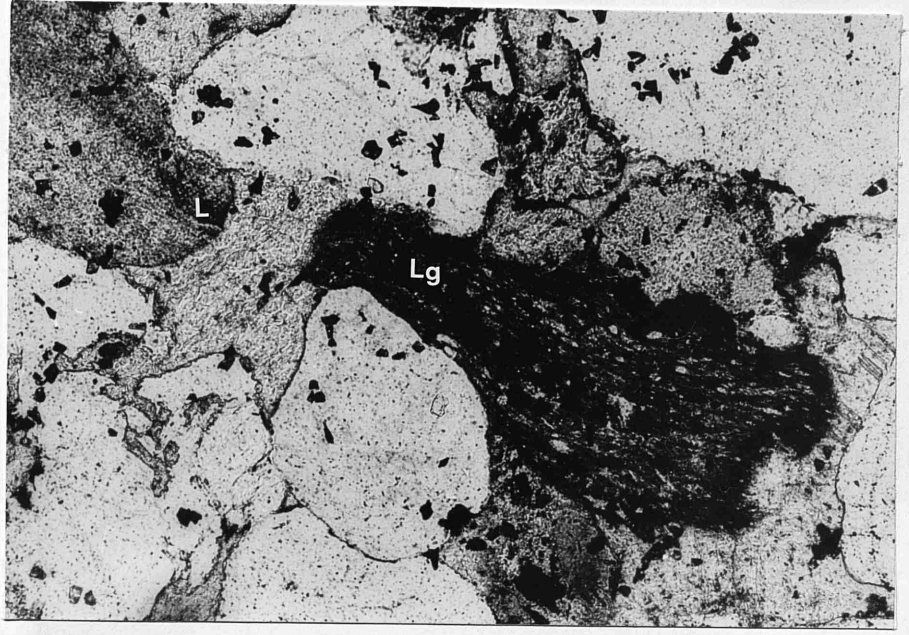

Fig 2.13 TS photomic, PPL, X25.2. Sandstone, Portencross. Plastic deformation of sedimentary lithic material (L, Lg) by adjacent detrital grains. Note 'gritty' appearance of mudstone clast Lg, and iron oxide grain coating cement.

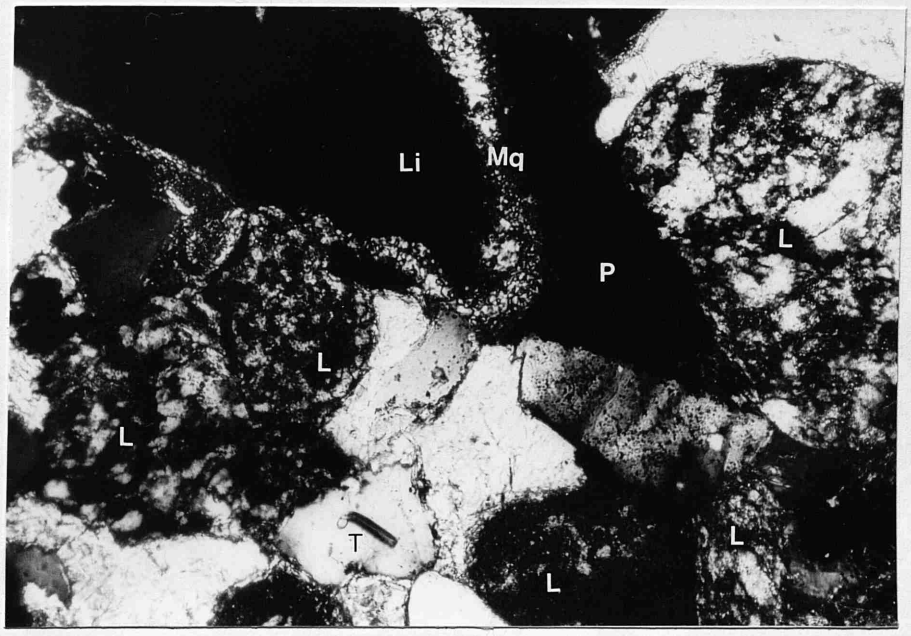

Fig 2.14. TS photomic, XPL, X40. Sandstone, Wemyss Bay. Intermediate and silicified acidic volcanic lithic grains (L, Li). Metamorphic quartz grain with euhedral pleochroic green/brown tourmaline inclusion (T). Infilling of porespace (P) by precipitation of microcrystalline quartz (Mq) on surface of intermediate volcanic grain (Li).

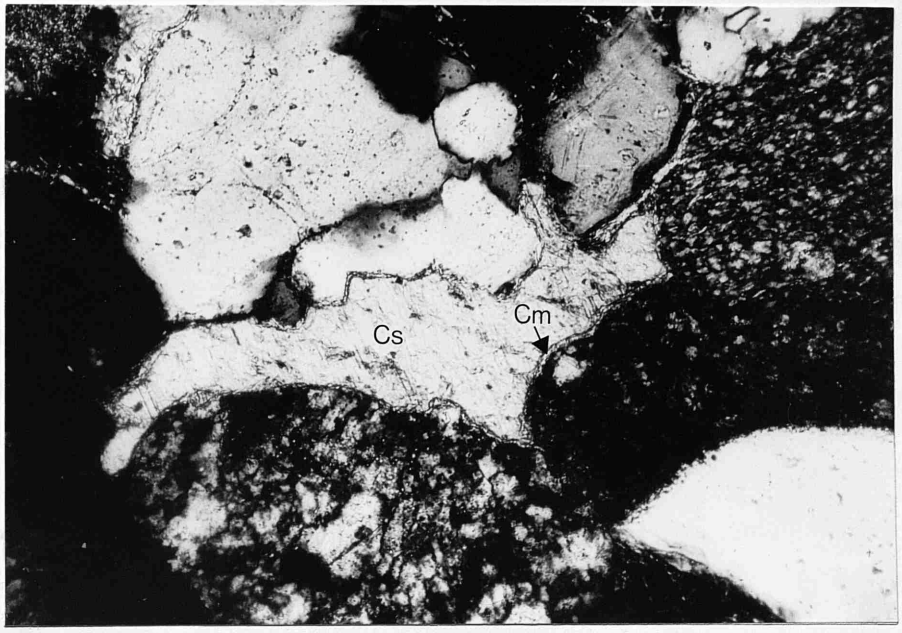

Fig 2.15. TS photomic, XPL, X40. Sandstone, Wemyss Bay. Fine micrite rim (Cm) lines pore space filled by main phase sparite (Cs). Detrital grains dominated by lithic clasts of intermediate and acidic volcanic material.

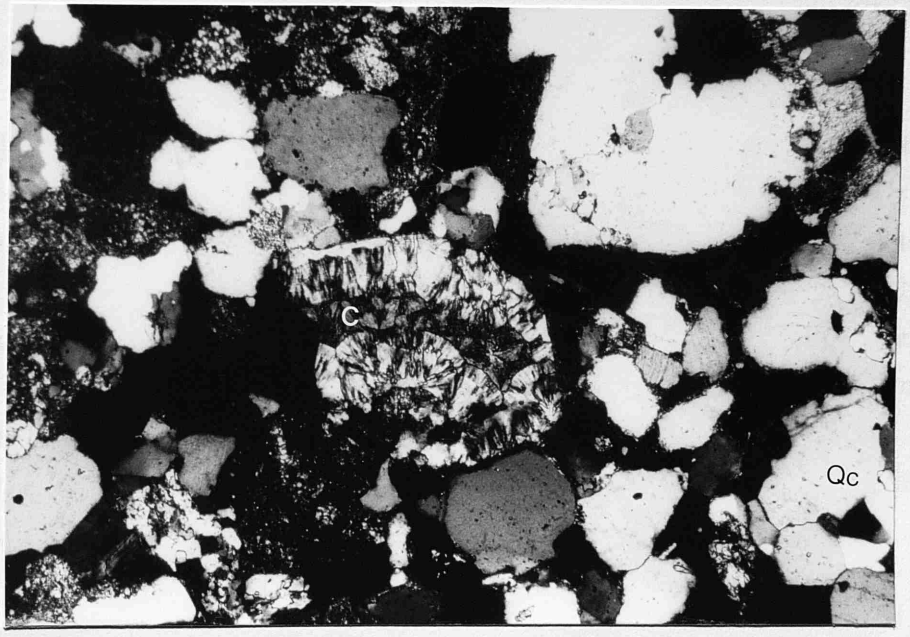

Fig 2.16. TS photomic, XPL, X10. Sandstone, Portencross. Rounded detrital chert fragment (C). Tightly packed composite quartz grains (Qc) form sedimentary lithic fragment with presumed Lower ORS origin.

conglomerate (section 3.3.7). Silicification of volcanic material occurred prior to incorporation into the UORS and often results in confusion with detrital chert which is present in all the conglomerates and sandstones (Fig. 2.16). These hydrothermally altered igneous rocks are presumably related to similar fragments described as silicified igneous material in Lower Carboniferous rocks in the NW Midland Valley (Tait 1973). This was interpreted as reworked UORS detritus.

Intermediate hypabyssal/volcanic micro-fragments are uncommon at Roseneath, where, however, they are present in large quantities as conglomerate clasts. Quartz-mica-(garnet) schist is the most distinctive lithic fragment at Roseneath. Black or dark grey shale fragments have been incorporated into the fine grained sediment and also occur as cobble sized detritus in the conglomerates. The large shale clasts occassionally contain a smooth, dichotomously branching flora (**Hostimella** sp. or a spineless **psilophyton** genus) of Lower/Middle Devonian age and must confirm reworking of LORS during UORS deposition. More precise dating of these shales was attempted by pollen and spore analysis (techniques described in Appendix I) but on etching were discovered to be barren.

2.3.4 Heavy Minerals

Heavy mineral separations were performed on 23 samples of sandstone interbedded with the basal conglomerates at Portencross, Wemyss Bay and Roseneath. In addition, sandstone, greywacke, granite and schist clasts, together with representative samples from the upper parts of the UORS succession in each area were also analysed. For the Portencross area, where LORS rocks are juxtaposed against basal UORS conglomerates, two samples of LORS sandstone were disaggregated and the heavy residue separated. The methods of separation are described in Appendix I and the results are presented in Table 2.5.

Tourmaline

The UORS conglomerate at Roseneath provided the most diverse suite of tourmalines of the three areas studied. Five varieties have been identified

Fig 2.17a. SEM photomic, 10um bars. Sandstone heavy mineral separate, Roseneath. Abraded (reworked) tourmaline grain.

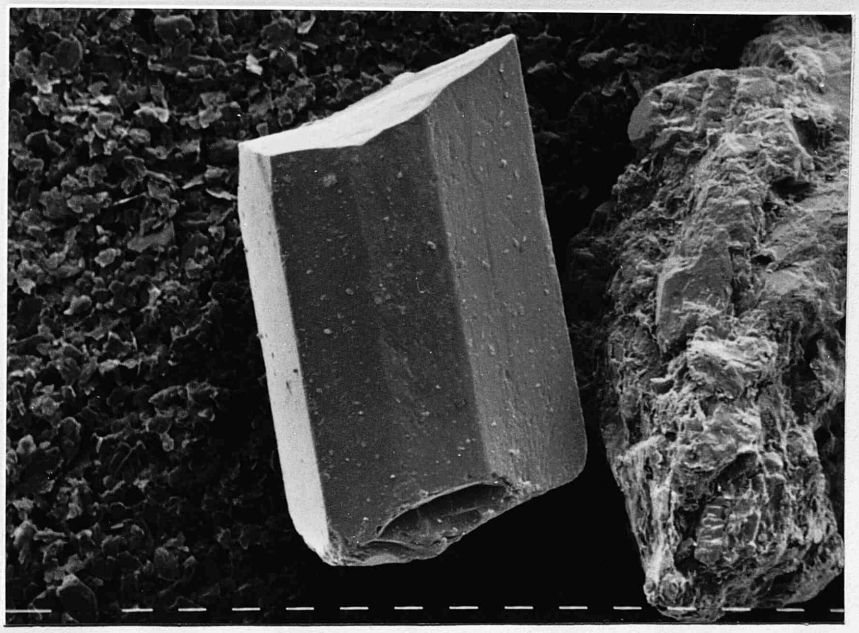

Fig 2.17b. SEM photomic, 10um bars. Sandstone heavy mineral separate, Roseneath. Unabraded (first cycle) tourmaline grain.

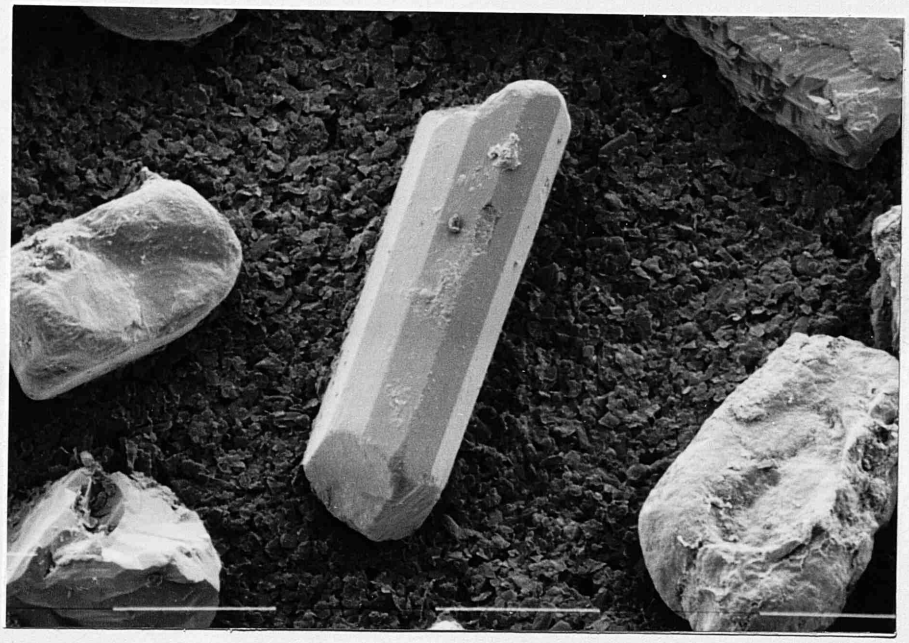

Fig 2.17c. SEM photomic, 150um bars. Sandstone heavy mineral separate, Wemyss Bay. Unabraded (first cycle) tourmaline grain.

	⟵ Sandstones in basal UORS ⟶											
SAMPLE TYPE:	PORTENCROSS	WEMYSS BAY	ROSENEATH	Ss clast PORTENCROSS	Gwacke clast PORTENCROSS	Ss clast ROSENEATH	LORS ss PORTENCROSS	Late UORS PORTENCROSS	Late UORS WEMYSS BAY	Late UORS ROSENEATH	Schist ROSENEATH	Granite ROSENEATH
LOCALITY:												
NO. OF SAMPLES:	6	7	10	3	5	3	2	3	2	2	3	3
1) Zircon:												
colourless	R	C	C	C	-	C	C	C	C	C	-	C
tan	R	C	C	R	R	C	-	-	-	-	C	-
purple	C	C	C	C	C	-	R	-	-	-	R	-
2) Tourmaline:												
colourless/lt pink	C	C	R	C	R	C	C	C	C	C	-	-
yellow - brown	-	R	C	-	-	C	-	-	-	R	R	-
olive - brown	-	C	C	-	-	C	-	-	-	-	C	-
dark pink	-	-	R	-	-	-	-	-	-	-	-	-
blue	-	-	R	-	-	-	-	-	-	-	R	-
3) Rutile	R	R	R	R	R	R	R	C	C	C	C	C
4) Garnet:												
green	R	-	-	-	R	-	-	-	-	-	-	-
pink	-	C	-	-	-	-	-	-	-	-	-	-
colourless	-	-	C	-	-	-	-	-	-	-	R	-
5) Epidote	C	R	R	-	C	-	-	-	-	-	-	-
6) Amphibole:												
hornblende	-	R	R	-	R	-	-	-	-	-	-	C
glaucophane	R	-	R	-	R	-	-	-	-	-	-	-
7) Apatite	C	C	C	R	-	R	R	R	R	R	C	C
8) Mica:												
chlorite	C	C	R	-	C	-	-	-	-	-	-	-
muscovite	-	-	C	-	-	-	-	-	-	-	C	-
biotite	-	R	C	-	-	-	-	-	-	-	C	C
9) Anatase	-	-	R	-	-	-	-	-	-	-	-	-

Table 2.5. Non-opaque heavy mineral abundances. C = common (>10%); R = rare (<10%); - = absent.

based on their strongly pleochroic colours:

i) Colourless/very light pink (dravite (Na) or Urite (Ca + Mg))

ii) Pleochroic golden yellow to brown (dravite (Fe) or schorlite (Mg - Fe))

iii) Pleochroic olive green to pale yellow/brown (Ca - Na - Fe Li elbaite or schorlite)

iv) Pleochroic deep pink to pale pink (rubellite (Li))

v) Pleochroic blue/turquoise to light mauve (Na - Fe - Li indicolite)

These correspond to the first five groups of tourmalines in Krynine's (1946) Pleochroic Formula. Only Group 6 (black to brown) in the Pleochroic Formula is not represented in the heavy mineral suites.

Krynine (1946) proceeded to relate the occurrence of a particular tourmaline type in clastic sediments to a 'type' provenance region. This results in the fivefold classification shown in Table 2.6. Interpreted in this way, the tourmaline suite in the base UORS at Roseneath is probably typical of a reworked sediment where several varieties of tourmaline from different source areas, eroded at different times, show many varieties of colour, internal morphology and rounding. Wilson (1971) has described a similar tourmaline assemblage from LORS rocks in the NW Midland Valley (sediments considered to underly those of the present study). Although a slightly different pleochroic scheme was used for the LORS, representatives from all five groups outlined above are clearly present. This would therefore be consistent with an inherited origin for the UORS heavy grains from LORS and possibly older rocks. However, from microscope and SEM studies, it is clear that, while many of the UORS tourmalines do display abraded surfaces (Fig. 2.17a), the *majority* do not (Figs. 2.17b and 2.17c) and must represent first cycle detritus.

It is interesting to note that all of the colourless tourmalines in the UORS are anhedral, almost spherical, and a very distal or polycyclical origin is implied. These have not been observed in suites from LORS rocks of this study, although colourless euhedral varieties are found in the middle and upper parts of the LORS sequences as reported by Wilson (1971). The rounded colourless types persist to high levels in the UORS, where none of the coloured varieties is present.

Tourmaline Type	Colour	Composition	Occurrence
1) Granitic	Dark brown, green pink (green cast)	Fe ± Li	Late stage growth in large plutonic masses - euhedral crystals full of bubbles and cavities.
2) Pegmatitic	Blue, mauve, lavender	Na ± Li	Pegmatites and vein rocks - very large crystals occurring as angular fragments in detrital sediments. Inclusions rare.
3) Metamorphic	Pale - deep, brown, colourless	Mg, Fe	Metaquartzites, quartz schists. Inclusions rare. Similar to granite type.
4) Authigenic	Colourless, pale blue	Mg ± Ca, Na	Outgrowths at end of c-axis only. Generally small (5-10% of nucleus). Root zone.
5) Reworked sediment			All tourmalines become more concentrated relative to other less stable species.

Table 2.6. Tourmaline provenance classification after Krynine (1946).

A broadly similar tourmaline assemblage to that present in the UORS has been described for the Craigmaddie Sandstone Formation of Lower Carboniferous age in the Western Midland Valley (Tait 1973). Again, a slightly different nomenclature and classification has been used, but enough information is available to graphically compare percentages of varieties present in both units (Fig. 2.18). Comparison of the two assemblages reveals significant differences in composition especially with regard to spherical colourless varieties which are probably not present in the Lower Carboniferous suite.

Other notable features of the UORS tourmalines include: optically continuous authigenic overgrowths on both euhedral and rounded varieties (Figure 2.19) with pitting and etching of the nucleus at the root zone (fully described by Krynine 1946 p71); development of euhedral overgrowths on cores of dissimilar composition (colour) - where cores are large in relation to overgrowths (zoned crystals, see Fig. 2.20 and 2.21) it is the outer part of the grain (overgrowth) which determines the grain's colour class (Tait 1973); and bubble or mineral inclusions in the nucleus (Fig. 2.19, 2.20 and 2.21), but not observed in pink, colourless or blue varieties.

The provenance of the basal UORS tourmalines suite is problematic. Whilst a considerable quantity (20 - 30%) has probably been reworked from LORS rocks, the vast majority of coloured varieties must reflect input of new, first cycle detritus into the UORS basin in the Roseneath area. Tourmalines found at Wemyss Bay are compositionally restricted, typically brown and euhedral, while no tourmalines are found in similar amounts at Portencross.

A similar source to that which provided the LORS tourmalines is suggested, and on the evidence of Krynine (1946) this source was probably a mixed terrain of metamorphics, granites and possibly minor pegmatite or vein rocks. Certainly the euhedral varieties crystallised under high temperature metamorphic or plutonic igneous conditions. Zoned crystals and tourmalines with cores and overgrowths of different compositions might indicate growth during two metamorphic episodes (Tait 1973) or metamorphic overgrowths on detrital grains.

A metamorphic and granitic basement providing detritus to UORS and LORS basins is consistent with clasts found in the basal UORS conglomerates. However, an additional source might be required since heavy mineral

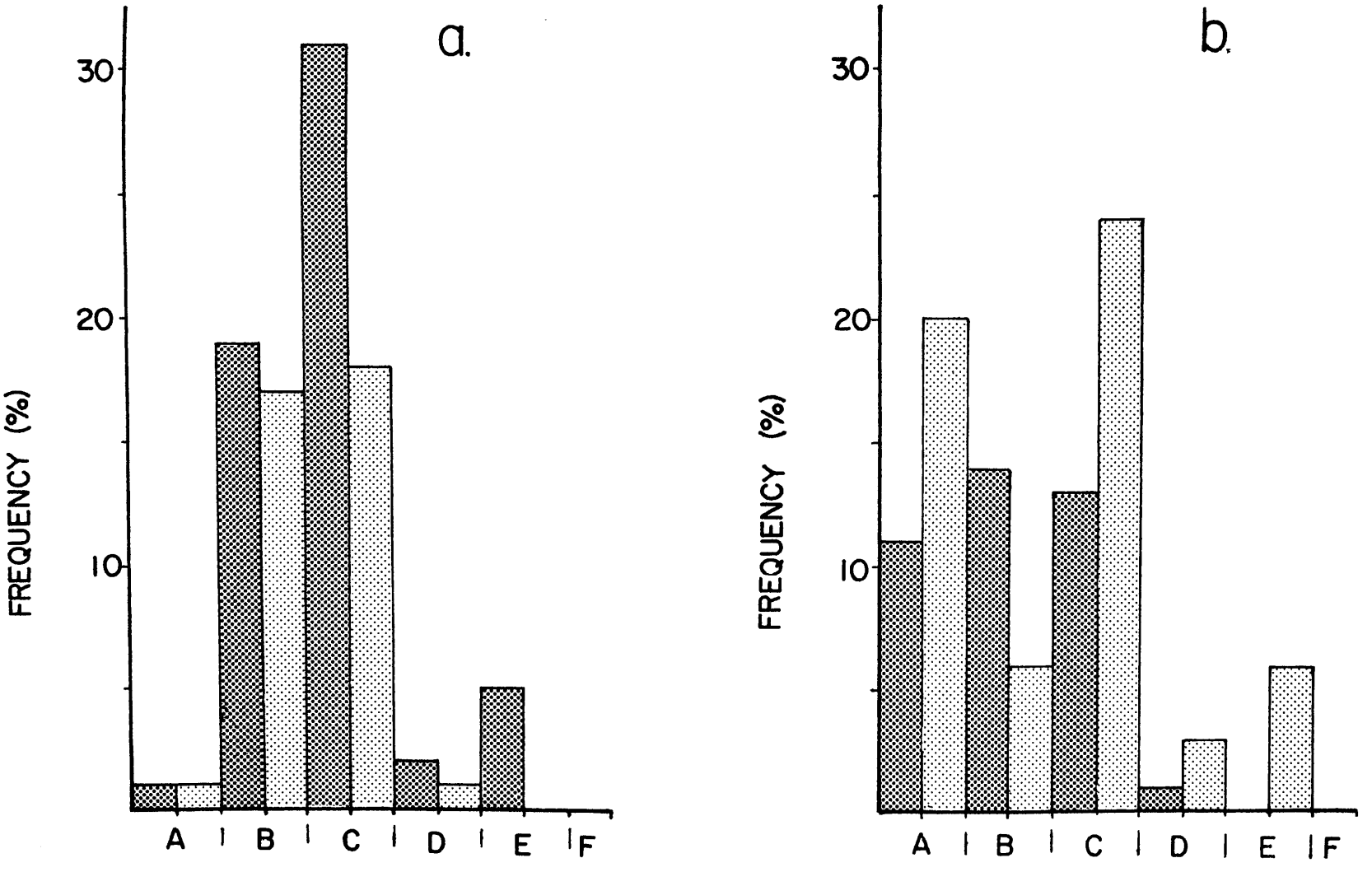

Fig 2.18. Comparison histograms of Tourmaline type from: a) Lower Carboniferous (Tait 1973) and; b) basal Upper ORS (this study). A colourless/light pink; B yellow/brown; C olive/yellow; D deep pink; E blue/turquoise/mauve; F black. Light and heavy stipple indicates presence or absence of inclusions for each variety respectively.

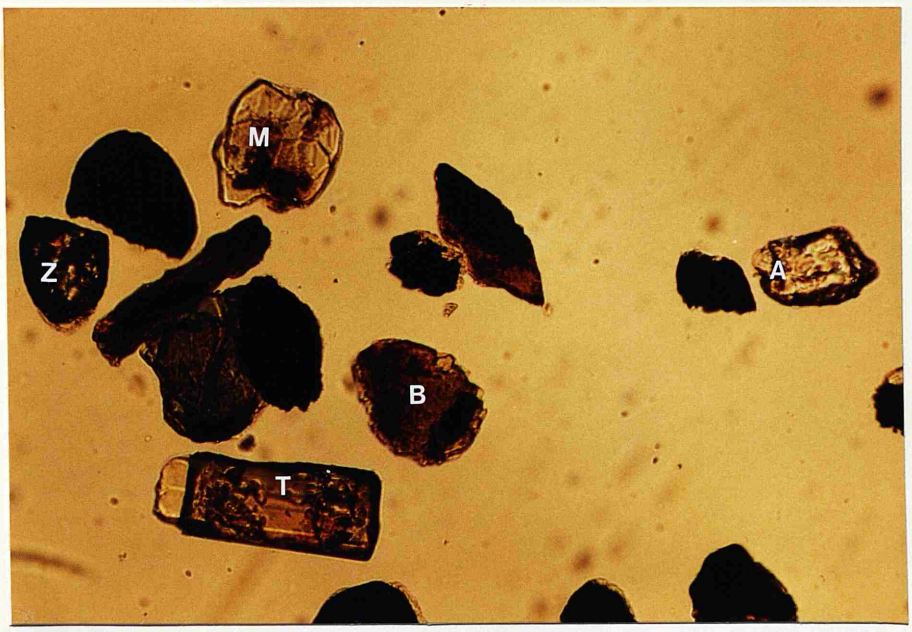

Fig 2.19. Grain mount photomic, PPL, X25.2. Sandstone heavy mineral separate, Roseneath. Euhedral yellow/brown tourmaline (T) with outgrowth and bubble inclusions. Highly rounded and broken zircon (Z); biotite flakes (B); muscovite flake (M) and; apatite (A).

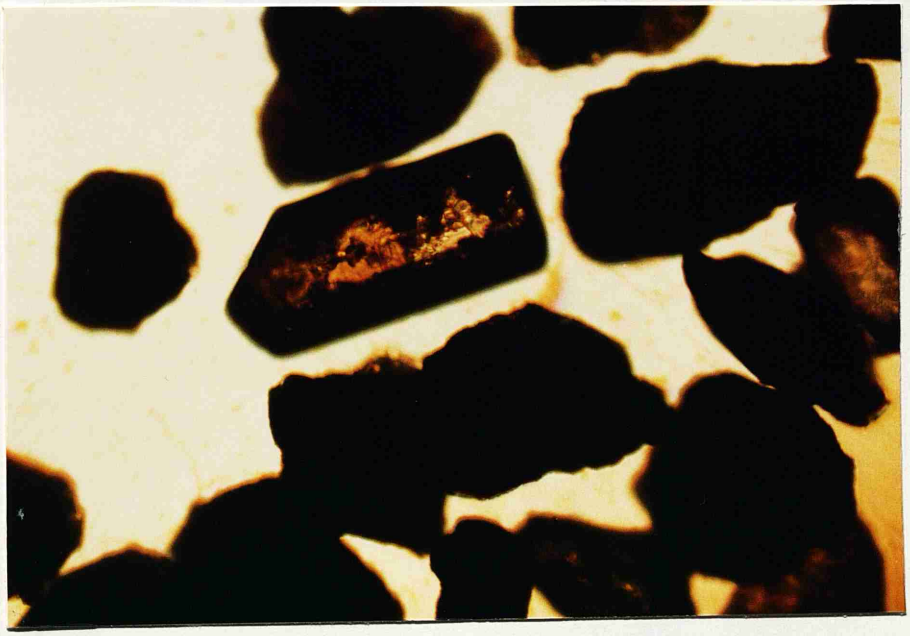

Fig 2.20. Grain mount photomic, PPL, X40. Sandstone heavy mineral separate, Roseneath. Euhedral zoned tourmaline grain. Overgrowth displays darker colour than nucleus.

Fig 2.21. Grain mount photomic, PPL, X25.2. Sandstone heavy mineral separate, Wemyss Bay. Euhedral zoned tourmaline grain. Overgrowth displays darker colour than nucleus.

separations performed on both granite and biotite schist clasts from Roseneath failed to produce tourmaline of sufficient variety to account for those in the sandstones. Indeed, although the presence of granitic tourmaline is indicated in the UORS, few of the Caledonian granites studied by Mackie (1928) contain any tourmaline at all, as is the case with the granitic clasts in the conglomerates at Roseneath.

Tait (1973) invoked a hybrid origin for Lower Carboniferous tourmalines in which an inherited assemblage of grains was derived from LORS and UORS and mixed with first cycle material from Dalradian metamorphic rocks. Euhedral tourmalines of similar type to those described for the UORS are certainly present in Dalradian metamorphic rocks of greenschist facies to the immediate north of Roseneath, and have been described by Tait (1973), Hill et al (1905), Kynaston and Hill (1908) and Chinner (1960).

Garnet

Each of the three areas of UORS contains a unique garnet suite. At Roseneath, large colourless garnets (Fig 2.22a) can provide up to 30% of the non-opaque heavy separate. At Wemyss Bay, smaller pink garnets (Fig 2.23) are very common (40 - 50% non-opaques), while at Portencross, tiny green garnets are found in small quantities (5% nonopaques).

At Roseneath and Wemyss Bay the garnets are relatively large, being concentrated in the 3 Phi seive fractions, and display etched and pitted surface textures (Figs. 2.22a,2.24 and 2.25). Pitted and faceted patterns on detrital garnets are well documented (Bramlette 1929, Smithson 1941, Rahmani 1973, Hemingway and Tamar-Agha 1975, Simpson 1976 and Gravenor 1979) and their origin has been variously ascribed to either chemical etching or new growth on a pre-existing nucleus. Gravenor and Leavitt (1981) have proved that both faceted surfaces and pits can be produced by synthetic etching in HF over a period of hours.

Like the tourmaline suite, it is difficult to provide a source for these garnets since garnet porphyroblast bearing schists are not widespread as conglomerate clasts. However, heavy mineral separation of biotite schist from the Roseneath conglomerates reveals that garnet growth was probably incipient in these rocks. Tiny colourless garnets found in the schists are probably compositionally equivalent to the larger detrital grains in the sandstones. At Wemyss Bay,

Fig 2.22. Grain mount photomic, PPL, X25.2. Sandstone heavy mineral separate, Roseneath. Abraded tan zircon (Z).

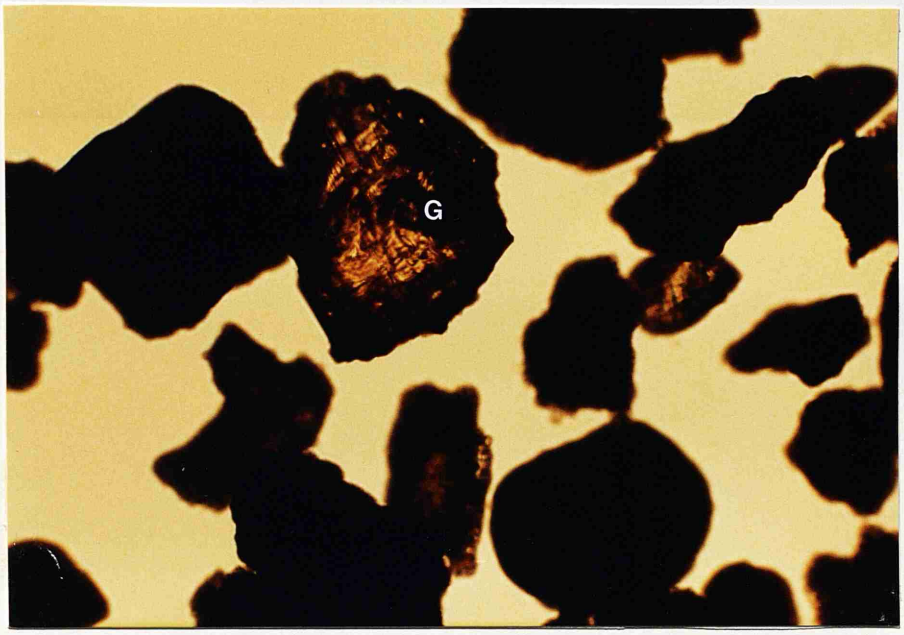

Fig 2.23. Grain mount photomic, PPL, X25.2. Sandstone heavy mineral separate, Wemyss Bay. Pink garnet (G) displaying faceted surfaces.

Fig 2.24. SEM photomic, 10um bars. Sandstone heavy mineral separate, Wemyss Bay. Garnet grain displaying faceted surfaces and pits.

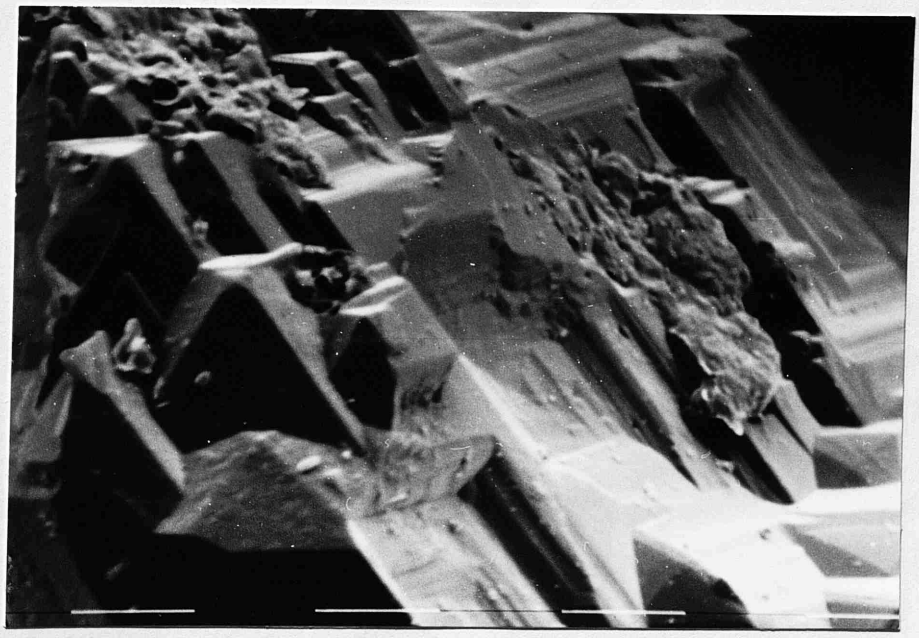

Fig 2.25. SEM photomic, 10um bars. Sandstone heavy mineral separate, Roseneath. Garnet grain displaying faceted surface.

a larger proportion of garnet is found in the non-opaque separate, and it is difficult to find a source for these in the metamorphic fragments of the conglomerates. These metamorphic rocks are of an even lower grade (chlorite) than those at Roseneath and the environmental conditions associated with their development would not facilitate garnet growth. The small green garnets obtained from the Portencross sandstones have been derived from the greywacke clasts in the conglomerates. These garnets do not appear fresh but do not display etched and pitted surfaces. The green cast in these grains indicates the presence of Fe or Cr and may be derived from a basic plutonic source.

Zircon

Zircons are ubiquitous at all levels in UORS sandstones of the western Midland Valley. In the basal parts three populations have been detected. Large purple zircons (Fig 2.28) and smaller colourless varieties dominate in the UORS and greywacke pebbles at Portencross and Wemyss Bay while small colourless and rounded tan (Fig 2.26) varieties occur at Roseneath. Generally, each does not occur to the exclusion of the other, and the Wemyss Bay and Roseneath sandstones contain representatives of all three types (colourless, tan and purple).

All three occur mainly in the 4 phi fraction and this appears to indicate that they are sorted during seiving according to width rather than elongation. They are commonly euhedral and rarely subhedral. Well rounded grains (obviously polycyclic) are not uncommon, though, but are usually confined to the tan and deep purple varieties.

Inclusions in the zircons are either mineral (probably rutile needles) or rounded inclusions of liquid or gas filled bubbles. It has been noted that the deeply coloured zircons often have opaque cores (Poldervaart 1956), but the purple zircons of this study commonly contain euhedral colourless/pale cores. Colourless varieties (including those separated from the granites) contain no inclusions, whereas the coloured zircons and more particularly the deeply coloured grains, are riddled with gaseous or liquid bubble inclusions.

It is generally considered that zircons are the most stable heavy mineral grains in clastic sediments (cf Pettijohn 1975). This means that a population will invariably represent a multi-source provenance. The variability of zircon

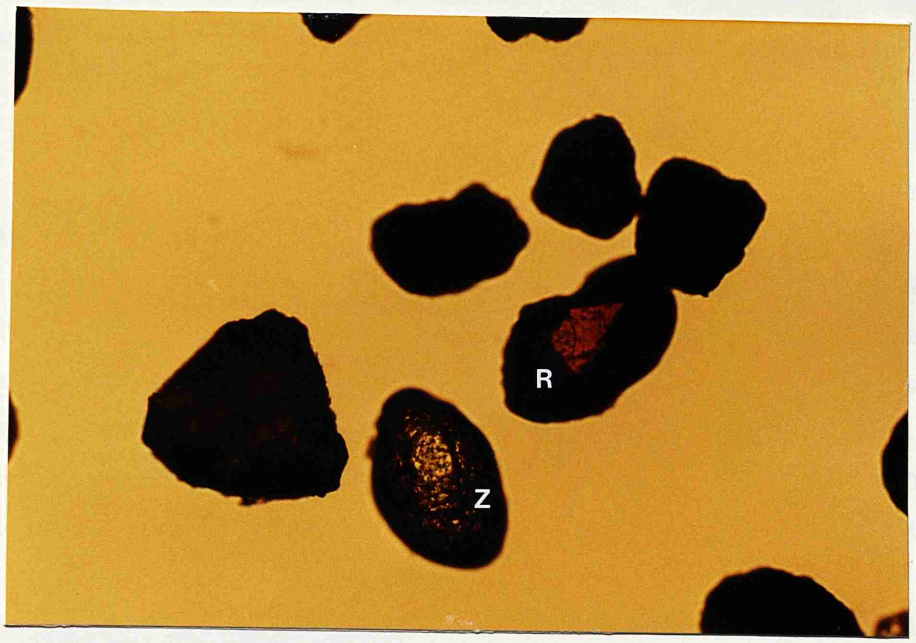

Fig 2.26. Grain mount photomic, PPL, X31.25. Sandstone heavy mineral separate, Roseneath. Abraded tan zircon (Z), rutile (R).

The variability of zircon populations has therefore received much attention. Heimlich et al (1975) discriminated between zircon populations on the basis of colour, rounding and elongation. Size analysis of zircon grains in the Wemyss Bay conglomerate was carried out in a similar manner to that described for the Sharon conglomerate (Heimlich et al 1975). The methods employed for this investigation are those described by Poldervaart (1955). 200 measurements were made of the maximum diameter for each grain encountered in a linear traverse. Broken grains are excluded in these measurements. Fig. 2.27 clearly displays a right-skewed bimodal distribution. This is a typical feature of transported zircons representing a mixture from two source regions (Poldervaart 1955).

Zircon is considered to primarily be of igneous origin (Deer et al 1977). However, a purely magmatic origin for zircons has been questioned in a controversial paper by Saxena (1966). He suggests that authigenesis in sediments and low-grade metamorphic rocks is not restricted to the formation of outgrowths, but in suitable environments, zircon can be completely formed by authigenesis in significant numbers. Although these authigenic zircons differ in morphological habit from magmatic zircons, they are difficult to distinguish in a reworked sediment. This has been dismissed by many authors (notably Kalsbeek 1967 and Marshall 1967), claiming that authigenic euhedral zircons probably only begin to develop after amphibolite facies has been achieved in the host rocks. Even under these conditions, authigenic zircons are confined to overgrowths on probably detrital cores formed under special metasomatic conditions (Taubeneck 1957 and Wyatt 1954).

The colour of zircons has frequently been used to characterise the provenance of sediments but more specifically to differentiate between granite intrusions. Heavy mineral separations from granite and schist clasts in the Roseneath conglomerate yield colourless and tan zircons (the latter from the schists) while colourless euhedral zircons have been recorded in Dalradian rocks (Teall, in Hill et al 1905). A source for the purple zircons is more difficult, but Mackie (undated manuscript) has attributed them to Lewisian rocks. Their occurrence in greywacke boulders at Portencross probably means that these are the immediate source for the UORS. The presence of purple zircons in the Silurian greywackes of the Southern Uplands (Mackie 1926) and in Ordovician greywackes from the Rhinns of Galloway (Kelling 1962) may suggest an origin for the greywacke pebbles.

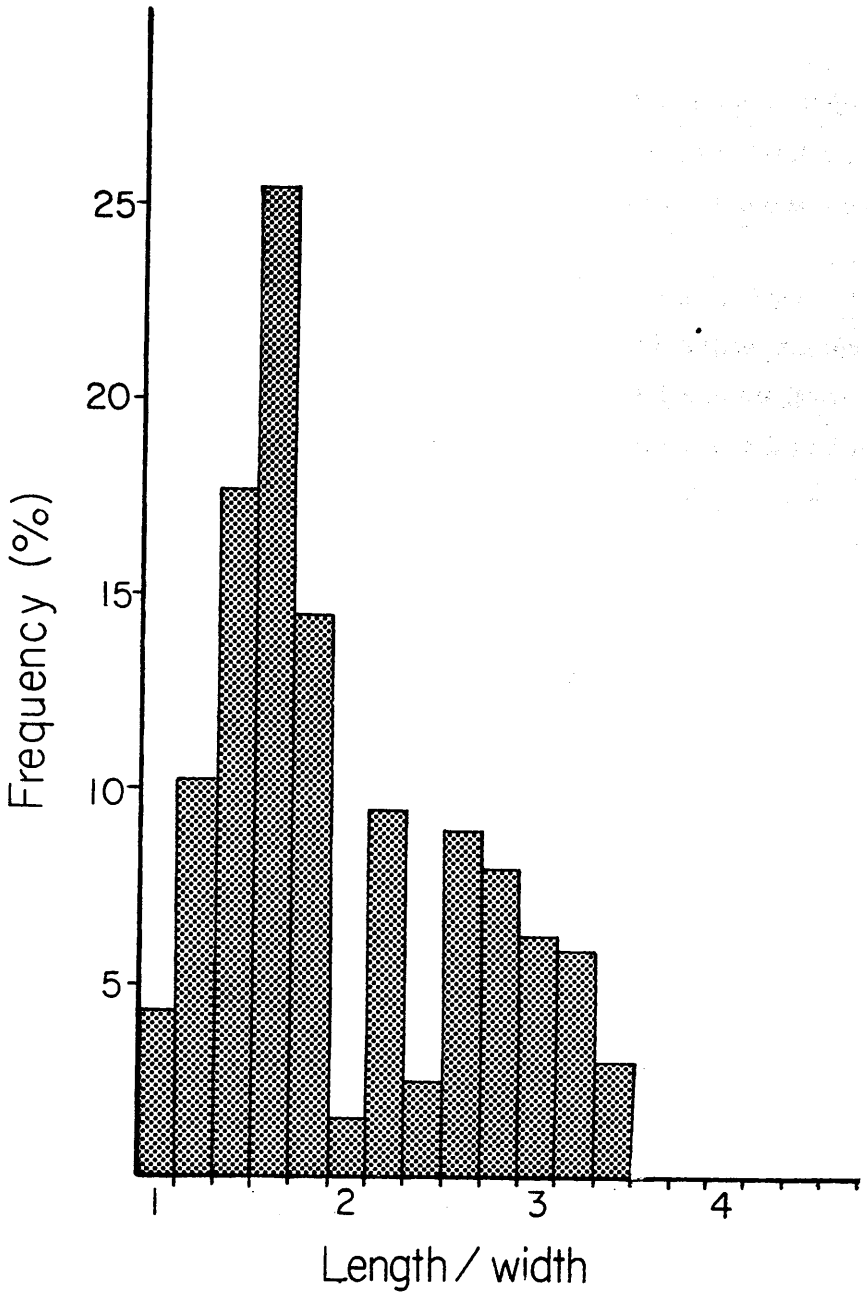

Fig 2.27. Zircon elongation histogram for basal Upper ORS at Roseneath.

Epidote

All three conglomerates contain epidote, but only at Portencross does it occur in significant quantities. It is found as large, well rounded grains in both sandstones and greywacke pebbles and displays pitted surfaces.

Epidote occurs principally in regionally metamorphosed basic rocks on the threshold of greenschist and epidote-amphibolite facies (Deer et al 1977). However, like purple zircon, the epidote has its *immediate* origins from the greywacke pebbles at Portencross. An ultimate origin for this mineral would be from a terrain similar to that found in Dalradian metasediments and volcanics around the region of Tayvallich in the Southwest Highlands or the variety of basic igneous and metamorphic rocks of the Ballantrae Complex of the Southern Midland Valley.

Rutile

Rutile is present in small quantities in each of the conglomerates investigated. These grains are only rarely rounded and commonly occur as small, euhedral, dark brown-red, twinned crystals of first cycle origin (Fig 2.26).

Heavy mineral separation of granite and schist clasts at Roseneath indicates that igneous and metamorphic clasts will provide an adequate source for these grains in the UORS.

Amphiboles

Amphiboles are present in small quantities in all three areas. Dissolution of mafic minerals (section 2.4) results in their scarcity in these rocks. Hornblende is the most common type and found as deep blue/green angular grains with a surprisingly fresh appearance.

The presence of glaucophane in heavy separates from Portencross and Roseneath is of particular interest. It is found in very small quantities (c.1%) as a highly pleochroic blue/violet platy mineral giving yellows or greens on rotation. Mackie (1928) reports the presence of glaucophane mainly in Silurian greywackes of Southern Scotland and indicates its presence in the UORS rocks at Heads of Ayr, Kilsyth and Auchenlea. It is also reported from Upper

Carboniferous sandstones in the Nith Valley. Floyd (1982) has indicated the abundance of glaucophane in the Ordovician flysch succession in the Southern Uplands. Mackie (1923) concluded that the Ben Ledi Grits (Dalradian) provided a detrital glaucophane source for the Silurian greywakces since these rocks at the time were the only known glaucophane bearing rocks in the vicinity of the Midland Valley. It is now also known that glaucophane schists are present in the Southern Midland Valley, within the Ballantrae Complex.

Other Heavy Minerals

Apatite is pervasive, especially in the sandstones in the northernmost conglomerates (Wemyss Bay and Roseneath). Medium sized and highly rounded grains are typical but this is not necessarily suggestive of a polycyclic origin due to its unstable nature. Acid clasts in the Roseneath conglomerate contain large amounts of apatite and may have contributed a large quantity of the mineral to the UORS. It has not been reported from the LORS (Wilson 1971), but is present in the basal part of the overlying Lower Carboniferous strata (Tait 1973). This is interpreted as indicating the increasing importance of granite in the source area after LORS deposition.

Micaceous minerals in the heavy residues are directly related to the metamorphic grade of the detritus in the conglomerates. Therefore at Portencross and Wemyss Bay, where greenschist facies dominates, many flakes of chlorite are observed. Biotite and muscovite are present to the exclusion of chlorite at Roseneath, where the metamorphic clasts are obviously approaching garnet grade.

Purely authigenic minerals are not well represented in these rocks. Less than 1% anatase is recorded and occurs as euhedral non-pleochroic yellow crystals (Fig 2.28).

Zircon-Tourmaline-Rutile Index

The concept of maturity in sandstones has received much attention and led Hubert (1962) to devise an index of maturity based on heavy mineral assemblages. The proposed zircon-tourmaline-rutile (ZTR) index is defined

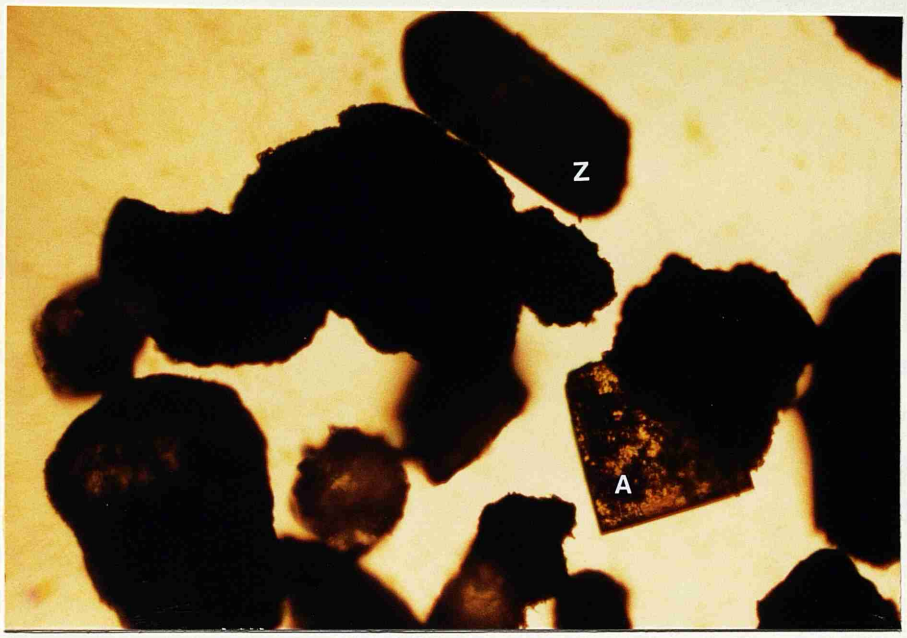

Fig 2.28. Grain mount photomic, PPL, X40. Sandstone heavy mineral separate, Wemyss Bay. Euhedral anatase (A). Subhedral purple zircon (Z).

as the percentage of combined zircon, tourmaline and rutile among the transparent, non-micaceous heavy residue:

$$ZTR = \frac{\text{zircon + tourmaline + rutile}}{\text{(total non-opaque heavy) - mica}}$$

Hubert (1962) discovered that the ZTR index was low in immature sediments (greywackes) and increased through transitional feldspathic and micaceous quartzose sandstones with an associated increase in quartz, chert and metaquartzite rock fragments to exceed 90% in most orthoquartzite sandstones.

Approximate ZTR indices determined for the basal UORS are obviously intermediate for the Wemyss Bay and Roseneath sandstones (c. 40 - 45%). At Portencross, however, low ZTR values are encountered (c. 25 - 30%) and must be associated with a heavy mineral suite derived largely from a primary source or perhaps minor reworking of Silurian or Ordovician greywacke.

The observed upward progression towards a homogeneous heavy mineral suite is also reflected in the ZTR index. In all 7 samples of late UORS analysed, ZTR values are high (c. 70 - 80%). Additionally, heavy residues from red/brown sandstone clasts (?LORS) at Portencross and Wemyss Bay also have high ZTR values. At Roseneath, sandstone cobbles contain a similar assemblage to that described by Wilson (1971) for the LORS in that area.

2.4 Diagenesis

Based on the textural relationship of grains and diagenetic features in thin section, and with the aid of XRD and SEM techniques, it is possible to interpret the relative sequence of diagenetic events in sandstones of the three basal conglomerates.

Sandstones from all three areas contain an essentially similar and time related diagenetic history which may be represented graphically. Fig. 2.29 is a schematic flow diagram showing the interpreted diagenetic sequence based on detailed analysis of the Wemyss Bay sandstones, which display the most completely presented diagenetic sequence and in which transitions from one event to the next are most easily determined. Portencross and Roseneath sandstones deviate from this path only insofar as a particular event may be locally absent or developed to a differing degree. The time order of events is always the same.

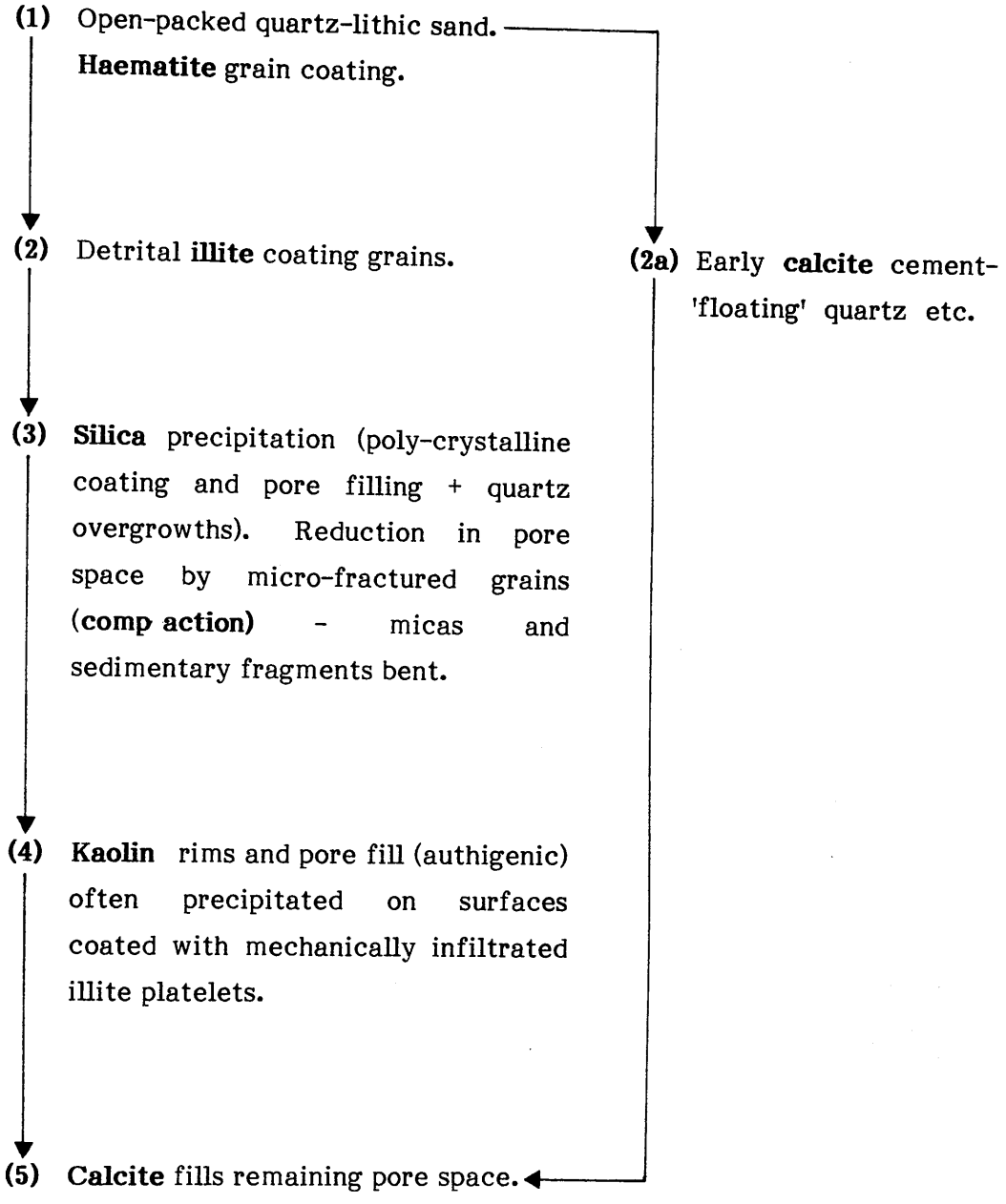

Fig 2.29. Flow diagram showing sequence of diagenetic events in the basal Upper ORS.

Observed Diagenetic Features

Six stages can be recognised:

Stage 1: Red-brown iron oxide grain coating cement formed very early in the burial history of the sandstones (Figs. 2.11, 2.12 and 2.13). Early formation of this cement in a loosely consolidated sand is indicated by:

i) The early coating of intergranular areas which subsequently underwent significant compaction.

ii) The absence of other (earlier) types of cementation or grain alteration in the sandstones that are thoroughly coated by iron oxide.

Stage 2: With slightly deeper burial, circulating pore solutions at times deposited carbonates but mainly coated the still uncompacted grains with detrital illite (Figs. 2.4a, 2.30 and 2.31).

Galloway (1974, 1979) was able to distinguish between clay 'coats' deposited as detrital minerals and clay 'rims' precipitated from solution, by the orientation of the clay flakes with respect to the surrounding framework. Clay rims are defined as flakes which are oriented perpendicular to the substrate, whilst clay coats are flakes which are either randomly orientated or parallel to the substrate. Although this distinction has subsequently been questioned by many authors (e.g. Burns and Ethridge 1979) it is clearly made here. Fairly large, highly birefringent illite grains lie tangentially on framework grains and separated from the latter by Stage 1 iron oxide coatings. A pre-compaction age for this coating is based on similar criteria to those for Stage 1. Especially important is the occurrence of illite flakes preserved in the contact zones of grains which are now firmly interlocked (Fig. 2.4a).

Carbonate deposited at this time takes the form of locally developed large calcite crystals commonly poikilotopically enclosing 'floating' framework grains (Fig 2.46,2.32) which often retain their iron oxide coatings. This early carbonate cement and pore fill frequently corrodes the silicate framework and is itself subject to dissolution at a later stage producing secondary porosity.

Stage 3: As depth of burial increased, compaction took place reducing porosity either by microfracturing siliceous grains (Fig. 2.33,2.34,2.35) or to a greater extent by compressing mica flakes and lithic fragments (Figs. 2.13 and 2.36). Thus compaction attains a higher degree of development in the Portencross sediments where sedimentary detritus forms a larger proportion of lithic fragments than in other areas (See Section 2.5.3). At Roseneath and more especially at Wemyss Bay, stress is released through fractures in quartz, feldspar, volcanoclastic and more siliceous metamorphic grains.

Authigenic silica precipitation began at about the same time as the onset of compaction or slightly earlier. Silica cement is present only in minor amounts in any sandstone and its restricted occurrence may be due to the abundance of clay accumulated at this time. It appears primarily in the form of microcrystalline aggregates (Fig. 2.14), mainly filling pore spaces but also occurs as rims to siliceous grains which it appears to be replacing. Crystalline quartz overgrowths are present in all sandstones but not at any significant levels. It is probably a pre-compactional feature as evidenced by compaction fractures in euhedral quartz grains (Figs. 2.34 and 2.35). Occassionally, when clay content is locally low, overgrowths reduce pore space and growth culminates with characteristic triple-point junctions. Pressure solution textures or highly sutured grain boundaries were not observed.

Stage 4: Authigenic kaolinite laths are found lining remaining pore spaces as compaction proceeds. These flakes are clearly rims as defined by Galloway (1974), radiating outwards from the substrate (Fig. 2.33). Further kaolinite precipitation resulted in pore filling by coarser well-formed booklets of clay (Fig. 2.30). This stage did not, however, develop at Portencross, where excessive development of Stage 2 illite can be seen filling pores.

Stage 5: The final phase of pore fill cement is carbonate. Precipitation of calcite is again patchy in distribution and may have been initiated by growth of Stage 2 carbonate or on small grains of calcite present in the framework.

This stage is charaterised by replacement features. Often, authigenic kaolinite pore fill has been consumed by calcite growth and a fibrous network may be seen within certain carbonate grains. It is also common for calcite

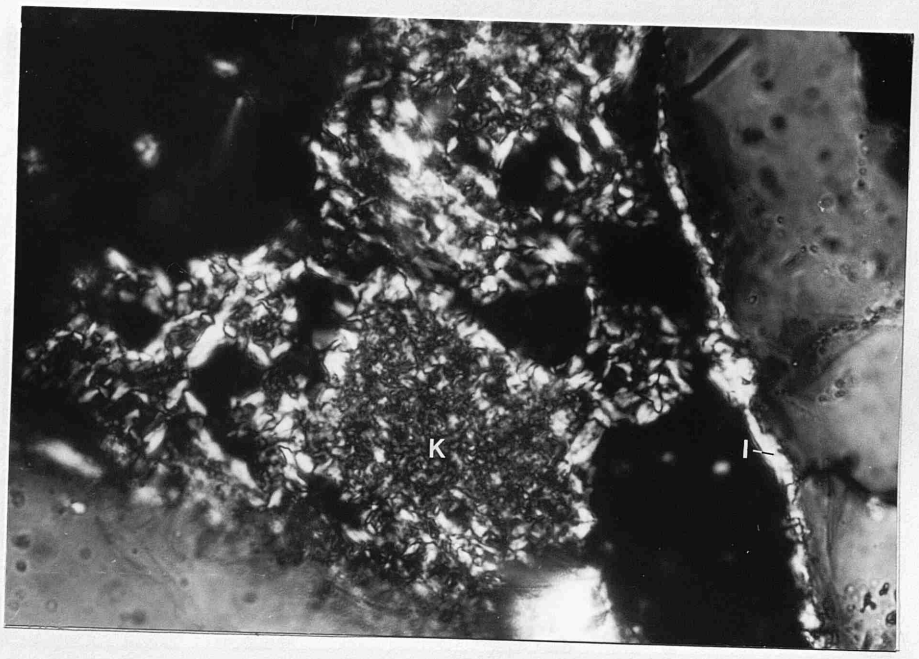

Fig 2.30. TS photomic, XPL, X160. Sandstone, Wemyss Bay. Stage 2 detrital illite (I) lines pores by coating uncompacted grains. Stage 4 authigenic kaolinite (K) fills pore space.

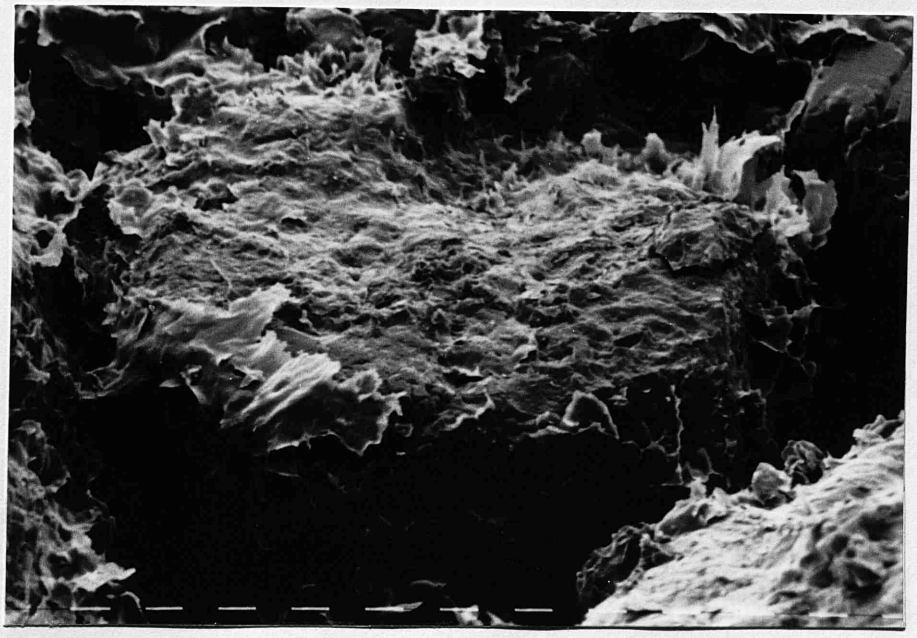

Fig 2.31. SEM photomic, 50um bars. Sandstone, Wemyss Bay. Stage 2 illite coat on detrital grain.

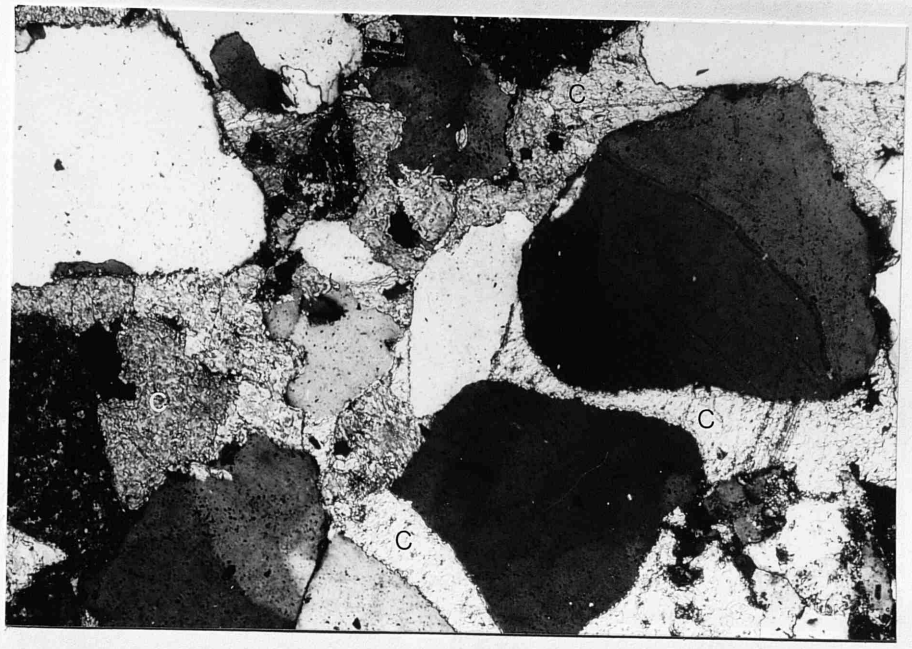

Fig 2.32. TS photomic, XPL, X40. Sandstone, Roseneath. Calcium carbonate (C) poikilotopically enclosing and corroding 'floating' framework grains.

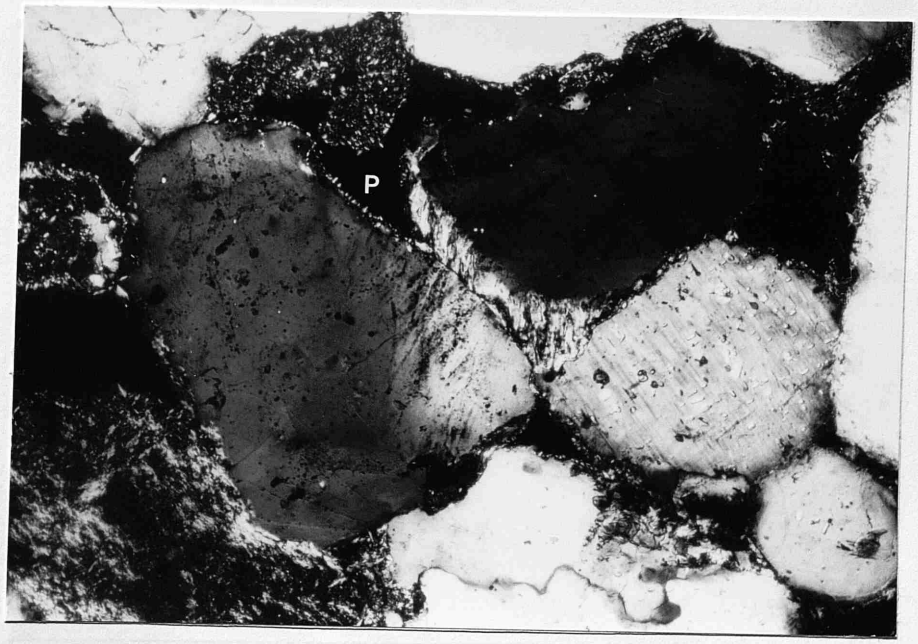

Fig 2.33. TS photomic, XPL, X40. Sandstone, Roseneath. Micro-fracturing of quartz grains. Authigenic clay rims radiating outwards from substrate in pore space (P).

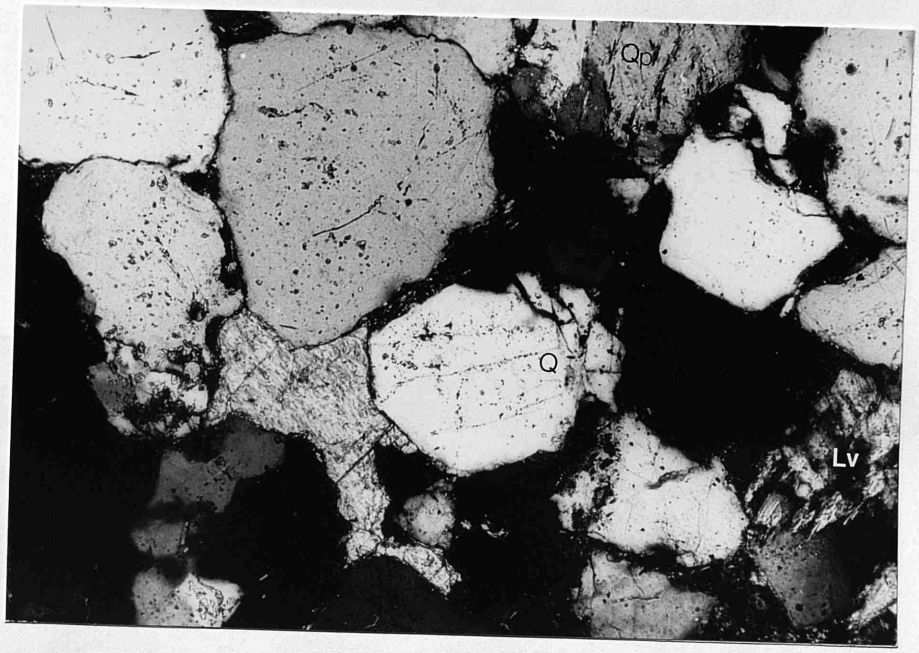

Fig 2.34. TS photomic, XPL, X40. Sandstone, Roseneath. Micro-fracturing of euhedral overgrowth on quartz grain (Q). Silicified igneous clast (LV). Mica fabric in meta-morphic polycrystalline quartz grain (Qp).

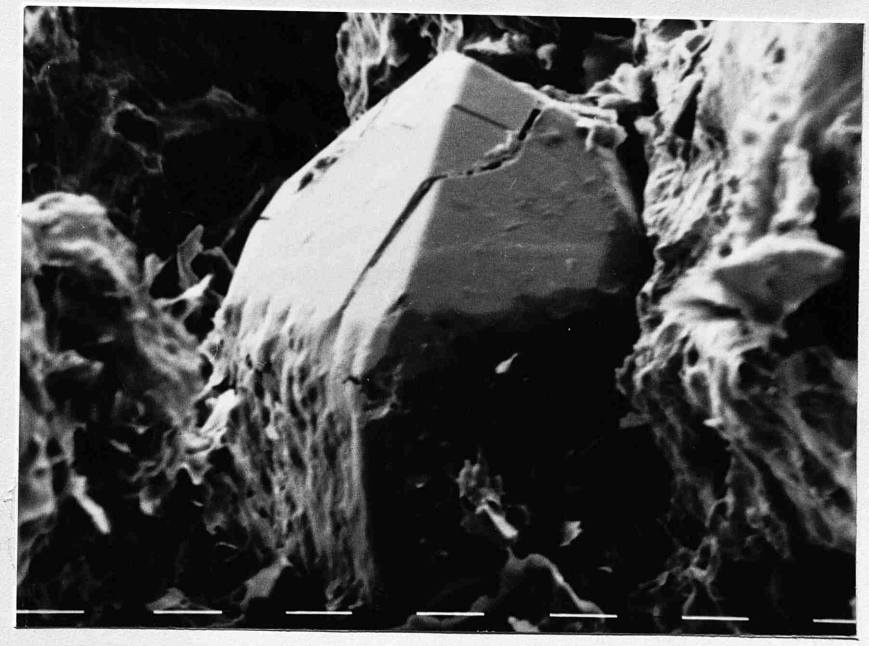

Fig 2.35. SEM photomic, 50um bars. Sandstone Roseneath. Micro-fracturing of euhedral overgrowth on detrital quartz grain. Large rhombohedral face indicating preferential growth at the distal end of the detrital grain c-axis.

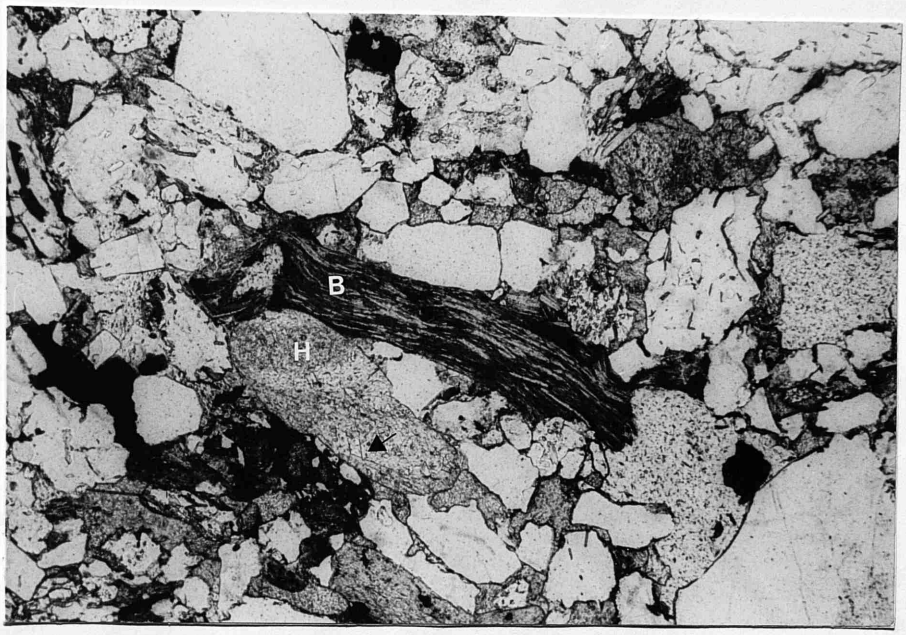

Fig 2.36. TS photomic, PPL, X10. Sandstone, Roseneath. Plastic deformation of biotite flake (B). Detrital amphibole grain (H) now entirely replaced by carbonate but retaining iron oxide ghost outline and cleavages (arrow).

to attack silicate minerals (Fig 2.4b, 2.32) leaving ghost outlines of the original grains (Figs. 2.37). In a few instances, the carbonate cement encloses poikilotopically uncompacted clastic silicate grains which may or may not post-date silica precipitation (overgrowths). Occassionally euhedral quartzes 'float' in the matrix carbonate. If these crystals are not corroded and display reasonable crystal faces then the carbonate is obviously late stage (see section 2.4.2).

The textures of Stage 5 carbonate pore filling cement suggest both phreatic and vadose environments of cementation, in the sense of Land (1970). Fine micrite rims seem to line pore spaces before main phase sparite (Fig. 2.15). These micrite linings have been interpreted as vadose precursors to phreatic calcite precipitation (Stalder 1975).

Subsequent solution of calcite has resulted in minor amounts of secondary porosity (Fig 2.38).

2.4.2 Factors Controlling Diagenesis

At the time of their deposition and initial burial, these coarse to medium grained sands must have had a moderate porosity. By removal of diagenetic effects, this porosity ranged from 21 - 25%. The net effects of diagenesis in the sandstones are the large scale reduction of primary porosity and minor development of secondary porespace. The processes involved may be divided into three broad categories: cementation and pore filling events; compaction features and replacement; and decementation features.

Cements and Pore Fills

From the previous discussion, up to 6 stages of cement are present in the UORS sandstones: iron oxide; silica; phyllosilicate (3 episodes); and calcite (2 episodes). These include both chemically and mechanically precipitated materials.

Iron Oxide: By analogy to modern deserts, it is generally agreed that the grains are not red when deposited, but redden with time as the sediments are buried below the water table. The alteration of ferromagnesian silicates has been shown to produce this red pigment (Walker 1967, 1974, 1976, Walker et al 1967, Van Houten 1968 and Walker et al 1978). A similar mechanism

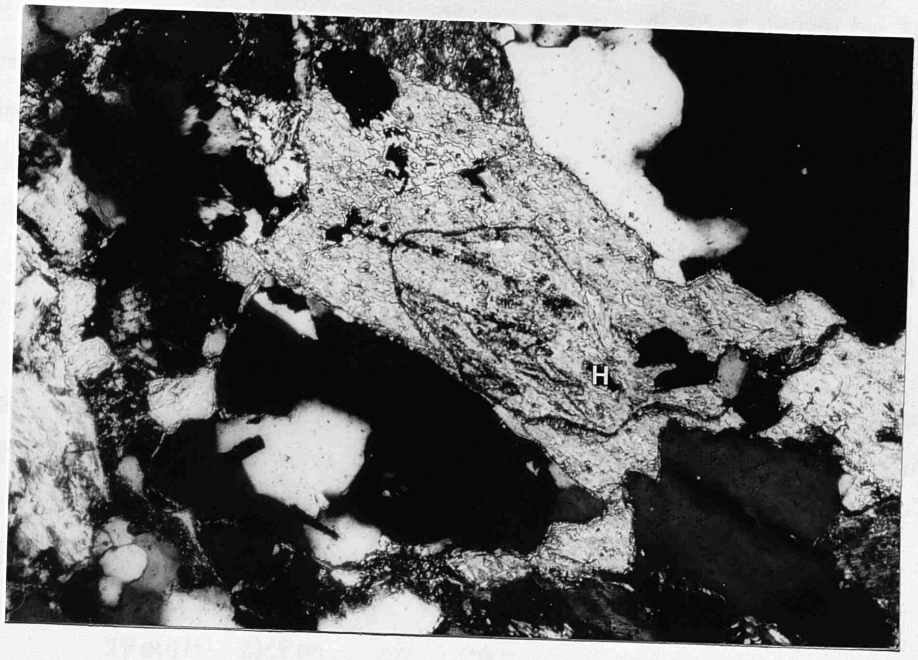

Fig 2.37. TS photomic, XPL, X40. Sandstone, Roseneath. Detrital amphibole grain (H) now entirely replaced by carbonate but retaining iron oxide ghost outline and cleavages.

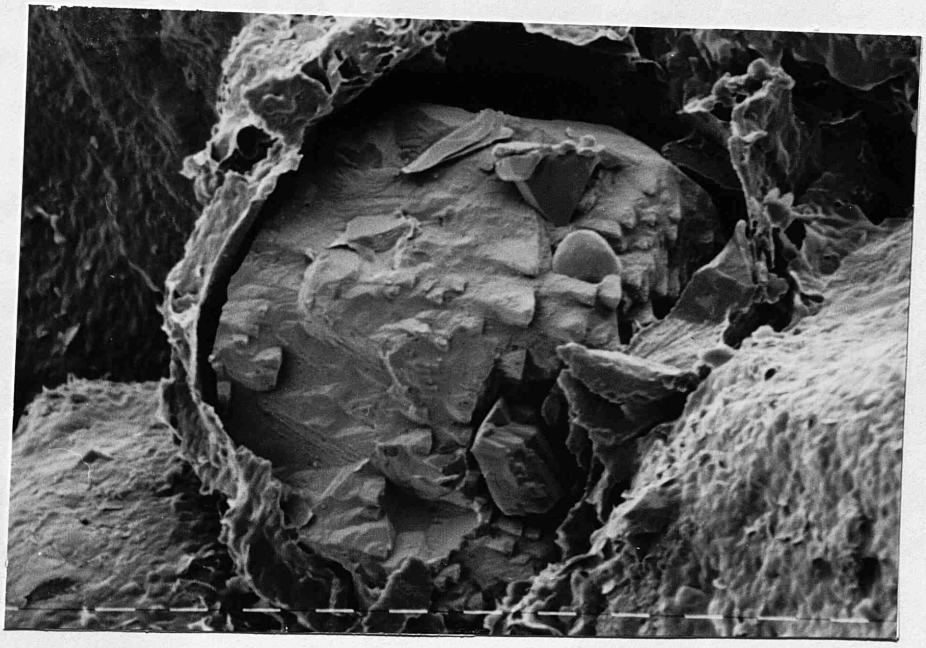

Fig 2.38. SEM photomic, 50um bars. Sandstone, Wemyss Bay. Dissolution of carbonate pore fill resulting in secondary porosity within detrital clay pore lining.

has been invoked for the Old Red Sandstone of the Midland Valley by Jawad Ali and Braithwaite (1977). They saw the in situ breakdown of mafic minerals (particularly pyroxenes, amphiboles and biotite) as producing the red colouration of the sediments and high levels of haematite. This view must be accepted in this study, where pyroxenes and amphiboles are now conspicuously absent from the sands. Where they do occur, however, the grains appear relatively fresh with little evidence of weathering.

Under favourable conditions of pH and Eh (7 - 14 and 0 - 0.6 respectively), iron passes into solution and rapidly reprecipitates locally as ferric hydroxide or oxide due to high Press 0_2 at the Earth's surface. A simplified reaction for this process has been put forward by Walker (1967):

$$2Fe(0H)_3\ 2HFe0_2 + 2H_20\ Fe_20\ Fe_20_3 + 3H_20$$

One million years is considered an adequate time to form the largest part of the red pigment (Blatt 1979).

Although the reddish-brown colour is common in the UORS, thin bands, lenses and spherical patches of green or grey-green sand are not uncommon and must be associated with locally developed reducing conditions. Identical spots have recently been reported from clastic sediments of Upper Proterozoic age in Sweden (Morad 1983). These patches may be either secondary, where ferric iron alters to the soluble green ferrous state during flushing (Glennie et al 1978) or due to the isolated occurrence of carbonaceous material as suggested by Sherlock (1947) and Trotter (1953). Due to the patchy development of this discolouration, the second alternative is favoured. In this process, organic matter would provide a source of acidic formation water formed by the release of CO_2 during the process of compaction and diagenesis.

Clay Minerals: Walker et al (1978) concluded that most coarse grained desert alluvium is essentially free of interstitial clay when originally deposited due to highly efficient stream sorting.

Clay minerals in these UORS sandstones are both detrital and authigenic in origin as determined by XRD, SEM and optical techniques. Relative proportions of each cannot be accurately determined since quantitive assessment of XRD analysis is of uncertain accuracy. However, what is

clear from thin section studies is that detrital illite occurs to the exclusion of authigenic kaolinite in the Portencross sandstones. At Wemyss Bay and Roseneath Point, a major phase of detrital illite preceeds a major pore filling phase of authigenic kaolinite (Stage 4). At the same time, XRD investigations (methods described in Appendix I) indicate illite crystallinity to be poor in all three areas of UORS and good in the underlying LORS and in sandstone boulders of presumed LORS affinity within the conglomerates.

It is difficult to invoke a mechanism which would result in this lack of correlation of clay mineralogies in the most southerly conglomerate with the other two exposures of basal conglomerate in what is by any standards a relatively small depositional basin. According to Blatt (1979), kaolinite precipitation requires circulating pore waters of meteoric origin where the value of log $(Na^+/H^+)^2$ cannot exceed 13 and the value of log $(K^+/H^+)^2$ cannot exceed 20. Values in excess of these would result in precipitation of illite or montmorillonite. Average river water values are 8 and 5 respectively, whereas sea water contents are 10^8 and 10^6. The required silica and aluminium for authigenic clay formation may be brought in by circulating waters or derived by the breakdown of aluminium silicates (feldspars) during weathering. Breakdown of heavy minerals can provide the cations in a similar fashion to the release of iron discussed previously. Since both stages of illite are clearly mechanical in origin, locally supersaturated meteoric waters (with respect to Na^+ and K^+) at Portencross can be disregarded as a buffer to kaolinite precipitation.

The chemistry of pore fluids cannot be analysed, and in any case, temporal changes in composition would be expected during extended burial. Variation in concentration of dissolved ionic species and pressure of CO_2, Eh and pH must exist but there appears to be no reason to suspect that thick sequences of sands should experience greatly disparate bulk geochemical conditions unless there are radical differences in sandstone composition.

Examination of the LvLmLs triangular diagram (Fig. 2.2d) indicates that each conglomerate sandstone unit has its own distinctive population of lithic fragments. However, Wemyss Bay and Roseneath each has a larger proportion of volcanic and igneous fragments than Portencross, where low grade metasedimentary and sedimentary fragments predominate. Conditions may therefore have been more conducive to kaolinite precipitation in the northern parts of this basin where presumably feldspar grains provided the raw material for authigenic clay.

The occurrence of detrital clay is thought to be concentrated above beds that have low permeability and therefore have served as barriers to downward migration of pore fluids. This type of clay is particularly abundant in deposits located at the proximal end of alluvial fans, where sediments are coarsest grained and recharge is most frequent (Walker et al 1978). The anomalous clay content of the Portencross sandstones may therefore either be explained by the differing composition of the sediments or by their geographical position on the fan.

Silica: Precipitation of quartz in all three areas can be pre-, post- and presumably syncompactional. It is not developed to any great degree, which is surprising since a paucity of silica crystallisation is normally a characteristic of very immature sediments. These rocks, whilst admittedly containing large quantities of lithic fragments, still contain a significant proportion of siliceous detrital grains which would serve both as a source of dissolved silica and as a substrate for precipitated silica. Lack of significant amounts of secondary quartz is probably due in part to thick Stage 2 illite coats resulting in the inability of quartz to seed on grain surfaces (Pittman and Lumsden 1968; Hawkins 1978).

Two forms of silica precipitation may be observed : monocrystalline quartz overgrowths and microcrystalline rims and porefills.

No evidence for pressure solution can be found and it seems that the silica for authigenic monocrystalline quartz has been brought in by pore fluids or has arisen from the breakdown of feldspars.

The origin of microcrystalline authigenic quartz is more difficult to explain, as has been noted by Hathaway (1970). Hawkins (1978) attributed microcrystalline silica to two primary sources : dissolution of sponge spicules present in an overlying sandstone, and alteration and devitrification of tuffaceous fragments. Although the first mechanism is certainly not a candidate for silica generation in the UORS, silica released to solution by alteration of volcanic ash might be a significant contributor.

Silica in solution may additionally reprecipitate with aluminium and potassium forming authigenic overgrowths of potassium feldspar. This was initially identified by interpretation of XRD traces (section 2.3.2) and is difficult to identify optically.

Carbonate: Calcite was introduced in variable amounts and at various stages as authigenic cement. Together with clay, these minerals are generally the most common causes of induration of the deposits. This variable temporal occurrence of calcite cement is commonly described for ancient sandstones, based on compactional relationships, tectonic considerations and hydraulic gradients produced by uplifts whose dates are known (Todd 1963, Wright 1964, Warner 1965, Stalder 1975 and Mankiewicz and Steidmann 1979). These studies seem to indicate that calcitic cementation occurred when the sands were at or near the surface, and is usually the latest cement in many sandstones.

The geochemistry of calcium carbonate precipitation has considerable complexity and is summarised by Blatt (1979). Essentially, precipitation depends upon increasing the (Ca^{2+}) $(C0^{2-})$ product in pore water by a rise in the pH of the environment, probably due to an increase in temperature (Bucke and Mankin 1971). The ease of precipitating calcite cement in sandstones increases with burial depth because calcite solubility decreases with increasing temperature. This explains why calcium carbonate is an important phase long after compaction and precipitation of other cements.

Compactional Features

Microfracturing of clastic grains is most conspicuous in the sandstones at Wemyss Bay and Roseneath Point. In these northern conglomerates, plagioclase feldspars are particularly affected, having inherent weaknesses along cleavage planes. Displaced twin planes are common.

Investigation of the microfractures in quartz grains reveals that conchoidal or straight fractures predominate and may be observed to terminate at grain/grain point contacts. At grain boundaries these fractures are often covered with a layer of Stage 4 kaolinite but are never infilled with calcite. Trails of liquid or gaseous inclusions can also be seen and may represent infilled and healed fractures but are probably post-depositional.

At Portencross, plastic flow is more important than brittle fracturing due to the higher content of sedimentary lithic material.

Replacement and Dissolution

Both stages of calcite accumulation can be observed to be a replacive cement in these sandstones. Replacive is used in a descriptive sense and not genetically: the calcite now occupies an area once occupied by quartz.

The dissolution of quartz during diagenesis was considered by Hurst (1981) to be a selective process, the variable location of which on grain surfaces is controlled by the surface energy characteristics of the individual grains. Experimental work carried out by Hurst (1981) indicates that a hierarchy of grain surface characteristics exists directly relating to the relative rates of dissolution during decomposition. This has been tabulated in Table 2.7. The numbering implies that if more than one surface characteristic is present on a grain, then the part with the highest scale number will be preferentially dissolved when etched. Also, in the case of two pores in the same sandstone with identical pore fluids, the pore with the highest average scale number for quartz faces at the pore boundary will be preferentially corroded and therefore enlarged. The situation is more complex if minerals other than quartz are present. Feldspars, for example, show that the presence of cleavages and twin planes are of greater importance than surface characteristics are for quartz.

However, this specific scale holds true for the UORS sediments. It is probably no coincidence that a large number of 'floating' quartz grains within Stage 2 and Stage 5 calcite porefills display well developed crystal faces.

2.5 Sandstone Texture

In order to investigate the textural nature of the sandstones, 8 thin sections were selected from each area (Roseneath, Wemyss Bay and Portencross) and determinations were made for the following parameters: grainsize; elongation and rounding; packing density; and packing proximity. The results of this investigation are displayed in Table 2.8.

2.5.1 Grain Size Analysis

For each thin section, the long axes of 200 quartz grains were measured with a calibrated eyepiece. Grains were selected in the same manner as for compositional analysis but without employing a minimum size cut-off.

Scale	Surface Characteristics
1	Low index faces
2	High index faces
3	Face edges
4	Junctions between edges
5	Faceted areas
6	Dissolution/replacement surfaces
7	Abraded surfaces
8	Fractures
9	Disturbed surface layers

Table 2.7. Relative rates of dissolution for 9 types of grain surface characteristic. From Hurst (1981).

AREA	SAMPLE	SIZE $\bar{x}$	SIZE σ	ELONG $\bar{x}$	ELONG σ	Pd $\bar{x}$	Pd σ	Pp $\bar{x}$	Pp σ	LITH %
Roseneath	DGD01	0.20	0.07	0.60	0.16	77.70	9.20	54.10	9.20	18
	DGD02	0.18	0.07	0.66	0.17	69.10	7.40	54.70	8.60	16
	DGD03	0.20	0.12	0.72	0.17	75.20	4.40	36.30	5.90	16
	DGD04	0.18	0.08	0.69	0.16	70.00	3.70	41.60	5.30	19
	DGD05	0.20	0.08	0.67	0.15	72.40	7.10	37.50	7.30	17
	DGD07	0.29	0.18	0.69	0.17	82.20	5.70	56.00	6.70	14
	DGD09	0.43	0.25	0.71	0.13	88.90	5.40	60.70	5.70	23
	DGD11	0.44	0.32	0.67	0.16	83.60	7.40	67.20	8.60	20
	Pop $\bar{x}$	0.27	0.15	0.68	0.16	77.40	6.30	51.00	7.20	17.9
Wemyss Bay	WBS01	0.22	0.10	0.69	0.18	75.50	6.60	50.20	2.80	32
	WBS02	0.24	0.16	0.66	0.17	78.10	6.30	62.60	11.30	38
	WBS04	0.25	0.15	0.70	0.17	77.20	6.00	61.40	4.60	49
	WBS06	0.42	0.20	0.67	0.14	91.20	7.10	67.80	5.10	44
	WBS07	0.23	0.14	0.71	0.14	71.80	4.20	50.50	8.00	34
	WBS08	0.21	0.11	0.63	0.13	65.30	6.90	33.40	4.80	26
	WBS09	0.20	0.09	0.62	0.19	73.10	8.60	59.90	5.80	34
	WBS12	0.22	0.12	0.62	0.16	68.30	5.30	41.30	3.10	31
	Pop $\bar{x}$	0.25	0.13	0.67	0.16	75.10	6.40	53.40	5.70	36.0
Portencross	DGP01	0.22	0.16	0.64	0.14	78.10	7.50	52.70	6.60	44
	DGP04	0.38	0.23	0.62	0.13	91.40	8.70	71.10	8.30	47
	DGP05	0.26	0.15	0.66	0.17	64.30	8.60	54.20	12.10	29
	DGP07	0.20	0.10	0.65	0.14	73.40	8.20	32.80	4.60	47
	DGP09	0.24	0.15	0.63	0.17	79.60	9.40	58.30	7.80	25
	DGP10	0.31	0.16	0.69	0.11	87.50	5.70	66.90	5.20	39
	DGP11	0.26	0.12	0.69	0.15	75.70	4.50	67.80	6.70	44
	DGP12	0.44	0.27	0.70	0.16	90.10	4.20	69.40	8.20	54
	Pop $\bar{x}$	0.29	0.17	0.66	0.15	80.00	7.10	59.20	7.40	41.1

Table 2.8. Means and standard deviations for size, elongation, packing density (Pd) and packing proximity (Pp) of Upper ORS sediment. Percent lithic content also indicated for individual samples.

Fig. 2.39a-c shows grain size curves for thin sections from the three areas plotted in phi units against cumulative frequency (probability scale). It is clear that there is very little difference between regions, and most of the 'curves' approximate straight lines with surprising precision.

Visher (1969) observed that such plots of grain size will rarely be straight lines, since a mixture of normal populations in the sediment should result in a number of straight line segments with different slopes. This implies that the majority of UORS sections investigated contain a single normal population. Histograms of grain size in phi units against frequency show this population with normal distribution (eg Fig. 2.40b). For the two coarsest sandstones investigated from the Roseneath conglomerate, however, a definite kink occurs in the probability curves between approximately 0 and 1 phi. The bimodality of these sediments is clearly shown in the size-frequency histograms (eg Fig. 2.40a). This may not be unusual, since bimodality appears to be especially common in coarser stream deposits while sands tend in general to have a single mode (Pettijohn 1975).

By inspection of the segments of probability curves, Visher (1969) recognises three grain size populations relating to their respective physical mechanisms of transportation. Comparison with Visher's diagram (Fig. 2.39d) may suggest that the main population was transported by saltation, while the 0 - 1 phi population might have had a traction or suspension mechanism.

It appears initially from Table 2.8 that there is little variation in grain size between areas, although Portencross sediments ($x = 0.29$, $\sigma = 0.17$) are marginally the coarsest and most variably sized, while Wemyss Bay ($x = 0.25$, $\sigma = 0.13$) are the finest grained and best sorted. These differences are not statistically significant (Section 2.5.4).

2.5.2 Rounding and Elongation Index

The sharpness of edges and corners of clastic fragments is difficult to quantify visually. However, using the roundness classification of Pettijohn (1975), the majority of UORS grains from all areas are classed as subrounded (i.e. rho values of 0.25 - 0.40 relative to a sphere of roundness 1.0).

The sphericity of sand grains has a direct relationship to the type and extent of transport process acting on clastic sediments. In thin section, though, it

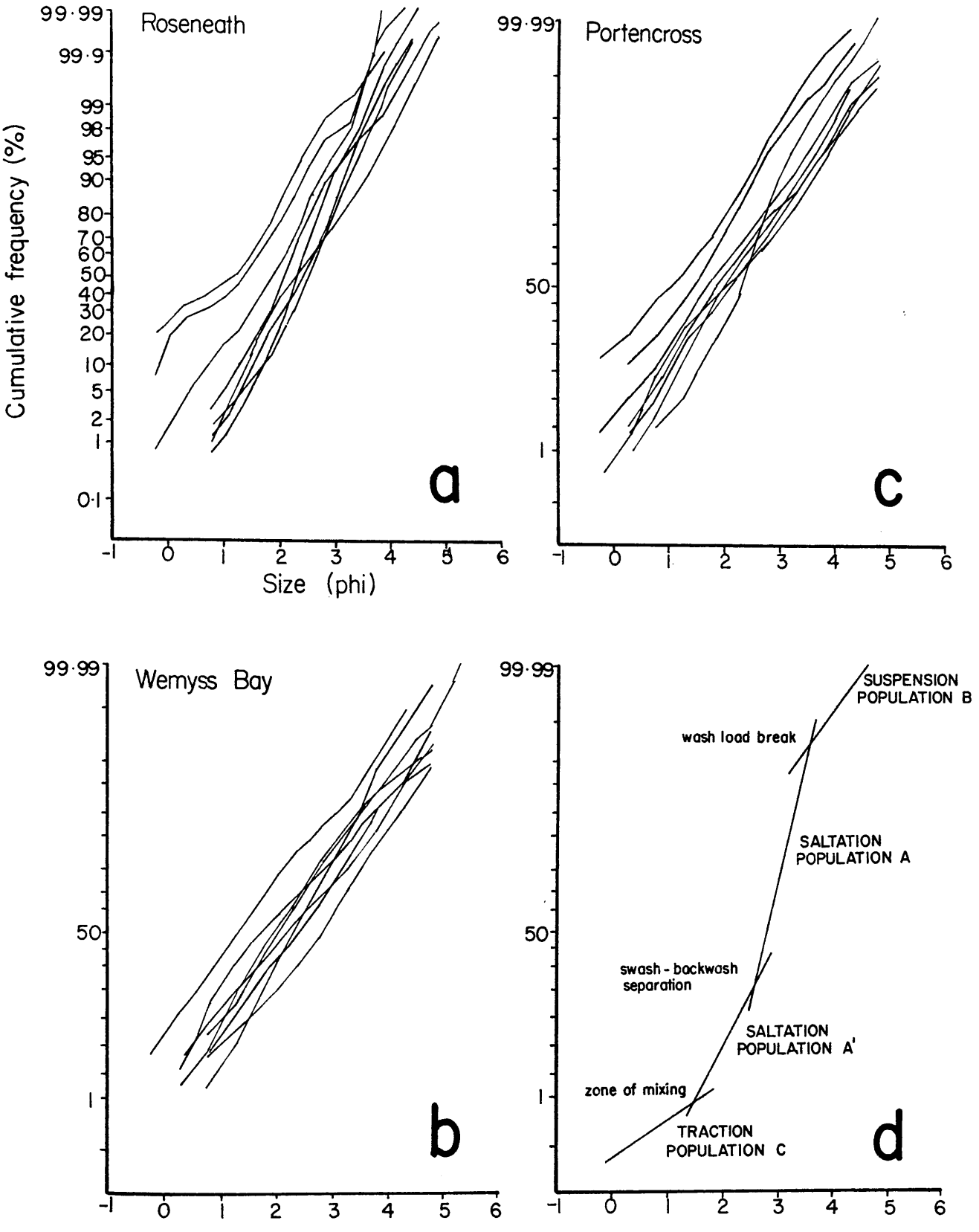

Fig 2.39. Cumulative frequency:grainsize curves for: a) Roseneath sandstones; b) Wemyss Bay sandstones; c) Portencross sandstones. d) Relation of sediment transport dynamics to populations and truncation points in a grain size distribution (after Visher 1969).

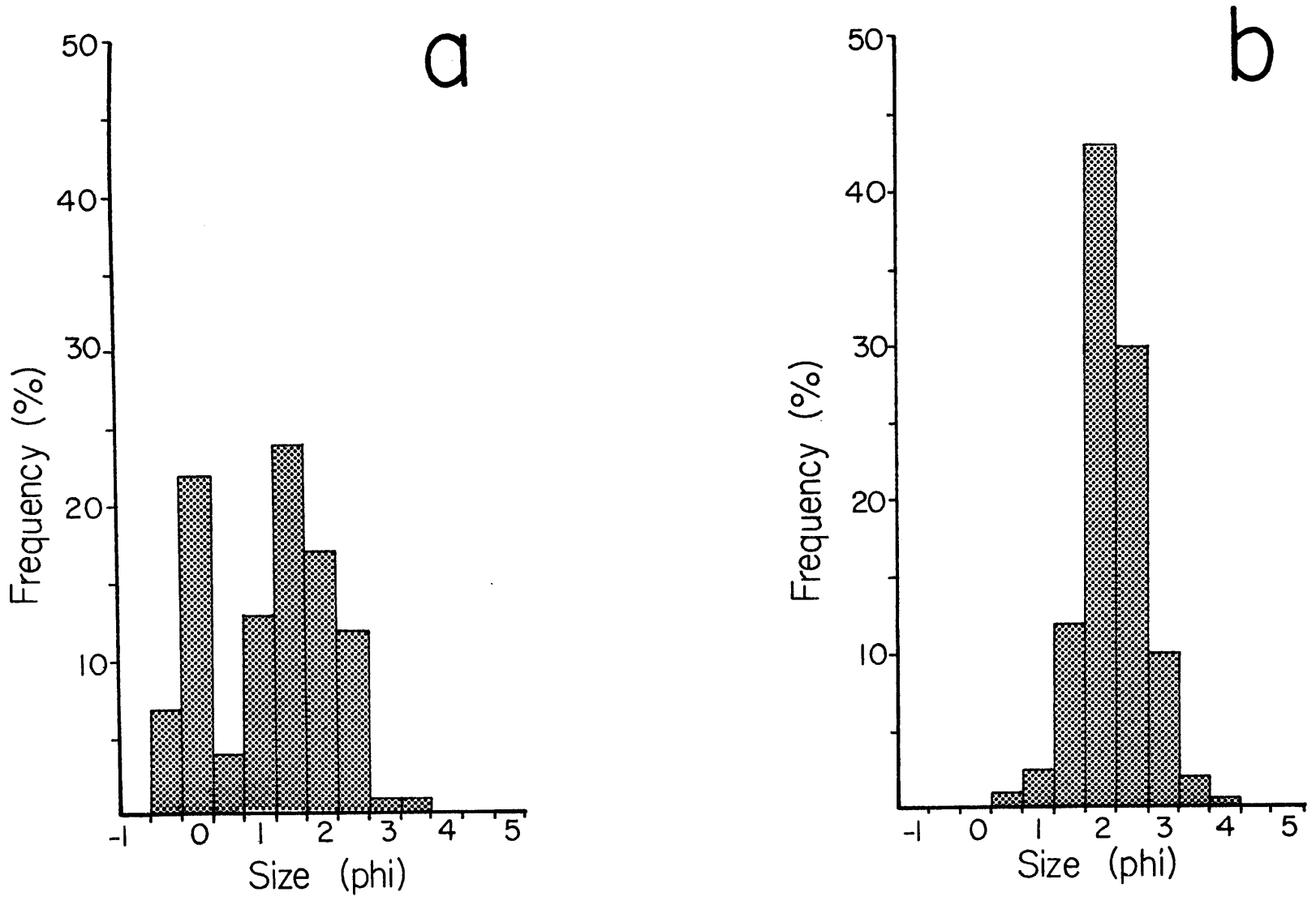

Fig 2.40. Typical size:frequency histograms for: a) coarse grained sandstone, Roseneath and; b) medium grained sandstone, Roseneath.

is impossible to measure, since true sphericity is a three dimensional ratio of a particle's long, intermediate and short axes. A best approximation to sphericity in two dimensions is the elongation index, defined as the ratio of the least-projection width of the grain (W) and maximum length (L) : W/L.

For eight thin sections from each UORS area, 200 elongation measurements were performed. Means obtained from the three areas indicate negligable variation in elongation between the conglomerates.

2.5.3 Packing

Kahn (1956a) defined packing in a sand sized sediment as:

'..... the mutual spatial relationship among the grains.'

and proceeded to propose two parameters by which packing could be calculated quantitatively:

i) Packing density (Pd) is a measure of the amount of space in a traverse occupied by grains and is given by:

$$Pd = \frac{m \sum_{i=1}^{n} g_i \cdot 100}{t}$$

where: n = number of grains; g = intercept size of ith grain; t = length of traverse; and m = magnification constant.
A sediment would be described as having 100% Pd when the entire traverse is occupied by grains.

ii) Packing proximity (Pp) is a measure of the closeness of the grains and is the ratio of grain/grain contacts to the total number of contacts:

$$Pp = (q/n) \cdot 100 \quad (0 \leq q \leq n)$$

where: q = number of grain/grain contacts and n = total number of contacts.

Packing proximity approaching 100% indicates that all grains are in contact with one another.

Both measurements are made simultaneously during six traverses of a thin section. Data from these traverses are used to calculate means and standard deviations for each thin section and population means calculated for each area (Table 2.8). Mean packing densities for the UORS are variable, but generally high, being in excess of that calculated by Kahn (1956b) for quartzites (68%) and greywackes (74%) but less than that for arkoses (82%). They are also considerably higher than those determined for the Silurian fluviatile Ringerike Group of Norway (Turner and Whitaker 1976). Mean packing proximities are also variable and again are higher than those calculated for quartzites and greywackes (43%) but lower than that for arkoses (60%). It is also worth noting that the highest packing density and proximity values are obtained from the lithic grain dominated Portencross conglomerate.

2.5.4 Statistical Analysis of the Data

a) Correlation Analysis

Table 2.9 is a correlation matrix showing the correlation coefficients (r) between all combinations of parameter pairings. Also included in this table are values obtained for percent lithic content from QFL compositions (Table 2.1) to determine whether a large quantity of lithic material affects sediment compaction. In this table critical values of r in excess of 0.40 (positive or negative) are significant at the 5% level (degrees of freedom = 22).

The following positive relationships are observed in decreasing order of significance:

i) Mean SIZE and standard deviation SIZE (0.93).

ii) Mean SIZE and mean PACKING DENSITY (0.82).

iii) Standard deviation SIZE and mean PACKING DENSITY (0.73).

iv) Mean PACKING DENSITY and mean PACKING PROXIMITY (0.71).

v) Standard deviation SIZE and mean PACKING PROXIMITY (0.54).

vi) Mean PACKING PROXIMITY and % LITHIC CONTENT (0.41).

	SIZE $\bar{x}$	SIZE σ	ELONG $\bar{x}$	ELONG σ	Pd $\bar{x}$	Pd σ	Pp $\bar{x}$	Pp σ	% LITH
SIZE $\bar{x}$		**0.93**	0.25	-0.34	**0.82**	-0.09	**0.54**	0.19	0.30
SIZE σ			0.25	-0.26	**0.73**	-0.09	**0.63**	0.21	0.28
ELONG $\bar{x}$				-0.05	0.19	0.10	0.08	-0.14	0.00
ELONG σ					-0.36	0.12	-0.05	0.16	-0.28
Pd $\bar{x}$						-0.20	**0.71**	0.00	0.36
Pd σ							0.07	0.30	-0.04
Pp $\bar{x}$								0.34	**0.41**
Pp σ									-0.12

Table 2.9. Correlation matrix showing r values between all combinations of parameter pairings for combined areas: degrees of freedom = 22; critical r at 0.04 ; pairings with significant correlation are in bold.

This implies the following:

a) The coarsest sediments are the most poorly sorted and have higher packing densities and packing proximities than finer sands.

b) Packing density and packing proximity are positively related, with the latter having a small but significant correlation with lithic content.

b) Textural variations between areas

The significance of textural variations between the three areas within the upper ORS basin was tested using the ratio difference of means/standard error of the difference (Reichmann 1961):

$$S = \frac{(\bar{x}_1 - \bar{x}_2)}{N\,((\sigma_1^2/n_1) + (\sigma_2^2/n_2))}$$

where $\bar{x}$ = mean, σ^2 = variance and n = number of samples

Differences can then be summarised as: statistically highly significant (S> = 4); significant (S = 3.00 - 3.99); probably significant (S = 2.00 - 2.99); and not significantly different (S< 2).

Sample populations from Roseneath, Wemyss Bay and Portencross basal upper ORS sandstones are compared in Table 2.10. There are no significant differences detected for textural variations between any of the areas compared in this investigation.

2. 6 Summary of Conclusions - Chapter 2

Conclusions concerning the petrology of sandstones interbedded with UORS conglomerate units are summarised below and illustrated diagramatically in Table 2.11.

Areas	Parameter	(x_1-x_2)	Standard Error	Significance	
Roseneath/Wemyss Bay	Size	0.02	0.04	0.50	**NONE**
	Elongation	0.02	0.04	0.50	**NONE**
	Packing density	2.33	3.48	0.67	**NONE**
	Packing proximity	2.38	5.38	0.44	**NONE**
	Lithic content	18.12	2.63	6.90	**HIGH**
Wemyss Bay/Portencross	Size	0.04	0.04	1.00	**NONE**
	Elongation	0.00	0.02	0.00	**NONE**
	Packing density	4.95	4.01	1.23	**NONE**
	Packing proximity	5.76	5.74	1.00	**NONE**
	Lithic content	5.13	4.05	1.26	**NONE**
Portencross/Roseneath	Size	0.02	0.04	0.44	**NONE**
	Elongation	0.02	0.04	0.44	**NONE**
	Packing density	2.62	3.85	0.68	**NONE**
	Packing proximity	8.14	5.64	1.44	**NONE**
	Lithic content	23.25	3.35	6.94	**HIGHLY**

Table 2.10. Standard error of the difference comparison of textural and compositional parameters for basal UORS at Roseneath, Wemyss Bay and Portencross.

LOCALITY		Portencross	Wemyss Bay	Roseneath
DOMINANT CONGLOMERATE CLAST TYPES (after Bluck 1980)		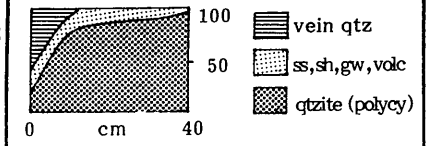	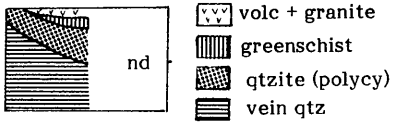	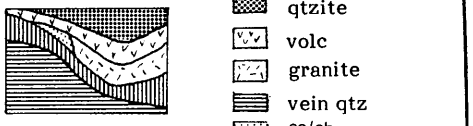
MICRO FRAGMENTS	CRYSTAL	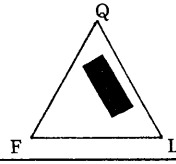 Qm < Qp plag > K-fs x-hatched K-fs	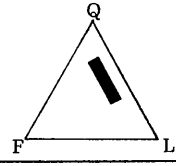 Qm Qp plag < K-fs volcanic quartz vein quartz myrmekitic plag	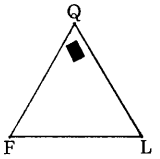 Qm > Qp plag < K-fs vein quartz
	LITHIC	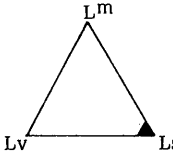 Quartzite Shale/mudstone Greywacke Immature sandstone	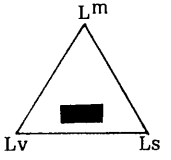 Volcanic Metaquartzite Shale Low grade pelite	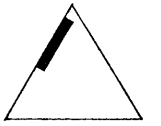 Quartzite Vein qtz (+ch sch) bt + gt schist Shale Mature sandstone
NON-OPAQUE HEAVY MINERAL COMPOSITION (approx visual est)		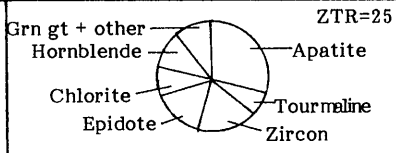	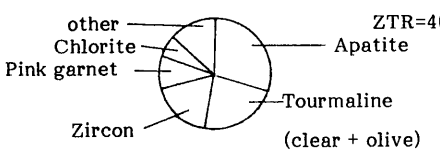	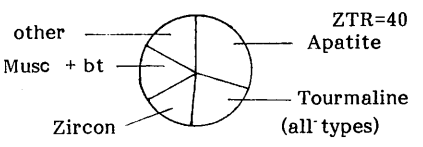
CLAY TYPE (xtalnty)		Illite (poor)	Illite (poor) < Kaolinite (good)	Illite (poor) < Kaolinite (good)
SANDSTONE TEXTURE		Size : 0.29mm Elongation : 0.66 Pd : 80.00 Pp : 59.20 Sorting : Poor Rounding : Subrounded	Size : 0.25mm Elongation : 0.67 Pd: 75.10 Pp : 53.40 Sorting : Poor Rounding : Subrounded	Size : 0.27 (bimodal) Elongation : 0.68 Pd : 77.40 Pp : 51.00 Sorting : Poor Rounding : Subrounded
IDEALISED STRAT SECTION - TOP DEVONIAN 1 cm = 1 km horiz.		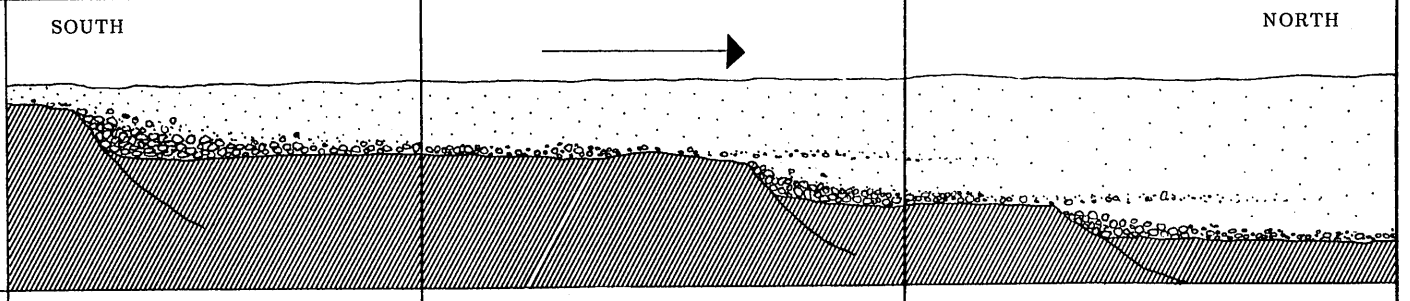		
INFERRED SOURCE COMPOSITION FOR BASAL UORS		? Silurian greywacke with shales, volcanics and distal or reworked basic plutonics.	Metagreywacke/phyllite in low green-schist facies. Unmetamorphosed volcanics and granite. Reworked LORS.	Schist in high greenschist facies (bt - gt) with large undeformed granite + volcanic input. Reworked LORS.

Table 2.11. Petrologic and provenance summary of basal Upper ORS detritus in the western Midland Valley.

i) The sandstones from all three areas studied are dominated by immature lithic arenites with low feldspar content. Compositional fields for Roseneath are always distinct from fields for Wemyss Bay and Portencross, and the latter are always indistinguishable on QFL, QmFLt and QmQpL plots. In QpLvLs and LmLvLs plots, distinctions are obvious amongst all three areas on the basis of lithic populations.

ii) Studies of polycrystallinity and extinction in detrital quartz suggests plutonic and/or higher grade metamorphic sources dominate at Roseneath and Wemyss Bay, whilst lower grade metamorphic and sedimentary sources are implied for Portencross. Volcanic quartz is particularly characteristic of Wemyss Bay sediment. Plagioclase/total feldspar ratios are highest at Portencross where abundant reworked greywacke clasts are considered to have provided a source. XRD analysis of K-feldspar reveals a high correlation between K-feldspar populations in the sandstones and those obtained from conglomerate clasts within specific areas; with the exception of probable authigenic feldspar at Portencross and Roseneath, there does not exist a single K-feldspar population in the sandstones whose source is not also represented as conglomerate clasts. Unique compositions for heavy mineral suites are also observed for each of the three areas. There does not appear to have been mixing of any of the above mentioned compositional components in a 'down flow' direction.

iii) Provenance estimations for UORS sandstones on the basis of compositional variations are as follows.

a) A substantial amount of reworking of older sediment is implied for all areas. Fragments of Southern Uplands type greywacke and sandstones and shales with LORS affinities imply that sediment of at least Silurian to early Devonian age were contributing detritus to the developing UORS basin. It is difficult to estimate this input quantitatively.

b) Metamorphic grade of the detritus increases in a northward/northwestward direction and ranges from very low greenschist facies in the southeast to garnet grade in the northwest. This is coupled with a trend from basic plutonics/volcanics to a more acid igneous input in a similar direction.

c) There is an upward progression in the sandstones in all areas to a more mature and homogeneous assemblage of grain compositions.

All of the above are compositional trends also displayed by conglomerate clasts.

iv) Post-depositional changes relating to burial generally follow a consistent sequential pattern which was uniformly developed throughout the basin. Local variations in compaction and diagenesis may be attributable to local variations in detrital composition.

v) Texturally, the sediments in the basal UORS are for the most part immature, but display an upward maturing indicative of more distal transportation. Grain size analysis reveals in general a single, normally distributed population although there is a tendency towards bimodality in coarser grained sand sized material. Statistically significant lack of elongation variation between areas and identical cumulative frequency:grainsize curves suggests clear similarities in type and degree of transportation. There is no detected down flow variation for any textural parameter.

CHAPTER 3

IGNEOUS CLAST PETROLOGY

3.1 Introduction

Igneous clasts of hypabyssal and plutonic types typify the UORS basal conglomerates at Roseneath Point, the most northerly of the three areas under investigation in this study (Bluck 1980). Since this detritus is of uncertain provenance (potential source terrains are not presently exposed in the *immediate* vicinity in the direction implied by the paleocurrent data) a number of analytical techniques have been applied to classify and place some constraints on the affinities of these clasts.

3.2 Petrography of the Igneous Clasts

3.2.1 Acid Hypabyssal clasts

The acid hypabyssal rocks occur in clasts of up to c 0.40m in size (maximum diameter) and consist dominantly of large (c 9mm) phenocrysts of plagioclase set in a fine to medium grained groundmass of quartz, plagioclase, biotite and K-feldspar.

The presence or absence of additional phenocryst phases has led to a three-fold classification of these rocks based on phenocryst mineral assemblages:

i) Plagioclase + hornblende + biotite + K-feldspar.

ii) Plagioclase + biotite (minor) + quartz + K-feldspar.

iii) Plagioclase + biotite + quartz + K-feldspar.

Virtually identical assemblages have been observed by Phillips et al (1981) in their study of the c. 400 Ma Criffel - Dalbeattie pluton, where a porphyrite porphyry series of dykes are associated with the final stages of main pluton emplacement. A fourth assemblage, however, is present at Criffell - Dalbeattie (plagioclase + hornblende + clinopyroxene) and is not observed in any of the igneous clasts at Roseneath. Since clinopyroxene occurs as relict masses enclosed within hornblende crystals, Phillips et al (1981) concluded that it

reacted with the magma at the onset of hornblende crystallisation. The absence of clinopyroxene bearing rocks at Roseneath might therefore be explained in this way.

Phenocryst plagioclase is of variable composition (albite, oligoclase or andesine), euhedral and always zoned (Fig. 3.1). Alteration to sericite is frequently highly developed and occassionally complete replacement by calcite can be observed. Examination of partially altered specimens indicates that alteration is selective and directly related to the composition of the zones. In a traverse from the rim to the core, three alteration zones are present in most altered plagioclases. The least altered parts of these phenocrysts are those around the rims. This is followed by one or two zones of intensive clay/mica alteration which may persist to the core. Finally, in many crystals the last clay/mica band encloses a core of calcite (Fig. 3.1). It may therefore be concluded that early plagioclase crystals had compositions more calcic than the overgrowths developed at later stages. This would agree with normal igneous trends.

Biotite is the second most abundant phenocryst phase. It can occur as large (c. 5mm) euhedral laths and is rarely altered to chlorite. Occassionally, small biotite flakes have developed at the edges of altered hornblende phenocrysts in a similar manner to that described by Phillips (1956) for the Criffell - Dalbeattie porphyries (Fig. 3.2). Muscovite phenocrysts were observed in only two samples and seem to occur to the exclusion of biotite.

Euhedral green-brown hornblende phenocrysts are common in the acid hypabyssal rocks. They are large (c. 5mm) and often completely altered to microcrystalline aggregates of chlorite, biotite, epidote or calcite, the latter two being most common (Fig. 3.3). Calcite replacement begins at the cores where the early hornblendes must have been especially calcic-rich.

Quartz phenocrysts are large (c. 6mm) and display characteristic embayed and resorbed textures (Fig. 3.4). They are commonly surrounded by a halo of microcrystalline quartz with a graduated transition into the phenocryst (Fig. 3.5). The 'pits' of the embayments are bulbous and sometimes contain grains of accessory minerals (zircon, apatite or rutile) of a size which is nearly always larger than the maximum aperture of the embayment neck. If the embayments do not actually contain an accessory mineral grain, then they are frequently seen to be developing in the general direction of one contained as an inclusion in the quartz.

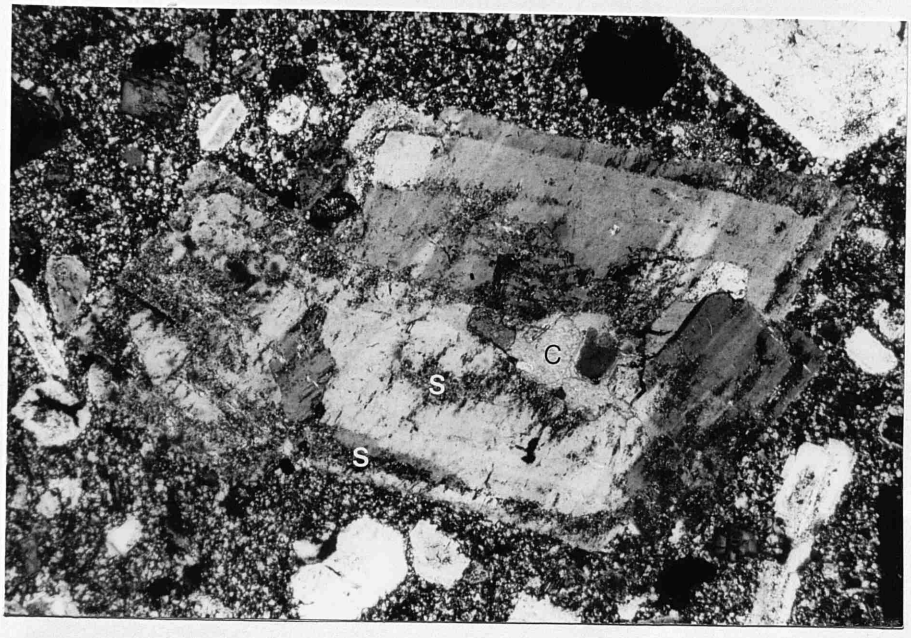

Fig 3.1. TS photomic, XPL, X10. Altered microgranodiorite, Roseneath. Albite plagioclase phenocryst showing sericite alteration zones (S) and carbonate core (C).

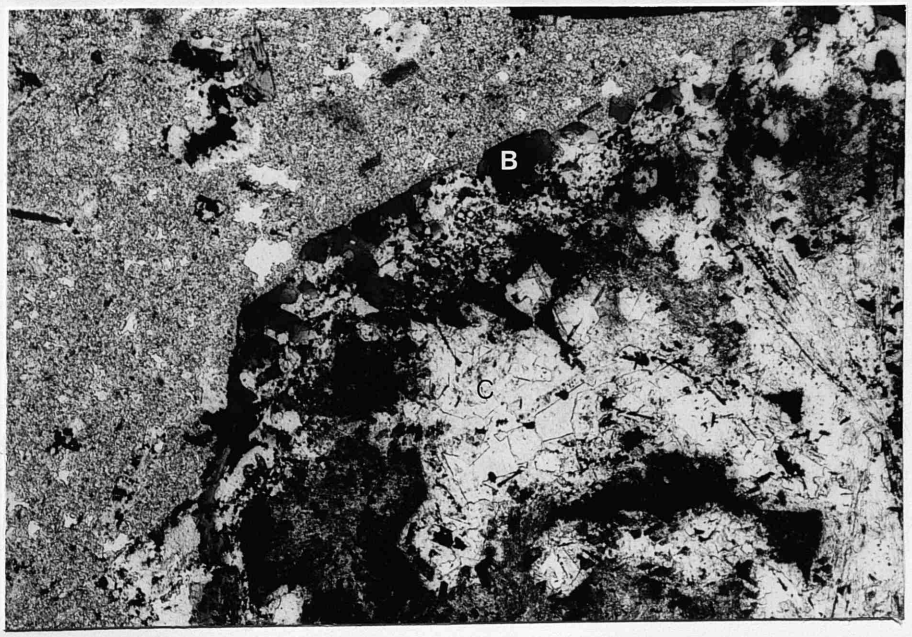

Fig 3.2. TS photomic, PPL, X40. Altered microgranodiorite, Roseneath. Hornblende phenocryst showing biotite (B) replacement at margins and carbonate core (C).

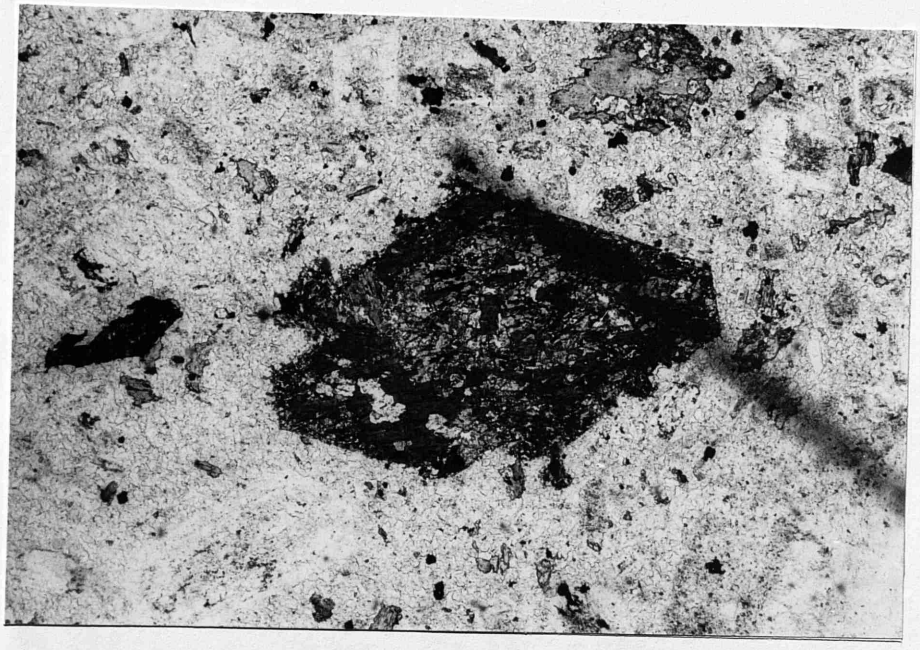

Fig 3.3. TS photomic, PPL, X10. Altered microgranodiorite, Roseneath. Hornblende phenocryst now entirely replaced by epidote aggregates.

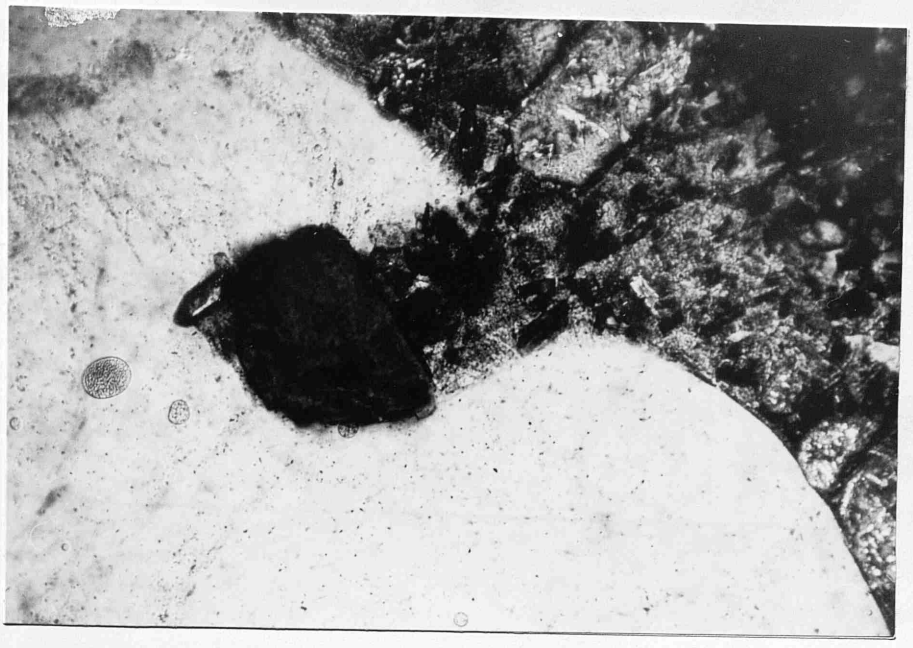

Fig 3.4. TS photomic, XPL, X40. Microgranodiorite, Roseneath. Quartz phenocryst showing embayment occupied by apatite.

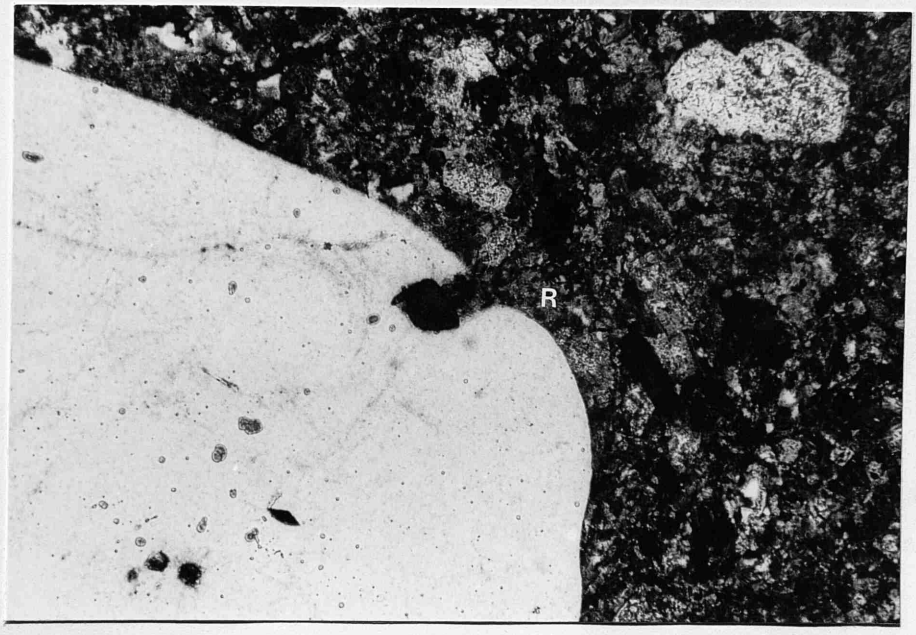

Fig 3.5. TS photomic, XPL, X10. Microgranodiorite, Roseneath. Quartz phenocryst with embayment and resorbed margin (R).

K-feldspar phenocrysts are also large (c. 6mm) and are relative unaltered in comparison to plagioclase. Minor kaolinite 'streaks' can be seen and the crystals display similar corrosion textures along the margins to those described for quartz above. Heavy mineral related embayments are also present.

3.2.2 Intermediate Volcanic/Hypabyssal clasts

These clasts are generally smaller than their acid equivalents (c. 0.25m maximum diameter). They are mineralogically and texturally less variable and on a petrographic basis may be termed hornblende bearing porphyritic andesites and spessartite lamprophyres. As far as can be determined, hornblende is almost exclusively the ferromagnesian phenocryst phase (biotite is rarely present and may be of secondary origin) and is present as large (c. 4mm) euhedral crystals which are now totally pseudomorphed by calcite and iron oxides (Fig. 3.6). However, unidentified phenocrysts of possibly anhedral hornblende or pyroxene, now pseudomorphed by calcite are also present in certain specimens (Fig. 3.7).

The groundmass in these rocks consists principally of plagioclase laths (with flow textures), small amounts of ferromagnesian minerals (chlorite/biotite) and iron oxides.

Optical identification of plagioclase compositions for the andesites and lamprophyres suggests a surprisingly low anorthite component. The plagioclase phenocrysts are both euhedral and interstitial, and carbonate alteration at the cores of euhedral crystals suggests that calcic compositions only characterised their early growth. Amphiboles, the vast majority of which have been altered to chlorite, are also large (c. 5mm), euhedral and display extinction angles appropriate for common hornblende.

3.2.3 Acid Plutonic Clasts

Within this grouping is a whole range of coarse grained plutonic material and includes a large proportion of porphyritic varieties. Maximum diameters for these types are of the order of 0.75m.

The granites and granodiorites are equivocably of the two-mica variety, containing up to 10% modal biotite but never more than 3% muscovite. However, muscovite is not pervasive and is absent in most samples. From

Fig 3.6. TS photomic, X10. Altered spessartite lamprophyre, Roseneath. Euhedral hornblende replaced by calcite and iron oxides.

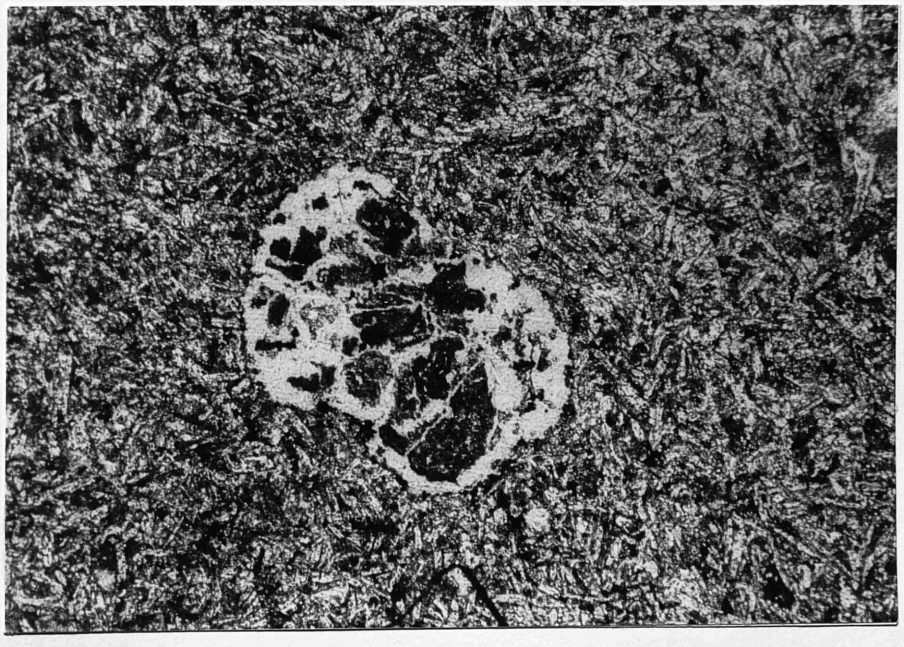

Fig 3.7. TS photomic,X10. Altered porphyritic andesite, Roseneath. Unidentified anhedral phenocryst (?hornblende/pyroxene) now replaced by calcite and iron oxides.

textural relationships, muscovite growth is considered to be early and not a late stage development under special conditions. Whether it is present in sufficient quantities to justify application on the term 'two-mica' is debatable.

Euhedral hornblende accompanies biotite and constitutes up to 10% of the mode. These crystals are often in various states of calcite, epidote, chlorite and iron oxide replacement (Fig. 3.8).

Non-porphyritic types have plagioclase and K-feldspar in roughly equal proportions, whereas porphyritic varieties approach alkali-granite in composition (K-feldspar> 2/3). Many of the K-feldspar megacrysts (c. 5cm) are probably phenocrysts (s.s.) as opposed to late stage interstitial cyrstallisation. This is based on the observation that most of the megacrysts are euhedral and do not enclose significant numbers of late-formed crystals. Blebs of quartz, however, are commonly observed in the phenocrysts [apparently defining former crystal boundaries (Fig 3.9)], as are small euhedra of hornblende and biotite.

Subhedral plagioclase is present both in the framework and occassionally as phenocrysts (c. 1cm) in porphyritic varieties. Zonation of these feldspars is common and, as with the acid porphyries, appears to be related to decreasing calcium content away from the core. Again one or two bands of heavy clay/mica alteration may be displayed with the rims being the least altered parts. Myrmekitic textures are occassionally displayed (Fig. 3.10).

The sequence of commencement of mineral crystallisation for the granites and granodiorites, based on textural relationships is shown below.

i) Apatite + sphene + biotite + hornblende.
ii) Plagioclase (Ca-rich) + muscovite + quartz (partially resorbed).
iii) K-feldspar (phenocrysts) + quartz + plagioclase.
iv) Plagioclase (becoming Na-rich) + quartz.
v) K-feldspar (interstitial and overgrowth).

It is clear from the petrography that the Group 1 clasts were not undersaturated with respect to H_2O. Applying the order of crystallisation for these rocks to the experimental work of Maaloe and Wyllie (1975) on a biotite granite at 2Kb pressure, it can been seen that the maximum permissable water content

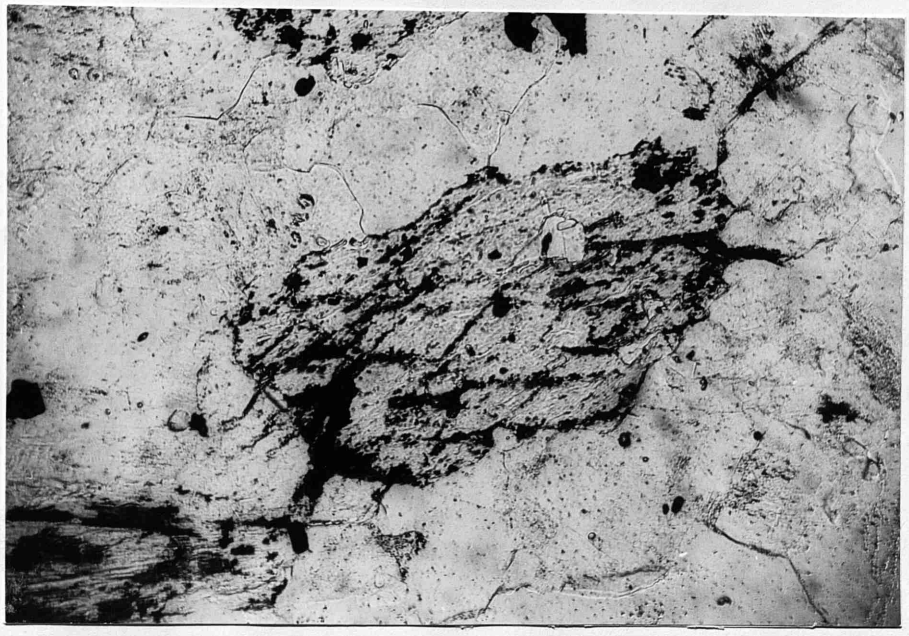

Fig 3.8. TS photomic,PPL, X10. Granodiorite, Roseneath. Hornblende phenocryst showing iron oxide replacement along cleavage planes.

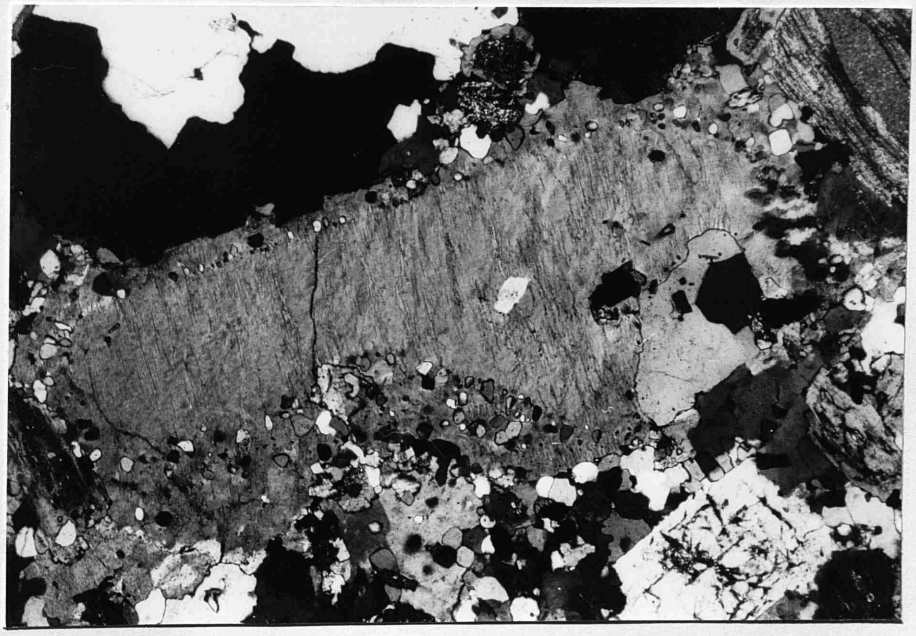

Fig 3.9. TS photomic, XPL, X10. Granodiorite, Roseneath. Small quartz blebs define early boundary of K-feldspar crystal.

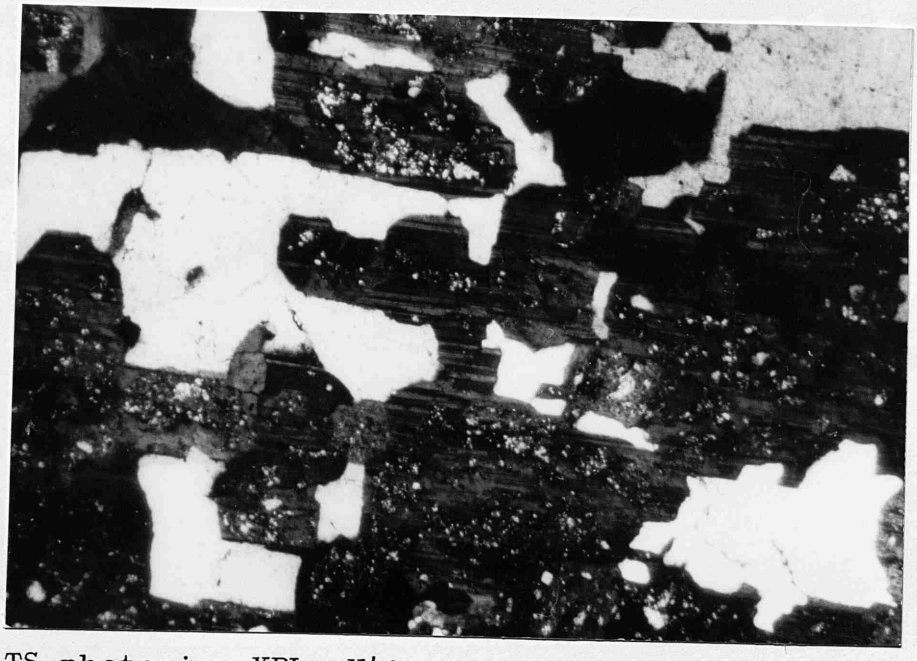

Fig 3.10. TS photomic, XPL, X40. Granodiorite, Roseneath. Myrmekitic texture (quartz-feldspar intergrowth) in albitic plagioclase.

of the Roseneath magma was an unlikely 20% (H_2O content of large bodies of batholitic granite magma rarely exceeds 1.5%). This H_2O supersaturated condition is probably unrepresentative of the Roseneath 'batholith' as a whole, but provides evidence that the portion of the pluton exposed during ORS deposition may represent a high level liquid-crystal mush. Here crystallisation of the anhydrous minerals, quartz and feldspar may have led eventually to water saturated conditions.

Accessory minerals are dominated by the early growth of apatite and large euhedral crystals of pale brown sphene (Fig. 3.11). Rutile, zircon and monazite are of minor importance. Tourmaline was not detected either in thin section or in any of the heavy mineral separations performed on the granites.

3.3 Whole-Rock Chemistry

3.3.1 Chemical Data and Sampling

A total of 41 samples, representing the least altered of more than eighty igneous clasts retrieved from the UORS conglomerate at Roseneath, were analysed for eleven major oxides and eighteen trace elements. This data is presented in Table 3.1, where loss on ignition values for the total volatile constituents (CO_2 + H_2O) are also shown. Full descriptions of analytical methods and sample preparation are given in Appendix II. Sample location NS 268 806.

3.3.2 Alteration

The clasts were sampled without any conscious bias towards either acid or intermediate types, and the proportions of each presented for analysis are largely controlled by the degree of alteration. Apart from the hydrothermal alteration of acid hypabyssal rocks to be discussed later (Section 3.3.5), the majority of clasts sampled showed the development of secondary minerals in thin section. The effects of this deuteric alteration (notably the appearance of chlorite, calcite and sericite) have been removed in the acid clasts by selecting for analysis only those specimens which appear fresh in thin section, that is, they exhibited no visible signs of weathering or alteration. However, in the case of the intermediate volcanic clasts with dimensions encountered in the Roseneath conglomerate, incipient alteration may be visually undetectable. This uncertainty must be considered during detailed geochemical investigations employing many major and trace elements.

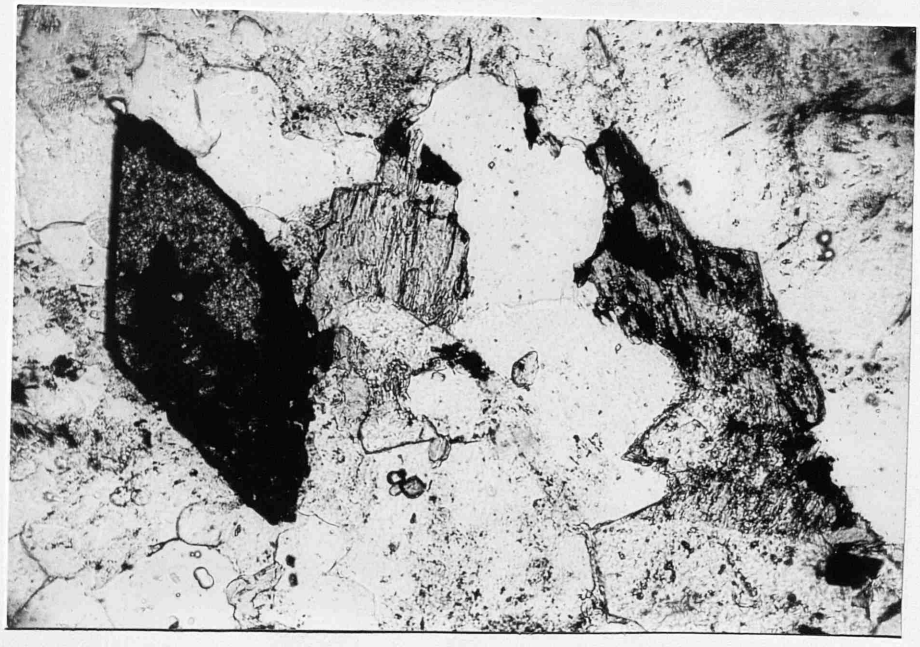

Fig 3.11. TS photomic,PPL, X40. Granodiorite, Roseneath. Large euhedral crystal of pale brown sphene (S). Note also interstitial apatine (A) and amphibole (Am).

	No	B12-27	B14-28	B15-29	B3-18	B6-21	B9-24	B16-30	A2-2
	Type	Granodiorite	Granodiorite	Adamellite	Micro-Granodiorite	Micro-Qtz-Monzonite	Micro-Granodiorite	Micro Granodiorite	Micro Granodiorite
Major (wt %)	Si02	67.15	65.54	68.16	71.40	67.22	67.69	67.06	68.30
	Ti02	0.41	0.38	0.36	0.37	0.41	0.43	0.41	0.40
	A1203	15.87	16.30	14.77	14.41	15.73	16.01	14.86	15.57
	Fe203	1.59	2.26	1.22	1.60	1.54	2.53	1.39	1.60
	FeO	0.74	0.94	0.82	0.67	1.22	0.94	0.94	0.98
	MnO	0.04	0.08	0.03	0.00	0.04	0.02	0.05	0.00
	MgO	1.43	2.22	1.35	1.52	1.53	0.51	1.44	1.52
	CaO	1.96	1.08	1.11	1.73	2.23	2.32	2.22	2.34
	Na2O	4.64	4.00	4.42	4.46	6.02	4.44	4.87	4.98
	K20	3.50	2.16	3.72	3.14	3.16	3.33	3.44	3.24
	P205	0.12	0.12	0.09	0.12	0.12	0.10	0.10	0.13
	L0I	1.99	5.37	3.17	1.40	1.81	1.09	2.43	2.14
	Total	99.44	100.45	99.22	100.82	101.03	99.41	99.21	101.20
Trace (ppm)	Ba	1039	530	981	1233	1208	1653	961	1199
	Ce	21	23	19	44	37	32	26	47
	Co	12	14	7	5	5	0	8	3
	Cr	20	24	45	20	26	17	25	26
	Cu	17	11	33	15	16	1	9	47
	Ga	18	16	17	16	20	15	17	19
	La	12	7	13	20	18	19	21	18
	Nb	13	9	10	13	9	5	17	9
	Ni	14	11	14	8	12	0	8	10
	Pb	17	0	14	14	8	14	20	14
	Rb	91	60	100	71	80	99	85	66
	S	33	35	47	33	21	23	35	55
	Sr	688	288	498	661	783	572	702	743
	Th	10	3	11	12	8	12	4	7
	U	3	1	1	3	3	1	2	2
	Y	7	11	5	8	7	3	6	13
	Zn	28	49	25	18	19	15	31	38
	Zr	155	144	142	167	168	77	156	162
CIPW norm	Ap	0.28	0.28	0.21	0.28	0.28	0.23	0.23	0.30
	Il	0.78	0.72	0.68	0.70	0.78	0.82	0.78	0.76
	Or	20.68	12.76	21.98	18.56	18.68	19.68	20.33	19.15
	Ab	39.25	33.84	37.39	37.73	50.93	37.56	41.20	42.13
	An	8.94	4.57	4.92	7.80	6.57	10.86	8.53	10.56
	C	1.17	5.71	1.67	0.82	0.00	1.12	0.00	0.00
	Mt	1.20	1.93	1.60	1.09	2.00	1.78	1.84	2.00
	Hm	0.76	0.93	0.12	0.84	0.00	0.12	0.27	0.22
	DiWo	0.00	0.00	0.00	0.00	1.56	0.00	0.76	0.08
	DiEn	0.00	0.00	0.00	0.00	1.23	0.00	0.66	0.07
	DiFs	0.00	0.00	0.00	0.00	0.15	0.00	0.00	0.00
	HyEn	3.56	5.53	3.36	3.04	2.26	2.59	2.88	3.71
	HyFs	0.00	0.00	0.00	0.00	0.27	0.00	0.00	0.00
	Q	20.77	27.72	24.07	28.25	14.19	22.88	19.37	20.06
	O1Fo	0.00	0.00	0.00	0.00	0.00	0.00	0.00	0.00

	No	A3-3	A4-4	A11-11	B2-17	B1-16	B8-23	B10-25	B11-26
	Type	Micro-Qtz diorite	Micro Granodiorite	Micro Granodiorite	Micro-Granodiorite	Granodiorite	Qtz-Monzo-Monzodiorite	Granodiorite	Granodiorite
Major (wt %)	Si02	66.18	68.26	67.17	68.34	67.99	66.24	65.12	65.04
	Ti02	0.46	0.40	0.38	0.44	0.41	0.46	0.49	0.48
	A1203	15.36	15.50	15.46	15.60	15.97	15.26	15.95	16.19
	Fe203	1.54	2.53	1.39	1.73	1.87	1.76	1.84	2.17
	FeO	1.10	0.54	1.02	0.69	0.58	0.82	0.80	0.74
	MnO	0.04	0.09	0.02	0.00	0.00	0.08	0.07	0.05
	MgO	1.53	0.51	1.44	1.08	1.18	0.76	1.22	1.43
	CaO	2.25	1.64	2.14	2.65	2.80	3.13	2.95	2.28
	Na2O	5.25	4.54	4.23	4.71	4.60	5.68	4.02	4.40
	K20	3.20	3.38	2.85	3.73	3.75	3.51	3.12	3.42
	P205	0.14	0.13	0.11	0.14	0.12	0.12	0.14	0.14
	L0I	3.12	3.57	2.98	1.99	1.65	0.96	3.81	4.52
	Total	100.17	101.09	99.19	101.10	100.92	98.78	99.53	100.86
Trace (ppm)	Ba	1145	1138	1324	1415	1247	937	952	855
	Ce	40	55	39	44	30	36	26	28
	Co	7	0	6	3	2	9	13	14
	Cr	55	22	35	23	24	25	30	32
	Cu	13	22	9	13	14	13	9	12
	Ga	17	18	20	19	18	19	19	20
	La	19	30	16	23	18	12	14	13
	Nb	11	32	11	11	17	19	17	15
	Ni	11	6	13	10	8	10	13	17
	Pb	9	16	11	18	11	18	18	19
	Rb	84	74	73	105	97	92	89	87
	S	60	32	28	56	45	47	42	39
	Sr	761	557	1061	849	805	816	784	675
	Th	7	9	6	11	9	9	5	5
	U	3	3	2	4	2	1	2	2
	Y	10	16	9	12	7	8	7	8
	Zn	16	18	26	24	23	24	31	31
	Zr	158	159	163	169	164	178	173	172
CIPW norm	Ap	0.32	0.30	0.26	0.32	0.28	0.28	0.32	0.32
	Il	0.87	0.76	0.72	0.84	0.78	0.84	0.93	0.91
	Or	18.91	19.98	16.84	22.04	22.16	20.74	18.44	20.21
	Ab	44.41	38.41	35.78	39.84	38.91	48.05	34.01	37.22
	An	8.90	7.29	9.90	10.41	11.85	5.77	13.72	10.40
	C	0.00	1.70	1.79	0.00	0.00	0.00	0.93	1.44
	Mt	2.21	0.58	2.02	0.95	0.68	1.31	1.16	0.99
	Hm	0.01	2.13	0.00	1.08	1.40	0.86	1.04	1.48
	DiWo	0.56	0.00	0.00	0.76	0.52	2.19	0.00	0.00
	DiEn	0.49	0.00	0.00	0.66	0.45	1.89	0.00	0.00
	DiFs	0.00	0.00	0.00	0.00	0.00	0.00	0.00	0.00
	HyEn	3.32	1.27	3.59	2.03	2.49	0.00	3.04	3.56
	HyFs	0.00	0.00	0.10	0.00	0.00	0.00	0.00	0.00
	Q	16.98	25.00	25.19	20.17	19.73	14.20	22.05	19.73
	O1Fo	0.00	0.00	0.00	0.00	0.00	0.00	0.00	0.00

Table 3.1 (and next 4 pages). Major oxide and trace element compositions of Roseneath igneous clasts.

	No	B12-27	B14-28	B15-29	B3-18	B6-21	B9-24	B16-30	A2-2
	Type	Granodiorite	Granodiorite	Adamellite	Micro-Granodiorite	Micro-Qtz-Monzonite	Micro-Granodiorite	Micro Granodiorite	Micro Granodiorite
Major (wt %)	Si02	67.15	65.54	68.16	71.40	67.22	67.69	67.06	68.30
	Ti02	0.41	0.38	0.36	0.37	0.41	0.43	0.41	0.40
	A1203	15.87	16.30	14.77	14.41	15.73	16.01	14.86	15.57
	Fe203	1.59	2.26	1.22	1.60	1.54	2.53	1.39	1.60
	FeO	0.74	0.94	0.82	0.67	1.22	0.94	0.94	0.98
	MnO	0.04	0.08	0.03	0.00	0.04	0.02	0.05	0.00
	MgO	1.43	2.22	1.35	1.52	1.53	0.51	1.44	1.52
	CaO	1.96	1.08	1.11	1.73	2.23	2.32	2.22	2.34
	Na2O	4.64	4.00	4.42	4.46	6.02	4.44	4.87	4.98
	K20	3.50	2.16	3.72	3.14	3.16	3.33	3.44	3.24
	P205	0.12	0.12	0.09	0.12	0.12	0.10	0.10	0.13
	L0I	1.99	5.37	3.17	1.40	1.81	1.09	2.43	2.14
	Total	99.44	100.45	99.22	100.82	101.03	99.41	99.21	101.20
Trace (ppm)	Ba	1039	530	981	1233	1208	1653	961	1199
	Ce	21	23	19	44	37	32	26	47
	Co	12	14	7	5	5	0	8	3
	Cr	20	24	45	20	26	17	25	26
	Cu	17	11	33	15	16	1	9	47
	Ga	18	16	17	16	20	15	17	19
	La	12	7	13	20	18	19	21	18
	Nb	13	9	10	13	9	5	17	9
	Ni	14	11	14	8	12	0	8	10
	Pb	17	0	14	14	8	14	20	14
	Rb	91	60	100	71	80	99	85	66
	S	33	35	47	33	21	23	35	55
	Sr	688	288	498	661	783	572	702	743
	Th	10	3	11	12	8	12	4	7
	U	3	1	1	3	3	1	2	2
	Y	7	11	5	8	7	3	6	13
	Zn	28	49	25	18	19	15	31	38
	Zr	155	144	142	167	168	77	156	162
CIPW norm	Ap	0.28	0.28	0.21	0.28	0.28	0.23	0.23	0.30
	Il	0.78	0.72	0.68	0.70	0.78	0.82	0.78	0.76
	Or	20.68	12.76	21.98	18.56	18.68	19.68	20.33	19.15
	Ab	39.25	33.84	37.39	37.73	50.93	37.56	41.20	42.13
	An	8.94	4.57	4.92	7.80	6.57	10.86	8.53	10.56
	C	1.17	5.71	1.67	0.82	0.00	1.12	0.00	0.00
	Mt	1.20	1.93	1.60	1.09	2.00	1.78	1.84	2.00
	Hm	0.76	0.93	0.12	0.84	0.00	0.12	0.27	0.22
	DiWo	0.00	0.00	0.00	0.00	1.56	0.00	0.76	0.08
	DiEn	0.00	0.00	0.00	0.00	1.23	0.00	0.66	0.07
	DiFs	0.00	0.00	0.00	0.00	0.15	0.00	0.00	0.00
	HyEn	3.56	5.53	3.36	3.04	2.26	2.59	2.88	3.71
	HyFs	0.00	0.00	0.00	0.00	0.27	0.00	0.00	0.00
	Q	20.77	27.72	24.07	28.25	14.19	22.88	19.37	20.06
	O1Fo	0.00	0.00	0.00	0.00	0.00	0.00	0.00	0.00

	No	A9-9	A10-10	A5-20	B7-22	V7-42	B4-19	BX-12	BX-9	BX-2
	Type	Micro Adamellite	Micro Granodiorite	Micro Granodiorite Qtz	Micro-Monzodiorite	Granodiorite	Spessartite Lamprophyre	Spessartite Lamprophyre	Spessartite Lamprophyre	Spessartite Lamprophyre
Major (wt %)	Si02	72.09	69.11	65.62	63.35	68.97	59.92	58.87	62.76	59.9
	Ti02	0.30	0.40	0.45	0.49	0.84	0.76	1.18	0.80	0.94
	A1203	14.17	15.37	15.78	15.78	13.50	15.96	15.19	15.26	15.06
	Fe203	1.73	1.34	1.65	2.04	1.09	3.02	4.01	3.34	3.68
	FeO	0.68	0.99	0.90	0.70	3.15	2.67	3.47	4.01	4.22
	MnO	0.06	0.06	0.10	0.02	0.04	0.06	0.10	0.06	0.08
	MgO	1.08	1.10	1.16	1.39	1.48	2.79	2.73	2.64	2.38
	CaO	1.50	2.19	2.88	1.92	0.46	2.92	2.68	2.56	2.41
	Na2O	4.48	5.01	3.72	5.01	3.75	3.92	3.75	3.53	3.72
	K20	4.28	3.57	3.50	3.35	3.98	2.83	3.46	3.12	3.60
	P205	0.09	0.12	0.12	0.13	0.13	0.28	0.09	0.06	0.12
	L0I	1.47	1.85	2.96	3.73	1.09	3.21	2.40	2.66	3.01
	Total	101.93	101.11	98.84	97.91	98.48	98.34	97.93	100.80	99.12
Trace (ppm)	Ba	587	963	1015	940	509	846	443	581	510
	Ce	39	23	23	31	23	26	26	23	26
	Co	0	6	5	18	16	8	19	17	19
	Cr	10	37	33	29	38	33	44	38	41
	Cu	10	6	7	12	8	7	12	14	6
	Ga	19	17	19	19	17	19	16	17	18
	La	21	10	12	15	9	7	6	9	11
	Nb	11	15	12	12	14	29	10	13	11
	Ni	5	8	9	14	11	9	14	12	14
	Pb	21	13	14	14	3	4	6	5	3
	Rb	107	80	75	90	83	75	74	112	87
	S	28	30	26	73	34	29	38	42	31
	Sr	462	650	578	642	333	85	197	170	146
	Th	9	12	8	9	3	10	4	6	4
	U	6	2	1	2	2	3	2	4	3
	Y	7	7	9	13	19	20	17	16	19
	Zn	16	26	37	26	32	54	53	61	59
	Zr	133	155	158	176	188	494	213	187	217
CIPW norm	Ap	0.21	0.28	0.28	0.30	0.65	0.30	0.93	0.31	0.93
	Il	0.57	0.76	0.86	0.93	1.44	1.60	2.28	1.52	1.82
	Or	25.29	21.10	20.68	19.80	16.72	23.52	20.57	18.35	21.13
	Ab	37.90	42.38	31.47	42.38	33.16	31.72	31.44	29.87	31.44
	An	5.92	8.91	13.50	8.68	12.66	1.43	12.51	12.79	11.12
	C	0.00	0.00	0.92	0.73	1.81	2.50	0.61	1.43	1.02
	Mt	1.32	1.94	1.60	0.84	4.38	1.58	5.80	4.87	5.34
	Hm	0.26	0.00	0.55	1.46	0.00	0.00	0.00	0.00	0.00
	DiWo	0.39	0.49	0.00	0.00	0.00	0.00	0.00	0.00	0.00
	DiEn	0.34	0.42	0.00	0.00	0.00	0.00	0.00	0.00	0.00
	DiFs	0.00	0.01	0.00	0.00	0.00	0.00	0.00	0.00	0.00
	HyEn	1.65	2.32	2.89	3.46	6.95	3.69	6.84	6.64	5.96
	HyFs	0.00	0.04	0.00	0.00	1.15	3.50	1.00	3.24	3.22
	Q	44.37	25.70	23.02	15.57	16.14	27.51	13.98	16.62	14.76
	O1Fo	0.00	0.00	0.00	0.00	0.00	0.00	0.00	0.00	0.00

	No	A8-8	A12-12	A14-14	A15-15	A1-1	A5-5	A6-6	A7-7
	Type	Silicified Micro-granodiorite	Silicified Micro-granodiorite	Silicified Micro-granodiorite	Silicified Micro-granodiorite	Silicified Micro-granodiorite	Silicified Micro-granodiorite	Silicified Micro-granodiorite	Silicified Micro-granodiorite
Major (wt %)	Si02	69.24	69.22	69.83	70.88	72.86	70.46	73.90	70.10
	Ti02	0.24	0.30	0.16	0.31	0.16	0.25	0.25	0.25
	A1203	14.34	14.61	14.46	14.62	13.99	14.30	14.23	14.86
	Fe203	2.09	1.84	1.40	1.96	1.56	1.79	1.39	2.14
	FeO	0.66	0.70	0.68	0.84	0.52	0.68	0.80	0.50
	MnO	0.04	0.06	0.04	0.07	0.00	0.07	0.04	0.02
	MgO	1.02	1.06	0.96	0.96	0.73	0.82	0.77	1.08
	CaO	1.68	2.22	1.20	2.04	1.92	2.68	4.06	1.97
	Na2O	0.55	0.00	2.13	0.00	0.70	0.66	0.36	1.12
	K20	4.39	2.84	5.18	2.88	4.82	4.22	4.04	4.22
	P205	0.09	0.13	0.07	0.12	0.09	0.14	0.11	0.12
	L0I	4.86	6.43	3.21	3.76	2.94	3.46	3.84	4.47
	Total	99.20	99.41	99.32	98.44	100.29	99.53	103.79	100.85
Trace (ppm)	Ba	644	475	692	458	502	1090		674
	Ce	176	192	115	216	123	124		130
	Co	0	1	3	0	0	0		0
	Cr	0	3	0	3	0	2		1
	Cu	50	97	19	80	61	59		61
	Ga	14	16	14	14	17	14		13
	La	94	98	53	102	56	54		66
	Nb	11	11	11	15	13	11		12
	Ni	1	0	3	0	1	1		0
	Pb	18	8	19	7	15	12		9
	Rb	97	59	126	53	112	89		93
	S	73	43	47	45	47	120		99
	Sr	145	143	122	144	140	132		102
	Th	9	12	8	10	6	8		12
	U	3	2	2	3	1	3		3
	Y	17	22	23	25	18	19		18
	Zn	18	28	26	26	29	25		18
	Zr	126	145	112	165	106	114		119
CIPW norm	Ap	0.21	0.30	0.16	0.28	0.21	0.32	0.26	0.28
	Il	0.46	0.57	0.30	0.59	0.30	0.48	0.48	0.48
	Or	25.94	16.78	30.61	17.02	28.48	24.94	23.88	24.94
	Ab	4.65	0.00	18.02	0.00	5.92	5.58	3.04	9.48
	An	7.75	10.16	5.50	9.34	8.94	12.38	19.42	8.99
	C	5.84	7.81	3.34	8.08	4.35	4.12	2.15	5.16
	Mt	1.43	1.39	1.73	1.81	1.21	1.47	1.85	0.89
	Hm	1.10	0.88	0.21	0.71	0.72	0.78	0.11	1.53
	DiWo	0.00	0.00	0.00	0.00	0.00	0.00	0.00	0.00
	DiEn	0.00	0.00	0.00	0.00	0.00	0.00	0.00	0.00
	DiFs	0.00	0.00	0.00	0.00	0.00	0.00	0.00	0.00
	HyEn	2.54	2.64	2.39	2.39	1.82	2.04	1.92	2.69
	HyFs	0.00	0.00	0.00	0.00	0.00	0.00	0.00	0.00
	Q	44.37	52.38	33.81	54.39	45.39	43.90	46.80	41.94
	O1Fo	0.00	0.00	0.00	0.00	0.00	0.00	0.00	0.00

	No	V5-40	V6-41	V8-43	V9-44	A13-13	V1-37	V2-38	B3-39
	Type	Andesite	Andesite	Andesite	Andesite	Andesite	Andesite	Andesite	Andesite
Major (wt %)	Si02	55.49	60.07	59.84	56.60	53.01	60.33	52.86	52.72
	Ti02	1.46	1.04	1.02	1.04	1.12	0.60	1.40	1.44
	A1203	16.06	16.79	17.00	15.96	17.28	16.72	16.07	16.21
	Fe203	3.19	2.54	2.11	4.29	4.61	2.24	6.36	1.55
	FeO	4.48	3.96	3.96	4.23	2.64	2.69	1.60	6.21
	MnO	0.10	0.14	0.08	0.12	0.10	0.10	0.14	0.10
	MgO	4.26	4.23	2.30	4.52	4.29	3.55	5.58	5.31
	CaO	2.84	0.98	2.36	1.77	2.02	2.14	4.19	4.16
	Na2O	4.38	3.20	4.18	3.17	2.94	5.16	5.29	3.79
	K20	1.82	4.49	2.87	3.16	4.30	2.81	2.06	2.11
	P205	0.27	0.20	0.25	0.31	0.16	0.22	0.30	0.27
	L0I	6.27	4.23	3.91	5.93	4.27	2.21	2.87	5.89
	Total	100.62	101.87	99.88	101.10	96.74	98.81	98.72	99.76
Trace (ppm)	Ba	285	1041	497	289	441	479		291
	Ce	23	29	40	14	27	32		36
	Co	31	25	13	13	31	19		36
	Cr	200	30	31	58	51	95		116
	Cu	20	33	15	11	33	21		32
	Ga	18	16	19	19	17	19		16
	La	10	7	14	6	16	11		15
	Nb	13	10	13	13	10	12		16
	Ni	64	15	7	15	36	22		66
	Pb	6	10	3	11	14	5		0
	Rb	34	113	66	89	148	84		52
	S	48	45	31	52	67	32		29
	Sr	441	229	236	200	122	358		373
	Th	0	7	2	5	4	3		0
	U	3	4	2	3	2	2		2
	Y	20	23	30	20	21	19		23
	Zn	100	102	75	129	105	77		108
	Zr	207	193	257	190	161	198		219
CIPW norm	Ap	0.68	0.46	0.58	0.72	0.37	0.51	0.70	0.63
	Il	2.77	1.98	1.94	1.98	2.13	1.14	2.66	2.74
	Or	10.76	26.54	16.96	18.68	25.41	16.61	12.17	12.47
	Ab	37.05	27.07	35.36	26.82	24.87	43.65	44.75	12.47
	An	12.33	3.56	10.08	6.76	8.98	9.18	14.02	18.87
	C	2.37	5.36	3.32	4.85	4.50	1.83	0.00	0.78
	Mt	4.62	3.68	3.06	6.27	5.26	3.25	1.10	2.25
	Hm	0.00	0.00	0.00	0.00	0.98	0.00	5.60	0.00
	DiWo	0.00	0.00	0.00	0.00	0.00	0.00	2.01	0.00
	DiEn	0.00	0.00	0.00	0.00	0.00	0.00	1.74	0.00
	DiFs	0.00	0.00	0.00	0.00	0.00	0.00	0.00	0.00
	HyEn	10.61	10.53	5.73	11.26	10.68	8.84	8.13	13.22
	HyFs	3.18	3.46	3.84	2.51	0.00	2.10	0.00	7.74
	Q	9.92	14.86	15.01	15.27	9.18	9.35	0.00	3.00
	O1Fo	0.00	0.00	0.00	0.00	0.00	0.00	2.83	0.00

The effects of deuteric alteration on bulk major element composition of volcanic rocks has been documented by Wilshire (1959), whilst Philpotts et al (1969) indicate mobility of K, Rb, Sr, Ba and certain Rare Earth Elements (REE) during weathering and metamorphism. Results of a study into compositional changes during alteration in Archaean volcanic terrains (Condie et al 1977) indicate that CO_2, H_2O, Fe^{2+}, Ti, Zn, Y, Nb, Fa and LREE are enriched, whilst Na, Sr, Cr, Ba, Fe^{3+}, Ca, Mn and U are depleted during carbonization-chloritization. In alteration of up to 10% carbonization the elements least affected are Ni, Co, Zr, Th and HREE. For the purposes of this study, particular attention is drawn to REE, Th, TiO_2, Na_2O, Y, Zr, Zn, Nb, Ga, Co, Fe total, Cr, Sr, Ni and Cu; elements considered by Condie (1982) to show little or no change during early alteration and metamorphism.

3.3.3 Classification by Nomenclature

Acid clasts

The inadequacy of the various different chemical approaches which can be applied to naming acid igneous rocks (SiO_2>62%) has been noted by many workers. Amongst the most popular classifications is that proposed by Streckeisen (1976a,b) using IUGS nomenclature. In this, a triangular plot is used with the three apices being: Q (quartz); A (alkali feldspar); and P (plagioclase). This diagram can be used in a modal sense (volume percent mineralogy) as intended, or using normative components (CIPW norms calculated from the major oxides). On the basis of their geochemistry (Fig.3.12) the majority of samples fall within the granodiorite field, although, according to Hatch et al (1972) may be more correctly known as adamellites using modal components (alkali feldspar and plagioclase approximately equal). From the Q:A:P diagram a significant number of clasts are classified as monzogranite and quartz monzonite.

Debon and Le Fort (1982) noted this general lack of agreement amongst chemical classifications and recognised the merits of Streckeisen's scheme. They have proposed the most comprehensive typology for common igneous rocks based mainly on major element data in which analyses are classified initially on a slightly modified QAP diagram using the nomenclature of La Roche (1966) and Streckeisen (1974, 1976a) and are qualified by plotting on additional diagrams which determine peraluminous/metaluminous nature

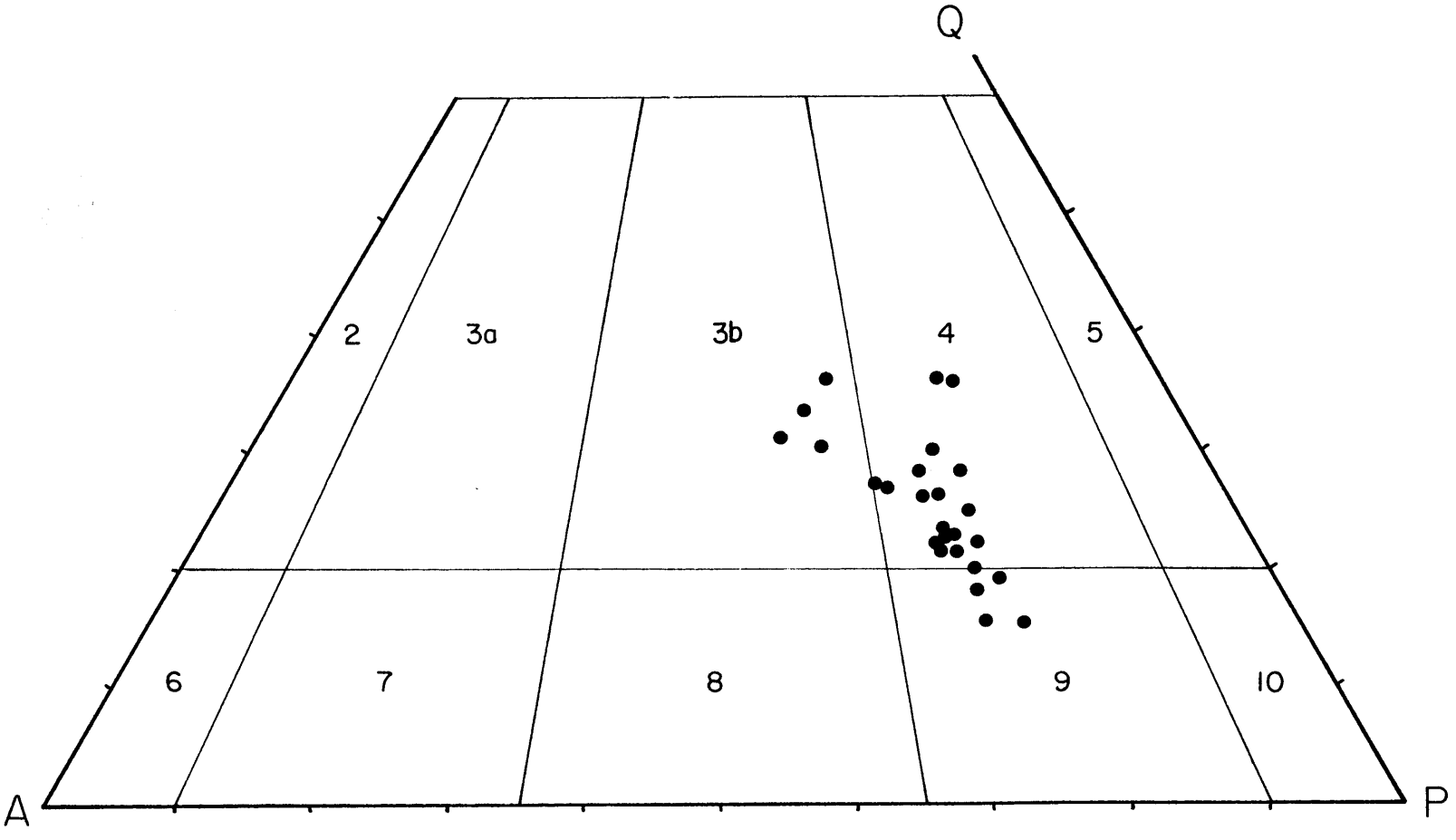

Fig 3.12. QAP nomenclature diagram (after Streckeisen 1976) showing fields for plutonic rocks: 2 alkali granite; 3a syenogranite; 3b monzogranite; 4 granodiorite; 5 quartz diorite; 6 alkali syenite; 7 syenite; 8 monzonite; 9 monzodiorite/monzogabbro; 10 diorite/gabbro.

and characteristic minerals. For acid plutonic and hypabyssal rocks the nomenclature obtained using the Q:P grid (Fig. 3.13) agrees well with that obtained by using mormative and modal components on the Q:A:P diagrams. The majority of acid clasts are classified as granodiorites but there are also representatives of adamellite, quartz monzodiorite and monzonite. Most of these compositions are poor in quartz but rich or very rich in feldspar in comparison with the average model composition for the relevant types (Debon and Le Fort). On the A:B plot (Fig. 3.14) the acid rocks straddle the sector III/IV boundary. As predicted by the diagram all analyses falling within sector IV (amphibole common) display hornblende phenocrysts in thin section whereas hornblende is consistently absent from all rocks in sector III (biotite common).

Intermediate rocks

Chemical classification and nomenclature for the volcanic/hypabyssal rocks of intermediate composition provide few problems. Using normative components on the Q:A:P triangular plot (Fig. 3.12) these clasts would be classified as trachyandesites, possibly more correctly known as quartz latites. On most of the discriminant diagrams devised by Winchester and Floyd (1977) employing immobile trace elements, the samples are andesite or transitional to quartz latite (Fig. 3.15). On the basis of texture and mineralogy however, many of these rocks are considered to be spessartitic lamprophyres (section 3.2.2.).

It is interesting to note that in comparison with model compositions of common intermediate rocks (Debon and Le Fort 1982). The Roseneath lamprophyres and porphyritic andesites are exceptionally depleted in CaO. This is clearly in agreement with the low anorthite component in plagioclases detected optically in thin section (see section 3.2.2) and may reflect an unusually highly evolved magma.

3.3.4 Classification by Multivariate Analysis

In the preceeding section, nomenclatural classification of the igneous clasts using major element chemistry suggested distinct clustering of samples, with similar compositions observed for many analyses. This is particularly true for the acid hypabyssal and plutonic clasts. To further investigate this grouping, and in an attempt to determine genetic relationships between acid

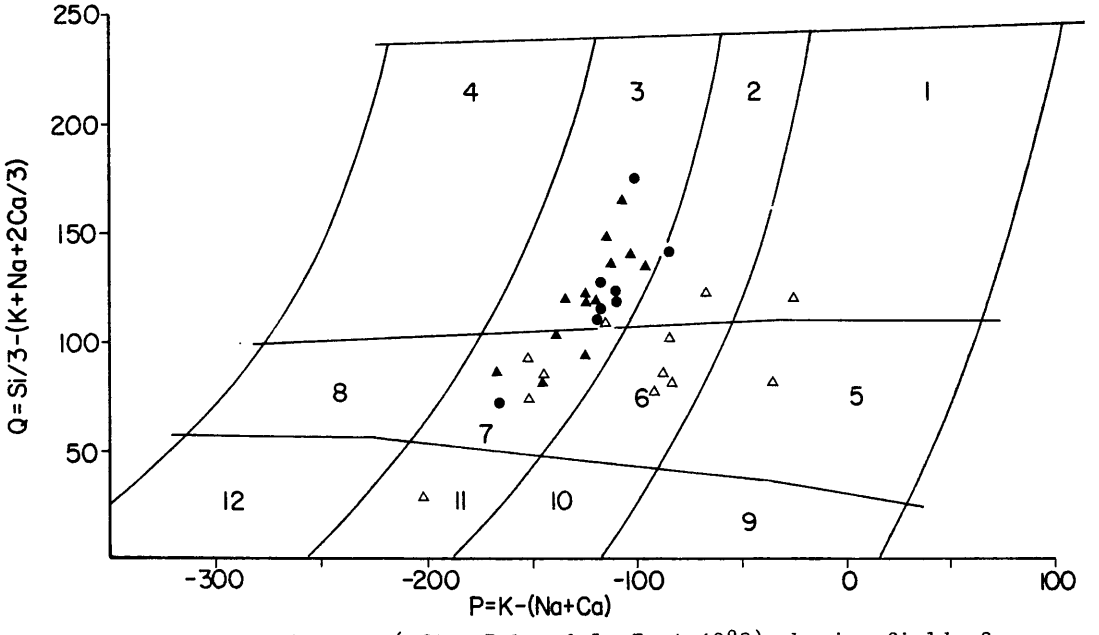

Fig 3.13. QP nomenclature diagram (after Debon & Le Fort 1982) showing fields for common igneous rocks: 1 granite; 2 adamellite; 3 granodiorite; 4 tonalite; 5 quartz syenite; 6 quartz monzonite; 7 quartz monzodiorite; 8 quartz diorite; 9 syenite; 10 monzonite; 11 monzogabbro; 12 gabbro. (●) Acid plutonic; (▲) acid hypabyssal; (△) intermediate hypabyssal.

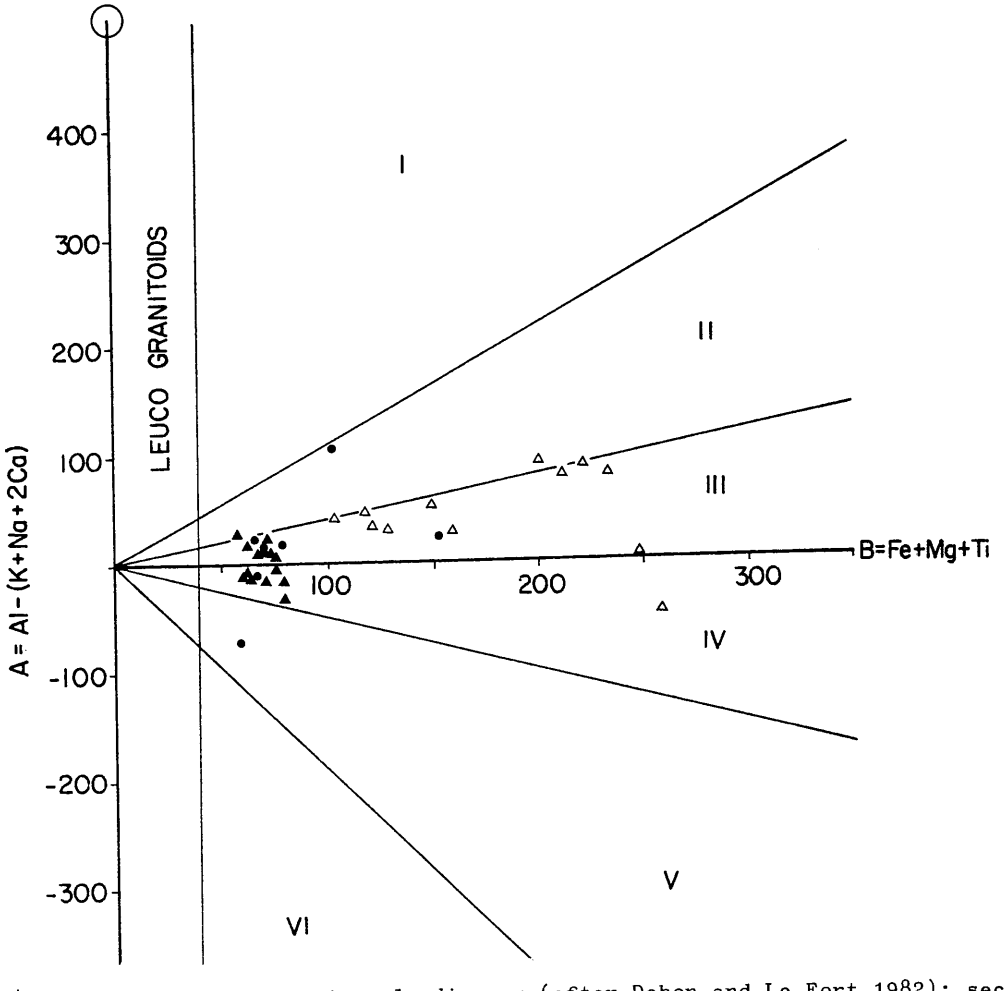

Fig 3.14. AB characteristic minerals diagram (after Debon and Le Fort 1982): sector I - muscovite alone or muscovite > biotite; sector II - biotite > muscovite; sector III - biotite alone; sector IV - amphibole and biotite common; sector V - clinopyroxene and/or epidote and/or sphene; sector Vi - exceptional compositions. Symbols as for Fig 3.13.

Fig 3.15. (next page). Immobile trace element discriminant diagrams for intermediate volcanic rocks (from Winchester & Floyd 1977): a) Zr/Ti:SiO2; b) Nb/Y:SiO2; c) Nb/Y:Zr/Ti; d) Ce:Zr/Ti; e) Ga:Zr/Ti. 1 rhyolite; 2 rhyolite/dacite; 3 andesite; 4 tholeiite; 5 alkali rhyolite; 6 trachyandesite; 7 olivine basalt; 8 trachyte; 9 phonolite; 10 basanite.

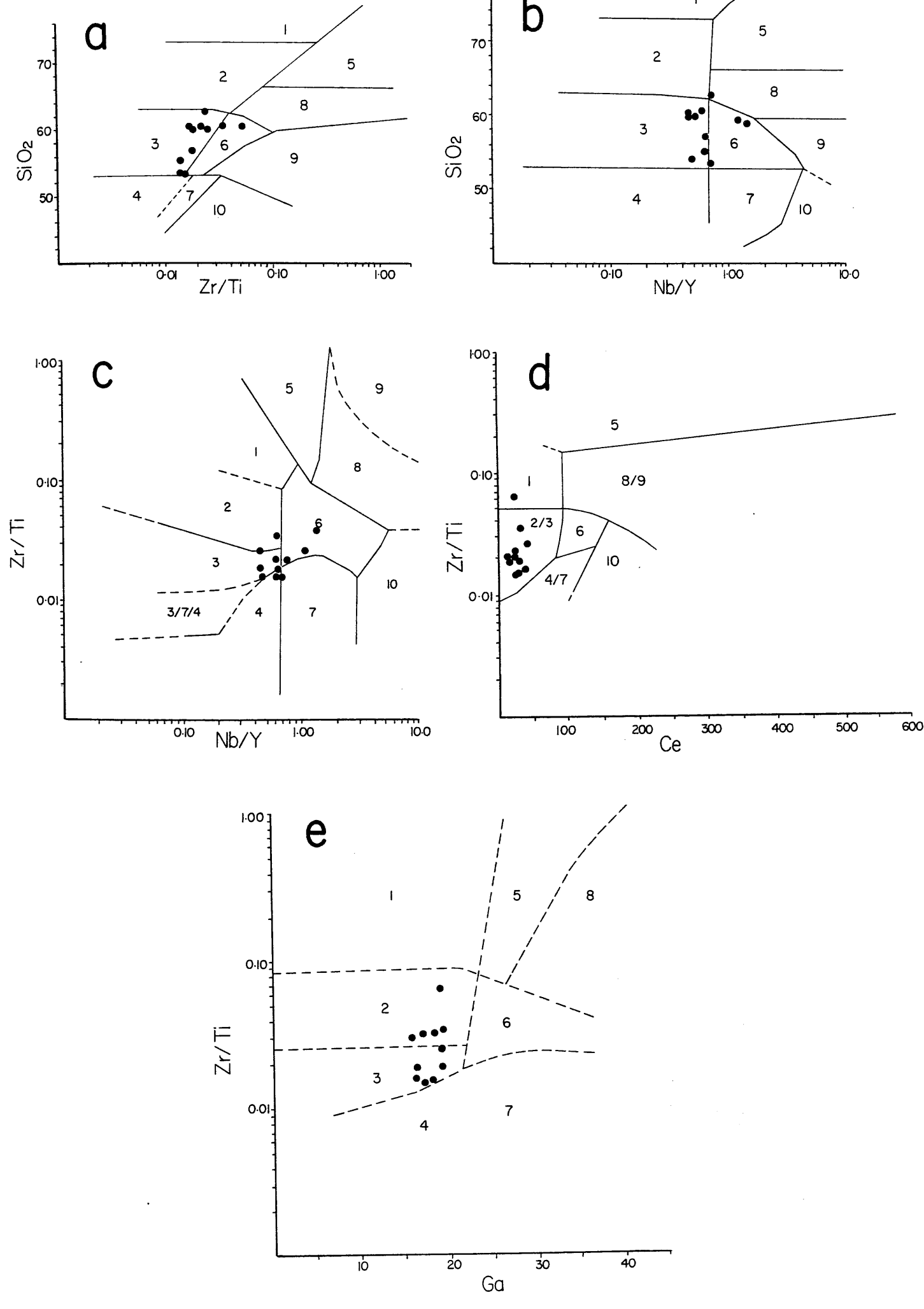
a
SiO2
70
60
50
Zr/Ti
0·01
0·10
1·00
1
2
3
4
5
6
7
8
9
10
b
SiO2
70
60
50
Nb/Y
0·10
1·00
10·0
1
2
3
4
5
6
7
8
9
10
c
Zr/Ti
1·00
0·10
0·01
Nb/Y
0·10
1·00
10·0
1
2
3
3/7/4
4
5
6
7
8
9
10
d
Zr/Ti
1·00
0·10
0·01
Ce
100
200
300
400
500
600
1
2/3
4/7
5
6
8/9
10
e
Zr/Ti
1·00
0·10
0·01
Ga
10
20
30
40
1
2
3
4
5
6
7
8

and intermediate types, trace element data were subjected to multivariate analysis. For the purposes of this study, cluster analysis was chosen in preference to factor analysis since it employs a more straightforward pair by pair comparison between variables (chemical elements) and samples, with definition of groups being possible at any desired level of similarity.

Method

As a preliminary to clustering, trace element concentrations are set up in a standardized data matrix where the concentration of all elements is transformed to range from 0 to 1.

Since it is known that several highly correlated elements can bias the results of a cluster analysis of samples (Q-type analysis), an R-type analysis (clustering of inter-element correlation coefficients) is first performed on the data matrix following the method outlined by Parks (1966). The resulting variable clustering by correlation coefficient is shown in Fig. 3.16. It is clear from this diagram that pairs and groups of many elements are not significantly related until low levels of correlation. However, two groups of elements (Ce, La, Cu and Cr, Ni, Co, Zn) have high enough correlation coefficients as to make their members redundant in a Q-type cluster analysis. One element is chosen to represent each group (in this case Cu and Cr respectively), the remaining elements being eliminated without much loss of information.

The final clustering of samples (Q-type analysis) is carried out using similar procedures to those in the R-type analysis except that the correlation coefficient is replaced by the distance function formula. The distance (D) or similarity between two objects in a multidimensional hyperspace of M dimensions (M = number of variables) is:

$$D_{1,2} = \sqrt{\left[\sum_{i=1}^{M} (X_{i1}-X_{i2})^2/M\right]}$$

where X is the normalized value of the variables. The distance function calculated ranges from 0 (greatest similarity) to 1 (greatest dissimilarity). Distance function clusters for 39 samples used in this study are shown in Fig. 3.17a.

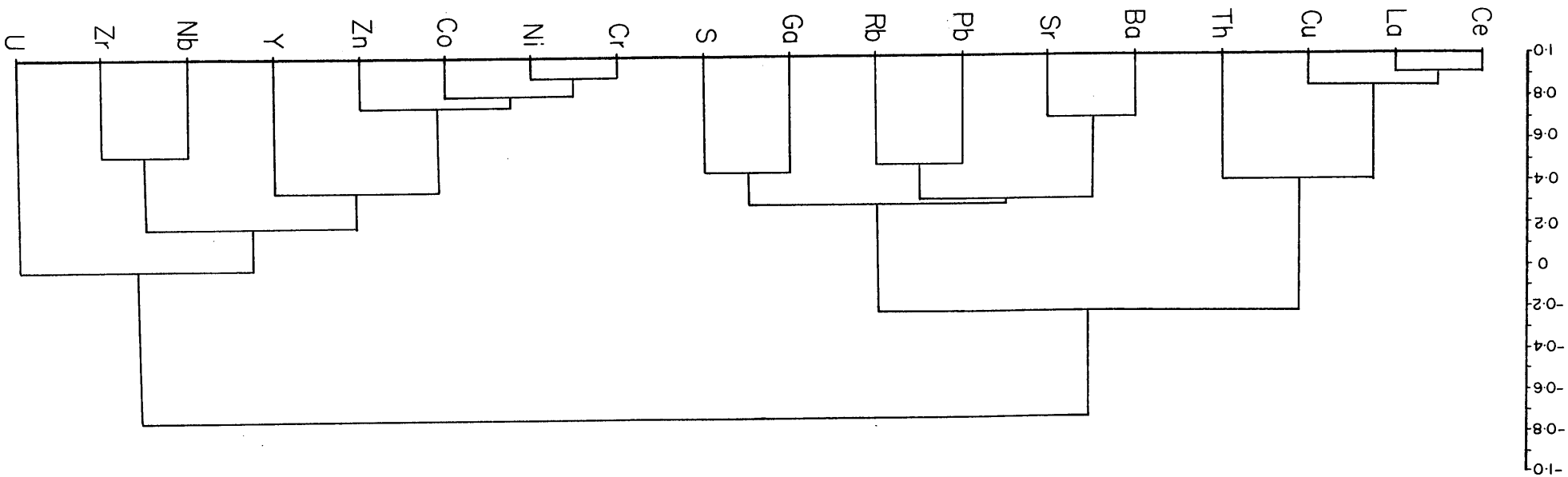

Fig 3.16. Trace element clustering (R-type) by correlation coefficient for Roseneath igneous clasts (all compositions).

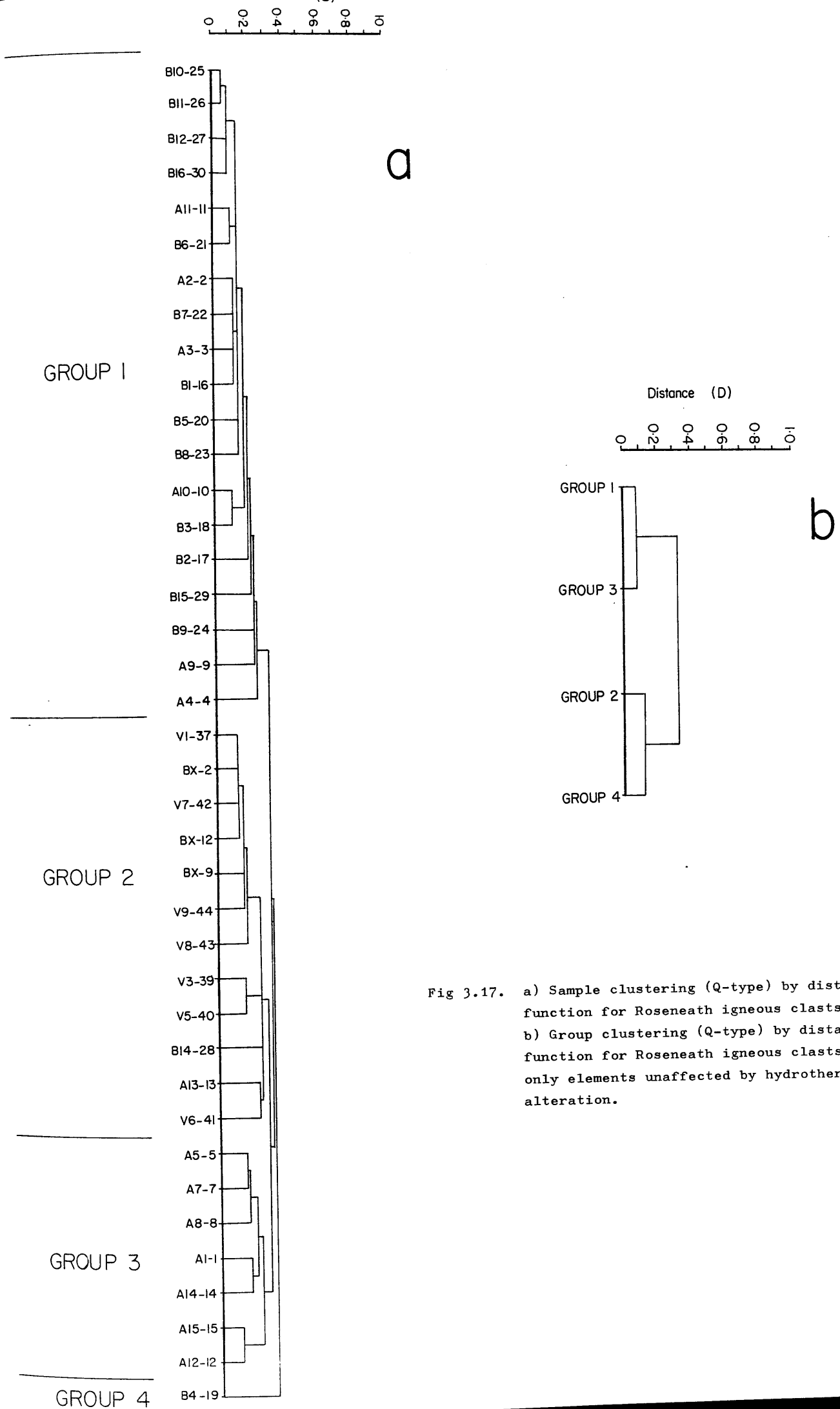

Fig 3.17. a) Sample clustering (Q-type) by distance function for Roseneath igneous clasts.
b) Group clustering (Q-type) by distance function for Roseneath igneous clasts using only elements unaffected by hydrothermal alteration.

Interpretation of Q-type Analysis

Unlike correlation analysis it is not possible to calculate a critical value for D at which clusters form at significant levels of similarity. With this in mind, a general observation from Fig. 3.17a is that four groups of clusters of samples are apparent at $D<0.25$. Group 1 contains the majority of acidic hypabyssal and plutonic clasts previously classified as granites, granodiorites or quartz monzonites. Group 2 encompasses all the intermediate clasts of trachyandesite composition. The hydrothermally altered acid rocks cluster into Group 3, whilst Group 4 contains only one sample, previously identified as granodiorite and now shown to display no significant similarities with any of the other three groups.

Another observation from the cluster diagram is the clear distinction between the predominantly intermediate Group 2 and the predominantly acidic Group 1. In fact Group 2 has greater similarities with the hydrothermally altered acid clasts of Group 3 than either has with Group 1. The apparent lack of similarity between the Group 1 acid clasts and the hydrothermally altered porphyries (Group 3) is not unexpected considering the major chemical modifications during alteration (Section 3.3.5). Cluster analysis using single sample representatives of the four groups identified above and only those elements whose concentrations are known to have been unmodified during alteration (see Fig. 3.2) produces the pattern shown in Fig. 3.17b. Clearly Groups 1 and 3 now have high similarities and are quite discrete from Groups 2 and 4, which themselves display interestingly high similarity.

3.3.5 Hydrothermally Altered Rocks

In thin section these rocks appear identical to the unaltered clasts of acid igneous material except that plagioclase feldspars are always in various stages of replacement (Figs. 3.18 to 3.19). The nature of the replacing mineral is unknown but seems to take the form of a fine grained microcrystalline aggregate of chert with clay and/or zeolite.

The major and trace element chemistry of whole rock samples (Table 3.1) is considerably modified relative to unaltered specimens with both enrichment and depletion of specific elements (Table 3.2), together with the dominance of Q in the CIPW norm. Those elements which are depleted relative to

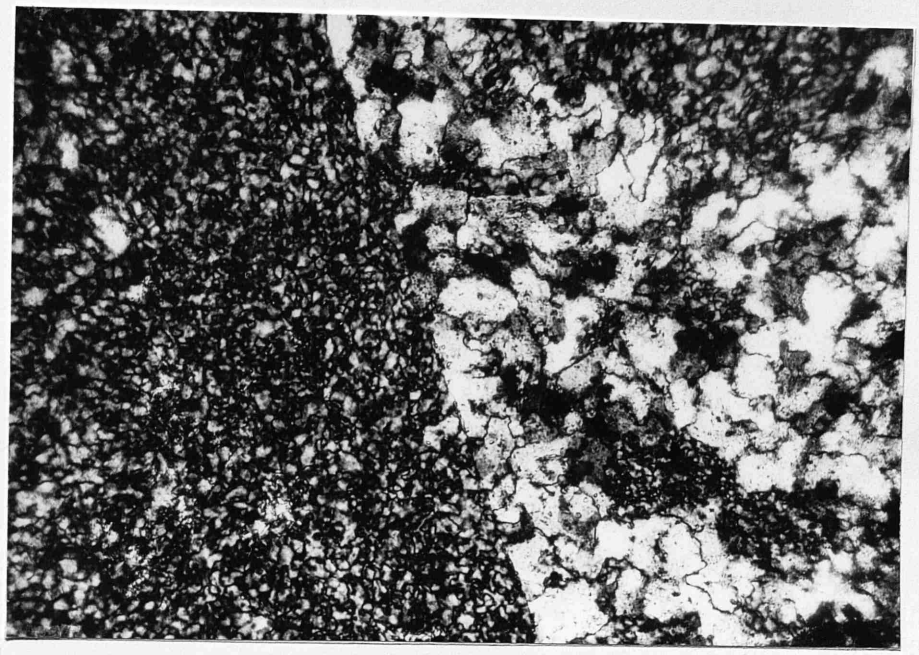

Fig 3.18. TS photomic, XPL, X10, silicified microgranodiorite, Roseneath. Replacement of matrix (top left quadrant) and large feldspar phenocryst by microcrystalline quartz.

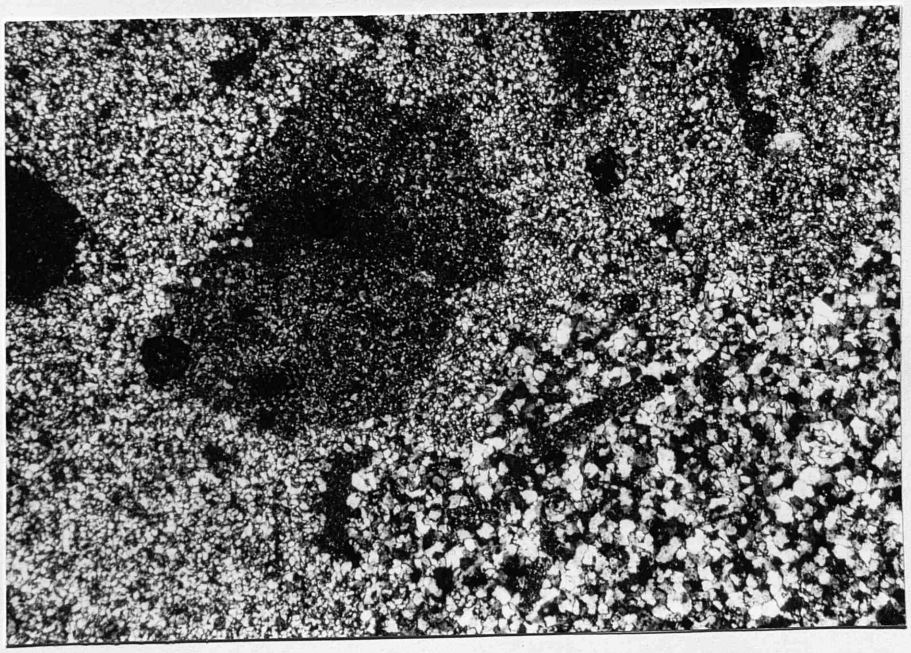

Fig 3.19. TS photomic, XPL, X10, silicified microgranodiorite, Roseneath. Detail of boundary between silicified matrix (left) and silicified feldspar phenocryst (right). Note the finer grain of the microcrystalline quartz replacing the feldspar.

	Enriched		Depleted		No Change
Major	SiO_2	+ 4%	Al_2O_3	- 6%	Fe_2O_3
			TiO_2	-42%	FeO
			Na_2O	-86%	MgO
					CaO
					K_2O
					MnO
					P_2O_5
Trace	S	+44%	Zr	-17%	U
	Cu	+74%	Sr	-82%	Rb
	Ce	+74%	Ga	-19%	Th
	La	+73%	Ni	-90%	Pb
	Y	+54%	Co	-86%	Zn
	(Ce + La)/Y	+42%	Cr	-95%	
			Ba	-48%	

TABLE 3.2 Percent enrichment or depletion of selected elements in altered porphyries relative to unaltered specimens.

unaltered porphyry concentrations are notably those contained within the Na-feldspar framework, indicating that plagioclase is probably the only mineral to be affected. Almost total removal of Na_2O dominates these changes.

The chert-like appearance of the replacive mineral might suggest that silification was the dominant process, as is the case in many high level volcanogenic environments (Grant et al 1977). However, these rocks differ from those in areas where silification has been documented (e.g. Lingren and Creveling 1928, Turneaure 1960 and Vikre 1981) insofar as silica values are only enriched by around 4% of their unaltered concentrations. Additionally, alumina, whilst depleted to a limited extent (c 6%), is still present in sufficiently large amounts to rule out simple silica replacement.

Co and Ni resemble each other in many physical and chemical properties and it is not surprizing that they have behaved similarly during replacement of the feldspar (Table 3.2). This is probably linked to an almost identical depletion in Cr (c 90%). Gallium mirrors aluminium in its behaviour and the relatively small depletion in Ga is approximately consistent with that observed for alumina. Sr and Ba show an expected sympathetic depletion. Larger quantities of Sr have been removed relative to Ba since K-feldspar will be the main Ba bearing phase in these rocks and has remained unaffected by alteration. The chemical behaviour of Y and the light rare earth elements (La and Ce) is quite similar and all three elements are enriched in the altered specimens. In addition, examination of the LREE/HREE ratio reveals that LREE are enriched by 42% relative to Y.

Cu is the most surprizing addition to the whole rock chemistry and attains levels approaching 100 ppm. Of the three valence states in which Cu exists in nature (Cu, Cu^+ and Cu^{2+}), Cu^+ is comparable in ionic size to Na^+, although there are large differences between the electronegativities of these two ions in melts (Wedepohl 1978). This, and since sulphur levels in the altered rocks appear to have been significantly enriched suggests that either Cu is present as a sulphide (although not visually identified) or that it has exchanged with Na to form an aluminium silicate incorporating Y, La and Ce. For the latter, a form of Cu-rich clay seems the most likely candidate to accompany the precipitation of quartz following dissolution of the feldspar. Possible contenders being ajoite, medmontite/cupromontmorillonite and copper vermicularite.

All the elements displaying concentration modifications, whether enriched or depleted, are reasonably easily transported in a chlorine or fluorine mobile complex and percolation of such a brine is envisaged for these rocks. Many documented examples in which this type of alteration has taken place employ a 2 phase mineralization model whereby Na is first leached from high level injected dykes by deep percolating saline solutions (with a marine source) followed by upward migration of a Cu bearing mobile complex as a late stage residue derived from the underlying plutonic mass. However, strong enrichment in LREE for these rocks probably indicates high pH and low water/rock ratios (Taylor and Fryer 1981). This is indicative of magmatic hydrothermal fluids rather than the involvement of meteoric fluids which would leach all REE and reduce the LREE/HREE ratio.

3.3.6 Geochemical Characteristics within a Caledonian Framework - Influences of Tectonic Setting

General Trends

Fig. 3.20 shows Harker-type variation diagrams for major oxides plotted against SiO_2 content for Groups 1, 2 and 4 defined in Section 3.3.3. For this type of diagram Bowen (1928) demonstrated that the shape and form of the variation curve for each oxide or trace element may be related to corresponding details in the crystallisation path when the rocks concerned all lie on a single liquid line of descent. However, as Groome and Hall (1974) observe, variation diagrams may be most significant if the rocks do not all lie on a single liquid line of descent, that is, if they do not show a smooth trend.

For major oxide data, the variation trends for the 406Ma Garabal Hill-Glen Flyne complex have also been indicated in Fig. 3.20 (data from Nockolds (1941) and Stephens and Halliday (1984)). Trends for this granitoid are typical of all Caledonian suites and comparison with Roseneath clasts are particularly important in view of the relative proximity of this complex to the Roseneath conglomerate (Fig 1.2) and clear trace element similarities to be discussed in the following sections. The clasts in the Roseneath conglomerate show general trends typical of calc-alkaline Caledonian igneous rocks originally described by Nockolds and Mitchell (1948). Al_2O_3, Fe_t, MgO, CaO, TiO_2, MnO and P_2O_5, all decrease with increasing values of SiO_2. K_2O and Na_2O show a positive correlation with SiO_2. It is also apparent that below about

Fig 3.20 (next page). Major oxide variation diagrams for Roseneath igneous clasts. Average Caledonian granitoid trends indicated. (●) Group 1 clasts; (o) Group 2 clasts.

Data from Nockolds (1941) and Stephens and Halliday (1984).

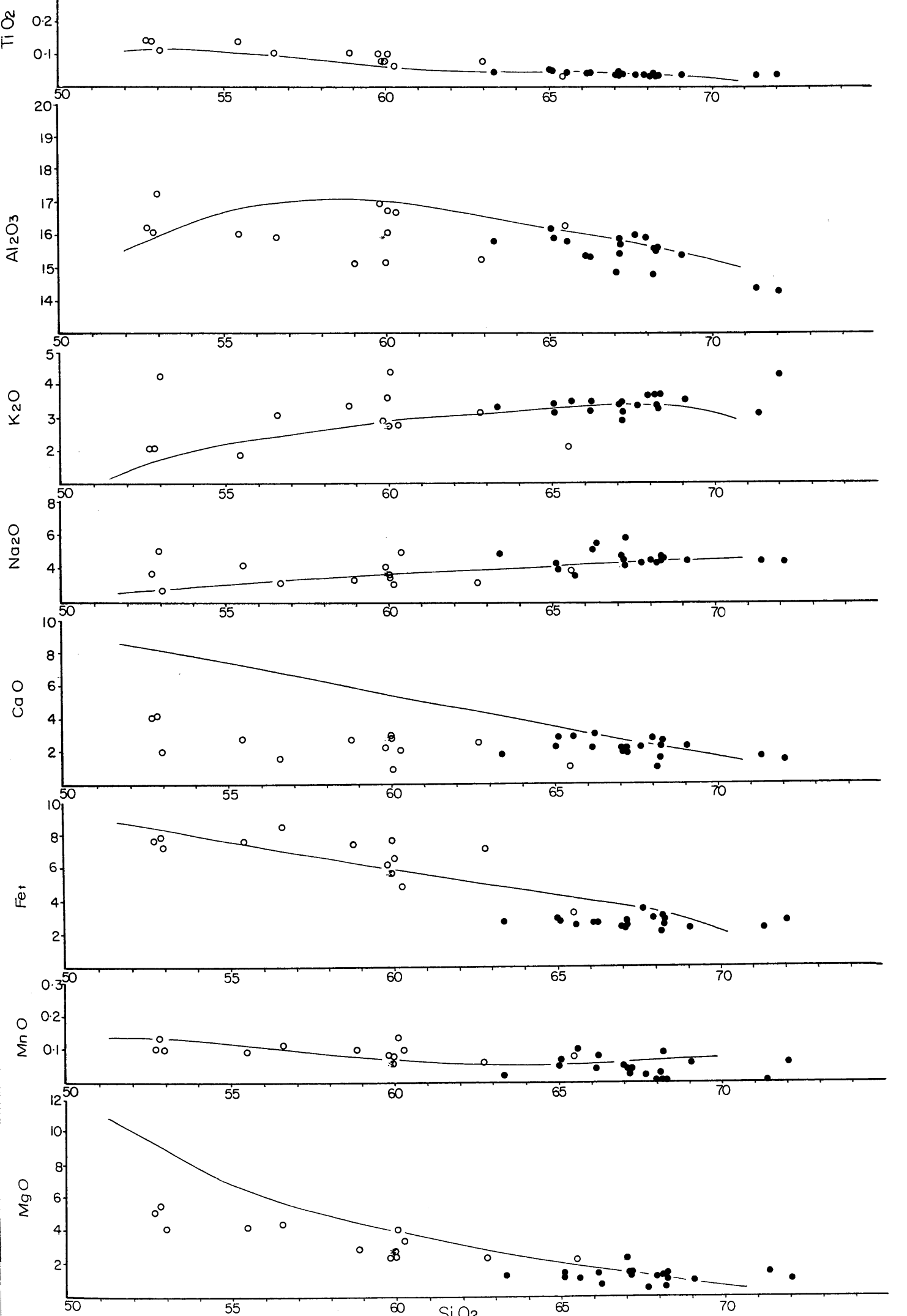
TiO2
0·2
0·1
50
55
60
65
70
Al2O3
20
19
18
17
16
15
14
K2O
5
4
3
2
Na2O
8
6
4
CaO
10
8
6
4
2
FeT
10
8
6
4
2
MnO
0·3
0·2
0·1
MgO
12
10
8
6
4
2
SiO2

63% SiO_2 there is a considerable scatter and best-fit lines become difficult to draw. This is also true for all Caledonian suites. For the Roseneath intermediate rocks, it is not thought that differing concentrations of suspended phenocrysts have caused the scatter in these diagrams since mineralogical variations in the acidic Group 1 types are not noticeably reflected in major oxide variations.

Despite these broad trends, there are distinct discontinuities between trends depicted from the acid and intermediate groups in certain Harker diagrams. This is particularly obvious in the MgO:SO_2 and Fe*O:SiO_2 plot. Such a pattern might be expected to arise after excessive deuteric alteration of the intermediate types relative to the acid clasts. Wilshire (1959) studied the bulk chemical changes in basic volcanic rocks caused by carbonate alteration. He showed that while most elements display major losses or gains, total iron showed only moderate changes (although the Fe^3/Fe^2 ratio generally increased). The total iron variation diagram Fig. 3.20 exhibits this discontinuity particularly well and implies a step at around SiO_2 60.5 to 63%. On Wilshire's evidence this is probably not due to alteration and may reflect differing evolutionary paths for the two major groups.

In fact, comparison with the Garabal Hill trend shows that the intermediate rocks probably have comparable levels of MgO and Fe*O with respect to Caledonian intrusions, and it is the acid group which displays significant depletions in both oxides. CaO levels are also low for the Group 1 acid clasts but depletions are more marked in this instance for the intermediate rocks. It is difficult to determine whether these deviations from normal Caledonian trends represent fundamental differences in parental magma compositions or simply modifications due to unusual fractionation conditions. For example the depletions can easily be explained in terms of low ferromagnesian phase contents in the granodioritic rocks and a low anorthite component for all compositions - features normally associated with highly fractionated rocks.

The overall calc-alkaline nature of the Roseneath igneous clasts is supported by the A:F:M ternary plot (Fig. 3.21) which shows an evolutionary trend associated with orogenic magmas and similar to that of Caledonian suites. This trend lies well within the calc-alkaline field of Irvine and Baragar (1971). The majority of analysed samples plot within the calc-alkaline field on the SiO_2:Fe/Mg diagram (Fig. 3.22) of Miyashiro (1974).

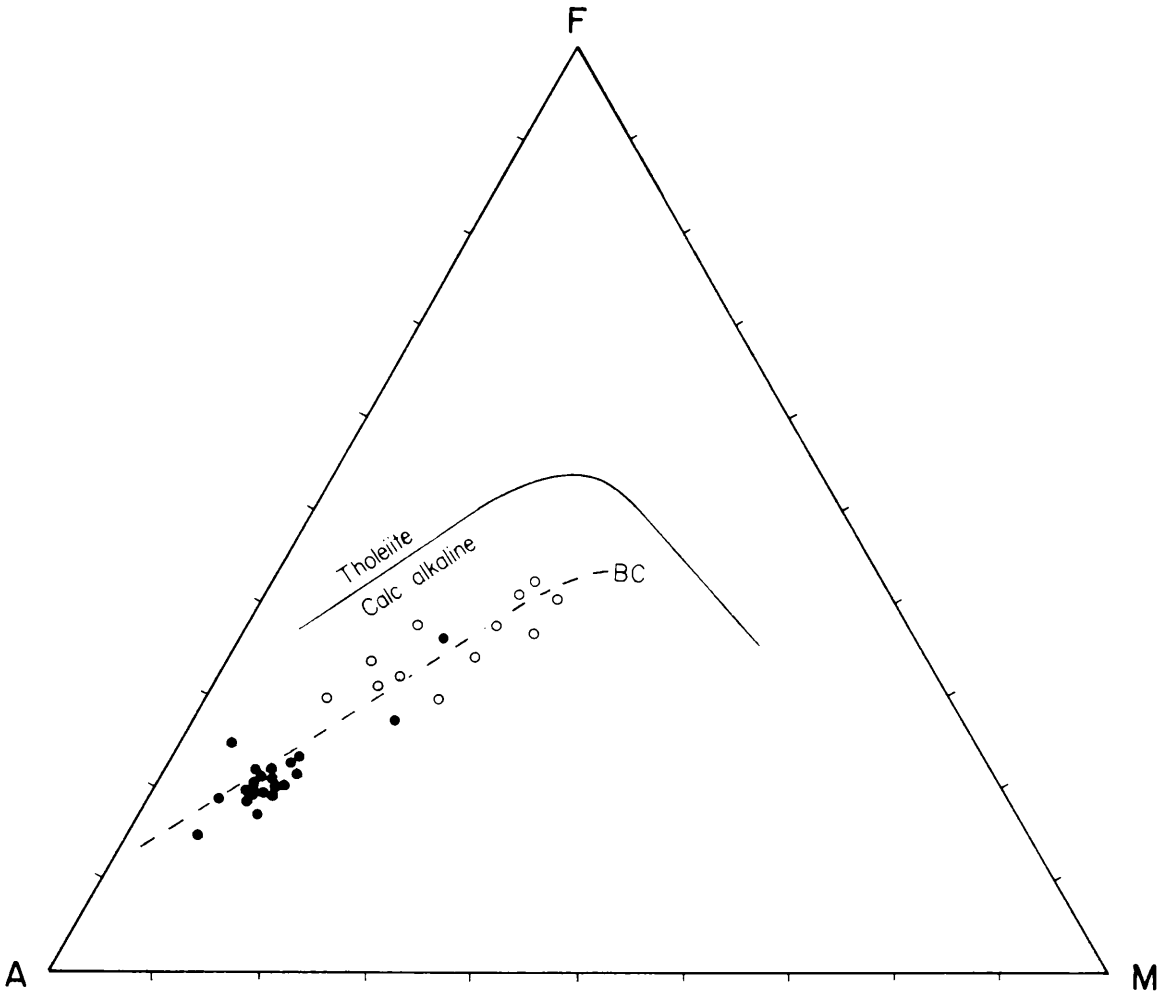

Fig 3.21. AFM ternary diagram for Roseneath igneous clasts. Symbols as for Fig 3.20.

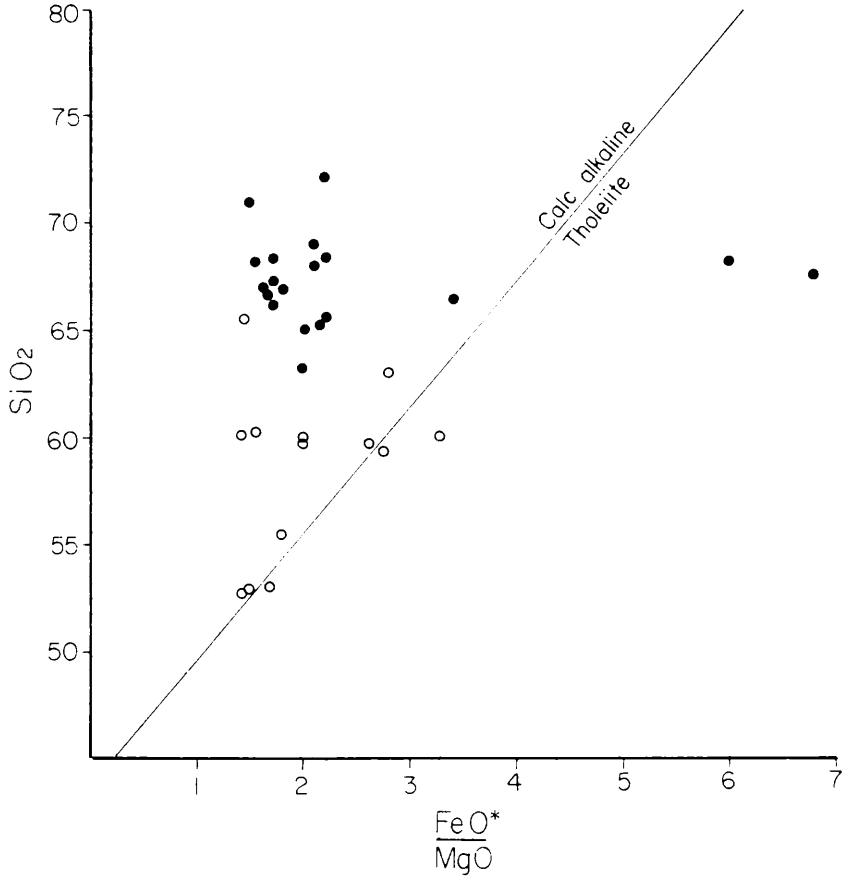

Fig 3.22. Fe/Mg:SiO2 calc-alkali diagram. Symbols as for Fig 3.20.

In Fig. 3.23a contents of K_2O against SiO_2 are compared with the four compositional fields (shoshonitic, high K, calc-alkaline and low K) of Peccerillo and Taylor (1976). With only minor exceptions the acidic Roseneath clasts fall into the field defined as high K calc-alkaline as do the majority of Caledonian granitoids (Stephens and Halliday 1984). The Group 2 intermediate and acid clasts are similarly enriched in K and this group may be transitional to the shoshonitic series (only distinguished in compositions with SiO_2<63%). In this respect rocks from both groups may be compared with orogenic hypabyssal and volcanic rocks of Tertiary to Recent age on the active continental margins of western South America (Andean), western USA (east and west subzones), and the Calabrian, Hellenic, Almerian and Anatolian regions of the Mediterranean. These contrast strongly with the island arc systems of the Western Pacific and South Shetland Islands (Ewart 1982). Both Group 1 and Group 2 clasts at Roseneath display the same slope and are equally potassic to typical continental margin suites in the K_2O:SiO_2 plot of Fig. 3.23b (generalised by Rogers and Ragland (1980) from Rogers and Novitsky-Evans (1977). However, a continental margin origin on the basis of K enrichment alone may be misleading without considering evidence from other areas. K enrichment need not be restricted to within plate continental margins (Pearce and Gale 1977).

Group 1 Clasts - Detailed Geochemistry I : Major Oxides

It has already been noted that highly homogeneous major and trace element chemistry is an important feature of all the acid clasts of Group 1 and, whilst this reinforces a comagmatic origin for the rocks, it also hinders interpretation of general magmatic trends. Similarly uniform chemical characteristics were observed by Lynch and Pride (1984) in the study of a high level, highly evolved portion of an acid magma chamber in Canada. Like the Canadian example, Group 1 analyses plot very close to the medium pressure (pH_2O = 5kb) water saturated eutectic on the Q:Ab:Or: diagram (Fig. 3.24). The predominance of samples falling within the plagioclase + alkali feldspar + liquid + vapour field illustrates the dominance of potassium feldspar as a crystallising phase.

Brown (1979, 1982) has used the calc-alkali ratio versus silica diagram calc-alkali ratio = CaO/Na_2O+K_2O)) to determine trends for various igneous provinces. Most of the Group 1 clasts plot reasonably tightly about or slightly

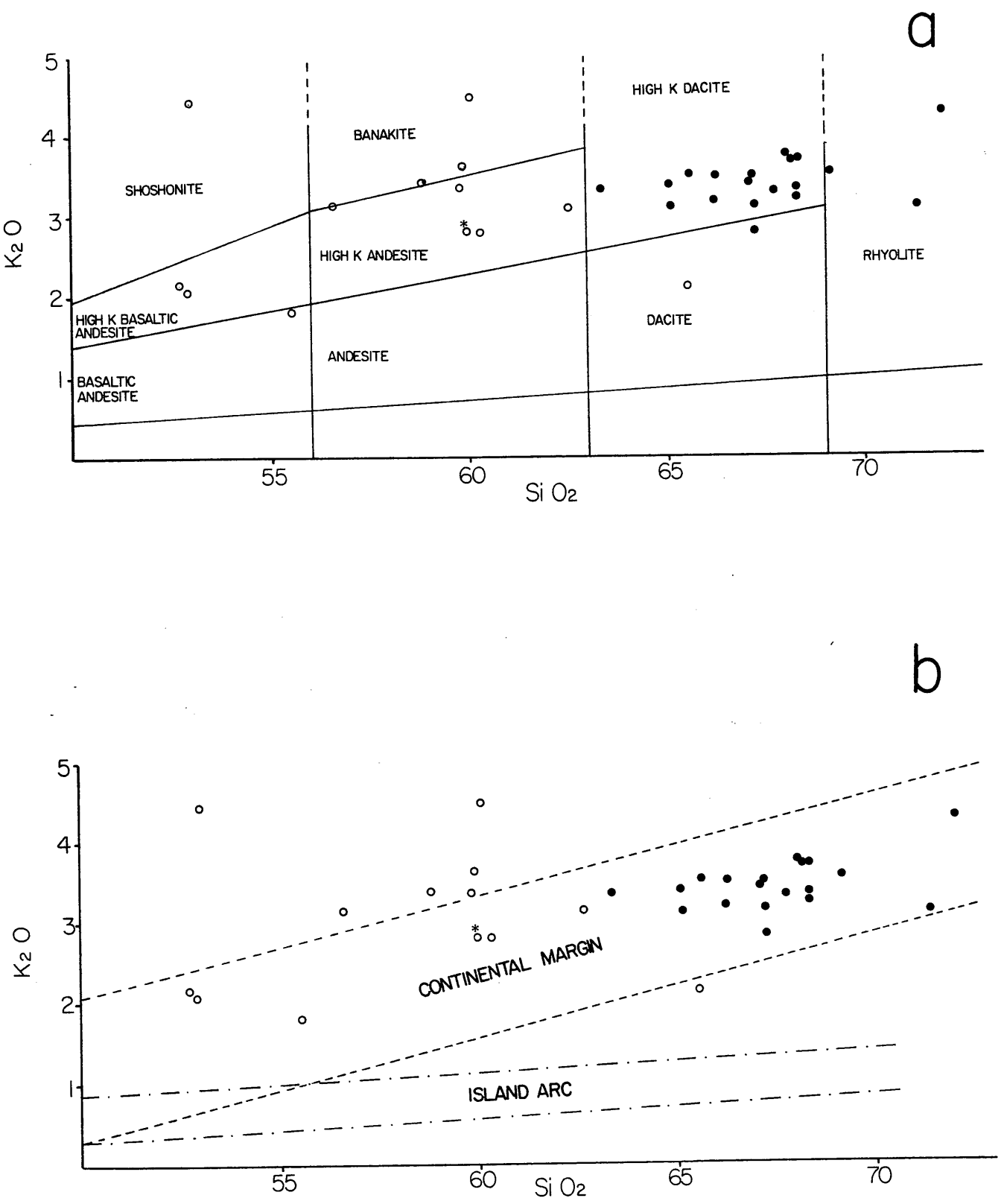

Fig 3.23. a) K20:Si02 nomenclature diagram. b) K20:Si02 diagram showing fields for continental margin and island arc granitoids. Symbols as for Fig 3.20.

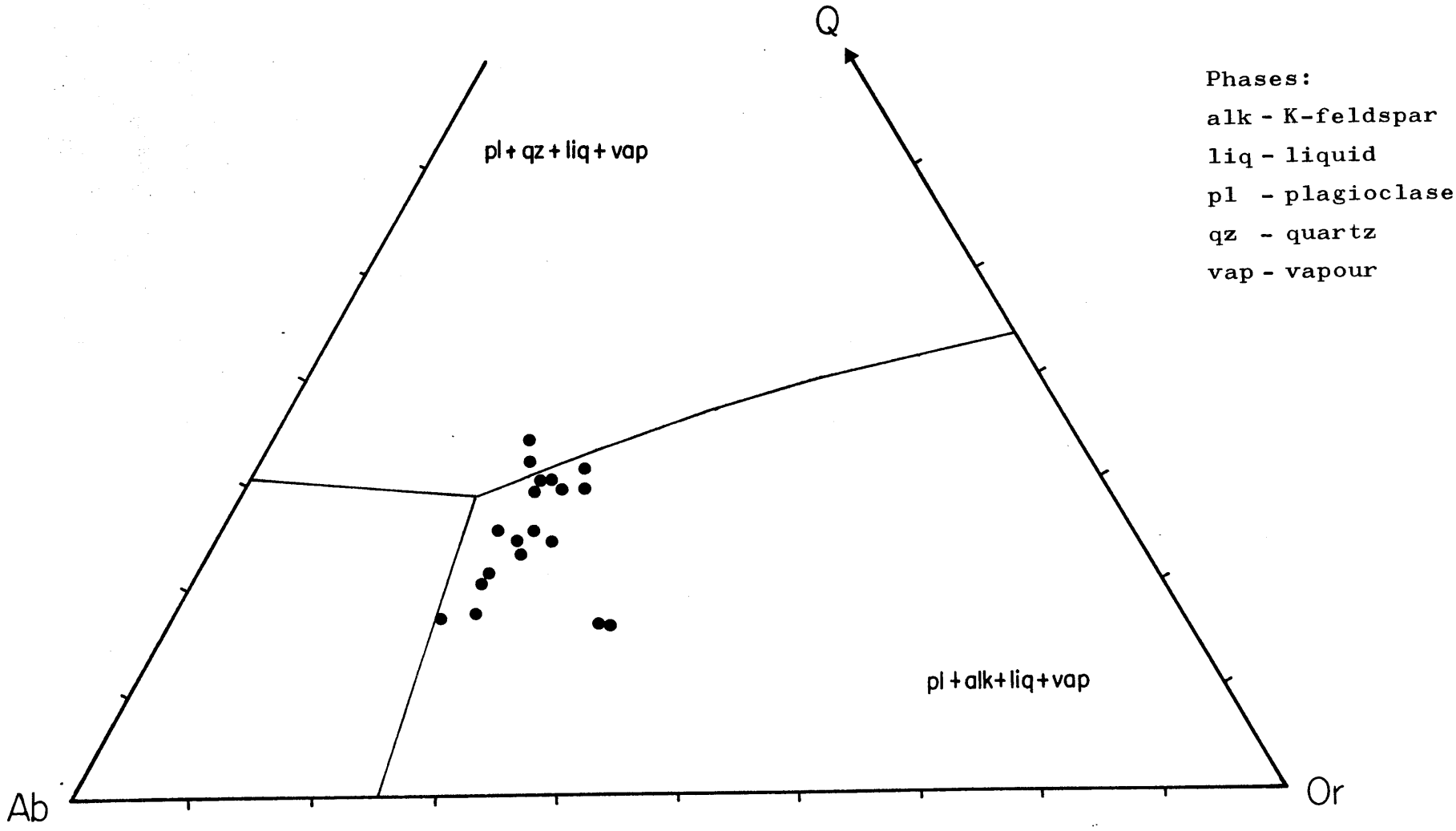

Fig 3.24. Q:Ab:Or diagram for Roseneath acid clasts showing med pressure water saturated eutectic.

below the British Caledonides calc-alkali trend, but the presence of more alkaline samples is also observed (Fig. 3.25).

The presence of more alkaline clasts is most readily apparent by reference to alumina saturation. It has already been demonstrated that Group 1 analyses are either marginally peraluminous or metaluminous depending upon the presence or absence of hornblende as a phenocryst phase (Fig.3.13). This agrees with similar observations by Cawthorn and Brown (1976) who have proposed fractionation of hornblende from a diopside normative bulk composition to explain trends from diopside normative to corundum normative compositions with increasing SiO_2 in calc-alkali suites.

In a development of the alumina saturation index of Shand (1947), Halliday et al (1981) showed that many older Scottish Caledonian granites (lacking amphibole but commonly containing inherited zircons) display peraluminous characteristics attributed to melting of prealuminous sediment/metasediment whilst members of the 'Newer' biotite granite suite are metaluminous and were perhaps generated from melting at 'lower levels in the crust-mantle section'. Using their A/CNK:SiO_2 diagram (A/CNK is the molar ratio Al_2O_3 /(CaO + Na_2O + K_2O)) two sub-parallel trends are observed for Roseneath Group 1 clasts (Fig. 3.26). Both groups display a tendency for A/CNK to increase with SiO_2 (a characteristic linked by Halliday et al with increasing initial $^{87}Sr/^{86}Sr$ with Rb/Sr and SiO_2 as evidence for crustal contamination) but contrast strongly on the basis of alumina saturation at any given SiO_2 value. Caledonian newer granitoids displaying similar dual trends are demonstrably geochemically zoned (implying two magmatic episodes), unlike the Roseneath acid rocks.

The alumina saturation parameter is considered to be sensitive to deuteric transformations and particularly sericitization processes (La Roche 1979). It is therefore possible that alteration of plagioclase feldspars to, for example, sericite might result in the trends of Fig. 3.26. As previously discussed, however, this has largely been discounted since thin section examination reveals that plagioclase crystals are relatively fresh, at least in those samples submitted for analysis. An attempt to confirm this chemically was made by plotting niggli al/alk:c (Leake pers. comm. 1983). The advantage of this method is that various mineral fields can be plotted in addition to individual rock analyses. Any igneous trend may be defined as a vector towards the mineral phase which dominates in that process. Significant sericitization

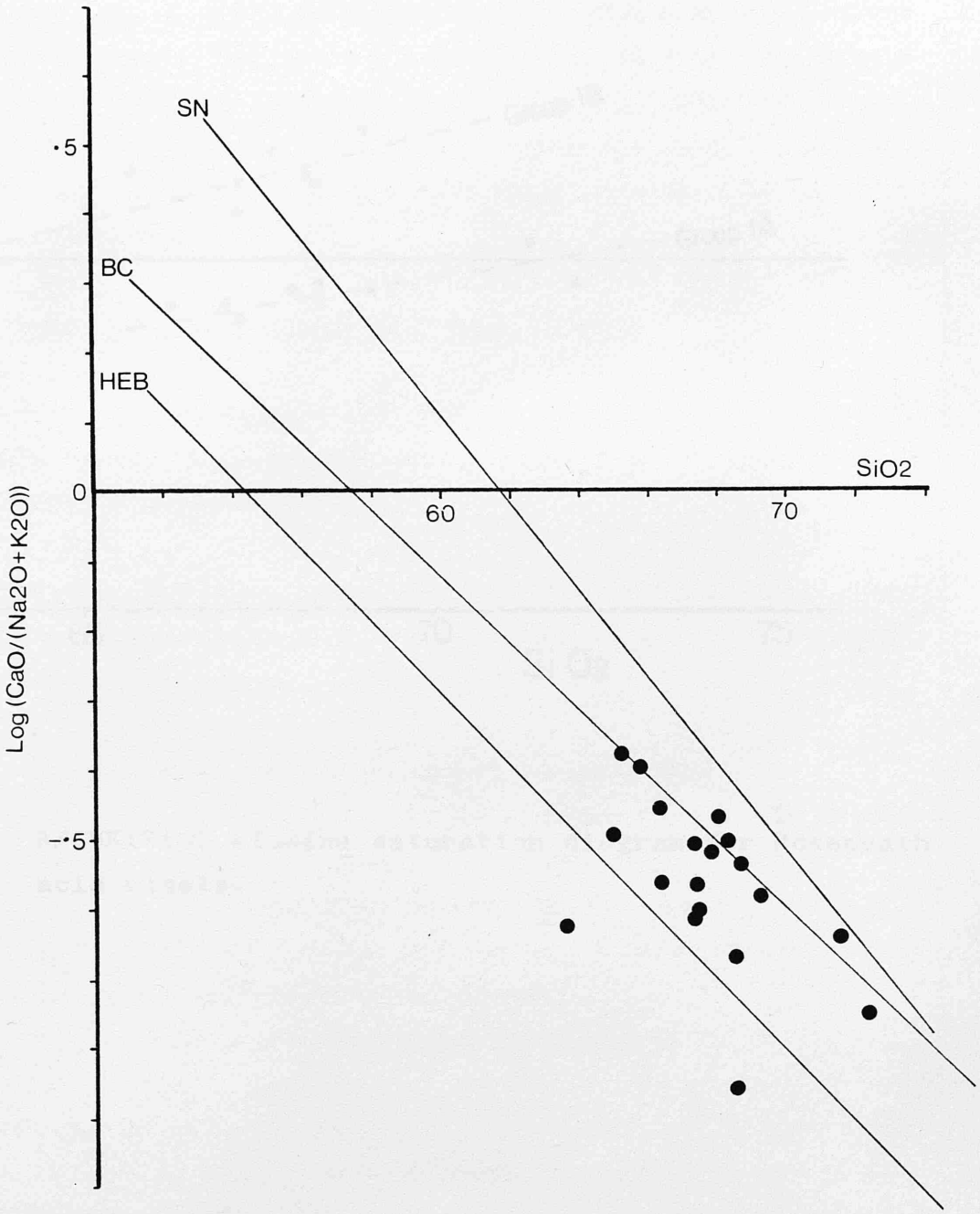

Fig 3.25. Calc-alkali ratio:SiO2 diagram for Rosenath acid clasts. Trends for Sierra Nevada and British Caledonides calc-alkali and British Tertiary alkaline suites indicated (SN, BC and HEB respectively). From Brown 1979.

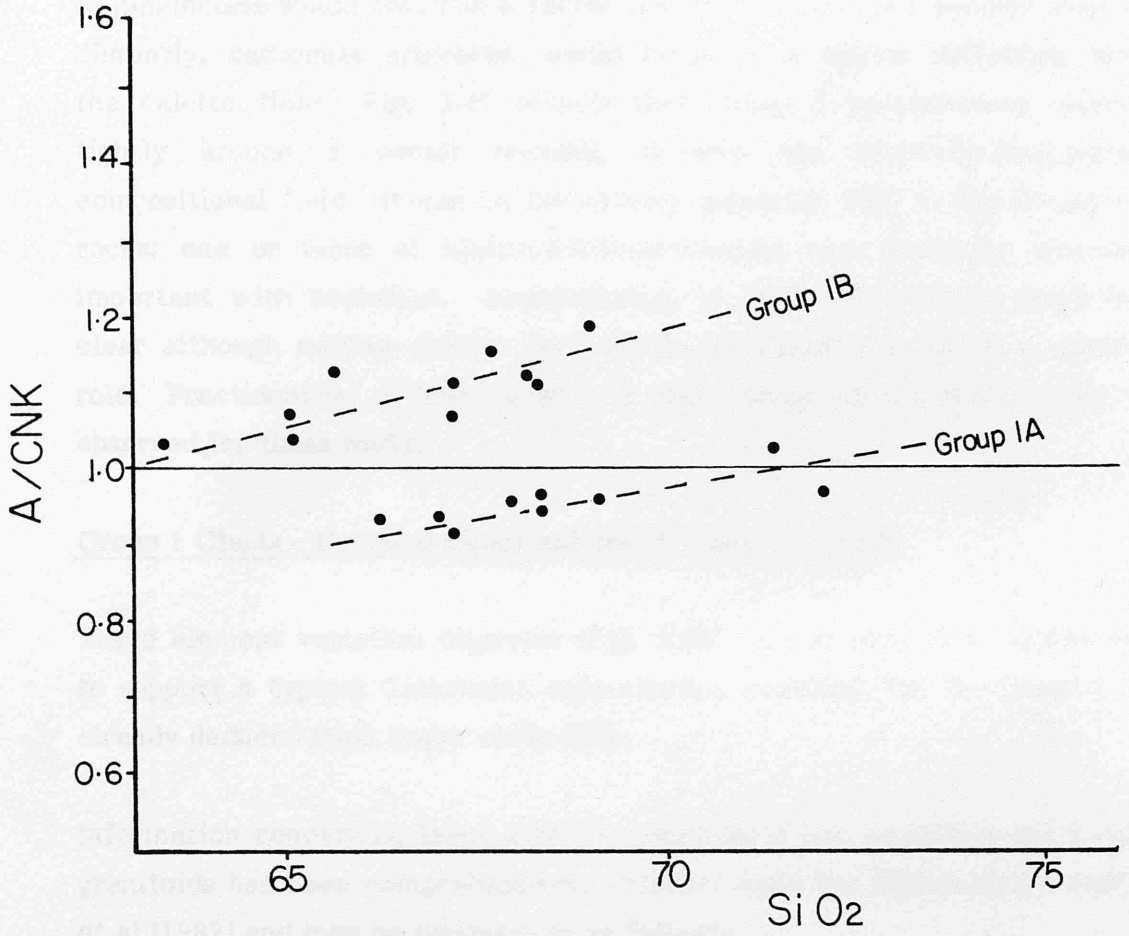

Fig 3.26. A/CNK:SiO2 alumina saturation diagram for Roseneath acid clasts.

of plagioclase would result in a vector towards the field occupied by muscovite. Similarly, carbonate alteration would result in a vector deflecting towards the calcite field. Fig. 3.27 reveals that Group 1 peraluminous clasts fall tightly around a vector trending towards the biotite/orthoclase/albite compositional field. It can be tentatively suggested that in the peraluminous rocks, one or more of biotite/albite/orthoclase was becoming increasingly important with evolution. Interpretation of the metaluminous trend is less clear although neither calcite nor sericite alteration has played a significant role. Fractionation of hornblende is a more likely explanation for the trend observed for these rocks.

Group 1 Clasts - Detailed Geochemistry II: Trace Elements

Trace element variation diagrams (Fig. 3.28) can be used to a certain extent to support a typical Caledonian calc-alkaline evolution for the Group 1 clasts already deduced from major oxide data.

Information concerning trace element abundances and variations in Caledonian granitoids has been comprehensively collated from the literature by Pankhurst et al (1982) and may be summarised as follows:

i) Ni, Cr, Co, Mn and Zn decrease with increasing SiO_2.
ii) Sr, Ba and Zr increase over intermediate compositions to very high concentrations in the acid rocks (>1000ppm).
iii) Rb, U and Th increase over the entire range of SiO_2.
iv) K/Rb ratios are variable, and decrease from intermediate rocks (400ppm) to more silicic types (100ppm).
v) Sr/Ca and Ba/Sr probably remain constant with increasing SiO_2.

Whilst the range of SiO_2 contents for the Group 1 clasts is admittedly small, making it difficult to establish general trends, these rocks conform closely to the Caledonian pattern. However, although the majority of elemental trends are typically calc-alkaline, certain major anomalies exist. For example, Zr shows a subtle but significant negative correlation with SiO_2 (Fig 3.28) whilst K/Rb ratios are up to four times those of typical Caledonian suites and display a positive correlation with SiO_2 (Fig. 3.29). These trends are also somewhat contrary to those expected during normal evolution of a granite magma. Zr and K/Rb are generally considered to be reliable indices of the degree of fractionation in most igneous suites (Taubeneck 1965). Under normal

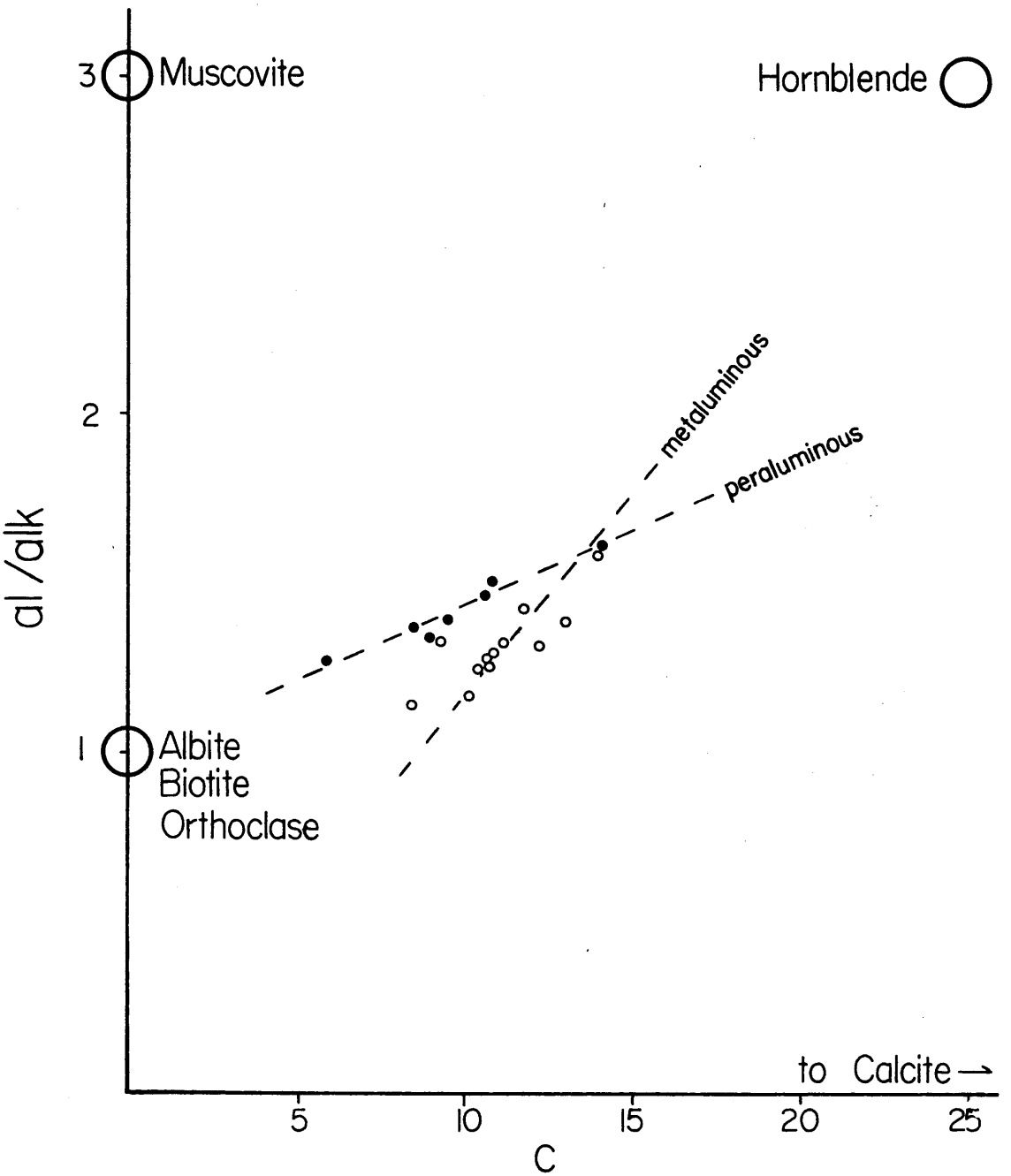

Fig 3.27. Niggli al/alk:c alteration diagram for Roseneath acid igneous clasts. (o) Group 1A, (•) Group 1B as determined from Fig 3.26.

Fig 3.28 (next 3 pages). Trace element variation diagrams for Roseneath igneous clasts. Symbols as for Fig 3.20.

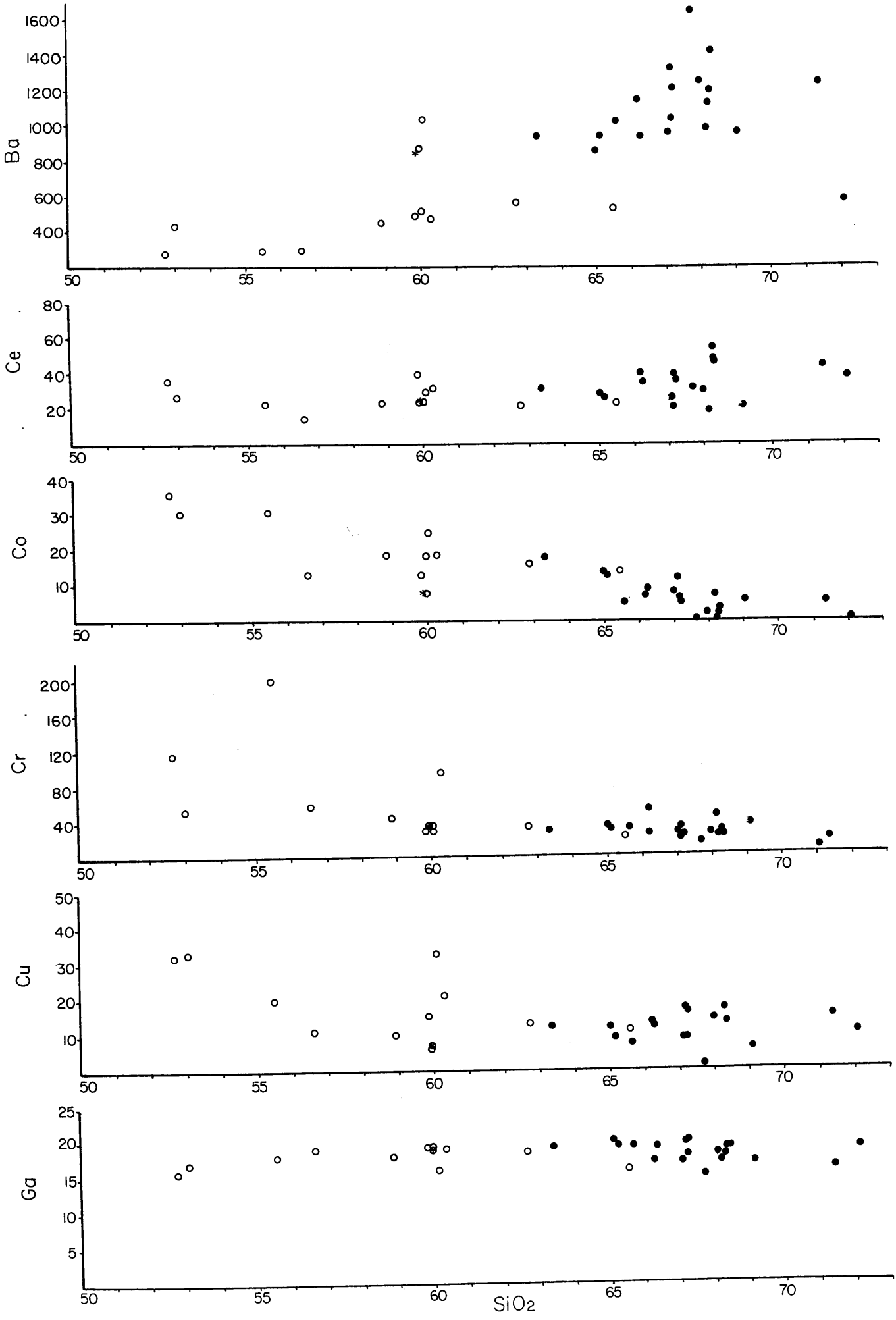
Ba
1600
1400
1200
1000
800
600
400
Ce
80
60
40
20
Co
40
30
20
10
Cr
200
160
120
80
40
Cu
50
40
30
20
10
Ga
25
20
15
10
5
50
55
60
65
70
SiO2

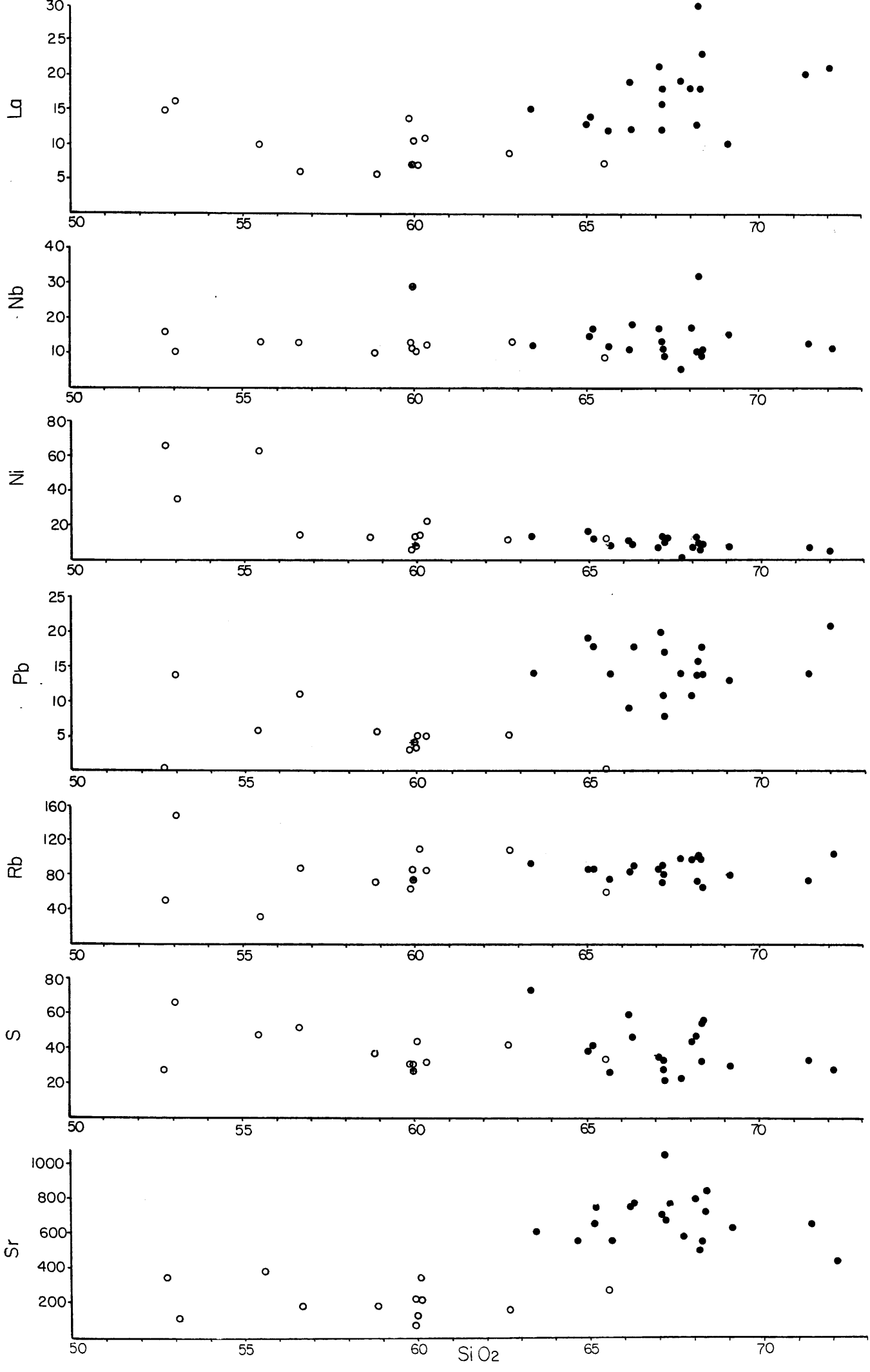
La
Nb
Ni
Pb
Rb
S
Sr
SiO2
50
55
60
65
70

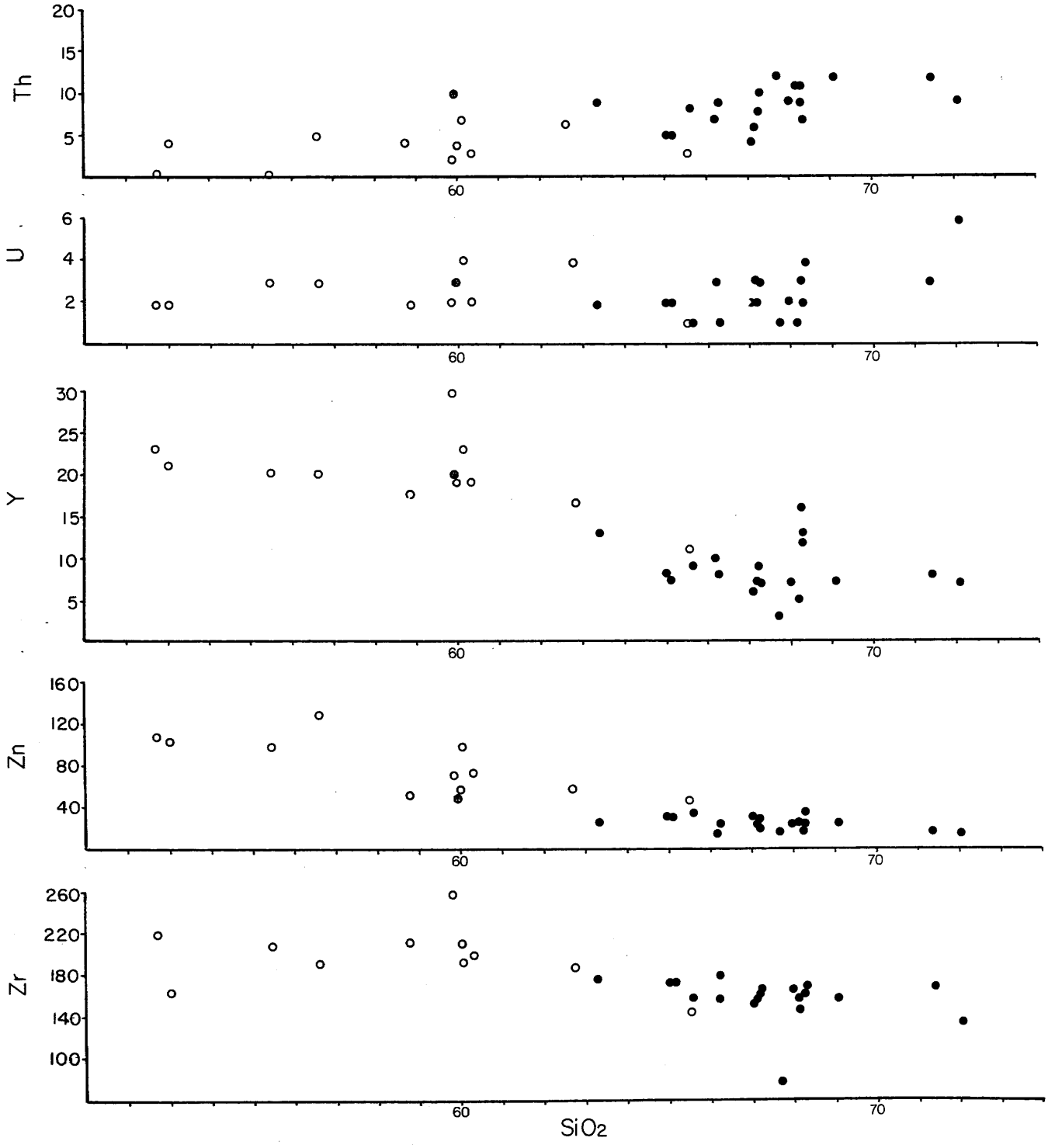
Th
20
15
10
5
60
70
U
6
4
2
60
70
Y
30
25
20
15
10
5
60
70
Zn
160
120
80
40
60
70
Zr
260
220
180
140
100
60
70
SiO2

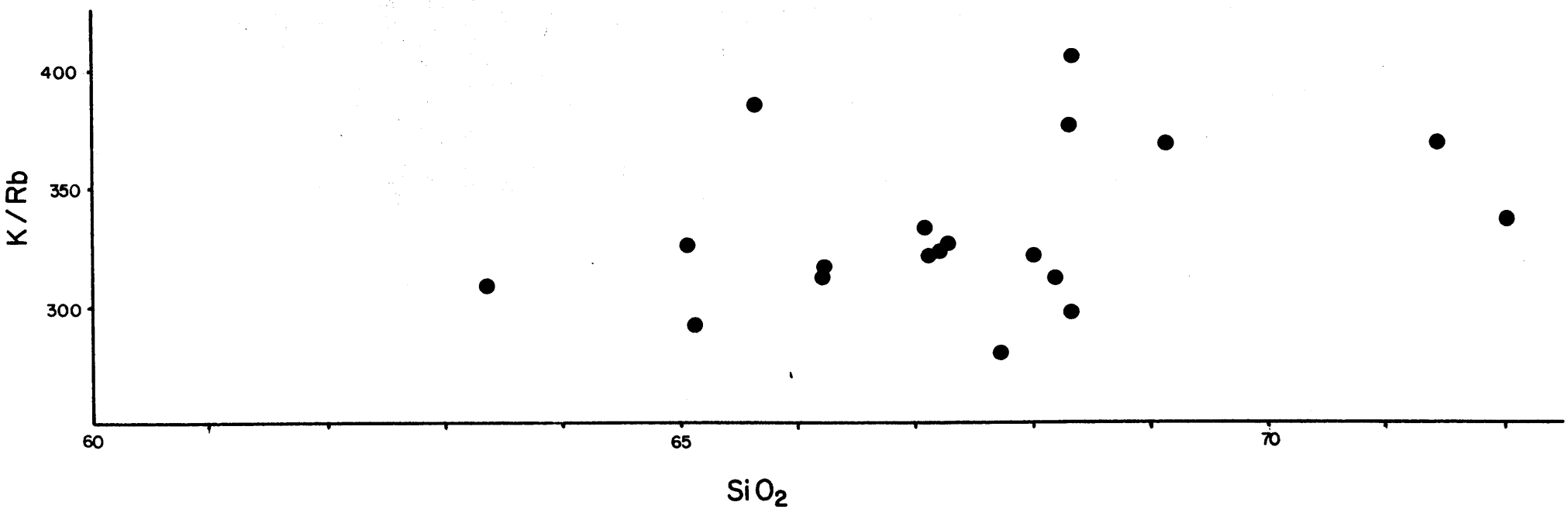

Fig 3.29. K/Rb:SiO2 variation diagram for Roseneath acid clasts.

fractionation K/Rb will decrease with SiO_2 and Zr should increase. It therefore becomes especially difficult to explain negative and positive trends with SiO_2 for Zr and K/Rb respectively in terms of simple fractionation.

High K/Rb (300-400ppm), however, is a characteristic of rhyolites and dacites in the southwest Highlands ORS Lorne lavas (Groome and Hall 1974) and appears to increase over the range 70% to 78% SiO_2. Recently published analyses of late Caledonian granitoids (Stephens and Halliday 1984) now reveals that while decreasing K/Rb is typical of Caledonian Newer granites as a whole (iv above), high and increasing K/Rb ratios with SiO_2 do occur but may be peculiar to plutons located in the southern Highlands. Garabal Hill, for example, attains K/Rb ratios identical to those for Group 1 clasts over comparable levels of SiO_2. Variation of other critical element ratios (Rb/Ba, K/Ba, Ba/Sr and Rb/Sr) all apparently decrease with increasing SiO_2 for many southern Highlands granites mirroring identical trends with Roseneath Group 1 rocks and contrast strongly with the majority of Caledonian granitoids.

A commonly used classification of subduction-related granitoid rocks is that in which the source material is deduced as having either a dominantly sedimentary (S-type) or igneous/mantle (I-type) character (Chappell and White 1974, White and Chappell 1977, 1983, Chappell 1978, Hine et al 1978). The distinguishing parameters of the two associations are set out in Table 3.3. A third association of non-subduction related peralkaline granitoids has been recognised by Pitcher (1983) and classified as A-type (anororgenic). Application of I- and S-type models to Caledonian intrusions is not always straightforward although members of both associations are clearly present. The majority of pre 450Ma Older granitoids for example display diagnostic features of S-type granitoids and appear to have been generated by melting of old crustal rocks during or shortly after the peak of Caledonian metamorphism. Many Newer granitoids, (c. 400ma), on the other hand, display undoubted I-type affinities and may have been derived from mantle sources or deep seated igneous material originally derived from mantle source. There is, however, a distinction made between Newer granitoids intruded in the southwest Highlands with undoubted I-type characteristics and those of the northeast Highlands which are generally of an I-type nature but display many indications of crustal anatexis (the transitional I- to A-type of Stephens and Halliday (1984)).

I-type

A Acid dominated end of wide compositional spectrum.

B Variation diagrams produce linear trends.

C Relatively high Na-content (Na_2O>3.2% in felsic varieties falling to 2.2% in more mafic types).

D CIPW normative diopside or <1% normative corundum.

E Mol. $Al_2O_3/(CaO + Na_2O + K_2O)$<1.1.

F Contain biotite + hornblende $\pm$ sphene $\pm$ magnetite.

G Low initial $^{87}Sr/^{86}Sr$ ratios (0.704 - 0.706).

H Association of prophyry copper type mineralization.

S-type

A Restricted acidic silica range.

B Variation diagrams are irregular.

C Relatively low Na content (Na_2O <3.2% in rocks with 5% K_2O, falling to less than 2.2% in rocks with 2% K_2O).

D CIPW normative corundum > 1%.

E Mol. $Al_2O_3/(CaO + Na_2O + K_2O)$ > 1.1%.

F Contain biotite $\pm$ muscovite $\pm$ cordierite $\pm$ garnet $\pm$ ilmenite.

G Higher $^{87}Sr/^{86}Sr$ ratios (>0.706).

H Association of tin mineralization.

Table 3.3. Differentiating characteristics of I and S type granitoids.

Application of the I-S system to Roseneath Group 1 rocks results in a relatively unambiguous I-type assignation. This is surprising in view of the large inherited zircon component (see section 3.3.9) and high Ba and Sr values suggestive of derivation from a largely crustal (sedimentary) source. A similarly paradoxical situation is observed for the I-type Newer southwest Highlands (Argyll) suite which is also enriched in Sr and Ba, has inherited zircons and displays O and Nd isotopic characteristics negating a significant mantle contribution (Hamilton et al 1979, Clayburn et al 1983, Halliday 1984, Stephens and Halliday 1984).

Brown et al (1984) envisaged a mantle source for all Caledonian granitoids and preferred to explain the observed geochemical differences between northeast Highlands intrusions and those of the Southern Uplands province by invoking a laterally variable (north-south) mantle source (a view shared by Stephens and Halliday and extended to the lower crust). To support this view, they produced Rb/Zr:Nb and Rb/Zr:Y diagrams which discriminated between the two provinces on the basis of relatively enhanced levels of high field strength (HFS) elements in the northern suite. Using the more comprehensive data for Caledonian granitoids of Stephens and Halliday (1984) the Rb/Zr:Y plot does not discriminate well due to poor north-south Y variability (Fig. 3.30). Roseneath granodiorites seem to be characterised by low Rb/Zr and Y most typical of plutons in the south and southwest Highlands.

The Rb/Zr:Nb plot (Fig. 3.31), however, discriminates well between the two provinces although the fields implied by Brown et al (1984) are clearly an oversimplication.

Unfortunately, the new fields for the Rb/Zr:Nb diagrams are not discrete enough to distinguish the Roseneath Group 1 rocks from southwest Highlands or Southern Upland granitoids but they obviously share the Low HFS characteristics of both and carry low levels of LIL (low Rb/Zr) which have been attributed to more primative arc suites.

Pearce et al (1984) used similar LIL-HFS relationships to discriminate intrusive settings for granitoid magmas. The Roseneath Group 1 rocks all lie within the arc field on Nb + Y: Rb and Y:Nb plots (Fig. 3.32 and 3.33), as do the majority of Caledonian plutons. Differences in fields for the Caledonian suites are attributed to heterogeneous mantle and/or source rock compositions rather than disparate environments of intrusion.

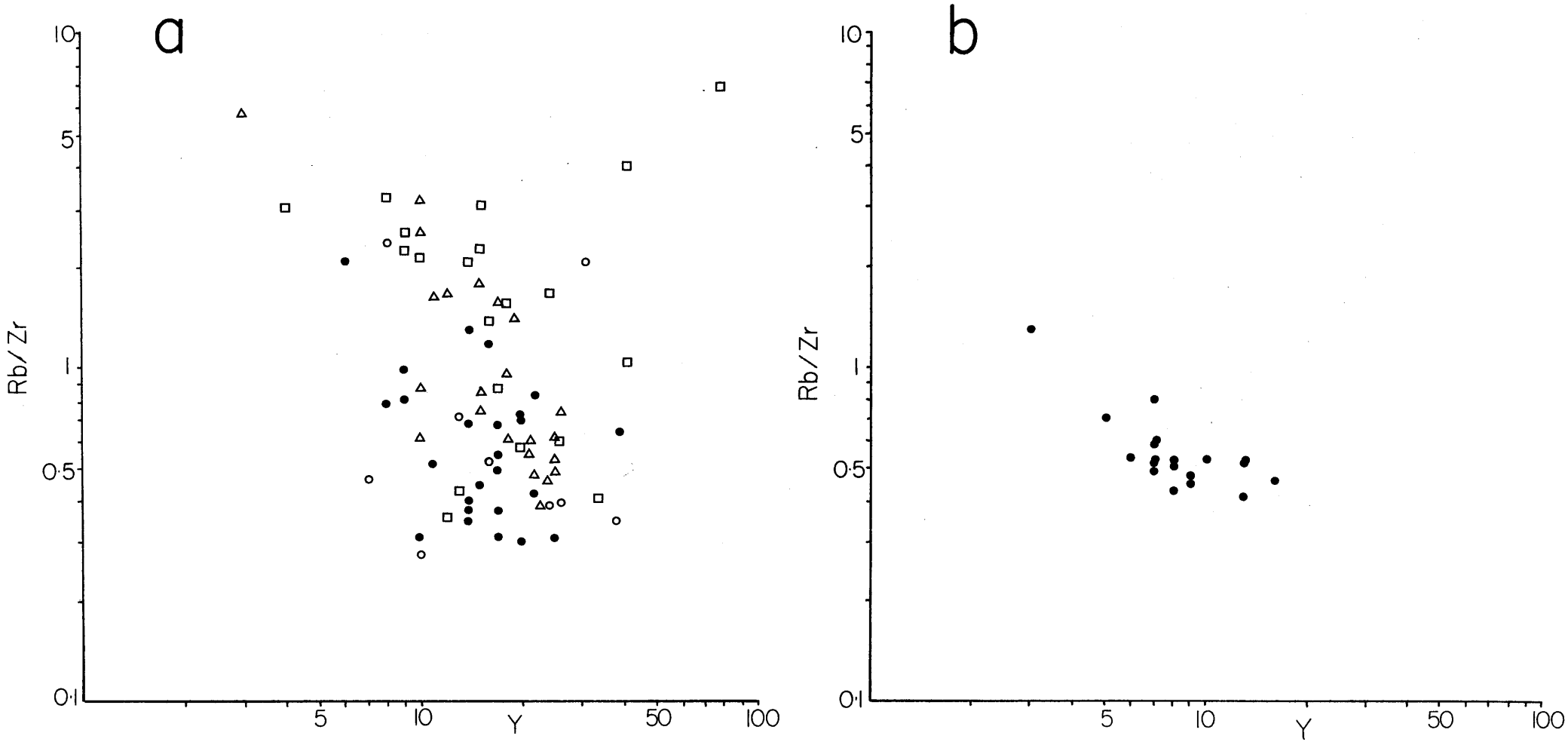

Fig 3.30. a) Rb/Zr:Y diagram for selected Newer Caledonian granitoids. (o) southern Highlands granites; (●) southwest Highlands granites; (□) central Highlands granites; (△) Southern Uplands granites. b) Rb/Zr:Nb diagram for Roseneath acid clasts.

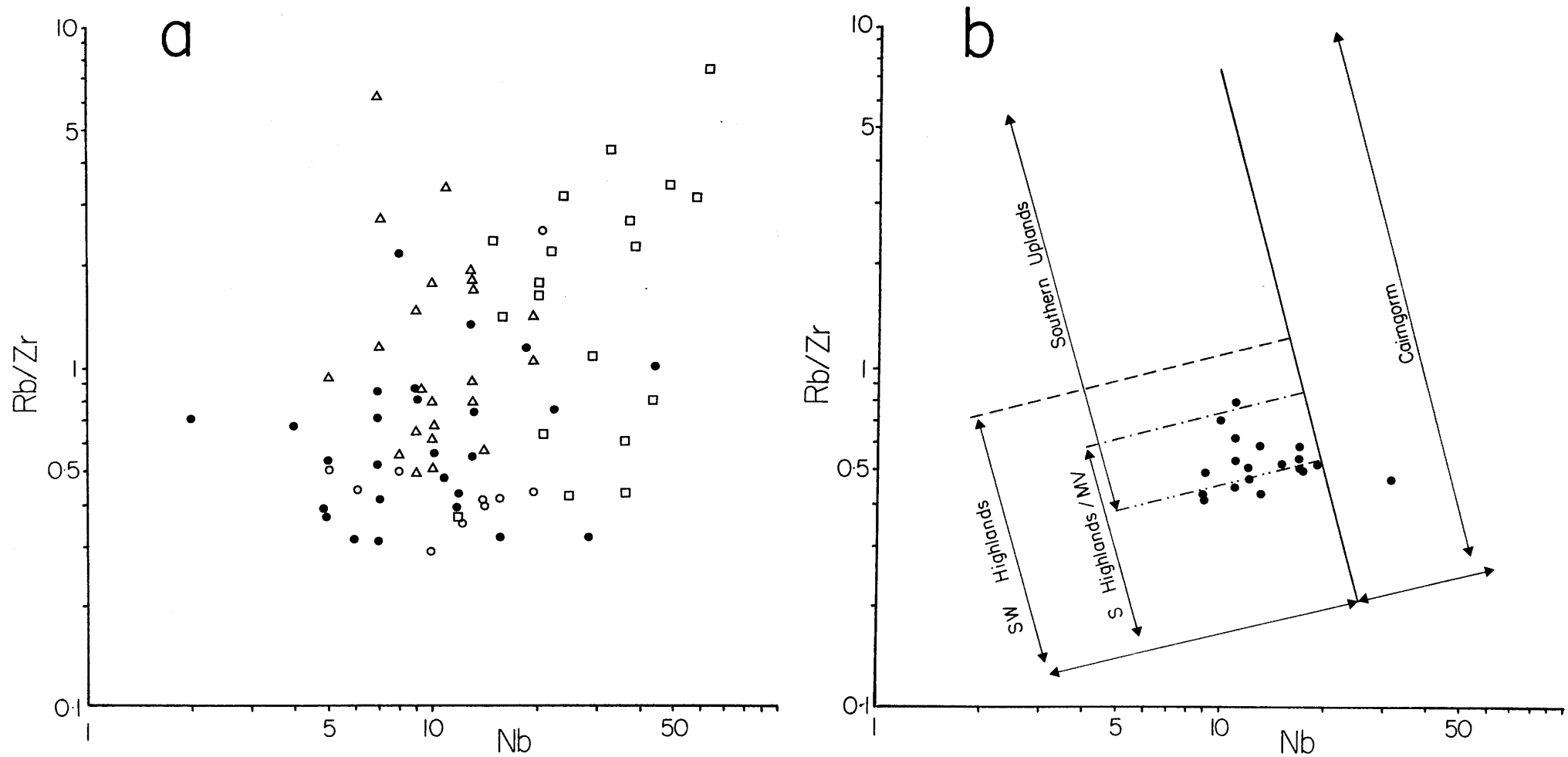

Fig 3.31. a) Rb/Zr:Nb diagram for selected Newer Caledonian granitoids. Symbols as for Fig 3.30a. b) Rb/Zr:Nb diagram for Roseneath acid clasts showing generalized fields from Fig 3.31a.

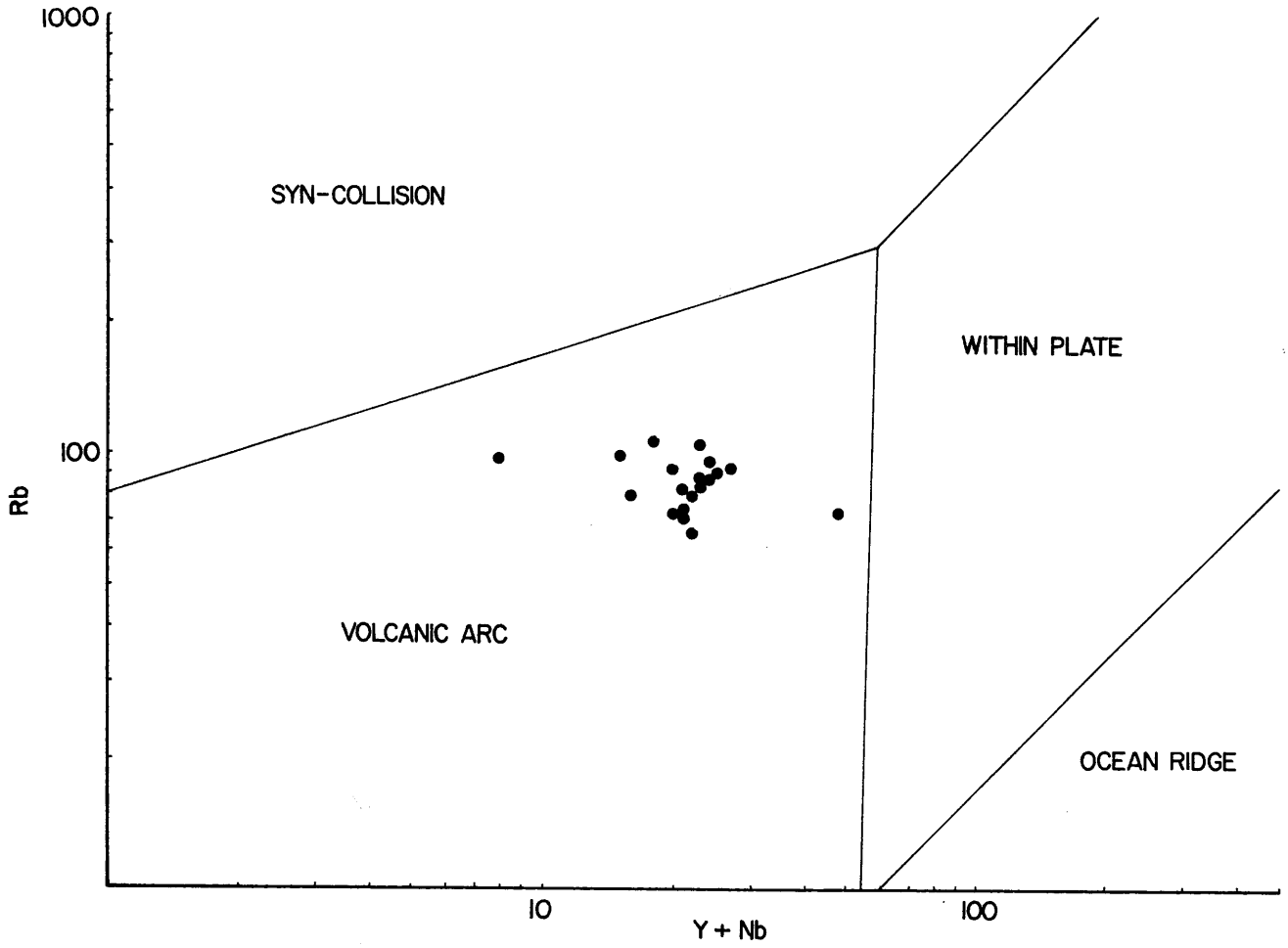

Fig 3.32. Nb+Y:Rb discriminant diagram for Roseneath acid igneous clasts.

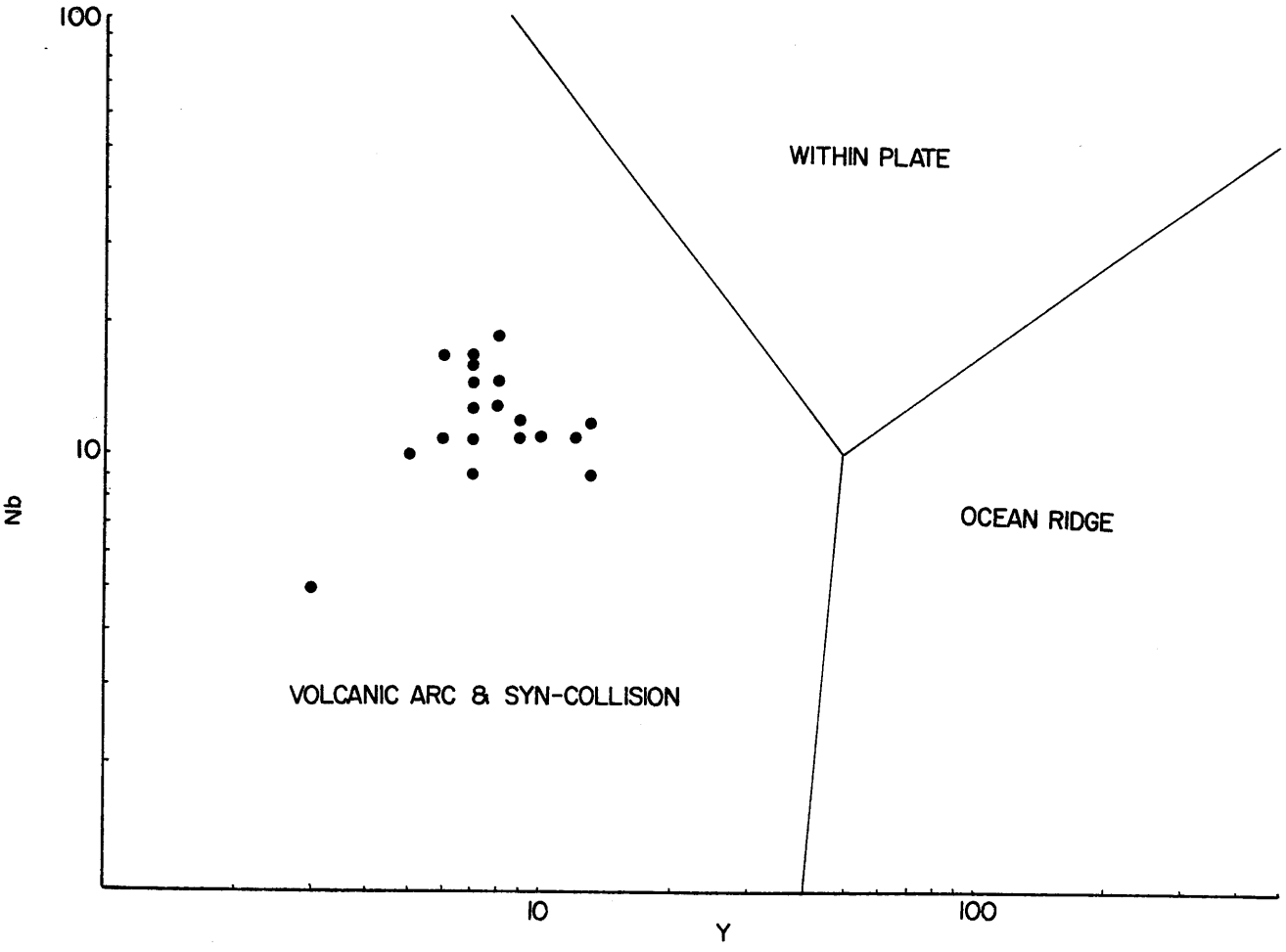

Fig 3.33. Nb:Y discriminant diagram for Roseneath acid igneous clasts.

Absolute abundances of LIL radio-elements (Th and U) in Group 1 rocks are low relative to 'average granite' (Rogers and Adams 1969), although the Th/U ratio is probably not significantly different. The Th/U ratio shows an unexpected positive correlation with SiO_2 (Fig. 3.34) and this deviation from predicted behaviour during fractionation must be linked with that of Zr, since Th^{4+} shows a preference for entry into early Zr^{4+} sites. A strong Th-Zr association may for example be explained in this way by the common occurrence of Th^{4+} in the zircon lattice.

Fig. 3.35 is a K:U:Th triangular plot devised by Tammemagi and Smith (1975) to determine fractionation trends for these radio elements. For comparison, the frationation trend for the late Caledonian (c. 400 Ma) Leinster granitoid (from O'Connor et al 1982) is superimposed. The clustering observed for Group 1 clasts seems to indicate that they were not fractionating with respect to K, U and Th. More significant perhaps is the observation that the Roseneath rocks, which have already been shown to represent a highly fractionated magma (see also following sections), cluster tightly in a position equivalent to the *least fractionated* parts of the Irish granite.

It has been suggested by Hall (1972) that the observed variations in the normative compositions of British granites is due to variations in the geothermal gradient. Elsdon and Kennan (1979) have cited a possible heterogeneous distribution of heat producing elements (e.g. U) in the crust to produce this effect and proposed that radio-element concentrations in granite plutons might reflect these changes in the source area. Paucity of data at that time prevented general conclusions to be made. Considerably more data has recently become available and absolute abundances of radio-elements for Irish and mainland British granites have been presented by (O'Connor 1981, O'Connor et al 1982, Stephens and Halliday 1984). With respect to Caledonian granites as a whole, the Roseneath rocks again display a marked depletion in U and Th but appear to be comparable to southwest Highlands Newer granites, for whose source Van Breemen and Bluck (1981) have invoked a substantial component of U, Th and Rb depleted Lewisianoid lower crust. Partial melting of Rb depleted Lewisian granulite lower crust would certainly explain the low Rb/Sr, Rb/Ba and high K/Rb observed for the Roseneath rocks and southwest Highlands Newer granites and is consistent with a proposed enrichment of K relative to Rb with increasing pressure (and depth) in lower crustal granulites where compositions are evolving towards the high K/Rb ratios of the mantle (Leake 1978).

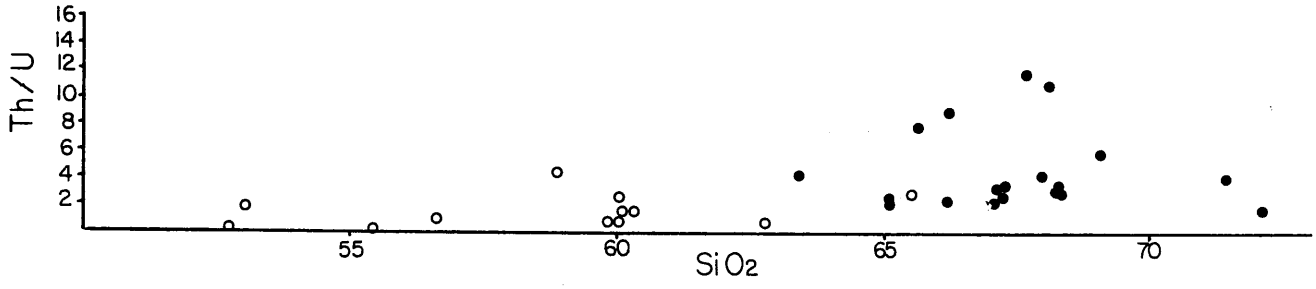

Fig 3.34. Th/U:SiO2 variation diagram for Roseneath igneous clasts. Symbols as for Fig 3.20.

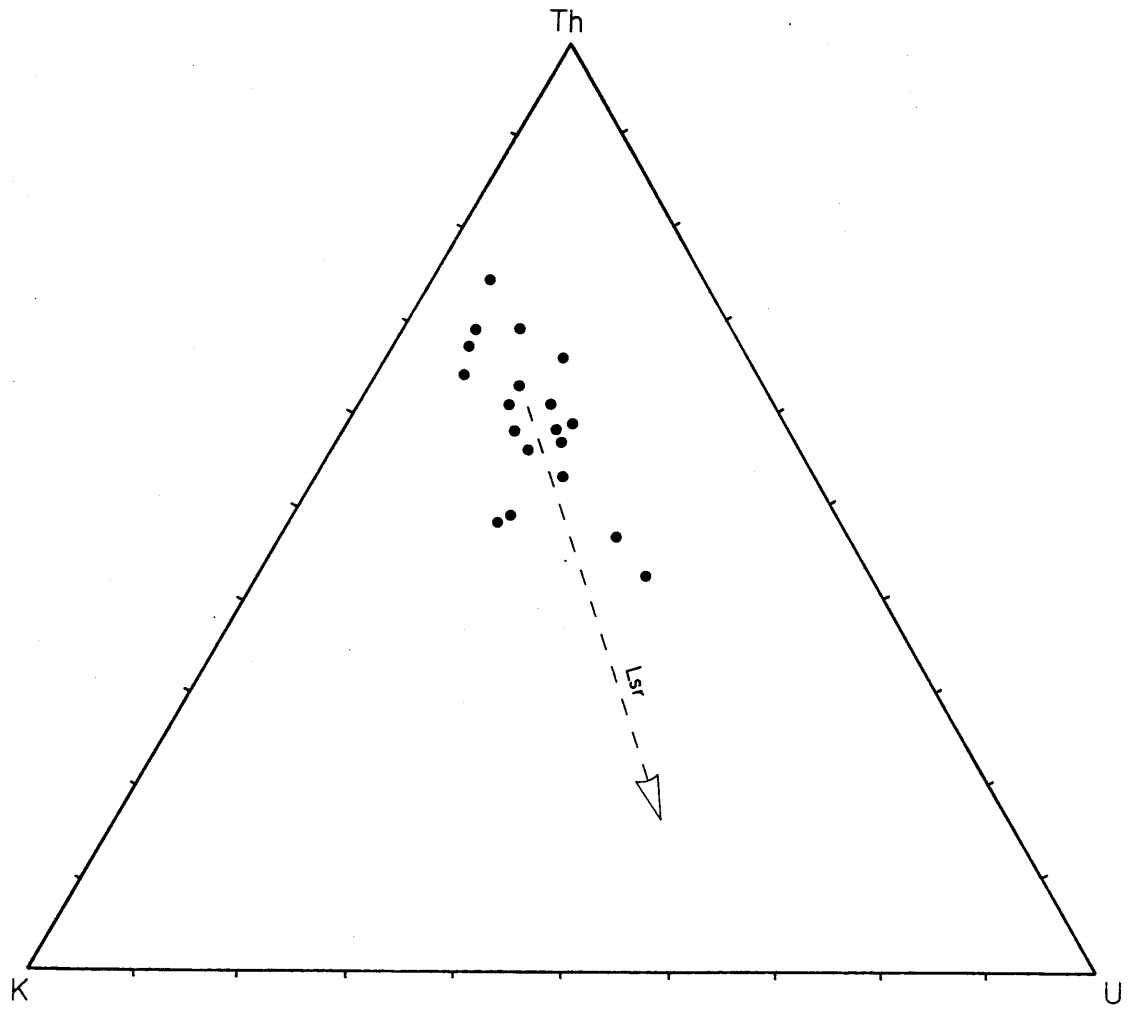

Fig 3.35. K:U:Th triangular diagram for Roseneath acid clasts. Lsr - fractionation trend of the Leinster Caledonian granitoid (from O'Connor et al 1982).

Group 2 Clasts - Detailed Geochemistry

Modern andesites can be divided into three categories based on composition and tectonic setting (Jakes and White 1972, Condie 1982). These are: arc andesites, occurring in immature oceanic island arcs and on the trench side of mature arcs; calc-alkaline andesites, most common in modern mature arc systems; and high K calc-alkaline andesites which occur in continental margin arcs underlain by thick lithosphere. Fig. 3.36 graphically compares the trace element composition pattern of the Group 2 andesites normalised against andesites from each of the above three categories. It is apparent that all three patterns differ significantly from Roseneath type andesite. Arc andesite exhibits both a depletion in elements of low ionic potential (K, Rb, Ba) and moderately incompatible elements (La, Ce, Zr, Ti) relative to Group 2 andesite. Similarly, calc-alkaline andesites are moderately depleted in elements of low ionic potential (except Sr), Zr and Ti, but with comparable concentrations of LREE. High K calcalkaline andesites are broadly comparable in terms of K, Rb, Ba, Zr and Ti but significantly enriched in Sr and LREE. As a general observation, however, the transitional elements (Y, Cr, Ni, Cu, Co, Zn) show least departure from Roseneath composition for all categories especially calc-alkaline andesites with the exception of Cu which is strongly enriched in all three types relative to Group 2 andesites.

Non-transition element abundances in the Group 2 andesites can best be interpreted in terms of combinations of arc type Sr, high K calc-alkaline K, Rb, Ba, Zr and Ti, and concentrations of LREE and transition elements (except Cu) characteristic of calc-alkaline andesites. The apparently anomalous behaviour (depletion) of Sr in the Roseneath andesites relative to other elements of low ionic potential (K, Rb, Ba) is of particular interest. Such relative depletion would normally be attributed to a moderately advanced fractionation (Pearce 1982), and in this instance probably relates to the low anorthite contents of these rocks.

Pearce et al (1977) established that MgO, FeO_t and Al_2O_3 are relatively immobile during the early stages of weathering and developed a triangular diagram which can be used to distinguish five tectonic environments of eruption (ocean floor and ridge, ocean island, continental, orogenic and spreading centre island). This discriminant diagram is valid for both basic and more intermediate volcanic rocks. While the Roseneath 'andesites' are

Fig 3.36 (next page). Average Roseneath 'andesite' normalised against: a) average arc andesite; b) average calc-alkaline andesite and; c) average high K calc-alkaline andesite.

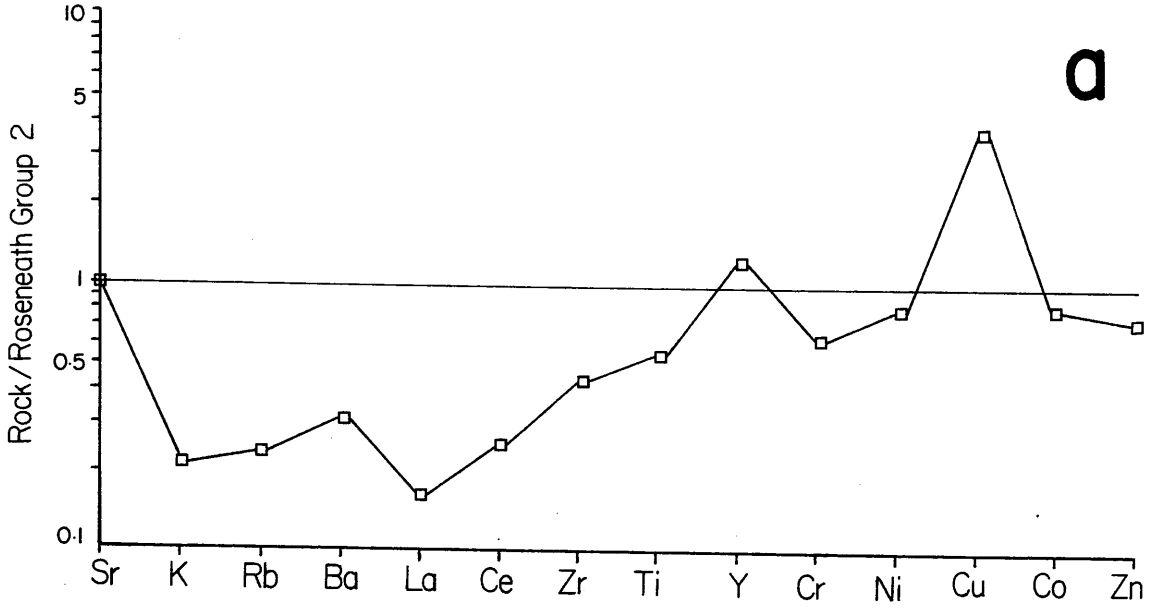
a
Rock / Roseneath Group 2
10
5
1
0·5
0·1
Sr K Rb Ba La Ce Zr Ti Y Cr Ni Cu Co Zn

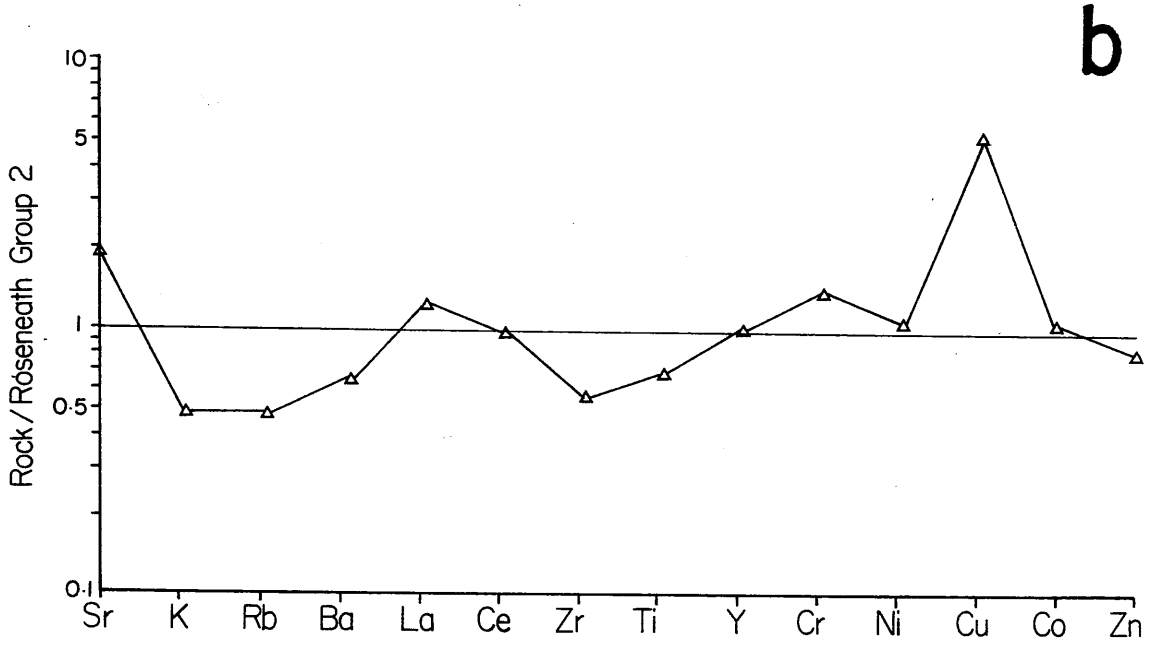
b
Rock / Roseneath Group 2
10
5
1
0·5
0·1
Sr K Rb Ba La Ce Zr Ti Y Cr Ni Cu Co Zn

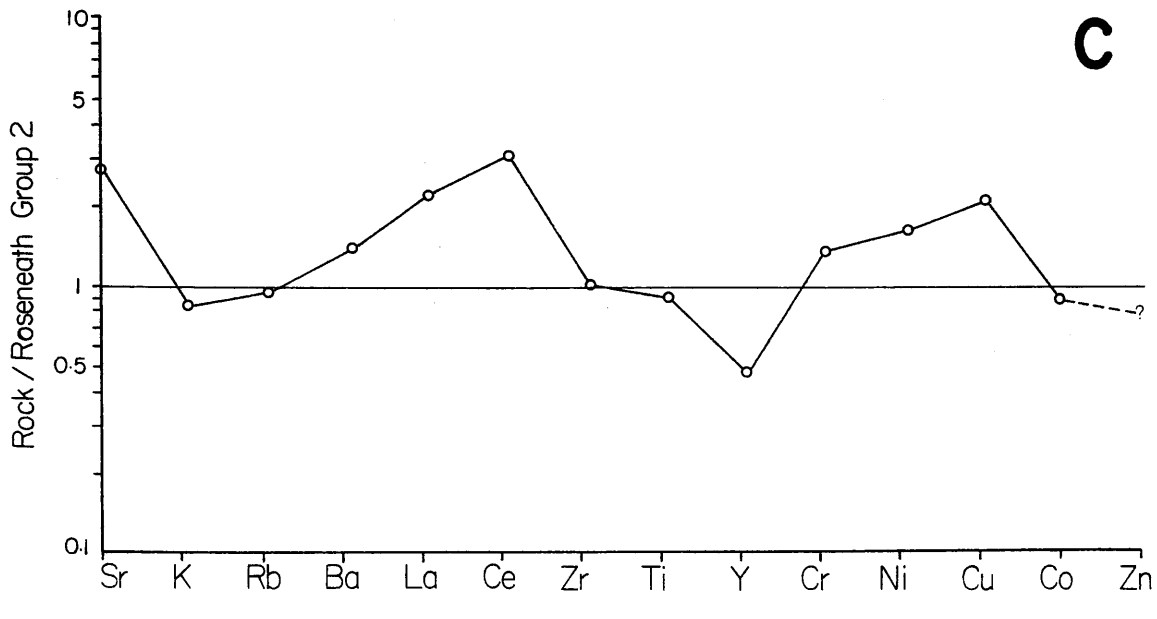
c
Rock / Roseneath Group 2
10
5
1
0·5
0·1
Sr K Rb Ba La Ce Zr Ti Y Cr Ni Cu Co Zn
?

probably more alkaline than the analyses used to construct the fields, they cluster within the 'orogenic' environment or possibly within the 'alkaline ocean island' field (Fig. 3.37). For comparison, analyses have also been plotted on this diagram for ORS andesites from Lorne (Groome and Hall 1974) and averaged compositions of ORS andesites from the north and south Midland Valley (Thirlwall 1981). These ORS andesites also cluster within the orogenic field and are indistinguisable from the Roseneath Group 2 clasts. Compositions within the orogenic environment are defined by Pearce et al (1977) to include volcanic rocks from island arcs and subduction related active continental margins.

Fig. 3.38 is a plot of TiO_2:Zr, regarded by Pearce and Norry (1979) and Pearce (1980) as the most realistic geochemical discriminator between arc and within-plate magmatic products. This plot utilizes the fact that volcanic arc lavas contain lower abundances of immobile elements than other magma types. Roseneath albitic andesites are clearly transitional, straddling the within-plate/arc boundary, as do the ORS intermediate volcanics from the SW Highlands, and north and south Midland Valley.

Pearce (1982) in a study of basaltic lavas from destructive plate boundaries discriminated between volcanic arc basalts and within-plate basalts using MORB normalized trace element patterns. A third group of lavas was identified using these diagrams as having hybrid geochemical components of island arc tholeiites, within-plate tholeiites and calc-alkaline basalts and therefore have parallels with Group 2 rocks. The effects of fractional crystallization unfortunately precludes accurate direct comparison of Roseneath andesite with these transitional volcanic arc basalts. However, particular similarities are apparent with the Aleutian Bogoslov Island pattern with an enrichment in elements of low ionic potential characteristic of island arc tholeiites and an enrichment in all elements from Sr to Ti characteristic of within-plate tholeiites.

A more satisfactory method for further investigating the affinities with Aleutian arc magmas are trace element patterns ('spidergrams') normalised against Aleutian tholeiitic and calc-alkaline magmas of andesitic composition (SiO_2 c 56%) using data drawn from Kay (1977). From Fig. 3.39, the trace element data for calc-alkali andesite from Mt. Recheschnoi, Umnak Island exhibits an astonishing match with the andesites from Roseneath, except for enrichment at Roseneath of K and Rb. Also, high K/La, Rb/La and Ba/La ratios for Aleutian volcanic arc samples (as opposed to the island arc

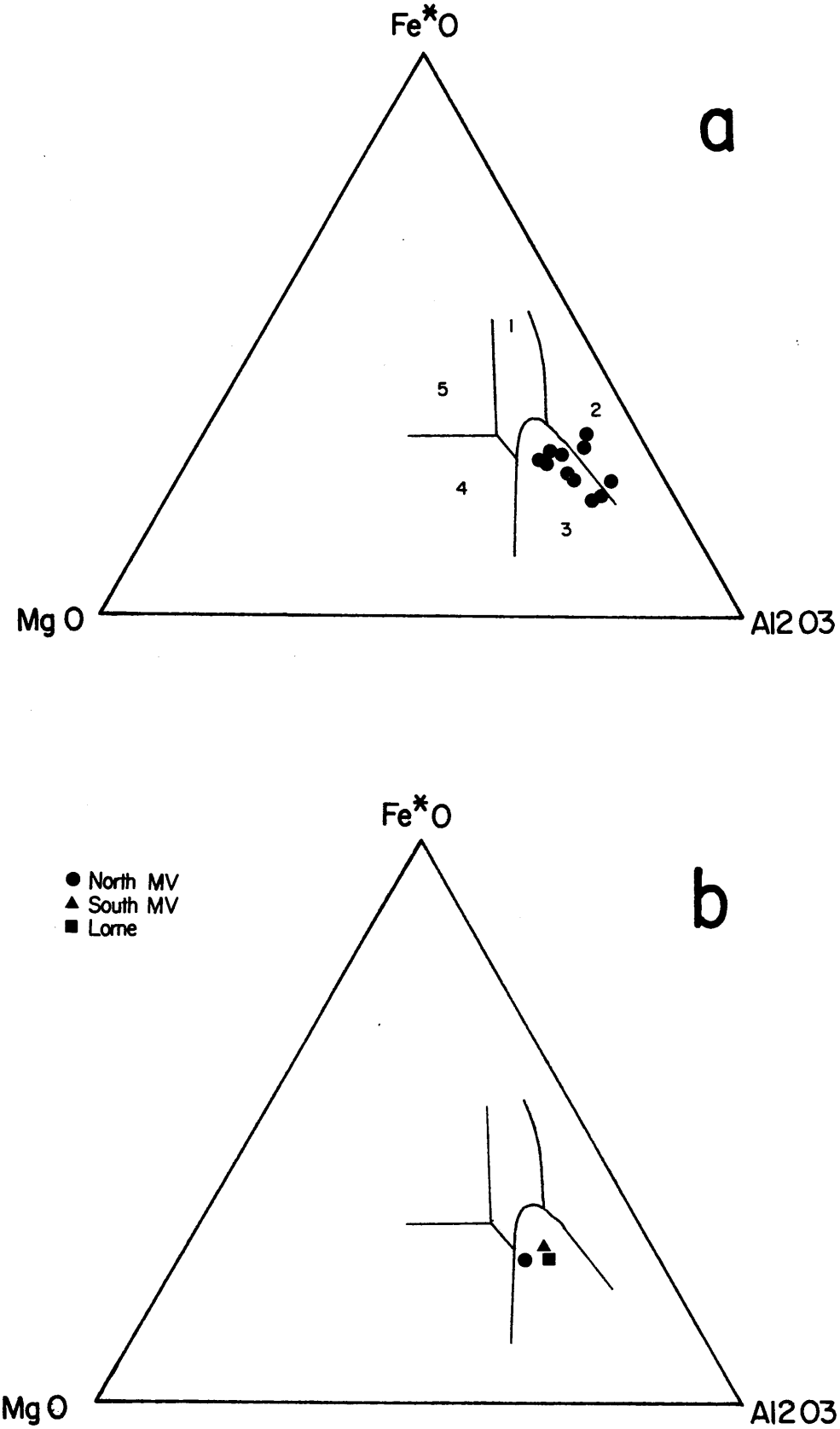

Fig 3.37. MgO:FeOt:Al2O3 discriminant diagrams showing: a) Roseneath intermediate clasts; 1 continental; 2 spreading centre island; 3 orogenic; 4 ocean ridge & floor; 5 ocean island and; b) average N Midland Valley, S Midland Valley and Lorne ORS lavas.

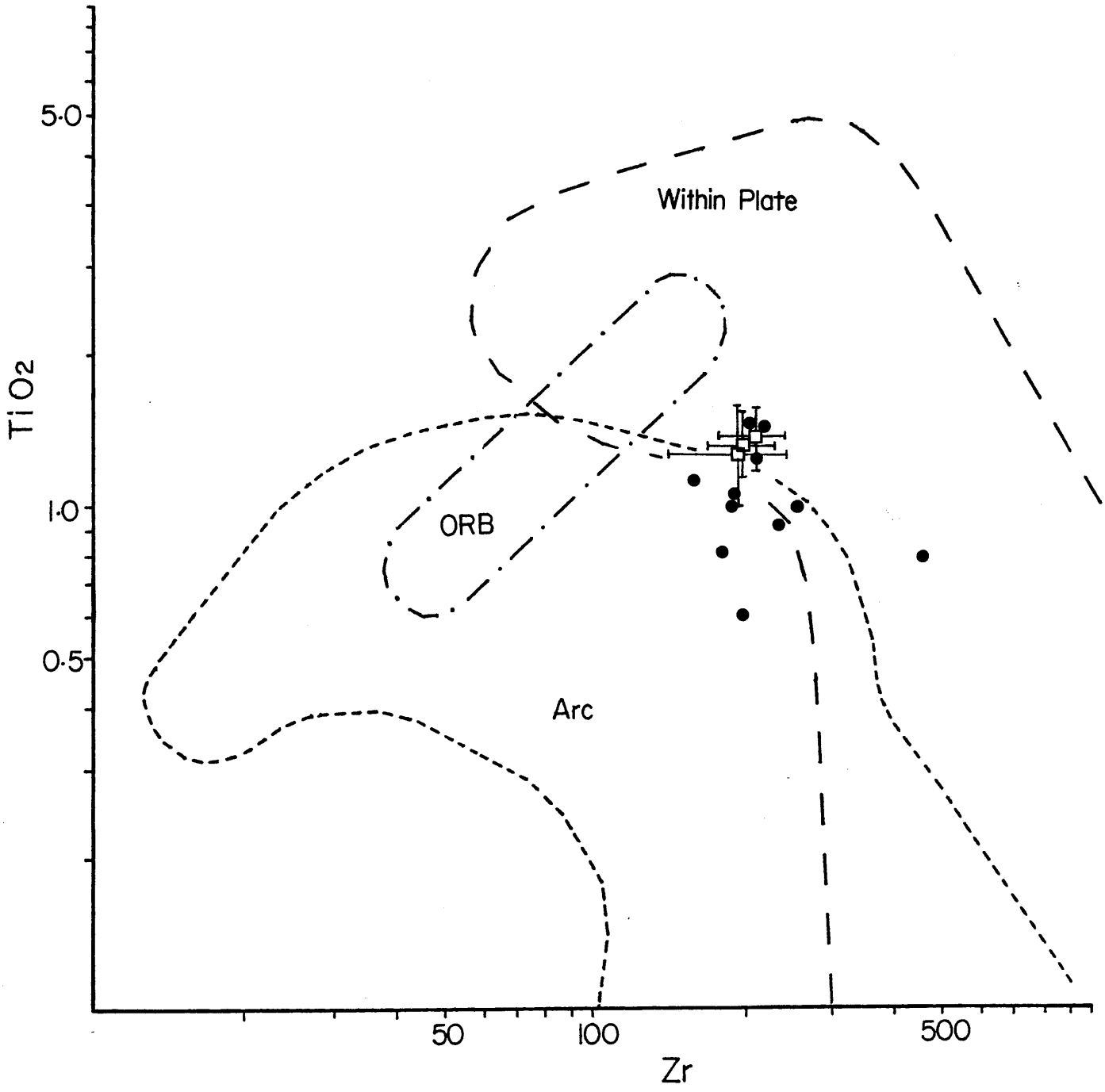

Fig 3.38. TiO2:Zr discriminant diagram for Roseneath intermediate rocks (●). Average southwest Highlands (1), north (2) and south (3) Midland Valley ORS andesites (with sd bars) indicated (□). Fields from Pearce and Norry (1979).

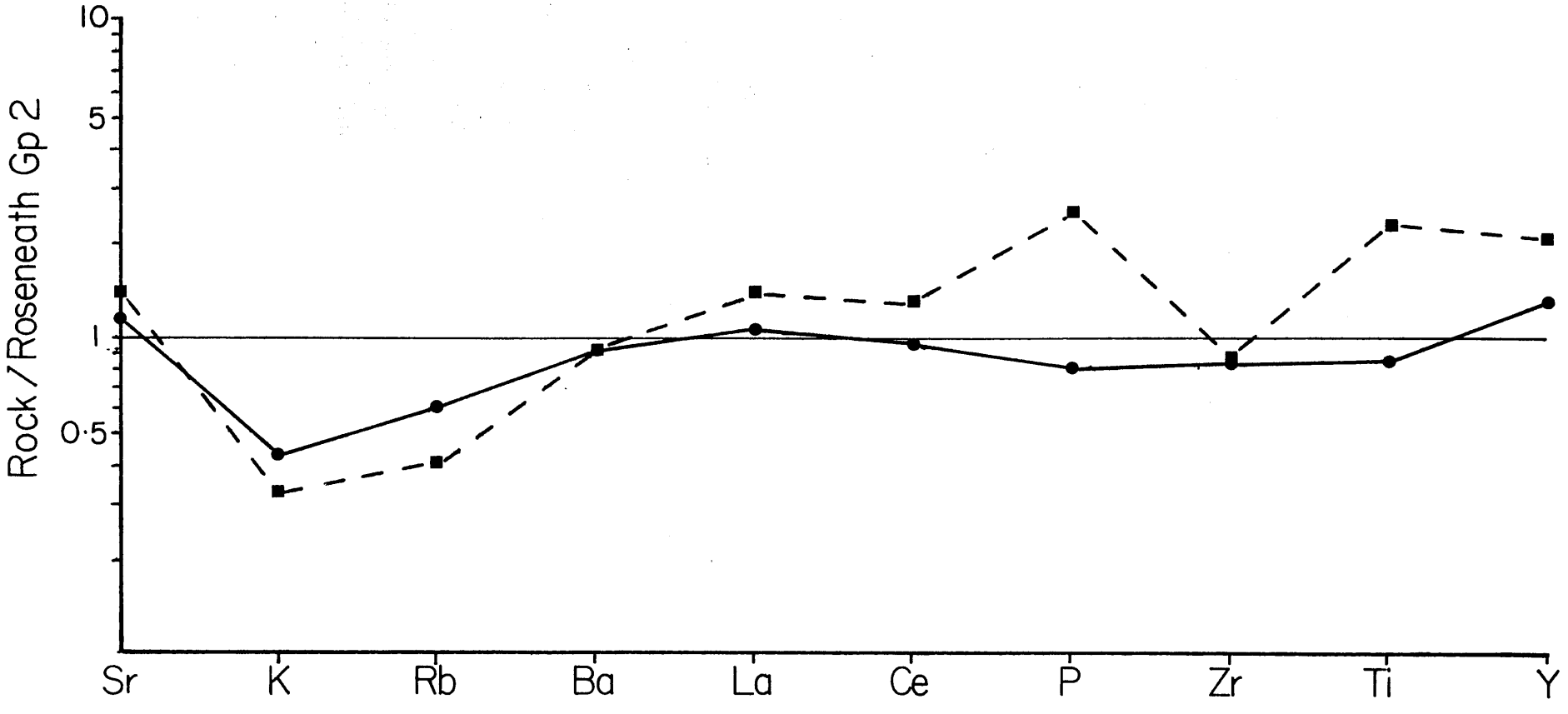

Fig 3.39. Roseneath average 'andesite' normalised against Aleutian calc-alkaline andesite (●) and Aleutian tholeiitic andesite (■). Data from Kay (1977).

tholeiites) is another common feature with the Roseneath andesites. Kay (1977) considered that the most likely mechanism to account for LIL enrichment relative to LREE would be an admixing of material with high LIL/LREE ratios and source rocks or magmas with low oceanic/island arc ratios. Sources in, or contamination by continental crust may not apply to the Aleutian magmas, but has already been suggested for the genesis of the Group 1 rocks (see above). This source would require to have been depleted in Sr and perhaps Ba relative to K and Rb, suggestive of plagioclase depletion during partial melting. An alternative explanation invokes a deeper source in a modified mantle wedge above subducting oceanic lithosphere. It is known that concentrations of incompatible LIL elements (eg. K and Rb) are high volcanic arc magmas (Pearce and Gale 1977). Since plagioclase is not a stable phase in the mantle, LIL ratios with Sr will be similarly high. The mantle wedge above a subduction zone would be further enriched if sediments were underthrust with the oceanic plate since high incompatible LIL contents (and ratios with La) of continental detrital and pelagic sediment have been documented (Church 1973).

Of the two models of magma genesis discussed above, low Nb concentrations and high Rb/Nb and K/Nb ratios of the Roseneath andesites favour a modified mantle origin. Nb^{5+}, being a small highly charged lithophile ion, is not strongly partitioned into acqueous fluids and mantle concentrations are low. By contrast, partial melting processes in a within-plate setting affect K^{+} and Nb^{5+} to an approximately equal extent producing melts richer in Nb. Nb concentrations are not quite low enough in these rocks, however, for a within-plate setting to be ruled out using the $Nb:SiO_2$ plot (Fig. 3.40) devised by Pearce and Gale (1977). On this diagram Group 2 intermediate rocks plot transitional between arc and mid-plate magmas but display Rb concentrations more typical of mid-plate types.

Broad similarities between the Roseneath andesites and volcanic rocks associated with Old Red Sandstone continental sedimentation in the Southern Uplands, Midland Valley and Southwest Highlands have been noted (eg. Figs. 3.37 and 3.38). However these correlations do not extend to concentrations of Sr, Ba, Th and LREE which are all depleted relative to ORS andesites. Similar depletions, coupled with lower La/Y for high Ni (> 100ppm) Shetland ORS lavas relative to Midland Valley and Southwest Highlands types led Thirlwall (1981) to conclude that the former lay closer to the surface trace of the Benioff zone (northwest subduction of Iapetus oceanic plate) than any other part of the province. This was based on the observation that Sr,

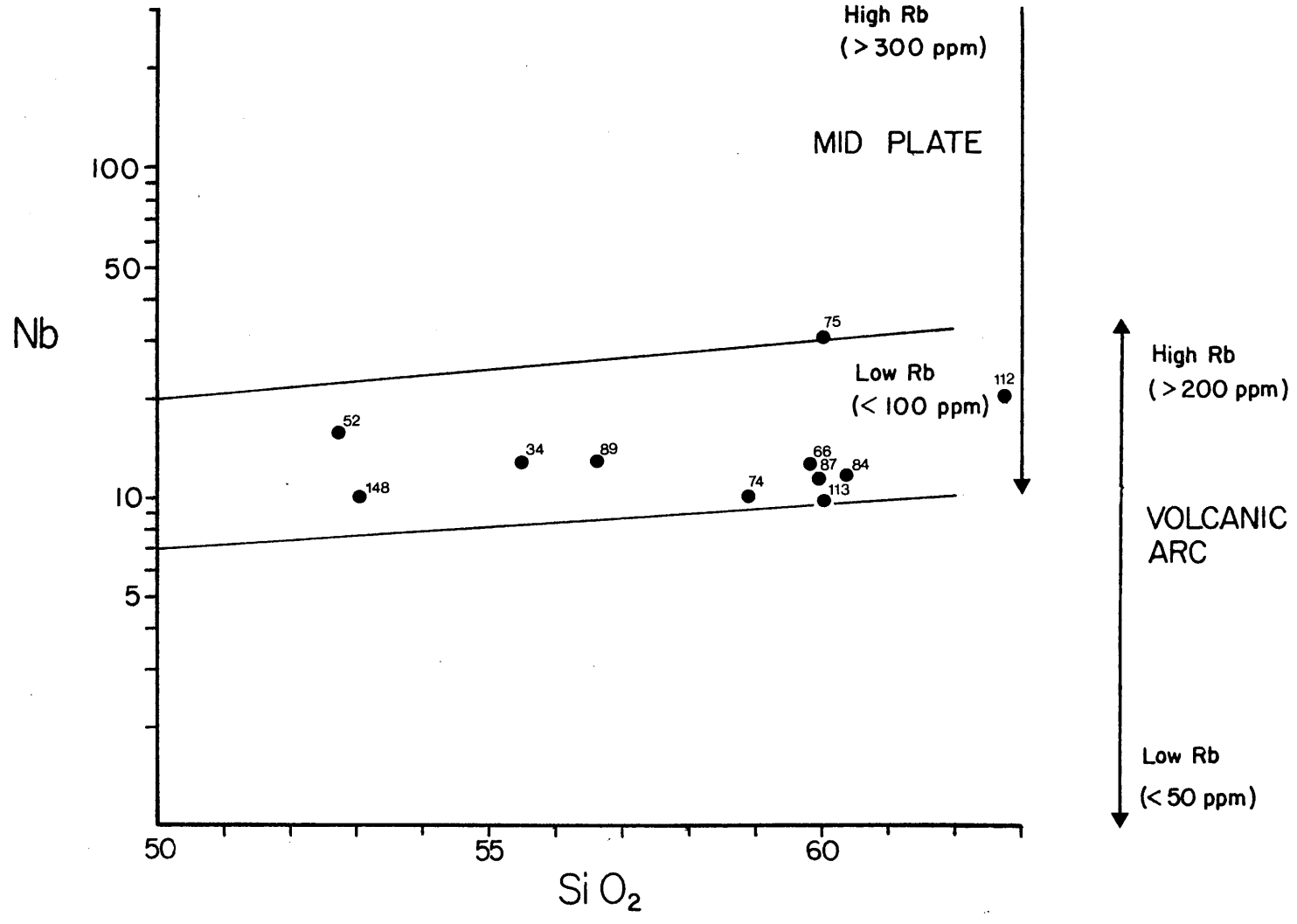

Fig 3.40. Nb:SiO2 discriminant diagram for Roseneath intermediate clasts. Rb concentrations (ppm) indicated for each clast.

Ba, and La/Y increase in a northerly/northwesterly direction, roughly perpendicular to the Iapetus suture for the Midland Valley/Southwest Highlands part of the province. Comparison with ORS lavas in La/Y:Sr and Ba:Sr diagrams (Figs. 3.41a,b) suggests distinct similarities between Roseneath andesites and Shetland/south Midland Valley equivalents. However low La/Y, Ba, Sr and Th are achieved in ORS lavas only in more primative rocks (higher Ni) than at Roseneath.

Comparison with analyses of Caledonian plutonic rocks (Stephens and Halliday 1984) reveals that LREE are also anomalously depleted for plutons closest to the Iapetus suture. In addition, low La/Y in these plutons is often accompanied by low Ba, Sr and Th, even in the most acidic types to a comparable level to that of the Roseneath Group 2 clasts. Plutons displaying these characteristics are not restricted to the palaeo-suture zone and can be found considerably north of this in the central Midland Valley (Distinkhorn) and Southern Highlands (Garabal Hill and Arrochar). Comparing Sr and Ba with Caledonian plutonic rocks over a similar SiO_2 interval (Figs. 3.42a,b and c) suggests that Group 2 clasts display characteristics of southern Highlands or Southern Uplands types, and Fig. 3.42c indicates that Group 2 andesites are probably also closest to Southern Highlands compositions with respect to high CaO and low Sr. As noted by Stephens and Halliday, geographic K/Ba distinctions are more ambiguous for Caledonian plutons but alkaline rocks depleted in Ba like Roseneath andesites are characteristic of Southern Highlands and certain Southern Uplands plutons.

3.3.7 Group 1/Group 2 Relationships and Fractionation Models

The observed variations and concentrations of most major and trace elements are consistent with the statistically deduced comagmatic origin for the majority of acid clasts in the Roseneath conglomerate. Wide scatter observed for many trace elements on Harker diagrams is resolved in many instances by plotting elemental ratios where the resulting neutral or slightly inclined lineages clearly indicate subtle fractionation trends in these rocks.

Major anomalies exist in the behaviour of certain elements suggesting that simple fractionation was not responsible for the observed trends. Nevertheless, several of the characteristic variations observed for Group 1 clasts are typical of the more siliceous parts of Caledonian Newer granites located in the Southern Highlands (Garabal Hill and Arrochar), and may

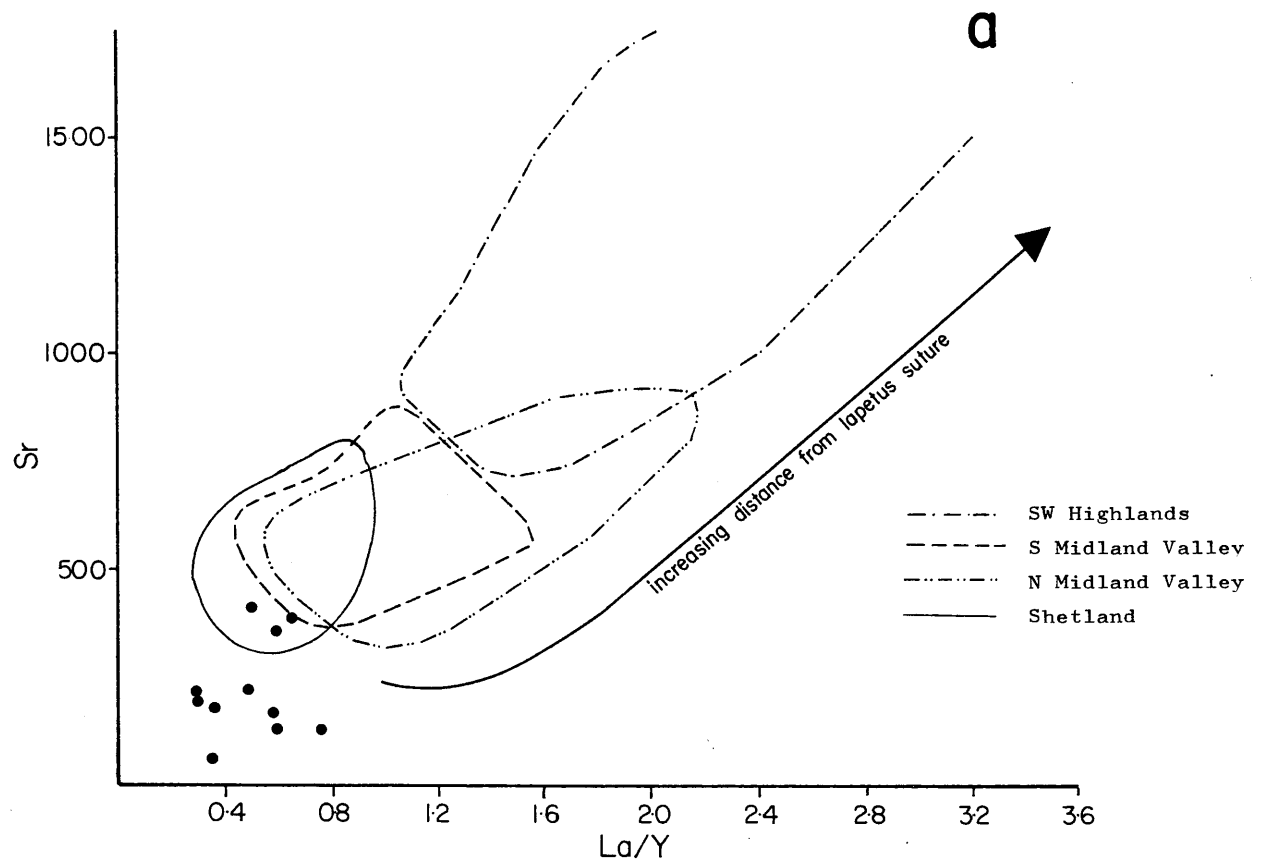

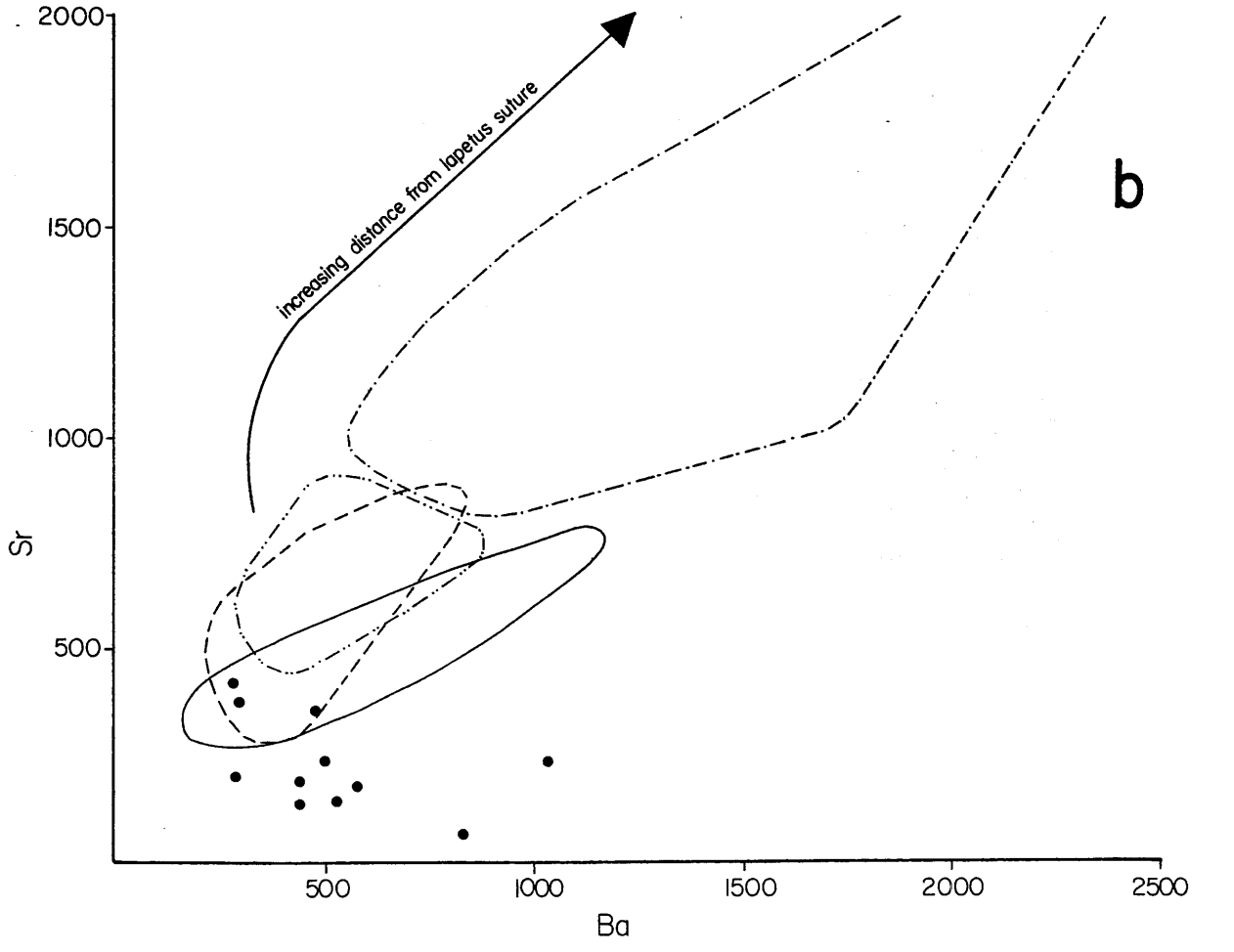

Fig 3.41. a) Sr:La/Y discriminant diagram for Roseneath intermediate clasts showing feilds for ORS volcanic suites. b) Sr:Ba discriminant diagram for Roseneath intermediate clasts.

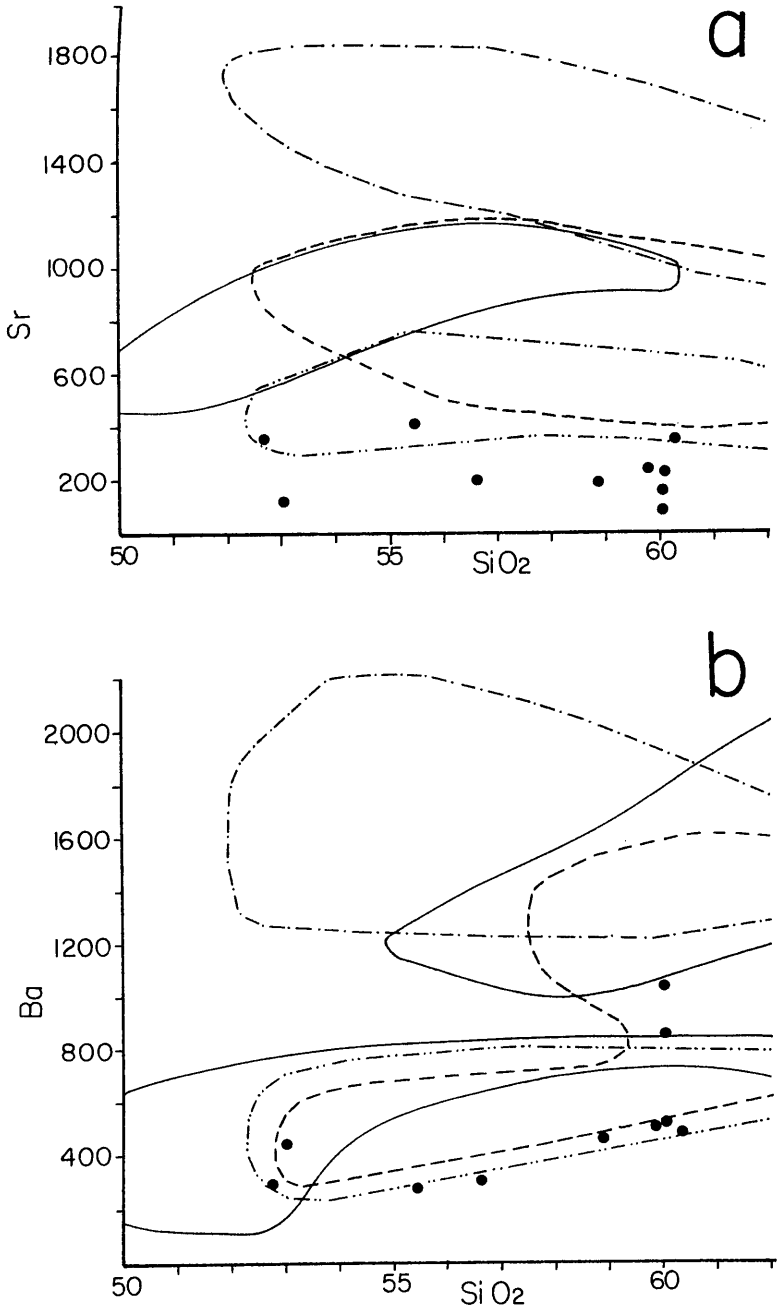

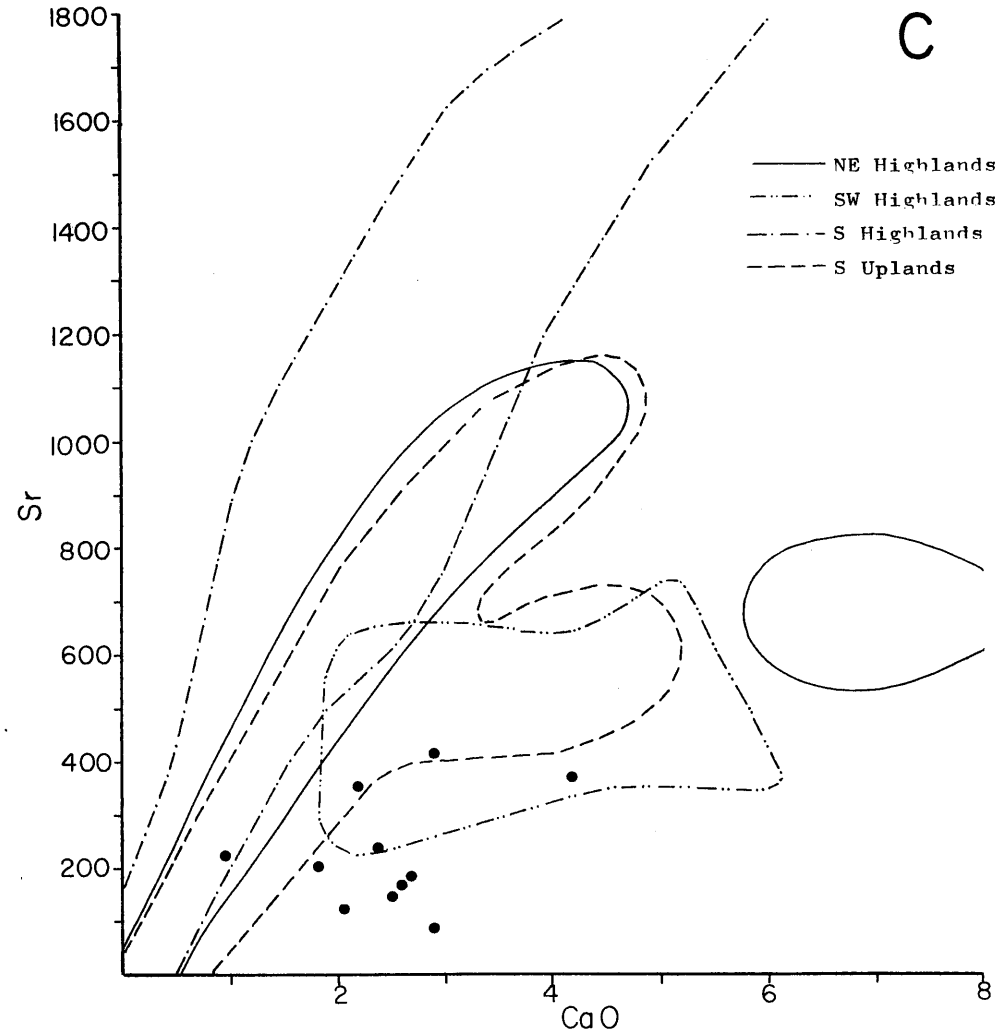

Fig 3.42. Diagrams comparing Roseneath intermediate clasts with fields for Caledonian plutonic rocks of similar composition using: a) Sr:SiO2; b) Ba:SiO2; c) Sr:CaO. All fields as in Fig 3.42c.

have resulted from crystal fractionation in an unusually evolved magma chamber. To understand the observed trace element behaviour further, and to investigate possible genetic relationships between Group 1 and Group 2 clasts, it is necessary to model these in terms of possible fractional crystallization processes.

The Zr/TiO_2 ratio plotted against SiO_2 content can be used as a rough measure of the degree of differentiation in igneous rocks (Winchester and Floyd 1977). Zr and Ti being relatively immobile during weathering enables incorporation of both acid and intermediate clast types in Fig. 3.43a. Group 2 rocks display increasing Zr/TiO_2 ratios but is less marked than that for Group 1 types. Despite the apparent dog-leg in the trend, the overall picture is not inconsistent with the evolution of a single magmatic series and is similar to a number of differentiation paths in Caledonian Newer granites. The Zr/TiO_2 ratio in conjunction with SiO_2 can also be used as an approximate index of alkalinity of a rock suite since Zr is apparently strongly concentrated in alkaline rocks (Winchester and Floyd 1977). From Fig. 3.43a, increasing alkalinity with increasing SiO_2 is characteristic of Group 2 intermediate rocks, whereas Group 1 types are only moderately evolving with respect to alkalinity.

The Nb/Y ratio is also an indicator of alkalinity (Pearce and Cann 1973, Winchester and Floyd 1977) because of Nb enrichment relative to Y in alkaline suites. Winchester and Floyd (1977) observed that this ratio remains constant or increases only slightly within a single magma series for increasing content of SiO_2. The $Nb/Y:SiO_2$ diagram (Figure 3.43b) shows a normal lack of Nb/Y variation for all Group 2 rocks over 53% to 71% SiO_2. This group is transitional between subalkaline and alkaline magma suites (Winchester and Floyd 1977). Group 1 clasts are obviously more alkaline than those of Group 2 ($Nb/Y>0.67$) and do not appear to form a coherent relationship with SiO_2. Once again, however, the general trend is not inconsistent with Caledonian granites, and particular similarities are noted with Southern Highlands types and most especially the Garabal Hill granitoid.

Because Zr/TiO_2 is a more reliable index of differentiation than SiO_2, a plot of $Zr/TiO_2:Nb/Y$ will be more helpful to determine possible genetic links between the two clast groups (Figure 3.44). Despite a considerable lack of homogeneity within Group 2 intermediate rocks, the differentiation path for the entire suite of Roseneath clasts once again resembles the

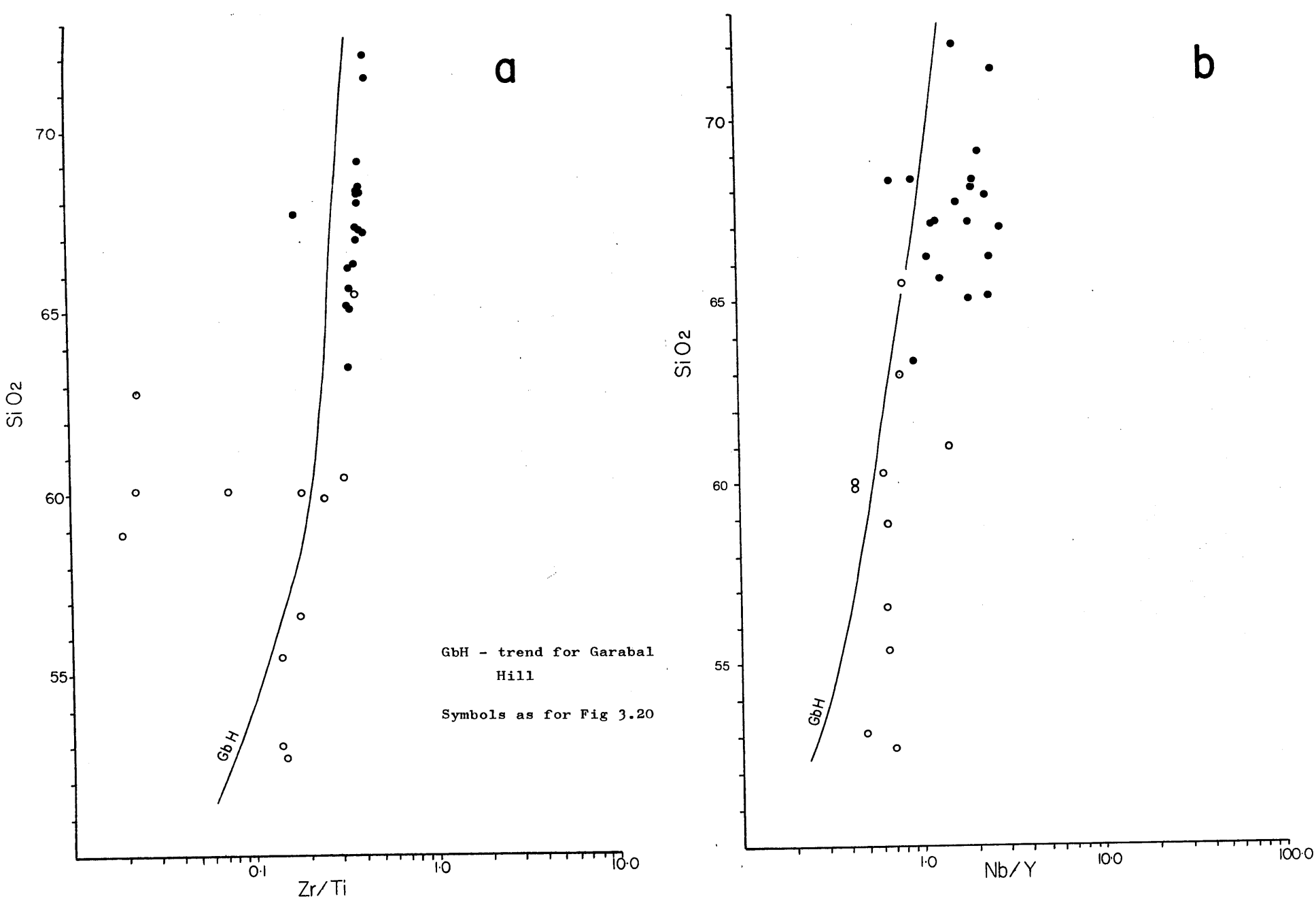

Fig 3.43. a) SiO2:Zr/Ti fractionation diagram for Roseneath igneous clasts. b) SiO2:Nb/Y fractionation diagram for Roseneath igneous clasts

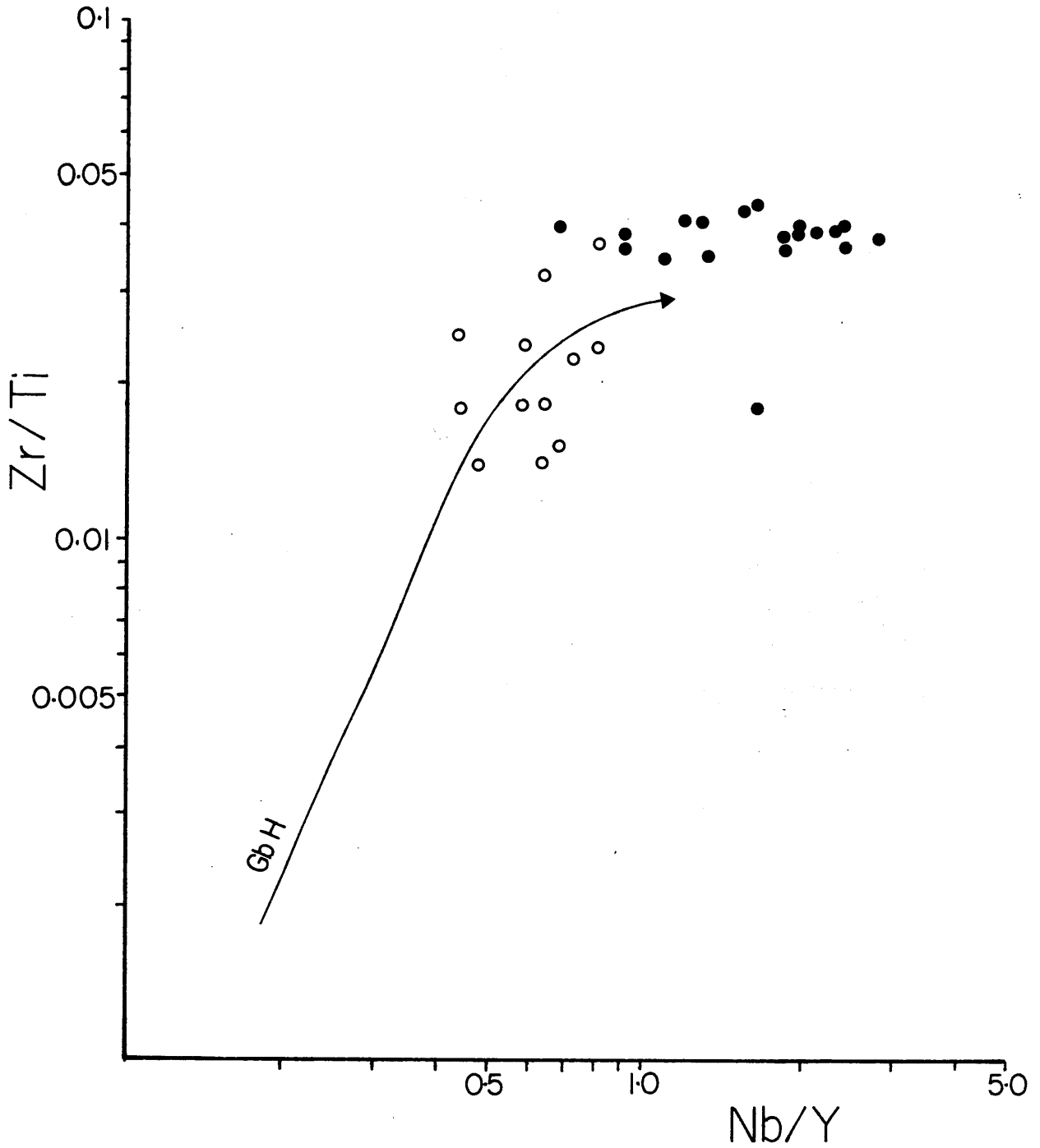

Fig 3.44. Zr/Ti:Nb/Y fractionation diagram for Roseneath igneous clasts. Symbols as for Fig 3.20.

fractionation trend for a single magmatic body. The evolutionary path is comparable with those of certain in situ Caledonian suites and similarities are again observed with Garabal Hill. The apparent divergence of the Roseneath fractionation trend from that of Garabal Hill at higher Nb/Y ratios is indicative of a more evolved magma type (higher Zr/TiO_2) than is presently exposed at Garabal Hill.

Fractionation paths for the evolution of volcanic suites have also been modelled by Pearce and Norry (1979) using the immobile elements Ti, Zr, Y and Nb. Compilation of mineral-melt distribution coefficients for these elements enables assignment of straight line portions of the trends to the fractionation of dominant mineral phases.

In the Zr:Ti diagram (Figure 3.45) Group 1 and Group 2 rocks seem to form a coherent fractionation lineage. The strengths of this correlation are particularly difficult to explain since Donnelly and Rogers (1979) showed that Zr and TiO_2 are closely correlated in ocean ridge basalts and primitive island arc suites but are unrelated in calc-alkaline assemblages. However, using models derived from distribution coefficients, decreasing Ti and Zr in Group 1 analyses is best achieved by considering biotite and/or K-feldspar as strong crystallizing phases. Similarly, in the Zr:Y diagram (Figure 3.46) the marked depletion in Y relative to Zr (best displayed by Group 1) is explained by amphibole crystallization, a characteristic not uncommon in acid and intermediate calc-alkaline rocks. Biotite and/or K-feldspar crystallization is also indicated from the most fractionated acid rocks in this diagram. The lack of a coherent fractionation path in the Zr:Nb diagram (Figure 3.47) is not anomalous, having been noted in suites from Andean type margins. The importance of amphibole and biotite/zircon as crystallizing phases causing fractionation trends to move back on themselves has been given as an explanation (Pearce and Norry 1979).

3.3.8 Geochemical Relationships with Caledonian Magmas - Group 1 Clasts Absolute Concentration Comparisons

Throughout the preceeding sections, similarities have been indicated between Roseneath igneous clasts and in situ plutonics and volcanics related to the Caledonian orogeny.

Abbott and Smith (1978), in their provenance study of rhyolite clasts in Eocene fluvial conglomerates of southwestern California and Mexico, successfully

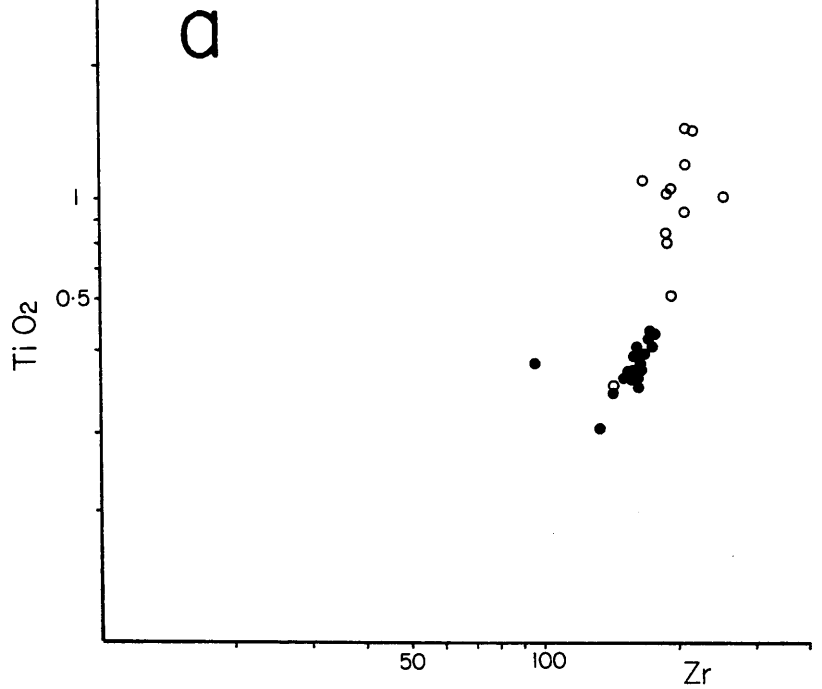

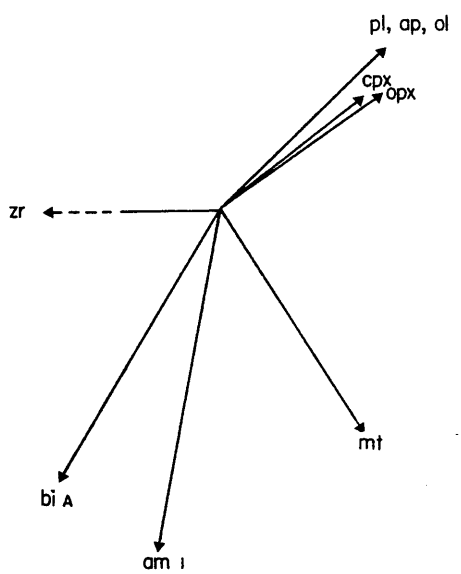

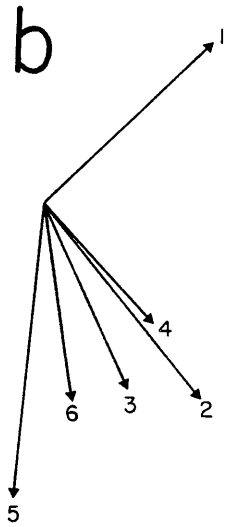

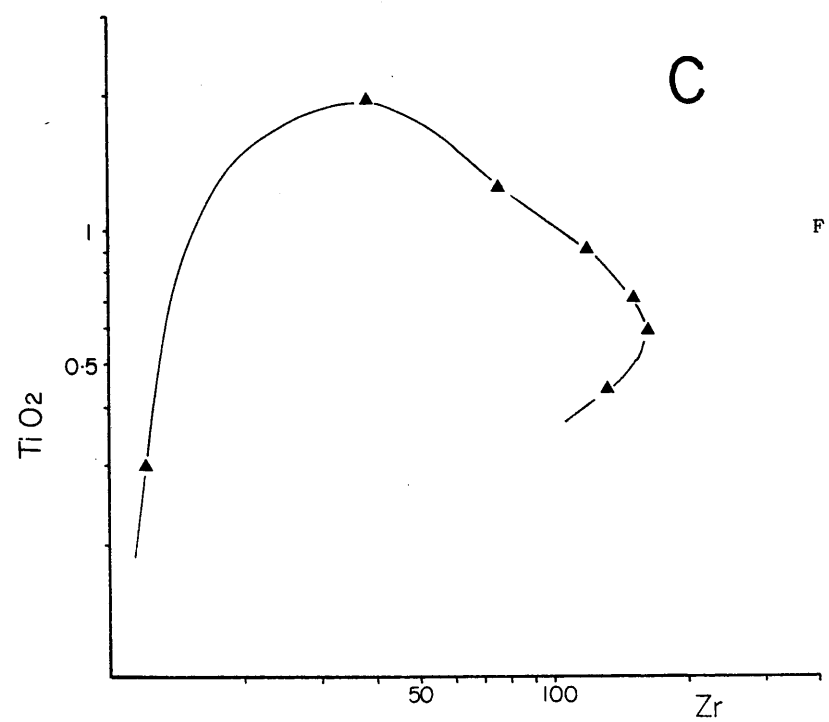

Fig 3.45. Zr:Ti fractionation diagram for: a) Roseneath igneous clasts, symbols as for Fig 3.20 and; c) Garabal Hill intrusion. b) fractionation vectors of dominant mineral phases (from Pearce & Norry 1979).

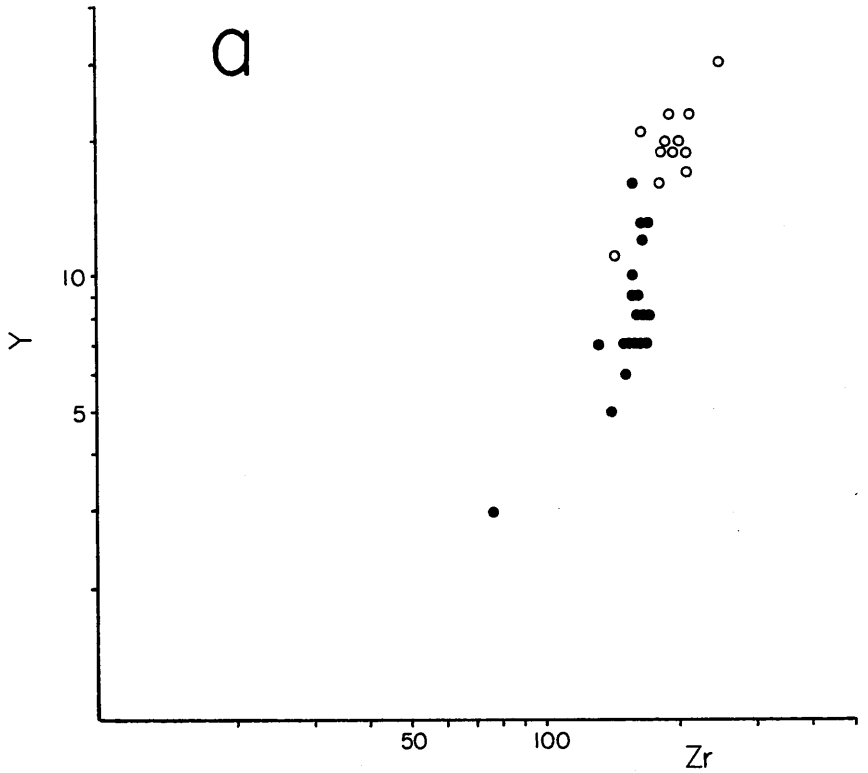

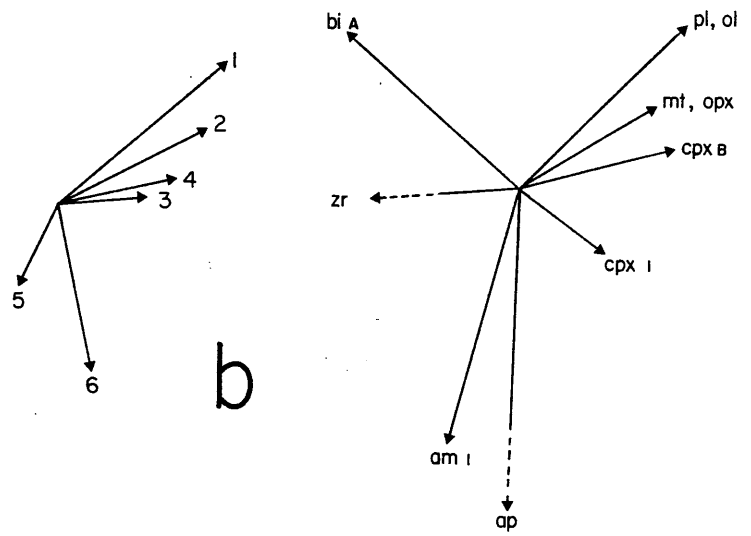

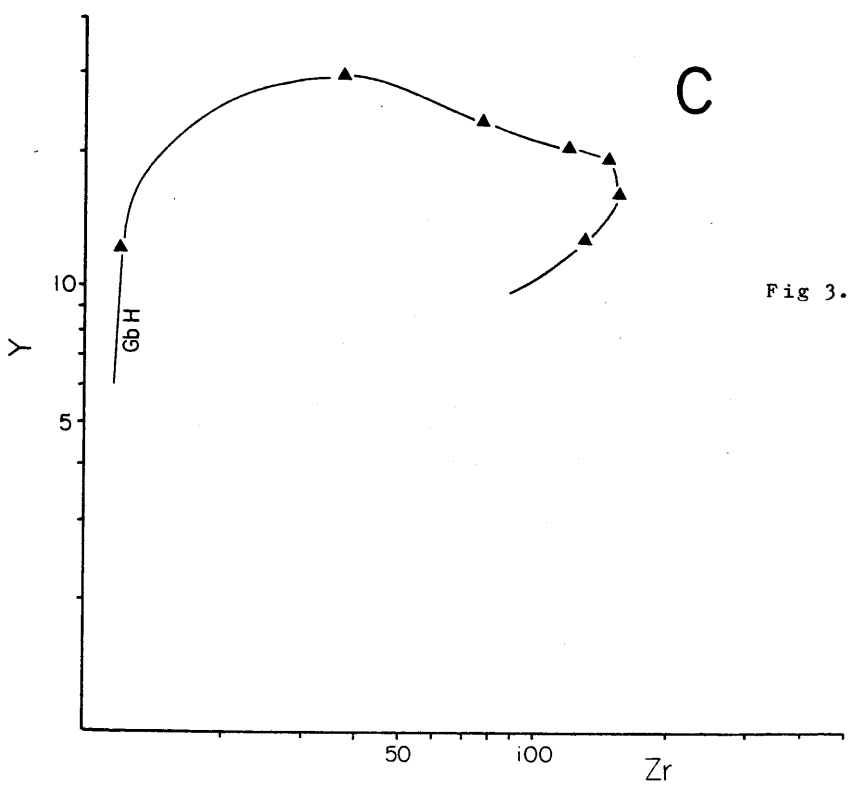

Fig 3.46. Y:Zr fractionation diagram for: a) Roseneath igneous clasts, symbols as for Fig 3.20 and; c) Garabal Hill intrusion. b) fractionation vectors of dominant mineral phases (from Pearce & Norry 1979).

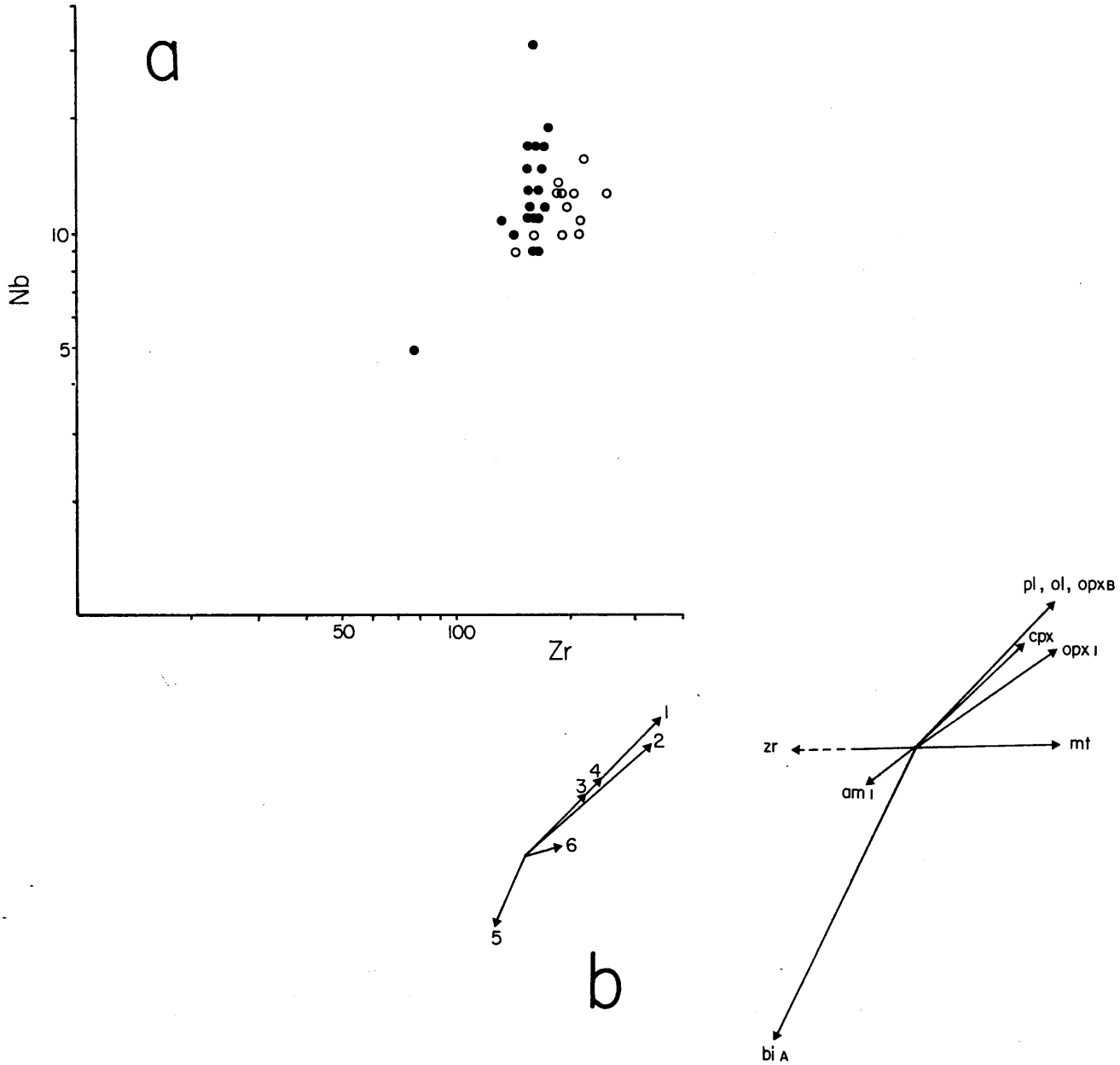

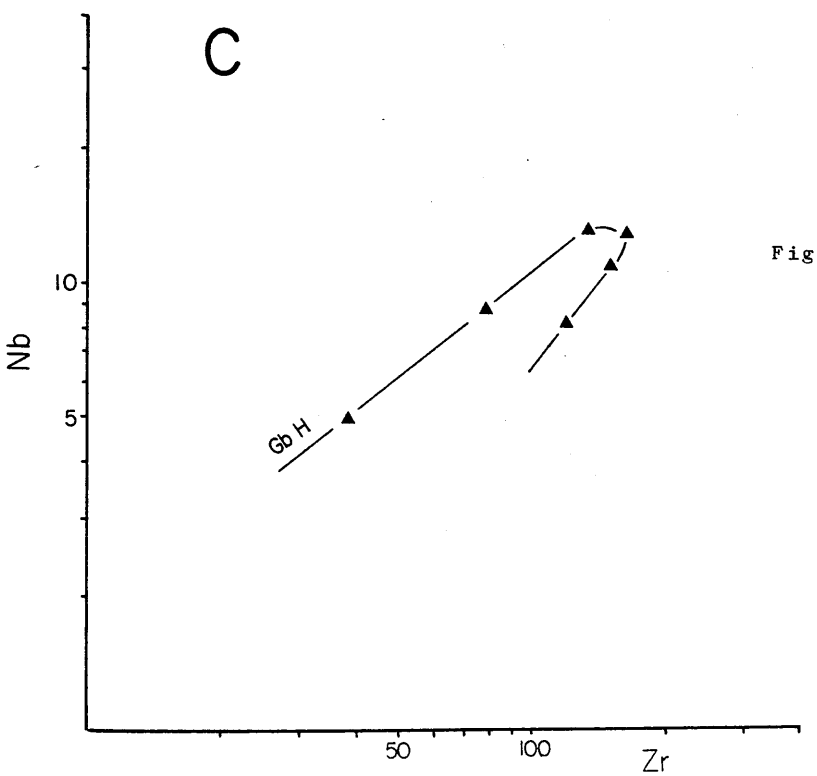

Fig 3.47. Nb:Zr fractionation diagram for a) Roseneath igneous clasts, symbols as for Fig 3.20 and; c) Garabal Hill intrusion. b) fractionation vectors of dominant mineral phases (from Pearce & Norry 1979).

pin-pointed previously suspected or unidentified source terranes by statistical matching of trace element 'fingerprints'. This was done by a series of systematic comparisons of means and standard deviations between the conglomerate clasts and likely source candidates of similar general acidic composition. For each element, the difference of means ($\bar{x}_1 - \bar{x}_2$) and standard errors of the difference (standard error = (($[\sigma_1^2/n_1] + [\sigma_2^2/n_2]$)) were calculated where σ is the standard deviation of a set of n variables. The significance (S) of the difference for each element comparison was determined using the ratio of these two parameters as follows:

$$S = \frac{(\bar{x}_1 - \bar{x}_2)}{(([\sigma_1^2/n_1] + [\sigma_2^2/n_2]))}$$

Differences in absolute concentration were then summarised as: statistically highly significant (S> 4); significant (S=3.00 to 3.99); and probably significant (S=2.00 to 2.99). No significant difference was interpreted only for values of S less than 1.99. Interpretation of probably significant S values was considered difficult, especially where small numbers of samples are used.

The publication by Stephens and Halliday (1984) of comprehensive information concerning trace element distributions within 38 late Caledonian granitoids has enabled detailed comparison with the bulk of Caledonian plutonic rocks. These granites are post-metamorphic, late Ordovician to Lower Old Red Sandstone in age and conform to the Newer Group (subgroups 2 and 3) of Pankhurst et al (1982) modified from Read (1961). However, whilst these intrusions are the most volumetrically significant, detailed analyses of Older granites and those emplaced at the climax of Caledonian metamorphism are still deficient in the literature. Comparisons with these Older granites are particularly pertinent in the light of the Rb-Sr whole rock age constraints for the Group 1 clasts (Section 3.3.9).

The second major source of data for Group 1 comparisons comes from granitic clasts in six major Ordovician conglomerates in the southern Midland Valley analysed by Longman (1980). These clasts are of middle Ordovician to middle/early Cambrian in age (c 450-590 Ma: Rb-Sr whole rock and mineral ages and U-Pb zircon ages) and have been considered to represent disintegration of a plutonic arc during the Ordovician. This arc is thought to have been located in the region now occupied by the Central Midland Valley (Longman et al 1979).

All comparisons were made using data from samples with $S:O_2$ contents > 63%; broadly comparable with those from the Roseneath clasts. These data are presented in Table 3.4.

Initial comparison with the Ordovician conglomerate clast suite in the statistical comparison table (Table 3.5) suggests impressive similarities with the Roseneath Group 1 clasts, especially for the moderately incompatible elements Th to Ti. However, many critical element ratios and concentrations (eg Sr, Rb, Ba, Rb/Sr and La/Y) are, at very least, significantly different. These differences probably negate the possibility that the Ordovician suite provided a source of polycyclic material, or that the two clast suites had a common provenance.

Stephens and Halliday (1984) classified all the Newer granites into three broad suites (Cairngorm, Argyll and South of Scotland) on the basis of unique geochemical characteristics. As an initial screening, average compositions for granite/granodiorite rocks from each of the three categories were compared with the Roseneath Group 1 clasts (Table 3.5). Few significant similarities are obvious for the Cairngorm suite, with 88% of the elements compared displaying significant or highly significant enrichment or depletion relative to the Roseneath suite. However, both the South of Scotland and Argyll suites correlate closely with Group 1, the Argyll suite providing the closest match. Particularly impressive are near identical concentrations of incompatible elements from Sr to Nb and the moderately incompatible P, Zr and Ti.

To further investigate these similarities, analyses for selected individual plutons of both Argyll and South of Scotland suites have been systematically compared (Table 3.5). Unfortunately, the reliability of statistical interpretation becomes less certain due to the reduction in the number of analyses used for each comparison. Where only one analysis is available for comparison it is clearly impossible to determine statistical significance. For the Argyll suite, both the Etive and Foyers plutons display near identical trace element characteristics to those of Group 1 clasts.

In addition, from the South of Scotland suite, Garabal Hill also exhibits similarities (cf analysis in Table 3.4), but slight enrichment in compatible elements for this intrusion is indicative of a less fractionated magma. Lack of data prevents statistical comparison but it would be fair to suggest that

	CAIRNGORM SUITE *		SOUTH OF SCOTLAND SUITE *		ARGYLL SUITE *		ORDOV. CLASTS +		STO *		FOY *		BNV *		ETV *		RNM *		BSH *		GBH 78 *		ROSENEATH ≠	
	$\bar{x}$	sd	$\bar{x}$	sd	$\bar{x}$	sd	$\bar{x}$	sd	$\bar{x}$	sd	$\bar{x}$	sd	$\bar{x}$	sd	$\bar{x}$	sd	$\bar{x}$	sd	$\bar{x}$	sd	$\bar{x}$	sd	$\bar{x}$	sd
Ba	461	325	758	235	1139	495	608	685	813	109	1255	403	1276	57	626	379	1513	468	1166	42	789		1094	233
Ce	71	51	60	33	64	21	34	21	64	9	62	26	94	8	50	16	46	10	90	16	50		34	10
Cr	5	6	36	39	31	48	27	15	100	100	13	15	8	11	18	22	50	20	12	13	99		28	10
Cu	5	3	18	19	31	95	17	12	8	3	14	6	9	2	7	3	6	1	225	294	4		15	10
La	43	32	33	19	40	9	16	11	30	2	42	9	49	7	40	6	35	3	50	8	27		17	5
Nb	31	15	12	4	13	10	11	12	9	2	25	16	9	3	10	3	6	1	21	3	13		14	6
Ni	9	6	19	16	21	18	4	6	47	29	12	5	11	7	18	12	33	8	12	6	42		10	4
Pb*	30	9	23	7	19	7	12	12	11	6	18	2	16	2	23	10	20	8	26	5	13		15	4
Rb	254	186	146	68	95	32	67	37	86	32	76	13	97	0	117	29	71	10	146	18	87		87	12
Sr	178	172	453	208	603	287	196	120	712	208	509	230	654	83	407	316	782	288	840	230	679		705	130
Th	25	16	18	8	13	10	10	5	11	8	6	4	10	1	13	6	17	15	28	12	6		9	2
Ti	2630	2080	5140	2080	4810	2820	2700	1500	6870	2750	4500	3050	4100	850	4220	3000	4070	1500	3500	1980	6000		4200	500
Y	23	18	17	8	15	5	20	17	17	3	15	8	16	1	14	5	10	1	18	3	16		8	3
Zn	34	14	37	18	38	16	38	22	50	14	38	19	28	4	35	19	37	11	40	19	54		25	7
Zr	131	72	167	67	153	53	150	147	153	16	156	70	204	13	136	62	103	12	166	74	163		157	22
n=	21		36		20		52		3		4		2		4		3		2		1		19	
n*=	11		22		20		52		3		4		2		4		3		2		1		19	

Table 3.4. Averaged trace element compositions of Caledonian granitoids and Roseneath clasts used for statistical comparison (Table 3.5). STO - Strath Ossian; FOY - Foyers; BNV - Ben Nevis; ETV - Etive; RNM - Rannoch Moor; BSH - Ballachulish; GBH - Garabal Hill.

* data from stephens and Halliday (1984); + Longman (1980); ≠ this study.

	CAIRNGORM SUITE	SOUTH OF SCOTLAND SUITE	ARGYLL SUITE	ORDOV. CLASTS	STO	FOY	BNV	ETV	RNM	BSH
Ba	Highly	Highly	NONE	Highly	Signif	NONE	Possible	Possible	NONE	NONE
Ce	Signif	Highly	Highly	NONE	Highly	Possible	Highly	NONE	NONE	Highly
Cr	Highly	NONE	NONE	NONE	NONE	NONE	Possible	NONE	NONE	NONE
Cu	Highly	NONE	NONE	NONE	Possible	NONE	Possible	Possible	Signif	NONE
La	Signif	Highly	Highly	NONE	Highly	Highly	Highly	Highly	Highly	Highly
Nb	Highly	NONE	NONE	NONE	Possible	NONE	NONE	NONE	Highly	Possible
Ni	NONE	Signif	Possible	Highly	Possible	NONE	NONE	NONE	Highly	NONE
Pb	Highly	Highly	Possible	NONE	NONE	Possible	NONE	NONE	NONE	Signif
Rb	Highly	Highly	NONE	Signif	NONE	NONE	Signif	Possible	Possible	Highly
Sr	Highly	Highly	NONE	Highly	NONE	NONE	NONE	NONE	NONE	NONE
Th	Highly	Highly	NONE	NONE	NONE	NONE	NONE	NONE	NONE	Possible
Ti	Signif	Possible	NONE	Highly	NONE	NONE	NONE	NONE	NONE	NONE
Y	Signif	Highly	Highly	Highly	Highly	NONE	Highly	Possible	Possible	Highly
Zn	Possible	Signif	Signif	Signif	Signif	NONE	NONE	NONE	NONE	NONE
Zr	NONE	NONE	NONE	NONE	NONE	NONE	Highly	NONE	Highly	NONE

Table 3.5. Statistical comparison (standard error of difference) of Roseneath acid clasts with selected Caledonian granitoid suites, selected intrusions and acidic igneous detritus from Ordovician conglomerates in the SW Midland Valley. Abbreviations as for Table 3.4.

the two compositions could easily have existed within a single fractionating system. Th, La, Y, and Ni concentrations are low and close to or below reliable detection limits for both Roseneath and Garabal Hill and therefore the minor discrepences around these elements can not be considered significant. Cu concentrations, however, are significantly enriched in the Roseneath rocks.

3. 4 Geochronology and Isotope Geochemistry

Isotopic determinations were performed on the Roseneath granodiorite boulders using Rb-Sr (mineral and whole-rock), K-Ar (biotite) and U-Pb (zircon) dating methods. These data are presented in Table 3.6. Analytical techniques are described in Appendix II.2.

Rb-Sr Whole-rock

The most reliable method of dating an in situ plutonic body using the Rb-Sr scheme is through the whole-rock method. This requires that a suite of rocks be collected from the intrusion which span as wide a range of Rb/Sr ratios as possible so that the data form a well defined line ('isochron') when plotted in co-ordinates of $^{87}Sr/^{86}Sr$ and $^{87}Rb/^{86}Sr$. However, the whole-rock system requires that all the analysed samples formed from the same parent magma with a homogeneous initial $^{87}Sr/^{86}Sr$ ratio. It is therefore difficult to apply to a suite of boulders in a conglomerate derived from an unknown source(s).

Since trace-element modelling (Section 3.3.7) and multivariate analysis (Section 3.3.4) has shown that the majority of acid clasts are probably genetically related by amphibole fractionation within a single pluton, 17 specimens were analysed using the Rb-Sr whole-rock method.

Ten samples which have previously been identified as unaltered by hydrothermal processes define a best-fit line with an age of 530 $\pm$ 70 Ma. Unfortunately, the limited range in $^{87}Rb/^{86}Sr$ and apparently heterogeneous initial $^{87}Sr/^{86}Sr$ ratios of the source render this a suspect isochron calculation. Seven hydrothermally altered clasts display much higher ($>$ 1.0) and more variable $^{87}Rb/^{86}Sr$ and generally scatter above the regression line through the unaltered samples. This is interpreted as reflecting enrichment in radiogenic Sr from either percolating hydrothermal fluids or through host-rock contamination.

1) UNALTERED CLASTS - Rb-Sr whole rock age

SAMPLE	Rb (ppm)	Sr (ppm)	87Rb/86Sr	87Sr/86Sr	2σ	(87Sr/86Sr)i	(87Sr/86Sr)516	AGE ±2σ
B9-24		870	.172	.70538	4	.7039±4	.70412	530±70
A11-11		1030	.195	.70518	3		.70375	
B3-18	70	644	.314	.70618	3		.70388	
B10-25	88	778	.328	.70649	3		.70409	
B1-16	94	714	.382	.70664	3		.70384	
B7-22	88	639	.400	.70698	3		.70405	
B12-27	90	649	.401	.70680	3		.70386	
B2-17	107	768	.405	.70678	3		.70381	
B15-29		547	.515	.70819	3		.70442	
A9-9		457	.653	.70867	3		.70389	

2) ALTERED CLASTS - isotopic data

SAMPLE	Rb (ppm)	Sr (ppm)	87Rb/86Sr	87Sr/86Sr	2σ	(87Sr/86Sr)i	(87Sr/86Sr)516
A15-15		139	1.011	.71604	3		.70863
A5-5		127	1.990	.72187	3		.70729
A6-6	113	155	2.102	.72141	3		.70601
V7-42		85	2.450	.72386	3		.70591
A1-1	112	127	2.557	.72543	3		.70669
A7-7		96	2.722	.72485	3		.70491
A14-14		114	3.094	.72473	3		.70206

3) Rb-Sr mineral ages

SAMPLE	MINERAL	Rb (ppm)	Sr (ppm)	87Rb/86Sr	87Sr/86Sr	2σ	(87Sr/86Sr)i	AGE ±2σ
B1-16	Biotite	529	33	47.40	.92975	3	.7049±2	332±3
	K-feld	92	929	.285	.70637	3		196±38
B2-17	Biotite	530	30	52.43	1.08934	5	.7038±1	516±5
	K-feld	164	821	.580	.70815	3		549±30
B3-18	Biotite	252	35	21.24	.83835	3	.7042±1	443±5
	K-feld	126	881	.415	.70677	4		410±40
A1-1	Biotite	313	45	20.25	.82853	3	.7092±8	449±5
	K-feld	100	87	3.337	.73086	3		489±26
A2-2	Biotite	250	113	6.432	.75276	3	.7056±20	508±8
	K-feld	104	132	2.274	.72175	3		139±32

4) K-Ar mineral age (provisional)

SAMPLE	MINERAL	AGE±2σ
B3-18	Biotite	374±8
A1-1	Biotite	391±8
A2-2	Biotite	397±8

5) U-Pb zircon

FRACTION	Pb (ppm)	U (ppm)	$\frac{206Pb}{204Pb}$	206Pb	207Pb	208Pb	$\frac{207Pb}{206Pb}$	$\frac{207Pb}{235U}$	$\frac{206Pb}{238U}$	$\frac{207Pb}{206Pb}$ AGE
+100NM	42.0	537	3139	80.4239	4.7000	14.876	.05849	.58478	.072569	931
-100NM	48.6	683	2339	81.8149	4.6735	13.512	.05712	.53272	.067632	945
-65+53NM	55.1	761	2060	80.1571	4.5327	15.310	.05654	.52539	.067380	932
-100+65NM	46.4	653	2073	81.8354	4.6664	13.498	.05702	.53069	.067495	966

Table 3.6 Rb-Sr (whole rock and mineral), U-Pb and K-Ar analytical data for Roseneath clasts.

Rb-Sr Mineral

Rb-Sr ages were also obtained from 5 individual boulders using biotite- and K-feldspar-whole-rock methods. This dating scheme is particularly applicable to metamorphic investigations since mineral phase Rb-Sr decay schemes are profoundly affected by modest increases in temperature whilst the rock as a whole remains unaffected with respect to isotopic abundances of Rb and Sr.

Rb-Sr mineral ages for the Roseneath clasts display enormous variability (332-516 Ma biotite-whole-rock; 139-549 Ma feldspar-whole-rock). However, the oldest biotite-whole-rock (516±5 Ma, IR=0.7038±1) and feldsparwhole-rock (549±30 Ma, IR=0.7036±2) ages and initial ratios are not only within error of each other but are also within error of the unaltered clasts' whole-rock determination (530±70 Ma, IR=0.7039±4).

The extreme variability of Rb-Sr mineral ages in these clasts which are demonstrably cogenetic using a variety of other techniques may be attributed to any of three influences:

i) Removal of radiogenic ^{87}Sr from mineral phases in a closed whole-rock system during reheating above mineral blocking temperatures will result in the date of the subsequent metamorphism, or the time of cooling and radiogenic closure after metamorphism. In this instance the oldest mineral age will provide a minimum crystallisation age for the intrusion.

ii) Deuteric removal of radiogenic ^{87}Sr and possible addition of Rb can also effectively lower Rb-Sr biotite and feldspar ages by up to 75% (Goldich and Grant 1966).

iii) Hydrothermal alteration may enrich selected mineral phases in radiogenic ^{87}Sr without significantly affecting whole-rock abundances. In this case anomalously old ages may be induced in detritus from a pluton whose date of intrusion was at least that of the youngest mineral age.

Sample A1-1 is known to have been affected by hydrothermal alteration which has clearly preferentially enriched feldspars and the whole-rock in radiogenic ^{87}Sr relative to biotite phases. Mineral ages for it are therefore suspect. Sample B1-16 yields both biotite- and feldspar-whole-rock ages (332±3 Ma and 196±38 Ma respectively) which are younger than the age of the conglomerate in which the clasts are contained. Since post-Devonian metamorphism of sufficient intensity to reset the mineral decay systems is unknown in the region, it appears that this boulder displays the deleterious effects of post-depositional weathering. The two remaining samples (B2-17 and B3-18) do not display features associated with the hydrothermal effects (^{87}Sr enrichment in whole-rock and feldspar analyses) and calculated mineral ages must therefore reflect the true age of emplacement or *younger* ages resulting from weathering or partial resetting during subsequent metamorphism.

K-Ar Biotite

Extremely low blocking temperatures for argon diffusion in biotite (c. 150-250°C) make K-Ar determinations on this phase particularly suitable for metamorphic and uplift studies. This dating method is particularly advantageous since it appears to be largely unaffected by incipient weathering (Goldich and Gast 1966; Obradovich and Cobban 1976; Wyborn et al 1982).

Three K-Ar biotite ages for the Roseneath boulders (Table 3.6) display a much reduced range (374-397 Ma) indicative of rapid uplift and cooling of the source terrain during the early to middle Devonian.

U-Pb Zircon

Three zircon fractions separated from granodiorite boulder B1-16 define a poor linear array which, if analytical errors are extended to equal geologic scatter, define a best-fit line whose lower and upper intersections with the concordia correspond to ages of 378^{+23}_{-60} Ma and 909^{+290}_{-230} Ma respectively. However, on the evidence of anomalously young Rb-Sr mineral ages for this boulder (above), post-depositional weathering has almost certainly resulted in considerable Pb loss. The lower intersection age of 378 Ma must therefore be considered as a minimum age of intrusion. Similarly, the upper intersection age should then be interpreted as a minimum age estimate of the source to a substantial inherited zircon population (basement).

Discussion

Geochronological analysis of the Roseneath granodiorite boulders is substantially hindered by the effects of post-depositional weathering, the narrow compositional range, and the apparently heterogeneous nature of the pluton with respect to initial $^{87}Sr/^{86}Sr$ ratios.

The most reliable minimum estimate of the intrusive age of the pluton (516±5 Ma) is given by the Rb-Sr biotite-whole-rock determination for sample B2-17, lying within error of the whole-rock age for ten unaltered samples (530±70 Ma). This date is obviously significant, placing the intrusion event prior to or contemporaneous with a period during which the Dalradian block was being subjected to peak metamorphic temperatures and major structural deformation (490-520 Ma - Dempster 1985). For this 'Older' Caledonian granite, the initial ratio of 0.7038±1 is considerably lower than its *in situ* Scottish counterparts (> 0.7117±3 - Insch) and is significantly lower than but more comparable with SW Highlands 'Newer' granites (> 0.7077±5 - Starav) for which many geochemical comparisons have already been made.

Low initial $^{87}Sr/^{86}Sr$ ratios combined with clear evidence of significant crustal Pb contribution reinforces the view based on trace element criteria that the parental magma was contaminated by or is a complete partial melt of Rb-depleted granulite basement similar to that presently exposed in north-west Scotland.

A complex crustal history is suggested by Rb-Sr mineral ages culminating in final uplift and erosion in the Devonian.

3.5 Summary of Conclusions - Chaper 3

1. Petrographically, undeformed igneous conglomerate material at Roseneath can be classified as: intermediate hypabyssal (porphyritic andesite and spessartite lamprophyre); acid hypabyssal (porphyritic microgranodiorite); or acid plutonic (porphyritic granodiorite). Acid hypabyssal types are further subdivided on the basis of phenocryst phases and the development in certain clasts of features associated with hydrothermal alteration (dissolution and silicification of Na-feldspar). Acid volcanic material has not as yet been recognised amongst the Roseneath assemblage.

2. Fractionation in a high level, H_2O supersaturated magma chamber is implied for the acidic rocks by the mineralogy and order of crystallization.

3. Geochemical classification emphasises a consanguinity between acid hypabyssal and plutonic species for which granodioritic compositions are predominant. Adamellites, quartz monzodiorites and a quartz monzonite are also recognised geochemically within the acidic group. Intermediate hypabyssal rocks belong to an unusually evolved group of Na-feldspar rich trachy andesites or quartz latites.

4. Multivariate cluster analysis of trace element data identifies at least four distinct groups of samples. Group 1 contains entirely acidic clasts of granodioritic composition. Group 2 is dominated by intermediate compositions. Group 3 is identified as the hydrothermally altered derivatives of Group 1, whilst the interpretation of the solitary acidic member of Group 4 is equivocal.

5. Geochemical analysis of hydrothermally altered acid hypabyssal clasts indicates almost complete removal of Na and associated depletion of Sr, Ni, Co, Cr and Ba. Changes associated with a phase of mineralization include enrichment in Cu, S and REE, and an increase in LREE/HREE ratios. These features are interpreted as the effects of percolation of magmatic hydrothermal fluids in a copper porphyry environment.

6. Fractionation modelling and multielement comparisons indicate magmatic links between Groups 1 and 2. It is clear by fractionation of amphibole and then biotite/K-feldspar that both groups share similar origins and environments of intrusion.

7. Clasts from Groups 1 and 2 display typical high K calc-alkaline volcanic arc geochemical characteristics together with features of intrusion into both continental margin and oceanic environments. Group 1 clasts not only display unambiguous I-type compositions, high K/Rb, low Rb/Sr and low HFS concentrations typical of mantle derived magmas but also unusually enhanced levels of Ba and Sr and a large inherited zircon component suggestive of derivation from a largely crustal (sedimentary) source. Group 2 clasts also display paradoxical features for which trace element abundances are best interpreted in terms of combinations of

island arc type Sr; high K calc-alkaline K, Rb, Zr and Ti; and concentrations of LREE and transition elements (except Cu) characteristic of calc-alkaline andesites. These features, together with high K/La, Rb/La and Ba/La ratios, point to derivation above or within a modified mantle wedge associated with a dehydrating, subducting oceanic plate and underthrust sediment. Crustal residence and contamination prior to final emplacement took place in U and Th depleted basement. Isotopic constraints suggest a host within depleted Grenvillian basement.

8. Statistical geochemical comparisons with in situ Caledonian intrusions and Ordovician grantitic detritus from the southern Midland Valley reveals that three Southwest Highland Newer granitoids (Foyers, Etive and Garabal Hill) are indistinguishable from Roseneath Group 1 rocks using trace element concentrations. There are significant differences for all other Caledonian intrusions and detritus from the proposed Midland Valley Ordovician volcanic arc. Of the three Newer granitoids with similar compositions to those at Roseneath, only the Garabal Hill intrusion provides a suitably proximal source, but does not display a sufficiently similar fractionation model path to compare with that of the Roseneath intermediate - acid clasts.

9. Data obtained by isotopic analysis for the granodioritic boulders suggests an emplacement age of at least 516 $\pm$ 5 Ma for an intrusion whose initial $^{87}Sr/^{86}Sr$ ratio was of the order of 0.704. A significant inherited crustal component is indicated for a substantial zircon population. The intrusion was subjected to final uplift and erosion in the Devonian. Hydrothermal alteration and a probably complex crustal history for the intrusion renders further interpretation largely conjectural.

CHAPTER 4
METAMORPHIC CLAST PETROLOGY

4.1 Introduction

Metamorphic detritus in the UORS conglomerates at Roseneath is dominated by cobble sized clasts of quartz-mica schist. These rocks have been subjected to high greenschist facies (biotite to garnet grade) metamorphism and polyphase deformation. Their most characteristic feature, however, is the development of abundant albite porphyroblasts.

The reported occurrence of albite porphyroblast schists in a southwest-northeast trending linear belt within the Upper Dalradian from northeast Antrim (Bailey and McCallien 1934) through Cowal (Gunn et al 1897) and Loch Lomond (Cunningham-Craig 1904) to the Balquidder district of Perthshire (Jones 1961) is of particular interest with regard to this provenance study. These schists occur more or less consistently within the outcrop of the Ben Ledi Grits but their distribution is considered to be dominantly controlled by the axis of the Cowal antiform and related minor folds, D3 upright structures trending ENE, parallel or subparallel to the stratigraphy (Figure 4.1). Their genesis has been variously ascribed to large scale reconstitution and Na metasomatism of grit bands (Gunn et al 1897, Reynolds 1942, Jones 1961, 1962, 1964, Trendall 1961, 1962), minor intraformational migration of Na during metamorphism of albite rich sediments (Bailey 1923, Tilley 1925, Cunningham-Craig 1904, Bailey and McCallien 1934, Bowes and Convery 1966), or through derivation from a source area rich in "trondjemitic" type rocks (Atherton and Brotherton 1982). Following a detailed investigation by Watkins (1983) it was demonstrated that the albite porphyroblasts resulted from localised redistribution of cations on a micro scale during retrogression of the original Barrovian metamorphic mineral assemblages as a result of hydrogen metasomatism. An influx of water acted as a catalyst by accumulating in the crests of F3 antiforms at a critical stage of retrogressive metamorphism.

4.2 Petrography of the Metamorphic Clasts

Metamorphic detritus in the Roseneath conglomerate occurs as clasts of up to c. 0.35m in size (maximum diameter). They are predominantly

Fig 4.1 (next page). Simplified pre-Carboniferous geological map of the northwest Midland Valley showing lithological variations within the Dalradian (see Fig 1.2 for key). (▬▬▬) encloses the albite porphyroblast zone (APZ); (▬ ▬) approximate position of the garnet isograd (ticks on high grade side).

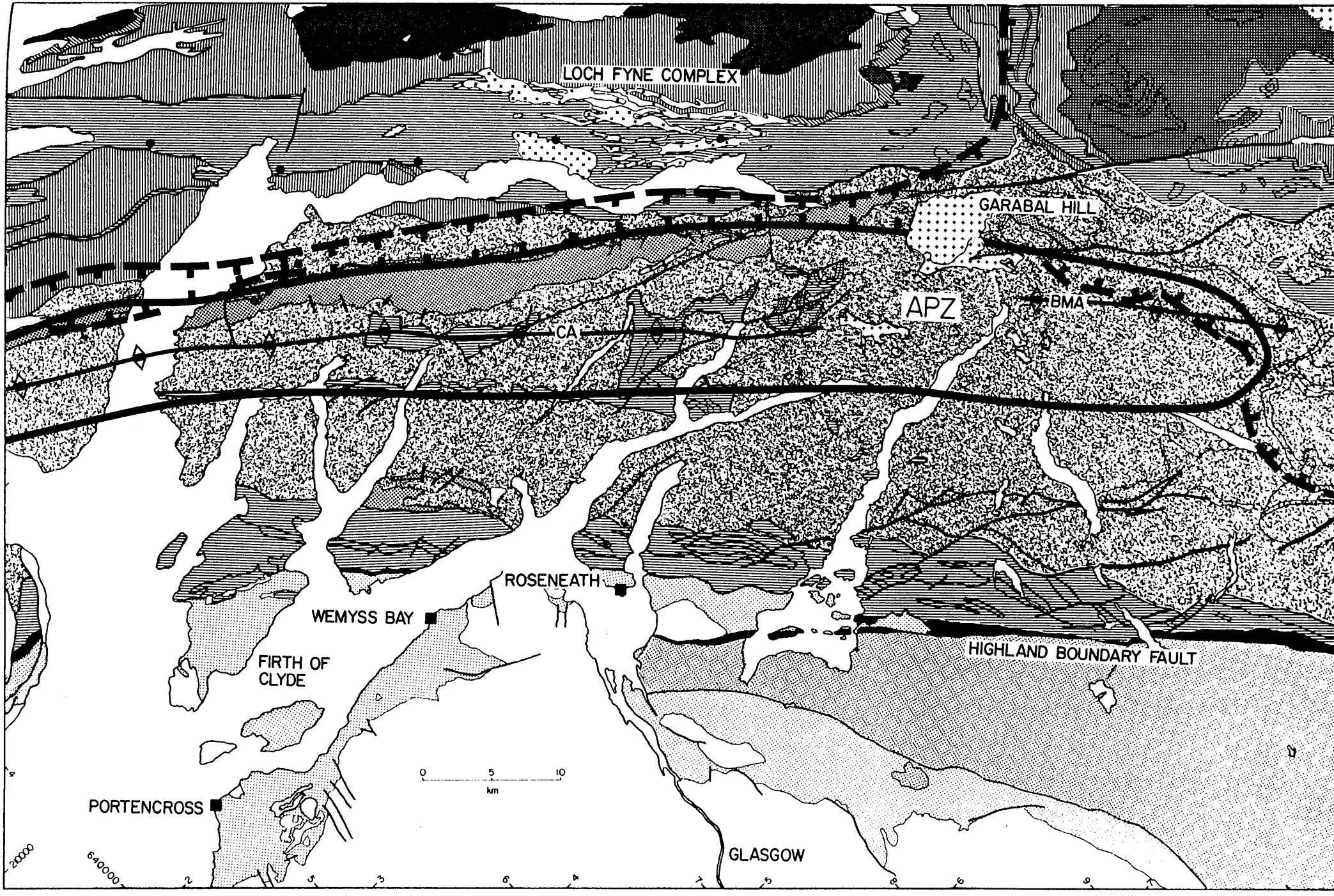
LOCH FYNE COMPLEX
GARABAL HILL
APZ
BMA
CA
ROSENEATH
WEMYSS BAY
FIRTH OF CLYDE
HIGHLAND BOUNDARY FAULT
0 5 10
km
PORTENCROSS
GLASGOW
20000
640000

quartzo-feldspathic (psammitic) or occasionally semi-pelitic reflecting generally high quartz/mica ratios, and display the following characteristic mineral assemblage :

$$qz + ab + bi + mu + chl + ksp + rut + tour \pm gnt \pm mt.$$

Albite porphyroblasts are present as large (<2mm) ellipsoid grains set in a medium to fine grained matrix of quartz feldspar and mica (Figure 4.2). Twinned and untwinned varieties occur and, where present, twin lamellae appear discontinuous and distorted. Irregular mica rich pelitic bands containing a concentration of porphyroblasts can be seen to alternate with quartz rich bands in both hand specimen and in thin section. Incipient chloritization of biotite grain margins in the pelitic bands is indicative of the onset of retrograde metamorphism. The porphyroblasts contain rotated inclusion trails of mica and small elongate quartzes which often achieve parallelism with the enclosing matrix but only at the very edges of the crystals.

Whilst not detected during thin section examination, tiny (0.2mm), colourless garnets with a pristine appearance were separated from the majority of schists clasts during heavy mineral separation. The implication is that these rocks were at some time located close to or enclosed by the garnet isograd.

4.3 Bulk Geochemistry

4.3.1 Chemical Data and Sampling

Eight specimens of quartz-mica schist from Roseneath have been analysed for eleven major oxides and seventeen trace elements (analytical techniques in Appendix II.1) This data, together with computed Niggli parameters, is presented in Table 4.1. All specimens submitted for analysis were extracted from the central portion of clasts not less than 0.2m maximum diameter, and were determined fresh by visual examination of thin sections.

Fig 4.2. TS photomic, XPL, X10, Qtz-gt-mica schist, Roseneath. Ellipsoid albite porphyroblast showing distorted twin lamellae and rotated inclusion trails of quartz and mica.

		DGS-1	DGS-2	DGS-3	DGS-4	DGS-5	DGS-6	DGS-7	DGS-8
Major (Wt%)	SiO_2	71.22	68.81	78.95	66.72	72.08	73.03	73.39	69.78
	TiO_2	0.73	0.72	0.49	0.78	0.58	0.60	0.62	0.67
	Al_2O_3	12.23	12.55	8.68	13.84	12.12	11.17	10.56	12.44
	Fe_2O_3	2.56	2.76	1.36	2.14	1.30	1.99	2.64	2.09
	FeO	2.65	2.91	1.54	3.34	2.54	2.51	2.03	2.51
	MnO	0.06	0.06	0.04	0.08	0.04	0.05	0.04	0.05
	MgO	2.48	2.99	0.72	3.14	1.69	2.01	1.82	1.86
	CaO	0.78	0.32	0.92	0.99	0.30	0.87	0.82	0.69
	Na_2O	3.53	4.22	1.74	3.26	3.80	3.47	3.62	3.94
	K_2O	1.67	1.67	1.93	2.20	2.01	1.84	1.46	1.75
	P_2O_5	0.08	0.07	0.02	0.16	0.10	0.11	0.04	0.07
	LOI	1.41	1.74	4.63	1.96	2.56	2.05	1.31	3.67
	Total	99.40	98.82	101.02	98.61	99.12	99.70	98.35	99.52
Trace (ppm)	Ba	701	280	747	554	503	907	272	531
	Ce	13	9	17	11	14	8	13	12
	Co	15	19	4	27	3	9	12	12
	Cr	67	71	40	139	52	60	54	66
	Cu	29	26	2	55	9	5	21	13
	Ga	12	13	10	15	8	14	10	9
	La	4	6	2	0	10	2	6	2
	Nb	10	11	8	9	15	12	9	12
	Ni	30	33	10	55	10	26	22	25
	U	2	2	2	2	3	1	2	2
	Pb	5	6	3	4	7	5	2	3
	Rb	75	77	61	60	70	60	64	60
	Sr	75	39	51	36	85	81	56	59
	Th	4	5	5	2	6	3	3	4
	Y	9	6	8	10	11	8	10	9
	Zn	57	70	33	83	40	64	47	51
	Zr	245	224	255	189	384	247	240	321
Niggli	al	35.28	33.83	41.24	35.67	39.57	35.21	34.69	37.60
	fm	38.66	41.01	27.29	39.73	31.14	35.53	35.66	33.30
	c	4.09	1.57	7.96	4.64	1.78	4.99	4.90	3.79
	alk	21.95	23.59	23.53	19.96	27.51	24.28	24.75	25.32
	si	348.69	314.74	636.50	291.80	399.29	390.71	409.09	358.21
	k	0.24	0.21	0.40	0.31	0.26	0.26	0.21	0.23
	ti	2.69	2.48	2.97	2.57	2.42	2.42	2.60	2.59
	mg	0.41	0.50	0.32	0.52	0.45	0.45	0.42	0.43

Table 4.1. Major and trace compositions and calculated Niggli values for eight Roseneath schist clasts.

4.3.2 Chemical Characteristics - Comparisons With In Situ Dalradian Lithologies

To enable direct comparison with in situ Dalradian lithologies, the averaged composition of Roseneath albite schist is presented in Table 4.2 together with mean composition of eighteen Pitlochry Schist semi-pelites from within the Dalradian albite porphyroblast zone (APZ) and three published analyses of ablite schist and gneiss from the Cowal district, Loch Lomond and County Antrim. All of the above are located within either biotite or garnet zones (Figure 4.1). In addition the mean composition of sixteen Ben Ledi Grits from outside the APZ (selected to compare with SiO_2 values in the Roseneath clasts) and analyses of Dalradian pelites (as a whole, and grouped both stratigraphically and according to metamorphic grade) are also presented in Table 4.2.

It is immediately apparent from Table 4.2 that the Roseneath schists have significantly higher SiO_2 contents than 'average' Dalradian lithologies but are broadly comparable in this respect to Dalradian biotite zone rocks. Al_2O_3 displays a negative correlation with SiO_2 for Dalradian rocks as a whole and reflects natural variations in maturity of the original sediments (quartz/feldspar + clay ratio). Low Al_2O_3 contents for Roseneath schists and Ben Ledi Grits are therefore not anomalous when compared with Dalradian rocks with similar SiO_2 content. Similarly low values of K_2O and especially TiO_2 can probably be explained by the relatively high maturity of the original sediment.

Na_2O contents of average Roseneath schist is significantly enriched relative to most Dalradian lithologies (except Ben Ledi Grits) including the majority of semi-pelitic rocks from within the APZ. Since Na_2O is negligably enriched in rocks within the APZ relative to identical lithologies outside (Watkins 1983), high Na_2O must be component of the original sedimentary material. Pettijohn et al (1972) devised a geochemical classification of clastic sediments in which recognition of mature and immature sandstones was based upon the variation of the SiO_2/Al_2O_3 ratio. Immature sediments are further divided by differences in the Na_2O/K_2O ratio. If a sedimentary origin is assumed for these rocks [the detrital nature of the Ben Ledi Grits is apparent in the least deformed rocks (Bowes and Jones 1958, Bowes and Convery 1966)] their original composition can be determined geochemically on a log (Na_2O/K_2O) : log (SiO_2/Al_2O_3) plot (Figure 4.3) using the nomenclature

		Dalradian Lower		Dalradian Middle		Dalradian Upper		Dalradian Biotite		Dalradian Garnet		Dalradian Pelite		Connemara Pelite		N.America Pelite		Ben Ledi bte+gt		Roseneath bte+(gt)	
		x	sd	x	sd	x	sd	x	sd	x	sd	x	sd	x	sd	x	sd	x	sd	x	sd
Major	SiO_2	64.10	4.68	58.48	10.27	59.84	11.27	69.48	9.85	59.68	10.85	59.88	10.87	55.39	5.53	61.54	4.68	71.99	4.86	71.75	3.44
(Wt%)	TiO_2	1.01	0.23	0.93	0.48	1.05	0.46	0.76	0.33	1.08	0.43	1.03	0.46	1.18	0.32	0.82	0.61	0.63	0.18	0.65	0.09
	Al_2O_3	17.57	3.24	19.86	5.84	19.12	6.22	13.56	4.45	19.03	5.47	19.15	6.02	20.75	3.79	16.95	4.21	12.04	2.01	11.70	1.46
	Fe_2O_3	2.54	1.21	1.90	1.22	2.61	2.47	1.36	0.92	2.05	0.95	2.49	2.28	2.69	1.75	2.56	1.97	1.18	0.51	2.11	0.52
	FeO	3.36	1.97	6.08	3.29	5.07	2.36	3.62	1.76	5.47	2.74	5.15	2.56	6.52	2.28	3.90	2.25	3.58	1.21	2.50	0.51
	MnO	0.19	0.17	0.10	0.07	0.12	0.09	0.08	0.08	0.11	0.09	0.12	0.09	0.15	0.08	N/A	N/A	0.07	0.08	0.05	0.01
	MgO	1.63	0.94	2.85	1.38	2.29	0.95	1.88	0.96	2.31	1.40	2.34	1.07	2.90	1.23	2.52	1.91	1.86	1.03	2.09	0.73
	CaO	0.75	0.86	1.16	0.84	1.02	0.71	0.93	1.06	1.05	0.77	1.03	0.75	1.36	0.99	1.76	2.03	1.25	1.07	0.71	0.25
	Na_2O	1.17	1.04	1.89	1.15	2.22	0.99	2.27	1.03	1.61	1.28	2.10	1.05	1.82	0.66	1.84	1.18	2.97	0.69	3.15	0.70
	K_2O	4.46	1.75	3.44	1.46	3.43	1.50	2.98	1.53	4.48	2.03	3.50	1.52	3.64	1.04	3.45	1.32	2.03	0.88	1.32	0.22
	P_2O_5	N/A	N/A	N/A	N/A	N/A	N/A	N/A	N/A	N/A	N/A	N/A	N/A	N/A	N/A	N/A	N/A	0.07	0.06	0.08	0.04
	M/FM	0.41	0.07	0.46	0.09	0.45	0.09	0.46	0.08	0.43	0.07	0.45	0.09	0.40	0.30	0.50	0.50	0.33	0.08	0.44	0.06
Niggli	al	46.11	N/A	42.05	N/A	42.63	N/A	39.92	N/A	43.72	N/A	42.69	N/A	41.16	N/A	40.13	N/A	37.93	6.34	36.64	2.43
	fm	32.59	N/A	39.01	N/A	36.81	N/A	34.61	N/A	34.66	N/A	36.99	N/A	40.18	N/A	36.30	N/A	33.22	4.90	35.32	4.29
	c	3.58	N/A	4.67	N/A	4.14	N/A	4.98	N/A	4.39	N/A	4.17	N/A	4.90	N/A	7.57	N/A	6.94	6.73	4.21	1.58
	alk	17.72	N/A	14.47	N/A	16.43	N/A	20.50	N/A	17.23	N/A	16.15	N/A	13.76	N/A	16.01	N/A	21.90	2.93	23.86	2.11
	si	285.47	N/A	210.16	N/A	226.45	N/A	347.16	N/A	232.71	N/A	210.33	N/A	190.32	N/A	247.27	N/A	400.17	102.61	393.63	99.46
	k	0.72	N/A	0.55	N/A	0.50	N/A	0.46	N/A	0.65	N/A	0.52	N/A	0.57	N/A	0.55	N/A	0.28	0.11	0.27	0.06
	ti	3.38	N/A	2.51	N/A	2.99	N/A	2.86	N/A	3.17	N/A	2.93	N/A	2.99	N/A	2.48	N/A	2.38	0.61	2.59	0.17
	mg	0.33	N/A	0.39	N/A	0.35	N/A	0.41	N/A	0.39	N/A	0.36	N/A	0.36	N/A	0.42	N/A	0.42	0.15	0.45	0.06

Table 4.2. Comparative compositions of various Dalradian grits and pelites, Connemara pelites, North American pelites, and Roseneath schist clasts.

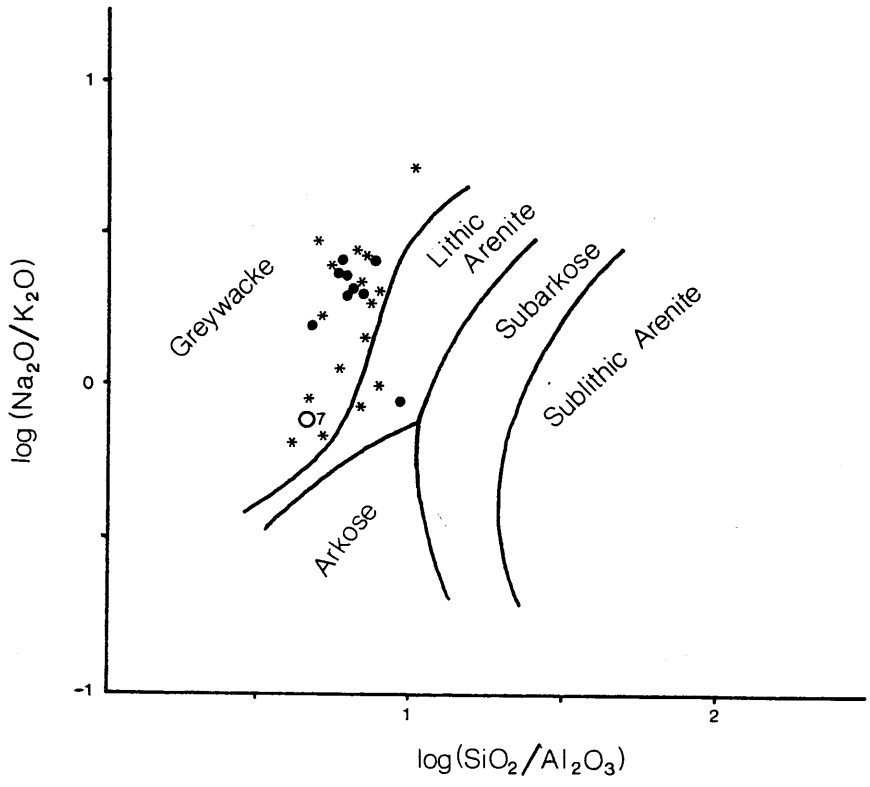

Fig 4.3. Log (Na2O/K2O):log(SiO2/Al2O3) sedimentary lithic type discriminant plot. (•) Roseneath schist clasts; (*) Ben Ledi grits; (o7) average Dalradian biotite schist.

fields of Pettijohn et al (1972). In this discriminant diagram, Roseneath schists (with only one exception) cluster tightly within the high Na greywacke field together with a number of Ben Ledi Grit analyses. High Na_2O/K_2O for these rocks suggests either an unusually high plagioclase content relative to K-feldspar or a distinctly muddier composition in comparison with average Dalradian sediment. In view of the trace element data discussed later in this section the former explanation is preferred.

Average oxidation and M/MF ratios for Roseneath schists are extremely high (0.58 and 0.42 respectively), and, whilst these values are not unknown in published analyses of Dalradian metasediments, they are considered to reflect excessive post-Devonian dueteric alteration of the clasts within the conglomerate. Bulk compositions plotted on AFM and AKF paragenesis diagrams are therefore probably meaningless.

Harker type variation diagrams using Niggli parameters (Figures 4.4a to d) are of limited use due to the paucity of data and restricted silica range of the clasts. For the Roseneath rocks a neutral or weakly positive correlation may exist for alk:si, and a slightly better defined positive correspondence is noted for al:si. This latter trend is particularly interesting and has been interpreted by workers in certain Connemara pelites as being indicative of deposition in a well aeriated sedimentary environment (Treloar 1978). Plots of mg:si and fm:si show a clear negative relationship, with MgO apparently decreasing more rapidly than total Fe with increasing SiO_2. Increasing Fe_t/Mg ratios similar to those displayed by the Roseneath schists (Figure 4.5), also found in Ben Ledi Grits, have parallels in Connemara pelites (Treloar 1978). It has been proposed that trends towards higher Fe_t/Mg ratios reflect a less saline depositional environment (Sholkovitz 1976, Eckert and Sholkovitz 1976, Boyle et al 1978). Treloar (1977) linked the sympathetic variation of Fe_t/Mg and Niggli al to propose a model in which more quartzo-feldspathic sediments were deposited during aeriated conditions of high run-off into a marine setting, resulting in low saline (presumably estuarine) water advancing in a seawards direction. Pelitic rocks, on the other hand, would be deposited in more saline conditions.

Average compositions for North American pelites, Connemara pelites and various combinations of Dalradian analyses have also been plotted on the Niggli variation diagrams (Figures 4.4a to d). Despite the fact that none of these analyses has been selected by SiO_2 content, average Dalradian biotite rock plots consistently within Roseneath and Ben Ledi fields away

Fig 4.4 (next page). Niggli variation diagrams. a) al:si, b) fm:si, c) mg:si and d) alk:si. (●) Roseneath schist clasts; (*) Ben Ledi schists; (o1-8) various matamorphic (1 average Dalradian pelite, 2 average Connemara pelite, 3 North American pelite, 4 average Lower Dalradian, 5 average Middle Dalradian, 6 average Upper Dalradian, 7 Dalradian biotite schist, 8 Dalradian garnet schist).

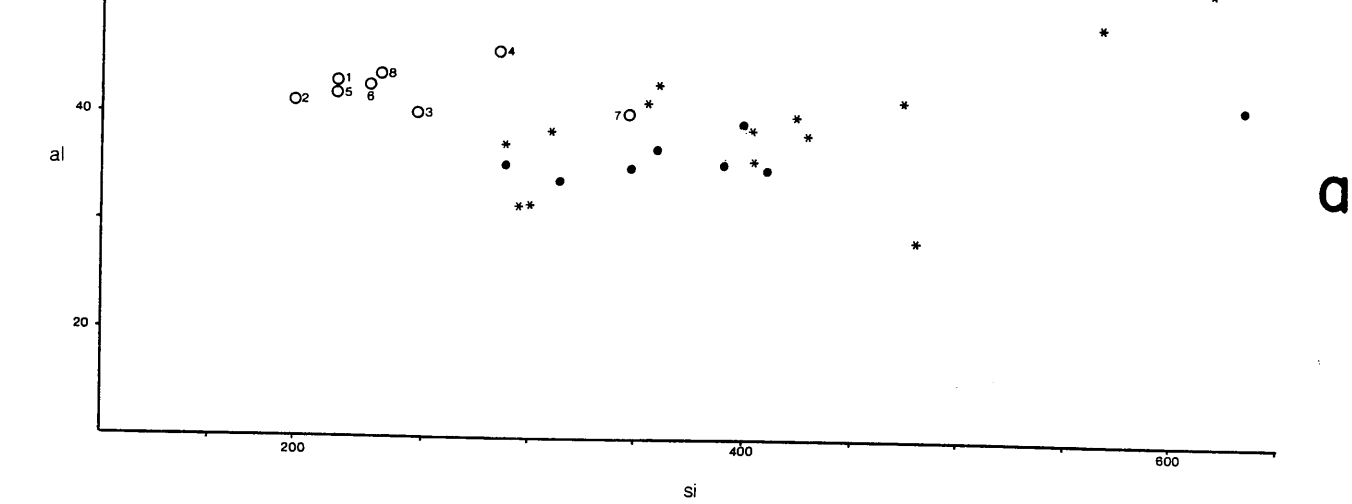
al
40
20
200
400
600
si
a

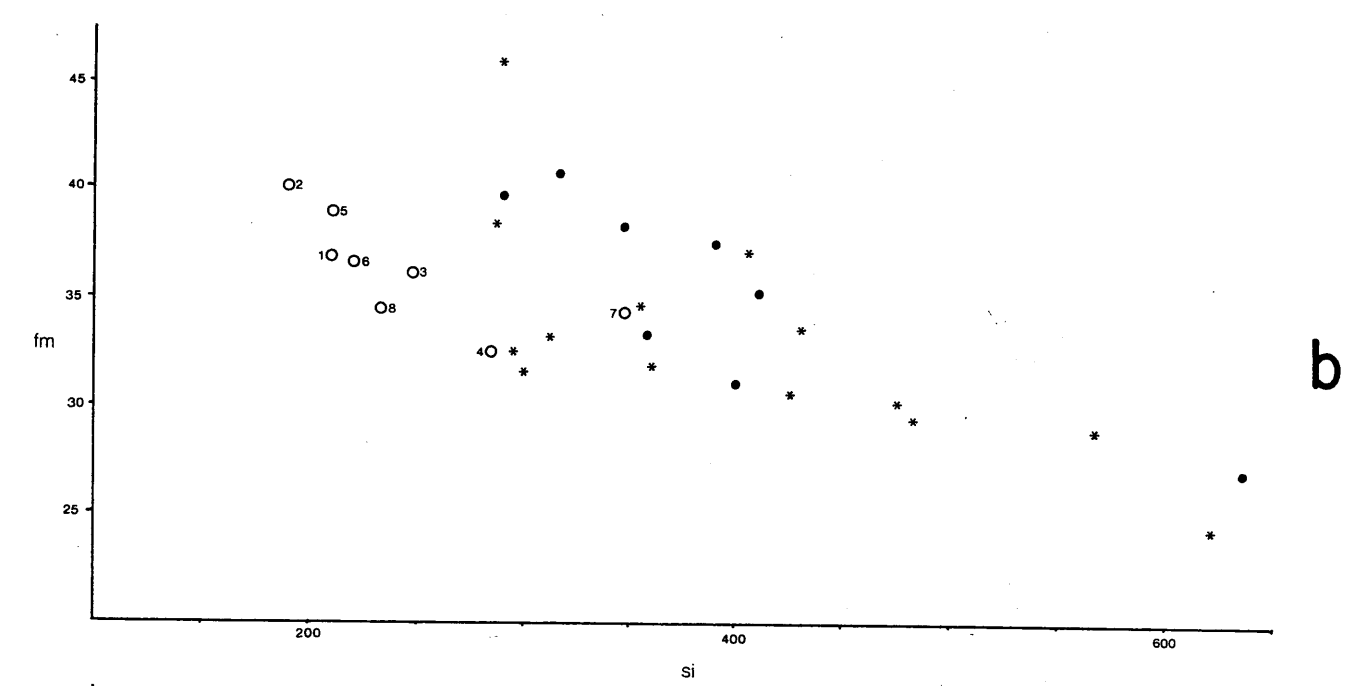
fm
45
40
35
30
25
200
400
600
si
b

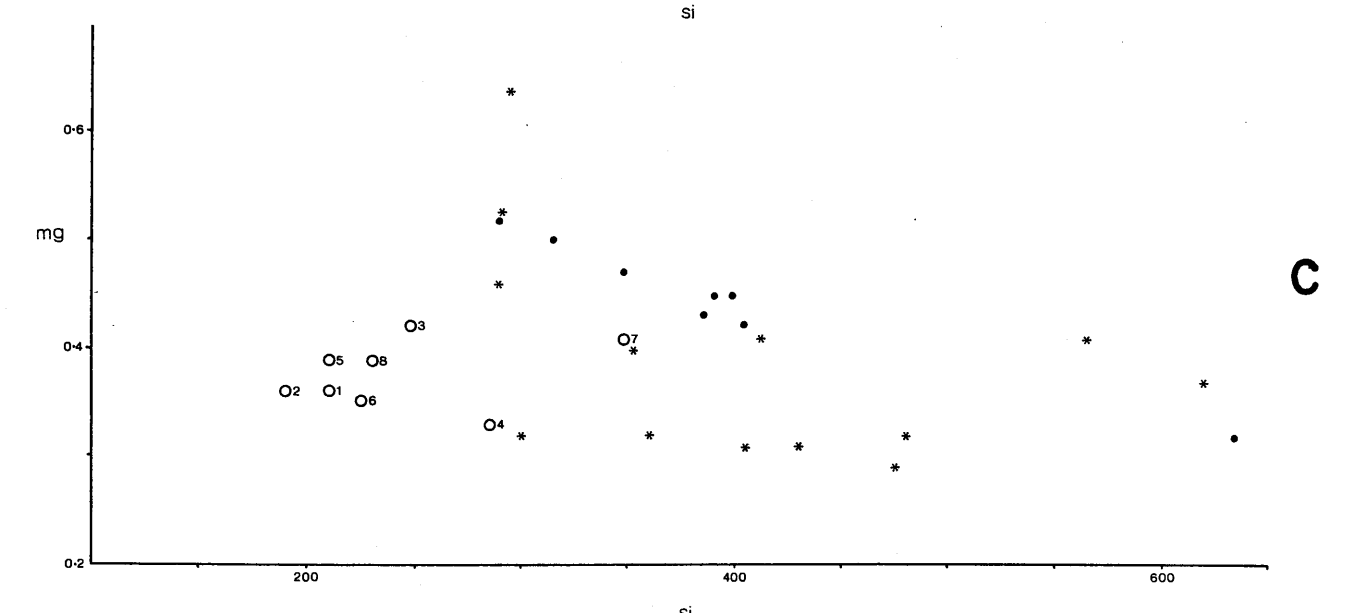
mg
0·6
0·4
0·2
200
400
600
si
c

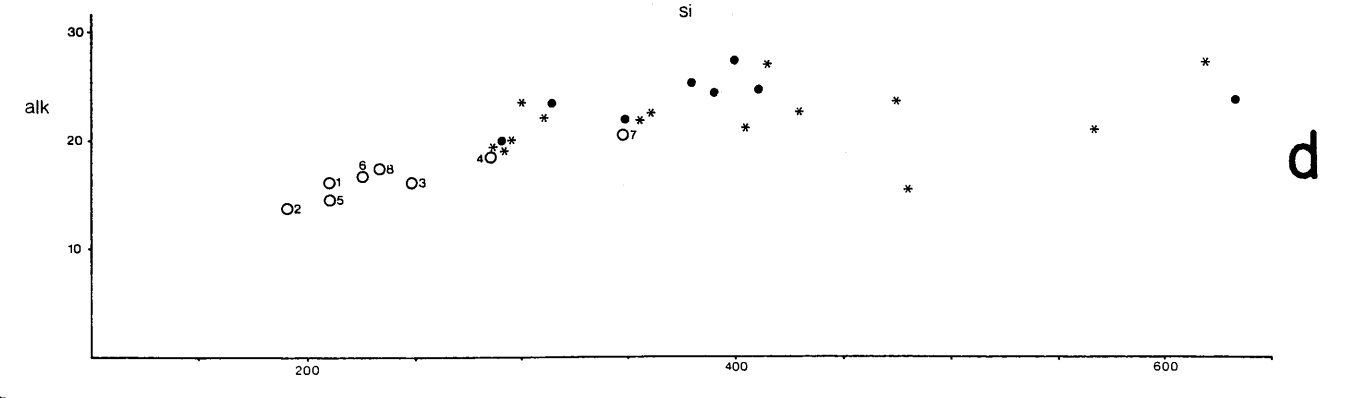
alk
30
20
10
200
400
600
d

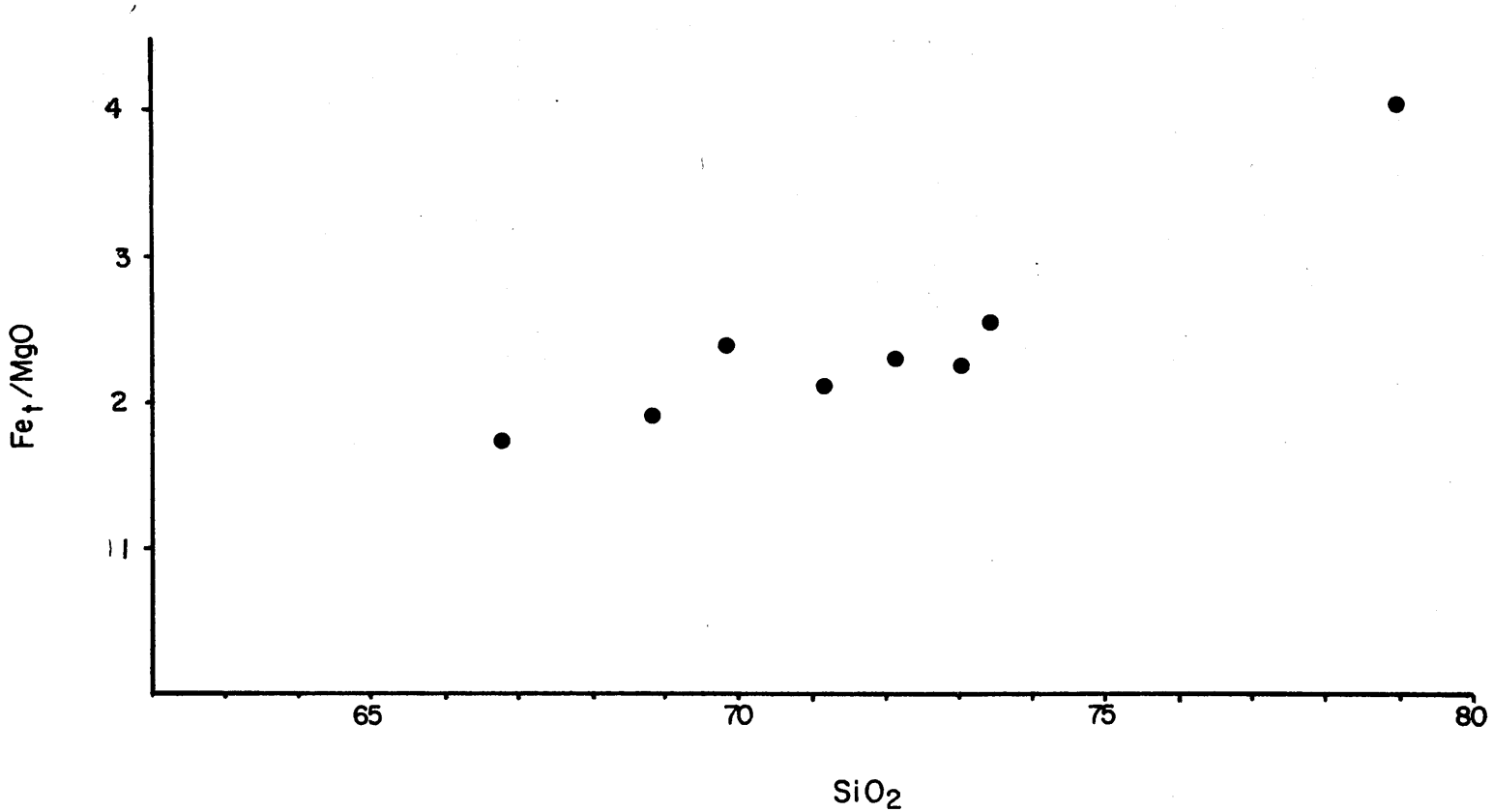

Fig 4.5. Fet/MgO:SiO2 plot for Roseneath schist clasts.

from pelites from other areas or Dalradian groupings. Changes due to variable silica concentration are effectively removed in plots of Niggli al, alk, fm, mg, c, k, and ti. Atherton and Brotherton (1982) used four diagrams independent of silica to define fields for Dalradian pelites. Figures 4.6a to d display the Dalradian fields for c:mg, k:mg, al-alk:c and 100mg:c:al-alk diagrams with analyses of Roseneath, Ben Ledi and averaged pelitic rocks from Table 4.2. The plot of mg:c (Figure 4.6a) shows that most of the albite schists are generally of Dalradian type. However in the remaining plots, involving either al or k parameters, many analyses fall outside the Dalradian field. This divergence from the bulk of Dalradian compositions must be linked with high Na_2O which, in the al-alk:c diagram (Figure 4.6b) is developed to such an extent that four Ben Ledi Grits plot within the field for igneous rocks. Similar observations by Atherton and Brotherton (1982) led to the conclusion that these albite schists were probably immature sediments derived from a source area rich in trondjemitic rocks. On the 100mg:c:al-alk triangular diagram (Leake 1964) the Roseneath schists display no evidence of being simple clay-calcite/dolomite mixtures, nor do they display any obvious igneous trends.

Trace elements, with their inherently higher discriminating resolution than major oxide variations, have been used with great success in stratigraphic correlation of metamorphic rocks. The use of supposedly mobile elements in petrologic studies of metamorphosed sediments has been validated for Dalradian and Moinian rocks by Lambert et al (1981) with the observation that wholesale homogenisation has not taken place. Unfortunately few published analyses of trace element concentrations are known to be available for Upper Dalradian rocks and it is therefore impossible to pursue the general similarities with Ben Ledi albite schists indicated by the preceding discussion. However, trace element concentrations of Lower Dalradian and Moine schists have received considerable attention in recent years with the work of Lambert et al (1981,1982) and Winchester et al (1981). Discrimination between and within Dalradian and Moine Divisions was achieved by simple boundary lines on plots of selected major and trace elements.

Figures 4.7a to f display the results of plotting the Roseneath data on diagrams used by Lambert et al (1981, 1982) to discriminate between Moinian and Lower Dalradian types. It is interesting to notice that the Roseneath schists do not have indisputible Lower Dalradian or Moine identities, and that in most cases the Roseneath schists lie surprisingly close to, or directly upon

Fig 4.6 (next 2 pages). Niggli discrimination plots. a)mg:c, b) al-alk:c, c) k:mg and d) 100mg:c:al-alk. Symbols as for Fig 4.4.

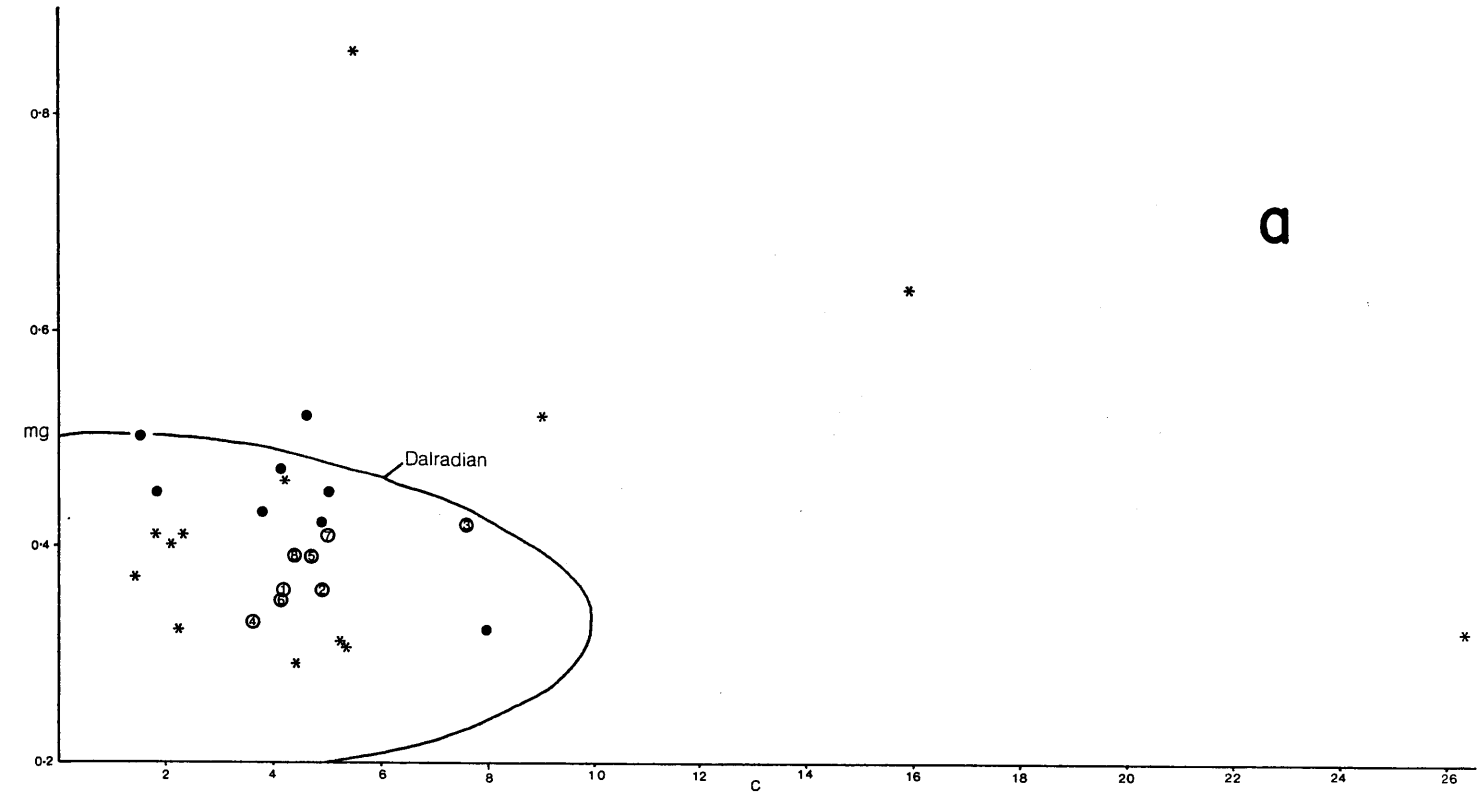
a
0·8
0·6
mg
0·4
0·2
Dalradian
2
4
6
8
10
12
14
16
18
20
22
24
26
C

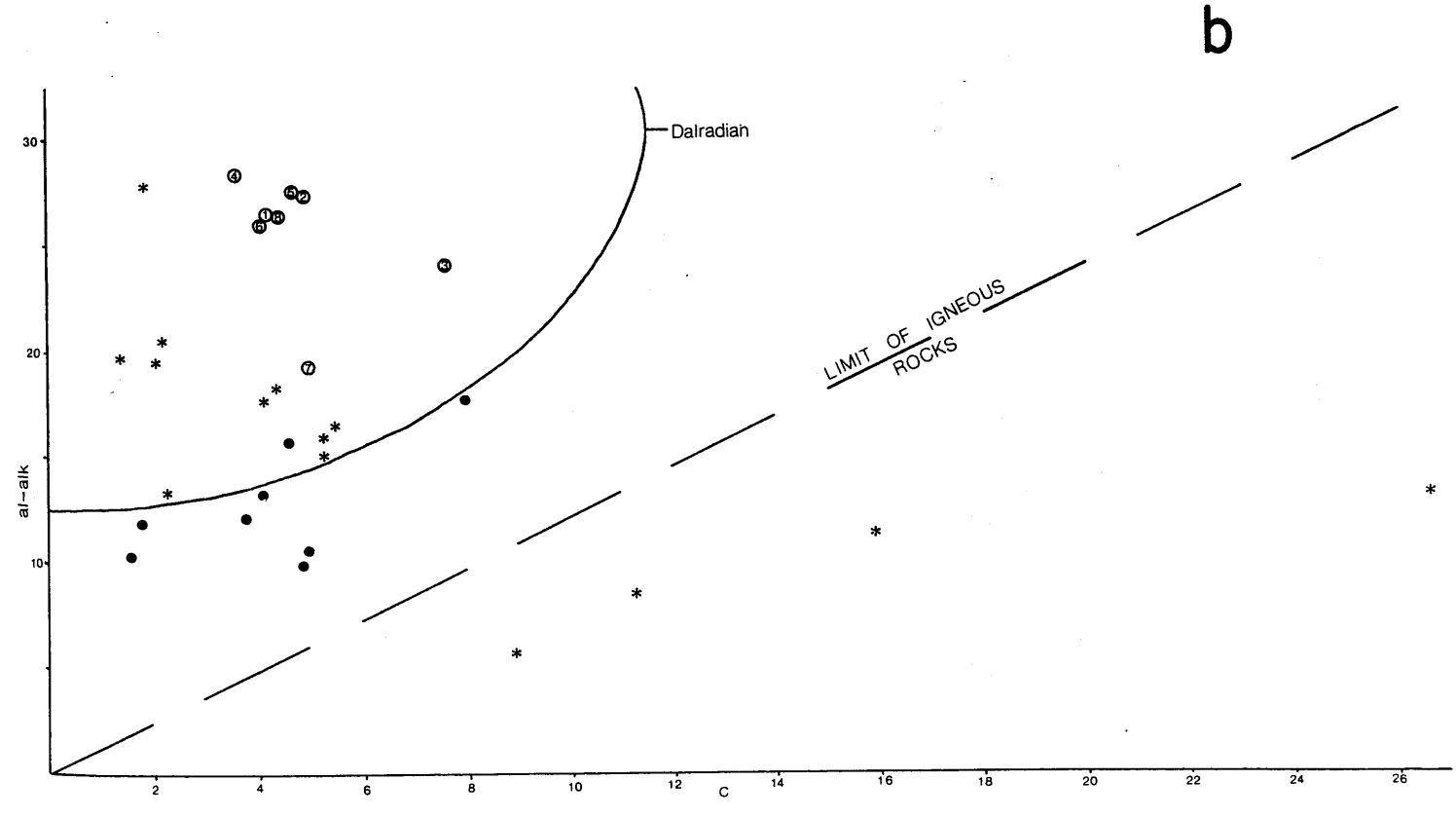
b
30
20
al-alk
10
Dalradian
LIMIT OF IGNEOUS ROCKS
2
4
6
8
10
12
14
16
18
20
22
24
26
C

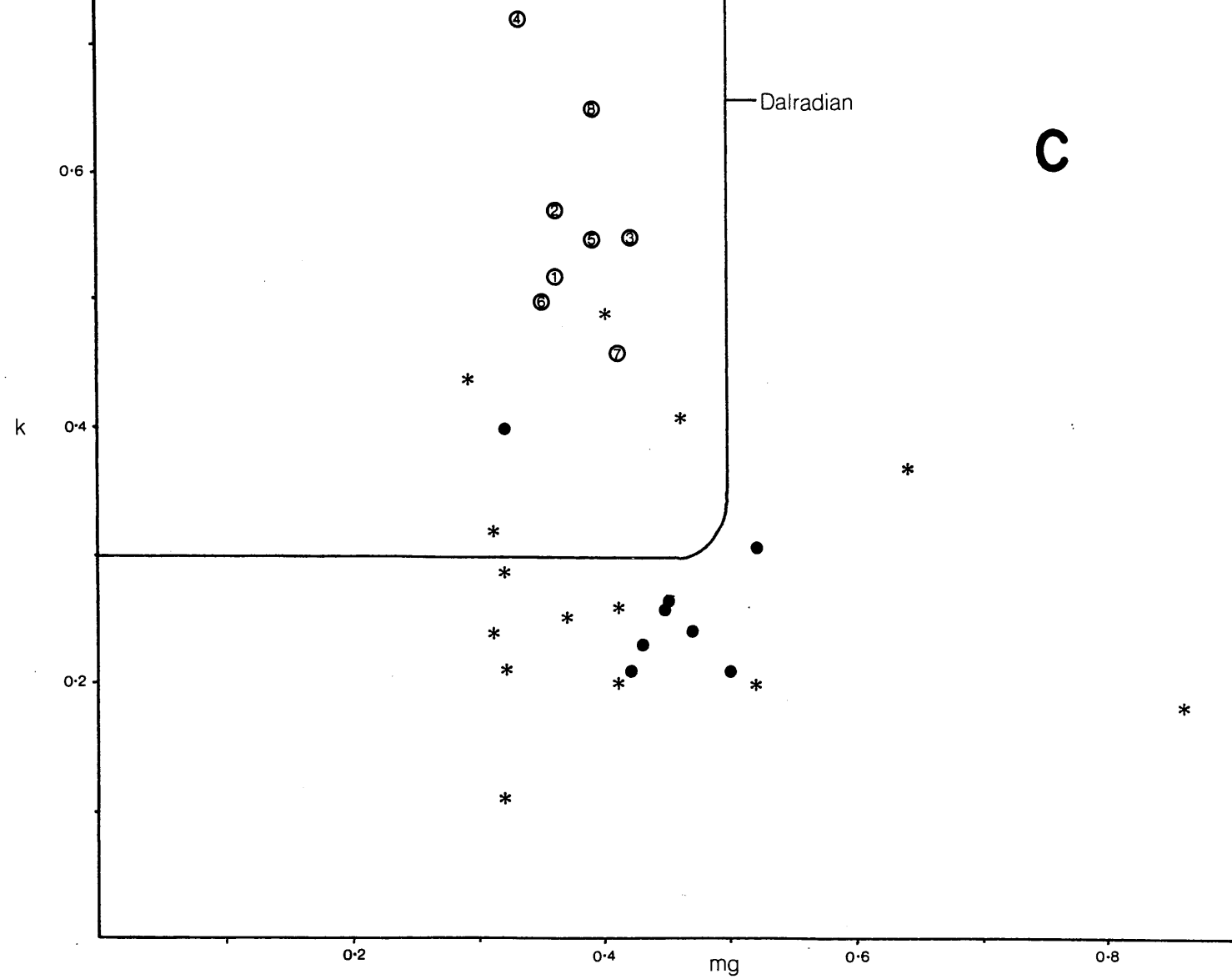
Dalradian
c
k
0·6
0·4
0·2
0·2
0·4
mg
0·6
0·8

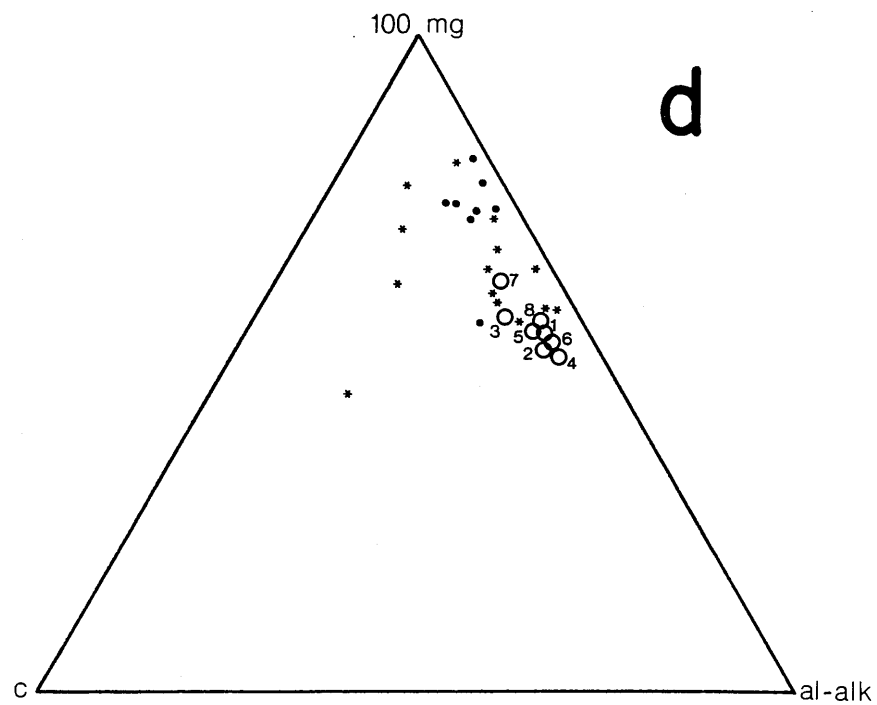
100 mg
d
c
al-alk

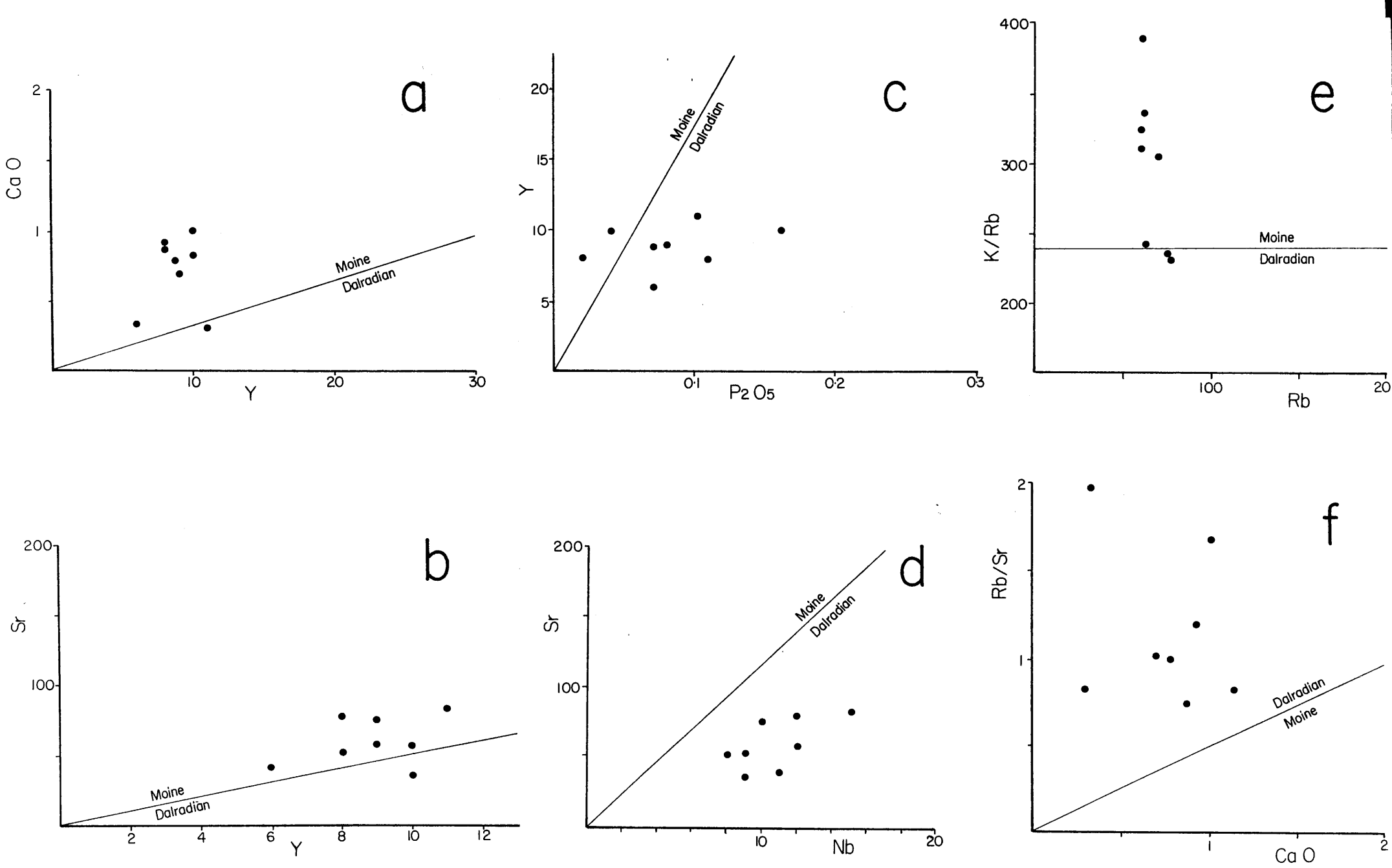

Fig 4.7. Moine/Lower Dalradian trace element discrimination diagrams showing Roseneath schists: a) CaO:Y, b) Sr:Y, c) Y:P205, d) Sr:Nb, e) K/Rb:Rb and f) Rb/Sr:CaO.

the discriminating boundary line. On the only two plots in which the Roseneath schists fall distinctly into one or other category, they are conclusively Moinian in terms of their K/Rb ratios (> 240) and Dalradian in terms of their Rb/Sr ratios (> 0.80).

A large plagioclase component of the primary sediment has been suggested by respective enrichment and depletion of Na_2O and K_2O. Sr, unlike Y, has a high distribution coefficient for plagioclase, and high Sr/Y (c 51) for these rocks also emphasises the importance of plagioclase. CaO and Sr contents are low for the schists and, whilst little quantitative information is known about the distribution of Sr with respect to the plagioclase end members (albite-anorthite) it is reasonable to assume that the depletion of these two elements is related and reflects a high albite/anorthite ratio in the sediment. It is of course possible that low CaO and Sr are merely diagenetic features reflecting a lack of calcareous pore filling cement immediately following deposition.

Despite the obviously high biotite content of these rocks, concentrations of Rb are surprisingly low. This, together with correspondingly low Al_2O_3 (after that required to combine with Na_2O for albite) and low Y, may imply a low illite content in the sediment. Low Y concentrations are also interesting in view of the observation by Balashov et al (1964) that Y is preferentially concentrated in marine argillaceous rocks but depleted in their fresh-water equivalents. This concurs with variations of Fe_t/Mg and Niggli al, cited above as evidence of deposition in a low saline estuarine environment.

4.4 Summary of Conclusions - Chapter 4

i) Albite porphyroblast bearing quartz-(garnet)-mica schist dominates metamorphic detritus in the Roseneath UORS conglomerates. These clasts petrographically resemble Dalradian albite schists located to the north of the study area.

ii) Despite displaying the high oxidation effects of deuteric alteration, the metamorphic clasts are geochemically indistinguishable from high silica Upper Dalradian equivalents

and in particular high Na albitic metasediments from the Ben Ledi Grits. The clasts do not have any notable trace element affinities with Lower Dalradian or Moinian metamorphic rocks. Trace element concentrations reinforce a high albitic component and, in conjunction with niggli parameters, suggest an original low saline estuarine environment of deposition. This is consistent with independent observations for Upper Dalradian lithologies.

CHAPTER 5
DISCUSSION

5.1. Provenance Models

For the basal Upper ORS in the NW Midland Valley, conclusions concerning the location of the source and its spacial variations in composition depend critically upon the correct identification of the detritus as being of a predominantly first cycle nature. It is clear, for example, that although derived essentially from the south and southwest, and cannot be matched to potential Dalradian source rocks in the immediate vicinity, much of the material in the northern conglomerates has distinct visual/petrographical and geochemical affinities with lithologies presently exposed deeper within the Dalradian metamorphic terrain to the north. This is a particularly important point, since a paucity of unequivocal local Dalradian material in Midland Valley conglomerates until the late Upper ORS is cited as amongst the strongest evidence that the Dalradian terrain did not achieve its present thrusted position relative to the Midland Valley block until late Devonian or early Carboniferous times (Bluck 1984).

Two provenance models are proposed to explain the detrital compositions of Upper ORS sediments in the study area:

a) Model I - Dalradian Source (polycyclic detritus) - Fig 5.1a

With assumptions that the southerly and southwesterly derived conglomerate material in the Upper ORS has a large polycyclic component, and that the allochthonous Dalradian block had been emplaced relative to the 'Midland Valley' block by c. 460 Ma (as is almost certainly the case in Connemara - Leake et al 1984), it is relatively easy to construct a specious Dalradian provenance incorporating many petrologic characteristics of the clasts discussed in the preceeding chapters.

The Upper ORS unconformably overlies Lower ORS south of the HBF at Ardmore Point, Portencross/Farland Head and in Arran. It is therefore difficult to envisage any provenance model which does not include a substantial component of reworked Lower ORS debris. Re-rounded quartzite boulders, highly abraded colourless tourmalines, abraded tan and purple

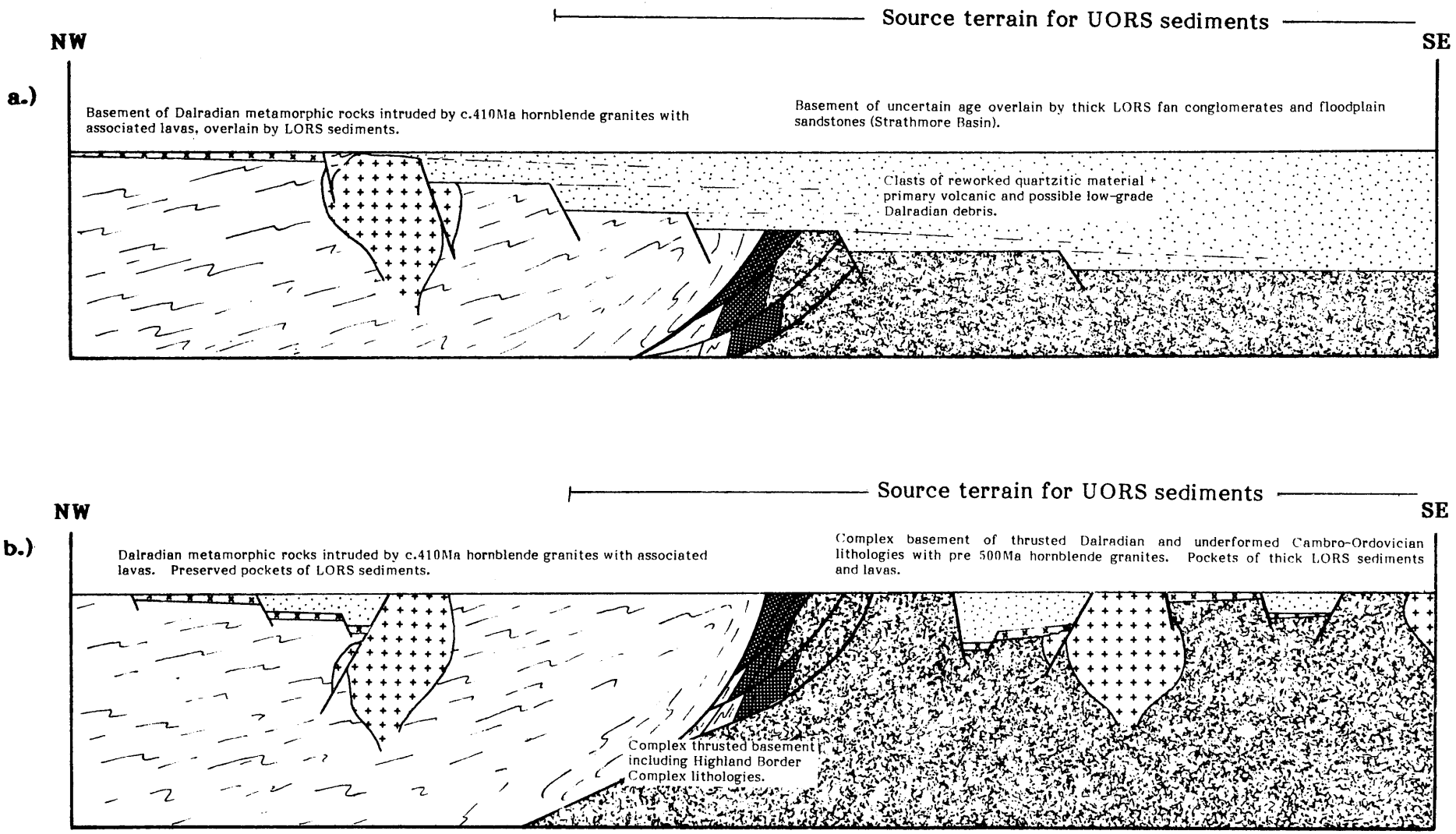

Fig. 5.1 : Alternative diagrammatic sections at base Upper Devonian (c.380Ma) in the NW Midland Valley. a.) Model 1 - UORS provenance = Dalradian (reworked LORS). b.) Model II - UORS provenance = Midland Valley basement (primary).

zircons, red sandstone and caliche cobbles, and shale clasts bearing a Lower Devonian flora provide circumstantial evidence of distal transport and reworking of Lower ORS material.

Lower ORS conglomerates within the middle and upper parts of the succession were derived from the north and northwest on the northern flank of a basin whose margins are considered to have lain some distance to the north of the present HBF (cf. Ch 1). These margins may have receeded even further periodically during the evolution of the basin. Vertical compositional variations within these conglomerates (upward trends from dominantly volcanic to medium greenschist material) have been interpreted as progressive unroofing of extensive volcanic fields in the north, exposing underlying Dalradian metamorphic rocks only during the late Lower Devonian. Progressively interior regions of the Dalradian block would be sampled by northerly receeding fans producing compositionally discrete stratigraphic packages. In this way, the oldest conglomerates would contain predominantly volcanic debris, whilst metamorphic material would be restricted to poorly exposed lithologies occurring in the southern part of the Dalradian province (low grade greenschist slates and phyllites). Overstepping younger conglomerates (distal fan facies) may contain smaller quantities of volcanic material but the appearance of higher grade metamorphic detritus would reflect changes in the underlying Dalradian lithologies. A thick cover of ORS sediment over the HBF could conceivably reduce dramatically the input of HBC and low grade Dalradian rocks especially towards the top Lower ORS.

Setting aside the geochronological work of the present study, there are striking similarities between the composition of the Roseneath Upper ORS conglomerates and lithologies presently exposed 35 km to the north, within the Upper Dalradian at the head of Loch Fyne (described by Hill et al 1905). There, the Ben Bheula schists and grits occur within a narrow albite porphyroblast zone, are transitional from biotite to garnet grade, and as far as can be determined using limited available data, are chemically and visually identical to metamorphic debris at Roseneath. These rocks are intruded by the 406 Ma Garabal Hill-Glen Fyne Complex, and associated lacolithic quartz porphyries form extensive exposures on the northern slopes of Loch Fyne (Fig 1.2). Porphyritic granodiorite rocks from this complex display distinctive compositions and unusual fractionation trends which can also be identified in porphyritic granodiorites and related hypabyssal

clasts at Roseneath. The occurrence of hornblende lamprophyres with a high albitic component at Garabal Hill (Nockolds 1941), petrographically equivalent to spessartite lamprophyre clasts at Roseneath is a further point of similarity. High level hydrothermal alteration and mineralization are known to have affected the Roseneath acid hypabyssal clasts by removal of Na and addition of Cu. From the account of Nockolds (1941), it is apparent that hydrothermal alteration involving dissolution and silicification of plagioclase has also severely affected plutonic and hypabyssal rocks of the Garabal Hill pluton and was ascribed to solutions emanating from the central non-porphyritic granodiorite. It is also pertinent in this respect that copper mineralization within the southwest Highlands is associated with porphyry copper style late Caledonian intrusions (Watson 1985) and is particularly well developed in the region of Loch Fyne (Wilson and Flett 1921) as shown on the geological map (Figure 1.2).

Outliers of Lower ORS and radiometrically dated Lower ORS lavas (Thirlwall 1983) resting unconformably upon Dalradian metamorphic rocks place constraints upon the level of erosion within the Dalradian at this time; the southern Highlands had more or less attained its present level of erosion prior to 410 Ma (see also Bluck 1984, p282). However, the high proportion of hypabyssal relative to plutonic types at Roseneath would seem to indicate that higher levels of erosion than are presently exposed at Garabal Hill were being sampled by the ORS fluvial system. The Garabal Hill complex, like all other Scottish Newer granites, was emplaced at very shallow crustal levels, and it is therefore only necessary to invoke an additional 1-2 km maximum of overlying Dalradian material to provide an ideal provenance terrain of greenschists, dyke/laccolith rocks, and exposures of very high level acid plutonic types. The attitude of the garnet isograd surface in this region of the Scottish Dalradian is known to be inverted, and dips at a very low angle (10-20°) to the northwest (Watkins 1984, 1985). The effect of adding, say 1000m, of extra Dalradian cover (perhaps locally) to that presently exposed would therefore be to move the surface trace of the garnet isograd approximately 4km to the southeast. This would place high levels of the Garabal Hill intrusion (present levels of which intersect the garnet isograd) firmly inside the high greenschist garnet zone and moves a potential low greenschist source (which demonstrably did not contribute significantly to the Roseneath conglomerates) southwards.

b) Midland Valley Source (primary detritus) Fig 5.1b

The identification of an ideal source in Lower ORS conglomerates ultimately provenanced from deep within the Dalradian terrain (Model I) is countered by impressive arguments for a primary south and southwesterly derivation:

1) Whilst undoubted polycyclic material can be identified within the basal Upper ORS, evidence of a primary origin for much of the remaining debris is strong:

   i) The large size of many Roseneath acid hypabyssal and plutonic boulders (c. 1m) may be used in an argument for a local primary source. However, despite experimental evidence to the contrary, it seems that in present day fluvial systems distal transport (or the order of 50km at least) need not necessarily produce a decrease in maximum or average size of clasts (Abbott and Peterson 1978; Bradley 1970; Bradley et al 1972; Breyer and Bart 1978). In any case, clast size must ultimately depend upon the initial size of material entering the system, for which no estimation can be made in ancient deposits. Most of the non-quartzitic clasts from the entire Clyde Upper ORS succession are moderately to well rounded. Again, this parameter cannot be used as a measure of transport since the degree of rounding is dependent not only on the distance travelled but also on the energy of transport and durability and size of the associated sediment load (see Laming 1966; Pearce 1971; Schumm and Stephens 1973). Abbott and Peterson (1978) produced a four division abrasion durability scale derived from tumble-mill experiments: weakly durable marble and schists; moderately durable basalt, granodiorite, gneiss and gabbro; durable obsidian, metabreccia and metasandstone; and ultradurable silicic rhyolite, quartzite and chert. The same experimental evidence also indicates that attrition rates of less durable types increases dramatically in polylithologic populations where ultradurable clasts are also present. Thus, the metamorphic and igneous detritus at Roseneath displaying moderate to large clast sizes and degrees of rounding are amongst the least durable lithic types. This is especially incompatible with a distal or polycyclic origin when it is considered that the associated conglomerate clasts for all areas are large ultradurable quartzites.

ii) Highly discrete heavy mineral, detrital feldspar and lithic fragment assemblages in sandstones across the Upper ORS basin are derived almost exclusively from source compositions identical to those supplying the equally discrete conglomerates. Such homogeneous assemblages within individual conglomerates would not be expected to result from significant mixing of polycyclic material or transport of primary detritus over any considerable distance.

iii) Upper ORS conglomerates in the Clyde area of proximal alluvial fan origin display a tendency for bed thickness to correlate positively with maximum particle size (and hence discharge). Good, positive MPS/BTh relationships were attributed to varying current competence and the derivation of predominantly primary detritus (Bluck 1967). Redeposition of older conglomerate material would display a poorer relationship with discharge.

iv) Lower ORS conglomerates in the NW Midland Valley are not well exposed but do not appear to contain compositions suitably rich in acid hypabyssal/plutonic and high greenschist metamorphic material to source the Upper ORS at Roseneath (assuming that it was not all removed during or prior to Upper ORS deposition). Whilst it is known that metamorphic input increased during the late Lower ORS, it does not approach the magnitude of that observed in the Upper ORS. The higher schist content of the base Upper ORS relative to the top Lower ORS can also be recognised in the sand sized detritus using geochemical means (Bowes 1963).

2) Radiometic age data for the undeformed and unmetamorphosed Roseneath granodiorite rocks indicates a crystallisation age of around 530-516 Ma. This in itself is sufficient to justify derivation from outwith the Dalradian block, since these ages probably pre-date the climax of Dalradian metamorphism. Scottish granites of this age or older (eg Carn Chuinneag 562-557 Ma; Inch Bae 560 Ma; Ben Vuirich 514 Ma; Dunfallandy Hill 506 Ma; Windyhills 497 Ma) were all deformed and foliated during peak Dalradian metamorphism. These granitoids of comparable age to the Roseneath clasts also display significantly higher initial strontium and Rb/Sr ratios together with other contrasting geochemical features associated with S-type granites. Provisional isotopic work on the garnet schists at Roseneath (Bluck pers. comm. 1985) seem to indicate that these clasts do not display Sm-Nd provenance ages of Dalradian greenschists but do appear to have shared a common uplift event with the local Dalradian at c 410 Ma (Rb-Sr and K-Ar mineral ages).

5.2 Implications For Midland Valley Basement

It is very difficult to reconcile the strong evidence for a primary southwesterly derivation within the Midland Valley for detritus which apparently predates but shows clear geochemical/petrographical affinities with Dalradian metamorphic lithologies and related Newer Caledonian intrusions to the north. Nevertheless, the sedimentological evidence for a primary southwesterly source must be considered overwhelming and, if accepted, has very important implications concerning the nature and evolution of the NW Midland Valley.

In the Midland Valley, the presence of metasedimentary and metaigneous granulite basement with certain 'Lewisian' - like characteristics at medium crustal levels beneath a thin (c 5km) but complete Lower Palaeozoic and younger cover is now reasonably well established using gravity, magnetic and seismological data (see Davidson et al 1984 and Hall et al 1984 for summary of previous and most recent work). Direct evidence for Lower crustal compositions beneath the Midland Valley is currently being determined from xenoliths present in deep rooted Carboniferous vents (see Upton et al 1984 for summary). Isotopic and petrologic investigations of the xenolith suites indicates that whilst an inherited Lewisian zircon component (c. 2 Ga) may be present in some metasedimentary xenoliths (Halliday et al 1984), the overriding impression is that this granulite continental basement has a predominantly Grenvillian to Knoydartian age (1100-700 Ma). This basement is therefore tentatively viewed as a continuation of that proposed to underly the Dalradian Supergroup of the Southern Highlands.

Dalradian greenschist and amphibolite facies rocks lie within the supposed Irish extension of the Scottish Midland Valley in Connemara and have a complex southward thrusted and rotated relationship to proposed Ordovician rocks which may be tentatively correlated with the HBC in Scotland (Leake et al 1983, 1984). Thus the two provenance models discussed above need not necessarily be mutually exclusive, with a southerly derivation from a preserved remnant of Dalradian block thrusted over a terrain containing the HBC and perhaps the unfoliated 530-516 Ma acid igneous material. However, evidence for pre-Upper Devonian/Lower Carboniferous thrusting along the HBF is lacking in Scotland and there is little independent evidence outwith the present study to support the presence of Dalradian-like lithologies preserved immediately south of the HBF.

No amphibolite or greenschist facies rocks have so far been recognised in any of the xenolith assemblages in the Midland Valley or southern Highlands. For the region occupied by the Upper ORS basin in the Firth of Clyde, as elsewhere in the Midland Valley, xenolith suites suggest a layered crust composed largely of anhydrous pyroxene granulite, anorthosite and gabbroic metaigneous rocks in the lower part, with foliated garnet bearing quartzofeldspathic granulite gneisses and unfoliated granite and trondjemite occupying mid crustal regions. The absence of greenschist Dalradian terrain south of the HBF is further supported by the Pb isotopic composition of galenas contained in veins in Silurian to Carboniferous rocks (Parnell and Swainbank 1984). An increase in radiogenic Pb southwards across the HBF was interpreted as reflecting the absence of Dalradian rocks in the Midland Valley, or at least that which includes a magmatic component of Pb. Pb isotopic compositions obtained from Lower and Upper ORS sediments near the HBF in Arran (Dickin 1984) correspond to a provenance age of c. 1800 Ma. This is indicative of a Laxfordian component which, to date, has not been recognised as a major contributor to the Xenolith assemblages. Additionally, whilst the Pb isotopic composition of many of the samples analysed deprecates a Dalradian low radiogenic composition, a number of analyses do display low radiogenic Pb compositions typical of the Grampian Highlands using the fields of Parnell and Swainbank (1984). It is also interesting that the most Dalradian-like ORS Pb composition was detected in a sediment containing 80% volcano-genic material (Dickin 1984).

5.3 Conclusions

The results of the present investigation may be summarised as follows:

1) A mixed composition of reworked Lower ORS and primary detritus derived from south of the HBF are identified in the basal Upper ORS in the Firth of Clyde.

2) The source of Primary detritus to the basin appears to have had a laterally variable composition in which the grade of metamorphic material decreases from garnet grade in the north through medium to low greenschist facies to predominantly nonmetamorphic sedimentary material in the south and southwest. Variations in this unidentified terrain therefore not

only reflect south-north grade trends within the Dalradian (chlorite→biotite→garnet) but also repeats lithologic trends in the same direction (greywacke and slates/phyllites to albite grits).

3) Primary metamorphic detritus with granulite compositions encountered in Carboniferous diatremes in the Midland Valley are not represented in the basal Upper ORS conglomerates.

4) Unfoliated late Cambrian-early Ordovician (530-515 Ma) plutonic and hypabyssal material in the Roseneath conglomerate does not have a Dalradian emplacement history and contains a probable Grenville inherited component. It is, however, indistinguishable petrographically and geochemically from Newer Caledonian granites (c. 400 Ma) in the southwest Highlands but does not display unequivocal similarities with Cambro-Ordovician plutonic detritus derived from the proposed Midland Valley volcanic arc (Longman 1980; Longman et al 1979). Similarities with southwest Highlands intrusions must therefore reflect continuity of magma source regions within the lower crust across the HBF zone and constrains the amount of strike-slip movement proposed for this fracture (cf. Bluck 1984, Curry et al 1984; Harte et al 1984).

5) The simplest provenance model required to explain the complex nature of the primary detritus in the Upper ORS conglomerates combines Dalradian and largely undeformed Cambro-Ordovician sources in a thrust related mixed terrain similar to that described for the Midland Valley extension in Connemara. Pb isotope constraints suggest, however, that if present, these Dalradian lithologies may only be of isolated occurrence.

6) In the absence of much more intensive isotopic and geochemical work in the Dalradian terrain around Loch Fyne and for Upper and Lower ORS sandstones and conglomerates in the Firth of Clyde, proposals for the provenance of igneous and metamorphic detritus in the Upper ORS must remain largely tentative.

APPENDIX I

SEDIMENTARY PETROLOGY TECHNIQUES

I. 1 Heavy Mineral Separation

Disaggregation sandstone was normally achieved either by hand or by gently crushing in an agate crucible. Treatment with HC1 was avoided since this is known to destroy apatite. For more consolidated samples such as silica cemented sandstone, schist and plutonic clasts in the conglomerates, slightly extended crushing in an agate crucible or occassionally a Tema mill was required to produce single crystals. This investigation agrees with the findings of Henningsen (1967), that gentle crushing in this manner does not result in mass fracturing and breaking of grains.

The disaggregated grains were dry seived using wire meshes and the 2Ø, 3Ø and 4Ø fractions collected. The fraction passing through the 4Ø seive was also retained for clay determination. Each size fraction was cleaned in an ultrasonic tank for at least 30 minutes during which the suspended fines were regularly poured off. This was followed by overnight oven drying.

Final separation of heavy grains was carried out using tribromoethane (bromoform - $CHBr_3$) and centrifuging for about 15 minutes at 3000 rpm.

I. 2 Clay Analysis by XRD

The clay portion of 4Ø seive fractions obtained from sandstone disaggregation (see Section I.1 above) was separated from silt and sand by a process of partial decanting and centrifuging with water, followed by filtration. Oriented mounts were prepared on ceramic tiles using a glass dropper and dried overnight in a dessication chamber at room temperature.

A preliminary diffractogram was run using Phillips PW2103/00 goniometer (Cu-K alpha radiation at 1° 2 θ per minute), and was followed by a second run after glycolation of samples in a dessicator chamber for 2 - 3 hours (montmorillonite determination). A third diffractogram was performed on all samples after heating in a furnace for 1 hour at 750°C (for kaolinite/chlorite at illite/muscovite peak separations).

L 3 K-feldspar structural state by XRD

Principles

The aluminosilicate framework shared by all feldspars is constructed of tetrahedra centred either by Si or Al atoms with O atoms forming the apices. If Si atoms form the centre of the tetrahedra, four oxygen atoms are required for electrostatic balance. However, when Al atoms are present, large cations (Na, K, Ca or Ba) are required to stabilise the structure. The type of cations present in the aluminium tetrahedra will therefore determine the composition of the resulting feldspar. Additionally, since Al and Si have similar structural properties and may mutually and randomly substitute, the distribution of Al and Si sites affects a feldspar's structural state. Random distributions of Al result in a disordered feldspar series (sanidine to high-albite). If most Al is locked in $T_{1(0)}$ sites the feldspar is ordered (microcline to low-albite). Intermediate stages of ordering are also possible.

It is the variation in distribution of Al and Si, and the resulting differences in length of, and angles between, unit-cell edges which are measured by X-ray diffraction. For the alkali feldspars, variations in the above parameters result in a continuous series from microcline through orthoclase to sanidine.

Martin (1974) outlined the physical and chemical controls on feldspar ordering:

i) Temperature is probably the most influential physical control. Although the process is only partially understood, it seems that high temperatures of equilibration induce a random distribution of Al and disordered alkali feldspars result (sanidine). With high temperature alkali feldspars, cooling rates apply additional control on ordering. The disordered feldspars which initially nucleate from an igneous magma gradually attain more stable, ordered forms provided cooling rates are slow. Therefore, rapidly quenched volcanic K-feldspars are commonly disordered. These disordered feldspars retain their structural state, unlike albites which appear to gradually order with time.

ii) The effects of deformation (more specifically shear stress) on feldspar ordering is probably only important on a local scale. The conversion of orthoclase to microcline in response to deformation in some granitic rocks goes some way to explain the regional trends towards ordered microclines with increasing grade in metamorphic rocks (Martin 1974).

iii) Reynolds (1963) showed a negative correlation between grain size and ordering for feldspars in carbonate rocks. Mackenzie (1952) observed a similar effect in simulated laboratory experiments. During authigenic growth there should be a greater ordering towards the cores of crystals. This, however, has not been reported.

iv) Chemical controls on structural state are probably dominated by the presence of an aqueous fluid. The role of water is seen as a catalyst upon which the strong T-O bonds of the feldspar tetrahedra are broken. This results in the development of more ordered crystals. The nature and composition of the fluid phase from which the feldspar crystallises is also important. The presence of excess Al_2O_3 at the solid-liquid interface apparently slows down the ordering process. Thus, peraluminous bulk compositions give rise to relatively disordered feldspars. On the other hand, ordering is promoted by the addition of alkali and silica to the fluid. The presence of H^+ may also be necessary in these conditions (Martin 1974). Where alkali feldspar has a maetasomatic replacement origin a complex relationship exists between ordering of the original feldspar (plagioclase) and that of the new crystal. Martin (1974) considered that a reasonably ordered plagioclase could be replaced by a fully ordered maximum microcline. The replacive microcline should not show grid twinning. Difficulties with this general rule occur if the plagioclase being replaced is particularly disordered or is more calcic than An_{28}.

v) The chemical composition of the feldspar influences the rate of ordering. Na and K exchange easily in the feldspar framework but the reactions involved are rapid compared with the ordering process (Laves 1952) and the amount of Na contained in the feldspar does not determine structural state. Ba substitution would probably not occur in a fully ordered feldspar and Rb and Cs are probably also preferentially incorporated into disordered varieties. Small

amounts of ferric iron, though, may increase the rate of ordering. The influence of boron is not fully understood.

vi) Composition of the host rocks is the final major chemical control on structural state. Microcline increases in plutonic igneous rocks with fractionation at the expense of orthoclase. The volatile content of the melt is thought to control the evolution of microcline at lower temperatures.

Method

The method of determining the structural state of alkali feldspars in this study is based on the 'three peak' method devised by Wright (1968) and a modified 'two peak' method proposed by Suttner and Basu (1977).

Of the many diffraction peaks which may be observed on an XRD trace of alkali feldspar, the five most intense peaks are particularly useful. These five peaks correspond to reflections from Miller indices $\bar{2}01$, 002, $\bar{1}13$, 060 and $\bar{2}04$. The 2θ positions and approximate intensities for each index are tabulated in Table I.3.1.

It was observed by Wright (1968) that a very close linear relationship exists between measured 2θ values of $\bar{2}01$, 060 and $\bar{2}04$ diffraction peaks and the a, b and c cell parameters respectively. Therefore the dimensions of the unit-cell and hence the structural state may be estimated from a plot of 2θ (060) against 2θ ($\bar{2}04$) upon which stability fields for feldspars of known structural state have been superimposed. The remaining cell parameter ($\bar{2}01$) for known feldspar states is also superimposed on this plot as cross contours (Figure I.3.1). The value of $\bar{2}01$ predicted from the plot should always agree with that observed for the $\bar{2}01$ peak on the trace. If it does not agree, then the feldspar is described as anomalous. These anomalous feldspars were not used by Wright (1968) for structural state determination.

Suttner and Basu (1977) noted that differences in predicted and observed values of $\bar{2}01$ rarely exceed $\pm$ 0.12° 2θ and proposed that scanning for the $\bar{2}01$ reflection was not necessary. In any case, the usefulness of anomalous K-feldspars in the plot was still considered to be credible. X-ray diffractions are ideally performed on powders of single crystals larger than 0Ø (1mm). However, considerable difficulty was

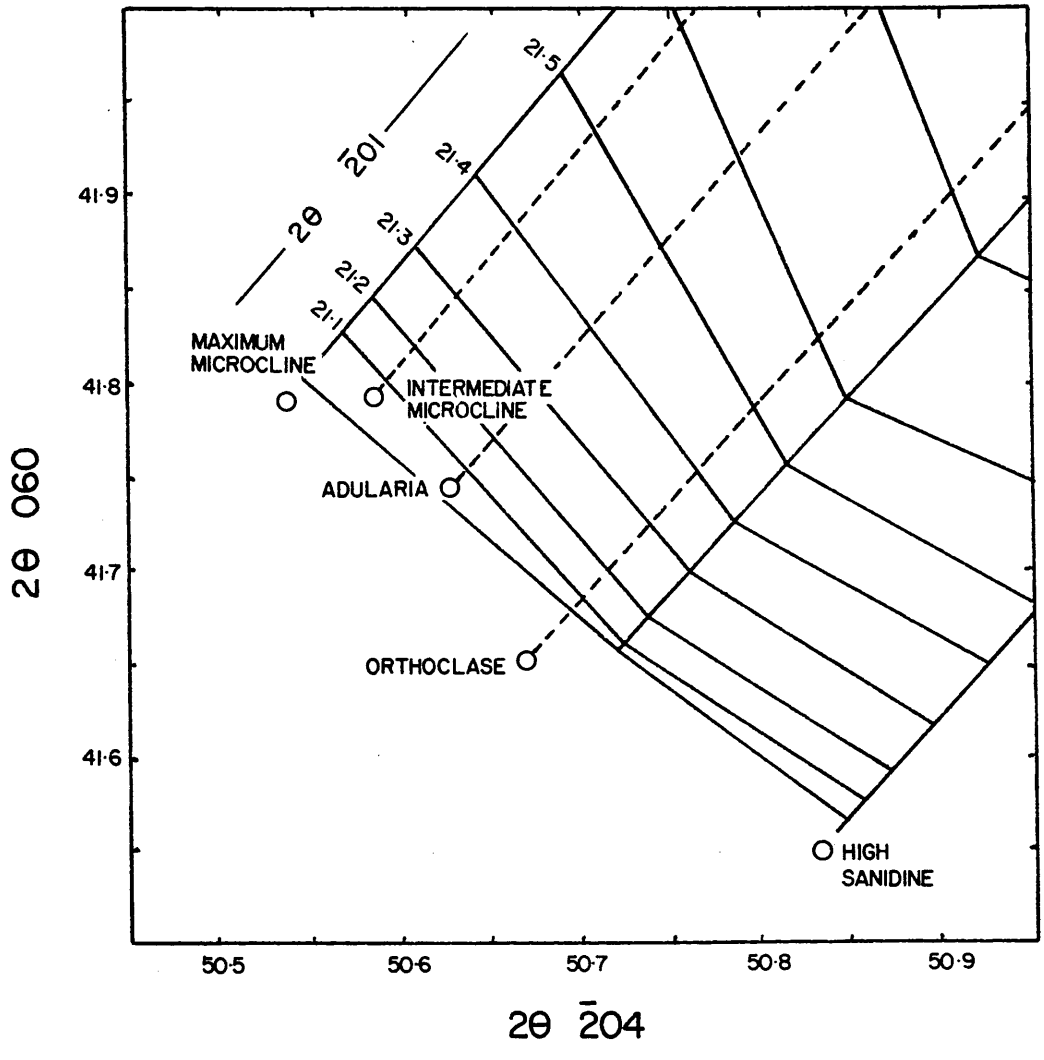

Fig I.3.1. Plot of 2θ(060):2θ($\bar{2}$04) showing alkali exchange paths and positions of maximum high and low structural states at KAlSi3O8 composition.

MILLER INDEX (hkl)	APPROX. INTENSITY	K-FELDSPAR 2θ	ANORTHOCLASE 2θ	ALBITE 2θ
$(\bar{2}01)$	40	20.8° - 21.2°	21.6° - 21.9°	21.9° - 22.1°
(002)	100	27.4° - 27.8°	27.8° - 28.0°	27.9° - 28.1°
$(\bar{1}13)$	8	38.6° - 39.0°	not present	not present
(060)	25	41.6° - 42.0°	41.7° - 42.0°	42.2° - 42.6°
$(\bar{2}04)$	30	50.5° - 51.1°	51.1° - 51.3°	51.2° - 51.5°

TABLE I.3.1 2θ positions and approximate intensities for the five major feldspar diffractogram peaks.

encountered in separating single grains from the sandstones of a large enough size that an aggregate grain method was devised. This was also applied to the igneous and metamorphic clasts from which K-feldspar was separated to use as a reference.

The sandstone samples were easily disaggregated either by hand or by gentle crushing in an agate crucible. Rock samples were normally around $6cm^3$ but high rates of success could still be achieved with smaller quantaties. The sands were then dry seived using wire meshes and the 0-3ø fraction collected and cleaned in an ultrasonic tank for at least 30 minutes. During cleaning the suspended fines were regularly poured off.

After thorough oven drying the grains were placed in a solution of tribromoethane and acetone with a specific gravity only slightly greater than that of K-feldspar. The correct specific gravity is achieved by floating large crystals of quartz and K-feldspar in the bromoform and adding acetone until only K-feldspar remains afloat.

For the igneous and metamorphic rocks used as references, a similar method is employed. Rock chips produced by jaw crushing are further broken down in an agate Tema mill for approximately 30 seconds until a fine sand is obtained. It is important that the samples should not be too finely powdered. These are then cleaned in the same way as the sandstones and dried before heavy liquid separation.

The K-feldspar separates obtained from centrifuging in heavy liquid (15 minutes at 3000 rpm) were powdered by hand using a corundum mortar and pestle. Crushing does not appear to affect the structural state of the crystals.

At this stage a small quantity of powder of known composition is added for use as an internal standard, to correct for any minor peak shift due to operator or mechanical error during analysis. Spec. pure SiO_2, $PbNO_3$ and CaF_2 were all used for this purpose, but it is thought that peaks caused by small quantities of quartz which survive the separation process may also be used with comparable precision. Acetone was added to the powder mixture and a small amount collected in a glass dropper. This solution was rapidly deposited as evenly as possible on one half of a glass slide (35mm x 35mm). Several attempts are sometimes required to produce an even application. One or two layers of adhesive tape (depending on

the thickness of the powder layer) are applied to the other half of the slide to compensate for the thin powder and to retain alignment inside the diffractometer. This last stage was found essential if reproducibility was to be achieved.

For each K-feldspar separate a single scan diffractogram is obtained from the goniometer (Phillips PW2103/00 this study) by running from 55° 2θ to 40° 2θ for the two peak method or down to 20° 2θ if the full 5 peaks are required. It is important to scan from high to low 2θ values since most published data are obtained in this way. Peaks will not occur in the same positions for repeated scans of the same sample if scanning direction is reversed on the second run.

Cu-K alpha radiation is used and the goniometer speed is set at 1° 2θ per minute. Chart speed is set at 2cm per minute and a range of 4 x 10^2 cps usually enables 2θ determinations of better than 0.01° precision.

In this study, the diffractogram was run a second time for each sample. If the peak positions were note identical to within 0.02° 2θ once corrected using the internal standard, the sample should be discarded. However, not one of the 50 determinations made, deviated by more than 0.01° 2θ and therefore repeat scanning may not be necessary. Occassionally the trace should be run to obtain the actual $\bar{2}01$ value to enable comparison with that predicted by the $\bar{2}04$ - 060 plot.

I. 4 Pollen and Spore Analysis

Preparation of shale samples for pollen and spore analysis in this study employs the techniques described by Brasier (1980).

Thorough cleaning of samples with a hard bristle scrubbing brush to remove organic surface deposits preceeded jaw crushing of samples into $1cm^3$ chips. These chips were disaggregated using both sodium hypochlorite (disaggregation time circa 3 months) and hydrofluoric acid (disaggregation time circa 4 days). In both cases thorough dilution of the supernatent liquid was followed by paper filtering and cleaning of the residue with distilled water.

Concentration of spores was attemped (unsuccessfully) by partial decanting into successive glass tubes after shaking and settling (Method H of Brasier 1980). Permanent mounts of the evaporated residue were made on glass slides using Canada Balsam.

APPENDIX II

GEOCHEMICAL TECHNIQUES

II. 1 Major and Trace Element Analysis

Elemental abundances were determined using X-ray fluorescence techniques for 10 major elements (SiO_2, TiO_2, Al_2O_3, Fe_t, MnO, MgO, CaO, Na_2O, K_2O and P_2O_5) and 18 trace elements (Ba, Ce, Co, Cr, Cu, Ga, La, Nb, Ni, Pb, Rb, S, Sr, Th, U, Y, Zn and Zr). Determination of FeO and total volatile content (H_2O + CO_2) was undertaken using wet chemistry and loss on ignition methods respectively.

Samples for analysis were obtained from the central portions of boulders larger than 30cm maximum diameter and selected to exclude xenoliths and veins. Initial scrubbing of the samples was followed by jaw crushing and grinding in an agate Tema mill to obtain 250µm whole rock powder. Major elements were measured on fused beads made from the 250µm powder mixed with flux (lithium tetraborate) in weight ratio 1: 5.3. Further grinding of the rock powder to 100µm was required to make pressed pellets for trace element analysis. Pellets were made from this whole rock powder and thermal binder (phenol formaldehyde) in weight ratio 6:1.

XRF techniques follow those described by Leake et al (1969) and were made on a Phillips PW1450 sequential automatic X-ray spectrometer using W, Cr and Mo detector tubes and Ge, LiF 220, LiF 200 P.E. and T.A.P. reflecting crystals.

II.2 Isotopic Techniques

Samples for Rb-Sr age determinations were obtained from the central portion of boulders larger than 50cm maximum diameter and selected to exclude xenoliths and veins. Initial scrubbing of the samples was followed by crushing into $1cm^3$ chips using a tungsten steel jaw crusher and grinding in a steel Tema mill until a coarse powder was obtained. The powders were seived and the portion remaining between 210µm and 175µm retained and thoroughly washed in water and acetone. Biotite and K-feldspar were separated from the whole rock powder using heavy liquid (tetrabromoethane) followed by several magnetic separations.

Preparation of samples for zircon U-Pb dating involved crushing of 25kg to a coarse powder using the techniques described above. Preliminary separation of heavy grains was made by washing the sample over a Wilty jigging table followed by heavy liquid separation in tetrabromoethane. Final separation of zircons by size and magnetic susceptibility was made by seiving and magnetic separation.

Isotopic compositions of Rb, Sr U and Pb were carried out by isotopic dilution on a V.G. Micromass 30B solid source mass spectrometer.

Preparation of samples for Rb-Sr age determination was made using the following method:

1) 0.1g of sample (Biotite separate, K-feldspar separate or whole rock powder) was weighed into teflon beakers together with known quantities of ^{87}Rb (99.2% Harwell) and ^{84}Sr (99.783% N.B.S.). 20cc of HF was added to this and heated overnight at 200°C. The samples were evaporated, the fluoride residue being dissolved in twice distilled Analar HNO_3, diluted by twice distilled water and evaporated again. Any remaining solids were then removed by centrifuging in 2.5N HC1.

2) The HC1 solutions were placed in ion exchange columns with Bio Rad AG50W-X8 200 - 400 mesh resin and fractions containing Rb and Sr collected. The 2.5 HC1 was evaporated on a hotplate.

3) Sr and Rb were loaded for isotopic analysis with a phosphoric and hydrochloric acid mixture on a tantalum filament bead, and with water on a triple tantalum filament bead respectively.

An on-line computer calculated average $^{88}Sr/^{86}Sr$ and $^{87}Sr/^{86}Sr$ for 15 sets of 10 peak height scans for each sample. $^{88}Sr/^{86}Sr = 8.37521$ is the accepted correction for mass fractionation. Mass of ^{85}Sr was monitored to enable correction for any ^{87}Rb present. For Rb determinations, average $^{85}Rb/^{87}Rb$ was calculated for 5 sets of data, sufficient to obtain precision greater than 0.0001.

'Isochrons' were calculated by computer using regression analysis and an Rb decay constant of $1.42 \times 10^{-11} y^{-1}$.

A different procedure to that described above was followed for U-Pb age determinations and has been described by Krogh (1973). Corrections for common Pb were made using $^{206}Pb/^{204}Pb$ = 17.3, $^{207}Pb/^{204}Pb$ = 15.5 and $^{208}Pb/^{204}Pb$ = 37.1 with decay constants taken as ^{235}U = 9.84850 x $10^{-10}y^{-1}$ and ^{238}U = 1.55125 x $10^{-10}y^{-1}$.

REFERENCES

ABBOTT, P.L. and SMITH, T.E., (1978). Trace element comparison of clasts in Eocene conglomerates, southeastern California and northwestern Mexico. J GEOL **86:** 753.

ABBOT, P.L. and PETERSON, G.L., (1978). Effects of abrasion, durability and conglomerate clast populations : examples from Cretaceous and Eocene conglomerates of the San Diego area, California. J SEDIMENT PETROL **48:** 31.

ALLEN, J.R.L. and CROWLEY, S.F., (1983). Lower Old Red Sandstone fluvial dispersal systems in the British Isles. TRANS R SOC EDINBURGH EARTH SCI **74:** 61.

ATHERTON, M.P. and BROTHERTON, M.S., (1982). Major element composition of the pelites of the Scottish Dalradian. GEOL J **17:** 185.

BAILEY, E.B. (1923). The metamorphism of the southwest Highlands. GEOL MAG **60:** 317.

BAILEY, E.B. and McCALLIEN, W.J., (1934). The metamorphic rocks of north-east Antrim. TRANS R SOC EDINBURGH **58:** 163.

BASU, A., YOUNG, S.W., SUTTNER, L.J., JAMES, W.C. AND MACK, G.H. (1975). Re-evaluation of the use of undulatory extinction and polycrystallinity in detrital quartz for provenance interpretation. J SEDIMENT PETROL **45:** 873.

BLATT, H. (1979). Diagenetic processes in sandstones. SPEC PUBL SOC ECON PALEONT MINERAL **26:** 141.

BLATT, H. and CHRISTIE, J.M. (1963). Undulatory extinction in quartz of igneous and metamorphic rocks and its significance in provenance studies of sedimentary rocks. J SEDIMENT PETROL **33: 559.**

BLUCK, B.J. (1967). Deposition of some Upper Old Red Sandstone conglomerates in the Clyde area: A study in the significance of bedding. SCOTT J GEOL **3:** 139

BLUCK, B.J., (1978). Sedimentation in a late orogenic basin: the Old Red Sandstone of the Midland Valley of Scotland. **In** Bowes, D.R. and Leake, B.E. (Eds.). Crustal evolution in northwestern Britain and adjacent regions. GEOL J SPEC ISSUE **10:** 249.

BLUCK, B.J., (1980a). Evolution of a strike-slip fault controlled basin, Upper Old Red Sandstone, Scotland. In Ballance, P.F. and Reading, H.G. (Eds.) Sedimemtation in oblique-slip mobile zones. SPEC PUBL INT ASSOC SEDIMENT **4:** 63.

BLUCK, B.J. (1980b). Structure, generation and preservation of upward fining, braided stream cycles in the Old Red Sandstone of Scotland. TRANS R SOC EDINBURGH **71:** 29.

BLUCK, B.J. (1984). Pre-Carboniferous history of the Midland Valley of Scotland. TRANS R SOC EDINBURGH **75:** 275.

BOWEN, N.L., (1928). The Evolution of the Igneous Rocks, Dover, New York.

BOWES, D.R., (1963). Note on the chemical composition conglomerates of Lower and Upper Old Red Sandstone age from Ardmore Peninsula, Dunbartonshire. TRANS GEOL SOC GLASGOW **25:** 17.

BOWES, D.R. AND JONES, K.A., (1958). Sedimentary features and tectonics in the Dalradian of western Perthshire. TRANS EDINBURGH GEOL SOC **17:** 133.

BOWES, D.R. and CONVERY, H.J.E., (1966). The composition of some Ben Ledi grits and its bearing on the origin of albite schists in the southwest Highlands. SCOTT J GEOL **2:** 67.

BOYLE, E.A., EDMOND, J.M. and SCHOLKOVITZ, E.R. (1977). The mechanism of iron removal in estuaries. GEOCHIM COSMOCHIM ACTA **41:** 133.

BRADLEY, W.C., (1970). Effect of weathering on abrasion of granitic gravel. BULL GEOL SOC AM **81:** 61.

BRADLEY, W.C., FAHNESTOCK, ROWEKAMP, E.T., (1972). Coarse sediment transport by flood flows on Knife River, Alaska. BULL GEOL SOC AM **83:** 1261.

BRAMLETTE, M.N., (1929). Natural etching of detrital garnet. AM MINERAL **14:** 336.

BRASIER, M.D., (1980). Microfossils. Unwin, London.

BREYER, J.A. and BART, H.A., (1978). The composition of fluvial sands in a temperate semi-arid region. J SEDIMENT PETROL **48:** 1311.

BROWN, G.C., (1979). The changing pattern of batholith emplacement during earth history. **In** Atherton, M.P. and Tarney, J., (Eds.). Origin of Granite Batholith, Shiva, Nantwich.

BROWN, G.C., (1982). Calc-alkaline intrusive rocks: their diversity, evolution and relation to volcanic arcs. **In** Thorpe, R.S. (Ed.) Andesites. John Wiley and Sons.

BROWN, G.C., THORPE, R.S. and WEB, P.C., (1984). The geochemical characteristics of granitoids in contrasting arcs and comments on magma sources. J GEOL SOC LONDON **141:** 413.

BUCKE. D.P. and MANKIN, C.J. (1971). Clay mineral diagenesis within interlaminated shales and sandstones. J SEDIMENT PETROL **41:** 971.

BURNS, L.K. AND ETHRIDGE, F.G., (1979). Petrology and diagenetic effects of listric sandstones : Paleocene and Eocene Umpqua Formation, southwest Oregon. SPEC PUBL SOC ECON PALEONT MINERAL **26:** 307.

CAWTHORN, R.G. and BROWN, P.A., (1976). A model for the formation and crystallization of corundum normative calc-alkaline magmas through amphibole fractionation. J GEOL **84 :** 467.

CHAPPELL, B.W., (1978). Granitoids from the Moonbi district, New England Batholith, eastern Australia. J GEOL SOC AUST **25:** 267.

CHAPPELL, B.W. and WHITE, A.J.R, (1974). Two contrasting granite types. PACIFIC GEOL **8:** 173.

CHINNER, G.A. (1960). Pelitic gneisses with varying ferrous/ferric ratios from Glen Clova, Angus, Scotland. J PETROL **1:** 178.

CHURCH, S.E., (1973). Limits of sediment involvement in the genesis of orogenic volcanic rocks. CONTRIB MINERAL PETROL **39:** 17.

CLAYBURN, J.A.P., HARMON, R.S., PANKHURST, R.J. and BROWN, J.F., (1983). Sr, O and Pb isotopic evidence for origin and evolution of Etive Igneous Complex, Scotland. NATURE **303:** 492.

CONDIE, K.C., (1982). Archean andesites. **In** Thorpe, R.S., (Ed) Andesites. John Wiley and Sons.

CONDIE, K.C., UILJOEN, M.J. and KABLE, E.J.D., (1977). Effects of alteration on element distributions in Archaen tholeiites from the Barberton greenstone belt, South Africa. CONTRIB MINERAL PETROL **64:** 75.

CUNNINGHAM-CRAIG, E.H., (1904). Metamorphism in the Loch Lomond district. QUART J GEOL SOC LONDON **60:** 10.

CURRY, G.B., BLUCK, B.J., BURTON, C.J., INGHAM J.K., SNETER, D.J. and WILLIAMS, A. (1984). Age evolution and tectonic history of the Highland Border Complex, Scotland. TRANS R SOC EDINBURGH EARTH SCI **75:** 113.

DAVIDSON, K.A.S., SOLA, M., POWELL, D.W. and HALL, J. (1984). Geophysical model for the Midland Valley of Scotland. TRANS R SOC EDINBURGH EARTH SCI **75:** 175.

DEBON, F. and LE FORT, P., (1982). A chemical-mineralogical classification of common plutonic rocks and associations. TRANS R SOC EDINBURGH 73: 135.

DEER, W.A., HOWIE, R.A. and ZUSSMAN, J., (1977). An Introduction to the Rock-forming Minerals. Longman, London.

DEMPSTER, T.J., (1985). Uplift patterns and orogenic evolution in the Scottish Dalradian. J GEOL SOC LONDON **142** : 111.

DICKIN, A.P., (1984). Provenance of the Old Red Sandstone : Pb isotape evidence from Arran, western Scotland. TRANS R SOC EDINBURGH **75:** 239.

DICKINSON, W.R., (1970). Interpreting detrital modes of greywacke and arkose. J SEDIMENT PETROL **40:** 695.

DICKINSON, W.R. and SUCZEK, C.A., (1979). Plate tectonics and sandstone compositions. BULL AM ASSOC PET GEOL **63:** 2164.

DICKINSON, W.R., BEARD, L.S., BRAKENRIDGE, G.R., ERJAVEC, J.L., FERGUSON, R.C., INMAN, K.F., KNEPP, R.A., LINDBERG, F.A., and RYBERG, P.T., (1983). Provenance of North American Phanerozoic sandstones in relation to tectonic setting. BULL GEOL SOC AM **94:** 222.

DONNELLY, T.W. and ROGERS, J.J.W., (1980). Igneous series in island arcs. The northeastern Caribbean compared with worldwide island-arc assemblages. BULL VOLC **43:** 347.

DOWNIE, C. and LISTER, T. R., (1969). The Sandy's Creek Beds (Devonian) of Farland Head, Ayrshire SCOTT J GEOL 5 : 193.

ECKERT, J.M. and SCHOLOVITZ, E.R., (1976).) The flocculation of iron, aluminium and humites from river water by electrolytes. GEOCHIM COSMOCHIM ACTA **40:** 847.

ELSDON, R. and KENNAN, P.S., (1979). Geochemistry of Irish granites. **In:** Harris, A.L., Holland, C.H. and Leake, B.E., (Eds). The Caledonides of the British Isles - Reviewed. SPEC PUBL GEOL SOC LONDON **8:** 713.

EWART, A., (1982). The mineralogy and petrology of Tertiary - Recent orogenic volcanic rocks : with special reference to the andesitic-basaltic compositional range. **In** Thorpe, R.S., (Ed.) Andesites. 24. John Wiley and Sons.

FLOYD, J.D., (1982). Stratigrpahy of a flysch succession : the Ordovician of W Nithsdale, SW Scotland. TRANS R SOC EDINBURGH **73:** 1.

FRANCIS, E.H., FORSYTH, I.H., READ, W.A. and ARMSTRONG, M., (1970). The geology of the Stirling district. MEM GEOL SURV UK.

FRIEND, P.F., HARLAND, W.B., and HUDSON, J.D., (1963). The Old Red Sandstone and the Highland Boundary in Arran, Scotland. TRANS EDINBURGH GEOL SOC **19:** 363.

GALLOWAY, W.E., (1974). Deposition and diagenetic alteration of sandstone in northeast Pacific arc-related basins: implications for greywarke genesis. BULL GEOL SOC AM **85:** 379.

GALLOWAY, W.E., (1979). Diagenetic control of reservoir quality in arc-derived sandstones : implications for petroleum exploration. SPEC PUBL SOC ECON PALEONT MINERAL **26:** 251.

GEORGE, T.N., (1960). The stratigraphical evolution of the Midland Valley. TRANS GEOL SOC GLASGOW **24:** 33.

GEORGE, T.N., (1965). The geological growth of Scotland. **In** Craig, G.Y., (Ed.). The Geology of Scotland. Oliver and Boyd, Edinburgh.

GLENNIE, K.W., MUDD, G.C. and NASTEGAAL, P.J.C., (1978). Depositional environment and diagenesis of Permian Rotliegendes sandstones in Leman Bank and Sole Pit areas of the UK Southern North Sea. J GEOL SOC LONDON **135:** 25.

GOLDICH, S.S. and GAST, P.W., (1966). Effects of weathering on the Rb-Sr and K-Ar ages of biotite from the Morton Gneiss, Minnesota. EARTH PLANET SCI LETT **1:** 372.

GRAHAM, S.A., INGERSOLL, R.V. and DICKINSON, W.R., (1976). Common proverance for listric grains in Carboniferous sandstones from Ouachita Mountains and Black Warrior Basin. J SEDIMENT PETROL **46:** 620.

GRANMAYER, A., (1978) Petrography and provenance of the Torridonian rocks, NW of Scotland. Unpublished MSc thesis, University of Glasgow.

GRANT, J.N., HALLS, C, AVILA, W. and AVILA, G., (1977). Igneous geology and the evolution of hydrothermal systems in some sub-volcanic tin deposits of Bolivia. **In** Volcanic processes in ore genesis. SPEC PUBL GEOL LONDON **7:** 117.

GRAVENOR, C.P., (1979). The nature of the late Palaeozoic glaciation in Gondwana as determined from analysis of garnets and other heavy minerals. CAN J EARTH SCI **16:** 1137.

GRAVENOR, C.P. and LEAVITT, R.K., (1981). Experimental formation and significance of etch patterns on detrital garnets. CAN J EARTH SCI **18:** 765.

GROOME, D.R., and HALL, A., (1974). The geochemistry of the Devonian Lavas of the northern Lorne Plateau, Scotland. MINERAL MAG **39:** 621.

GUNN, W., CLOUGH, C.T. and HILL, J.B., (1897) The geology of Cowal. MEM GEOL SURV GB.

HALL, J., BREWER, J.A., MATTHEWS, D.H. and WARNER, M.R., (1984). Crustal structure of the Caledonides from the 'WINCH' seismic reflection profile : influences on the evolution of the Midland Valley of Scotland. TRANS R SOC EDINBURGH EARTH SCI **75** : 97.

HALLIDAY, A.N., (1984). Coupled Sm-Nd and U-Pb (Zircon) systematic in the late Caledonian granites and the nature of the basement under northern Britain. NATURE **307:** 229.

HALLIDAY, A.N., STEPHENS, W.E. and HARMON, R.S., (1981). Isotopic and chemical constraints on the development of peraluminous Caledonian and Acadian granites. CAN MINERAL **19:** 205.

HALLIDAY, A.N., AFTALION, M., UPTON, B.G.J., ASPEN, P. and JOCELYN, J., (1984). U-Pb isotopic ages from a granulite-facies xenolith from Partan Craig in the Midland Valley of Scotland. TRANS R SOC EDINBURGH EARTH SCI **75:** 71

HAMILTON, P.J., EVENSEN, N.M., O'NIONS, R.K. and TARNEY, J. (1979). Sm-Nd systematics of Lewisian gneisses : implications for the origin of granulites. NATURE **277:** 25.

HARTE, B. BOOTH, J.E., DEMPSTER, T.J., FETTES, D.J., MENDUM, J.R. and WATTS, D., (1984). Aspects of the postdepositional evolution of Dalradian and Highland Border Complex rocks in the Southern Highlands of Scotland. TRANS R SOC EDINBURGH EARTH SCI **75:** 151.

HATCH, F.H., WELLS, M.K. and WELLS, A.K., (1972). Petrography of the Igneous Rocks. Murby. London.

HAWKINS, P.J., (1978). Relationship between diagenesis, porosity reduction, and oil emplacement in late Carboniferous sandstone reservoirs, Bothamsall

oilfields, E Midlands. J GEOL SOC LONDON **135:** 7.

HEIMLICH, R.A., SHOTWELL, L.B., COOKRO, T. and GAWELL, M.J., (1975). Variability of zircons from the Sharon conglomerate of northeastern Ohio. J SEDIMENT PETROL **45:** 629.

HEMINGWAY, J.E. and TAMAR-AGHA, M.V., (1975). The effects of diagenesis on some heavy minerals from clastics of the Middle Limestone Group in Northumberland. PROC YORKSHIRE GEOL SOC **40:** 537.

HENNINGSEN, D., (1967). Crushing of sedimentary rock samples and its effect on shape and number of heavy minerals. SEDIMENTOLOGY **8:** 253.

HILL, J.B., PEACH, B.N., CLOUGH, C.T., KYNASTON, H., TEALL, J.J.H. and FLETT, J.S., (1905). The geology of Mid-Argyll. MEM GEOL SURV GB.

HINE, R. and MASON, D.R., (1978). Intrusive rocks associated with porphyry copper mineralization, New Britain, Papua New Guinea. ECON GEOL **73:** 749.

HUBERT, J.F., (1962). A zircon-tourmaline-rutile maturity index and the interdependence of the heavy mineral assemblages with the gross composition and textures of sandstones. J SEDIMENT PETROL **32:** 440.

HURST, A.R., (1981). A scale of dissolution for quartz and its implications for diagenetic processes in sandstones. SEDIMENTOLOGY **28:** 451.

INGERSOLL, R.V., (1983). Petrofacies and provenance of late Mesozoic forearc basin, northern and central California. BULL AM ASSOC PET GEOL **67:** 1125.

IRVINE and BARAGAR, W.R.A., (1971). A guide to the classification of the common volcanic rocks. CAN J EARTH SCI **8:** 523.

JAKES, P. and WHITE, A.J.R., (1972). Major and trace element abundances in volcanic rocks of orogenic areas. BULL GEOL SOC AM **83:** 29.

JAWAD ALI, A. and BRAITHWAITE, G.J.R., (1977). Penecontemporaneous weathering of the Old Red Sandstone of the Midland Valley of Scotland. SCOTT J GEOL **13:** 305.

JONES, K.A., (1961). Origin of albite porphyroblasts in rocks of the Ben More-Am-Binnein area, western Perthshire, Scotland. GEOL MAG **98:** 41.

JONES, K.A., (1962). Origin of albite porphyroblasts. GEOL MAG **99:** 92.

JONES, K.A., (1964). Metamorphism of the Ben More-Am-Binnein area, western Perthshire Scotland. QUART J GEOL SOC LONDON **120:** 51.

KAHN, J.S., (1956a). The analysis and distribution of the properties of packing in sand-size sediments. 1. on the measure of packing in sandstones. J GEOL **64:** 385.

KAHN, J.S., (1956b). Analysis and distribution of packing properties in sand sized sediments. 2. The distribution of the packing measurements and an example of packing analysis. J GEOL **64:** 578.

KALSBECK, F., (1967). Evolution of zircons in sedimentary and metamorphic rocks - a discussion. SEDIMENTOLOGY **8:** 163.

KAY, R.W., (1977). Geochemical contraints on the origin of Aleutian magmas. **In** Talwani, M. and Pittman, W.C., (Eds.) Island Arcs, Deep Sea Trenches and Back-arc Basins. 229. American Geophysical Union, Washington, D.C.

KELLING, G., (1962). The petrology and sedimentation of Upper Ordovician rocks in the Rhinns of Galloway, south-west Scotland. TRANS R SOC EDINBURGH **65:** 107.

KROGH, T.E., (1973). A low contamination method for hydrothermal decomposition of zircons and extraction of U and Pb for isotopic determinations. GEOCHIM COSMOCHIM ACTA **37:** 485.

KRYNINE, P.D., (1946). The tourmaline group in sediments. J GEOL **54:** 65.

KYNASTON, H. and HILL, J.B., (1908). Geology of Oban and Dalmally. MEM GEOL SURV UK.

LA ROCHE, H. de, (1966). Sur l'usage du concept d'association minerale dans l'etude chimique des roches : models chimiques, statistique, représentation graphiques, classification chimico-minéralogique. C R ACAD SCI PARIS **262D:** 1665.

LA ROCHE, H. de, (1979). Muscovitisation deutérique, caractère alumineux des leucogranites et classification des granites subsolvus. BULL SOC GEOL FR **21:** 87.

LAMBERT, R.St J., HOLLAND, J.G. and WINCHESTER, J.A., (1981). Comparative geochemistry of petites from the Moinian and Appin Group (Dalradian) of Scotland. GEOL MAG **5:** 477.

LAMBERT, R. St J., HOLLAND, J.G. and WINCHESTER, J.A., (1982). A geochemical comparison of the Dalradian Leven Schists and the Grampian Division Monadhliath Schists of Scotland. J GEOL SOC LONDON **139:** 71.

LAMING, D.J.C, (1966). Lubrication, palaeocurrents and other sedimentary features in the Lower New Red Sandstone, Devonshire. J SEDIMENT PETROL **36:** 940.

LAND, L.S., (1970). Phreatic versus vadose meteoric diagenesis of limestones: evidence from a fossil water table. SEDIMENTOLOGY **14:** 175.

LAVES. F., (1952). Phase relations in the alkali feldspars : I. Intoductory remarks. J GEOL **60:** 436.

LEAKE, B.E., (1964). The chemical distinction between ortho- and para-amphibolite. J PETROL **5:** 238

LEAKE, B.E., (1978). Granite emplacement : the granites of Ireland and their origin. **In** Bowes, D.R., and Leake, B.E., (Eds.). Crustal evolution in Northwest Britain and Adjacent Regions. GEOL J SPEC ISSUE **10:** 221.

LEAKE, B.E., HENDRY, G.L., KEMP, A., PLANT, A.G., HARREY, P.K., WILSON, J.R., COATS, J.S., AUCOTT, J.W., LUNEL, T., and HOWARTH, R.J., (1969). The chemical analysis of rock powders by automatic x-ray fluorescence. CHEM GEOL **5:** 7.

LEAKE, B.E., TANNER, P.W.G., SINGH, D. and HALLIDAY, A.N., (1983). Major southward thrusting of the Dalradian rocks of Connemara-western Ireland. NATURE **305:** 210.

LEAKE, B.E., TANNER, P.W.G., MACINTYRE, R.M. and ELIAS, E., (1984). Tectonic position of the Dalradian rocks of Connemara and its bearing on the evolution of the Midland Valley of Scotland. TRANS R SOC EDINBURGH **75:** 165.

LEEDER, M.R., (1982). Upper Palaeozoic basins of the British Isles - Caledonide inheritance versus Hercynian plate margin processes. J GEOL SOC LONDON **139:** 479.

LINGREN, W. and CREVELING, J.G., (1928). The ores of Potosi, Bolivia. ECON GEOL **23:** 233.

LONGMAN, C.D., (1980). Age and affinity of granitic detritus in Lower Palaeozoic conglomerates, SW Scotland. Implications for Caledonian evolution. Unpublished PhD thesis, University of Glasgow.

LONGMAN, C.D., BLUCK, B.J. and BREEMEN, O., (1979). Ordovician conglomerates and the evolution of the Midland Valley. NATURE **280:** 578.

LYNCH, G.V. and PRIDE, C., (1984). Evolution of a high-level, high-silica magma chamber : the Pattison pluton, Nisling Range alaskites, Yukon. CAN J EARTH SCI **21:** 407.

MCBRIDE, E.F., (1963). A classification of common sandstones. J SEDIMENT PETROL **33:** 664.

MACGREGOR, M. and MACGREGOR, A.G., (1948). The Midland Valley of Scotland. BR REG GEOL SURV MUS.

MACKENZIE, W.S., (1952). The crystalline modifications of $NaAlSi_3O_8$. AM J SCI **255:** 481.

MAALOE, S. and WYLLIE, P.J., (1975). Water content of a granite magma deduced from the sequence of crystallization determined experimentally with water undersaturated conditions. CONTRIB MINERAL PETROL **52:** 165.

MACK, G.H., (1981). Composition of modern stream sand in a humid climate derived from a low-grade metamorphic and sedimentary foreland fold-thrust belt of north Georgia. J SEDIMENT PETROL **51:** 1247.

MACK, G.H., JAMES, W.C. AND THOMAS, W.A., (1981). Orogenic provenance of Mississippian sandstones associated with southern Appalachian-Ouachita orogen. BULL AM ASSOC PET GEOL **65:** 1444.

MACK, G.H., THOMAS, W.A. and HORSEY, C.A., (1983). Composition of Carboniferous sandstones and tectonic framework of southern Appalachian-Ouchita orogen. J SEDIMENT PETROL **53:** 931.

MACKIE. W., (1926). Preliminary report on the heavy minerals of the Silurian rocks of southern Scotland. Unidentified typescript in Dept. of Geology library, University of Glasgow.

MACKIE. W., (1928). The heavier accessory minerals in the granites of Scotland. TRANS EDINBURGH GEOL SOC **12.**

MANKIEWICZ, D. and STEIDTMANN, J.R., (1979). Depositional environments and diagenesis of the Tensleep sandstone, eastern Big Horn Basin, Wyoming. SPEC PUBL SOC ECON PALEONT MINERAL **26:** 319.

MARSHALL, B., (1967). The present status of zircon. SEDIMENTOLOGY **9:** 119.

MARTIN, R.F., (1974). Controls of ordering and subsolidus phase relations in the alkali feldspars. **In** MacKenzie, W.S. and Zussman, J., (Eds). The Feldspars. Manchester University Press, New York.

MIYASHIRO. A., (1974). Volcanic rock series in island arcs and active continental margins. AM J SCI **274:** 321.

MORAD, S., (1983). Diagenesis and geochemistry of the Visingso Group (Upper Proterozoic), southern Sweden: A clue to the origin of colour differentiation. J SEDIMENT PETROL **53:** 51.

MORTON, D.J., (1976). Lower Old Red Sandstone sedimentation in the North-west Midland Valley and North Argyll areas of Scotland. Unpublished PhD thesis, University of Glasgow.

MORTON, D.J., (1979). Palaeogeographical evolution of the Lower Old Red Sandstone basin in the western Midland Valley. SCOTT J GEOL **15:** 97.

NOCKOLDS, S.R., (1941). The Garabal Hill - Glen Fyne igneous complex. QUART J GEOL SOC **46:** 451.

NOCKOLDS, S.R. and MITCHELL, R.L., (1948). The geochemistry of some Caledonian plutonic rocks. A study in the relationship between the major and trace elements of igneous rocks and their minerals. TRANS R SOC EDINBURGH **61:** part II, No. 20.

OBRADOVICH, J.D. and COBBAN, W.A., (1976). A time scale for the late Cretaceous of the western interior of North America. SPEC PAPER GEOL ASSOC CAN **13:** 31.

O'CONNOR, P.J., (1981). Radioelement geochemistry of Irish granites. MINERAL MAG **44:** 485.

O'CONNOR, P.J., HENNESSY, J., BRUCK, P.M. and WILLIAMS, C.T., (1982). Abundance and distribution of uranium and thorium in the northern units of the Leinster granite, Ireland. GEOL MAG **119:** 581.

PANKHURST, R.J., SUTHERLAND, D.S., BROWN, G.C. and PITCHER, W.S., (1982). Caledonian Intrusive Rocks. **In** Sutherland, D.S., (Ed.). Igneous Rocks of the British Isles. Wiley, Chichester. 129.

PARNELL, J. and SWAINBANK, I, (1984). Interpretation of Pb isotope compositions of galenas from the Midland Valley of Scotland and adjacent regions. TRANS R SOC EDINBURGH EARTH SCI **75:** 85.

PATTERSON, E.M., (1951). The Old Red Sandstone rocks of the West Kilbride-Largs district, Ayrshire. TRANS GEOL SOC GLASGOW **21:** 207.

PEARCE, J.A., (1980). Geochem evidence for the genesis and eruptive setting of lavas from Tethyan ophiolites. PROC INTERNAT OPHIOLITE SYMP NICOSIA CYP, 261.

PEARCE, J.A., (1982). Trace element characteristics of lavas from destructive plate boundaries. **In** Thorpe, R.S., (Ed.) Andesites. 526. John Wiley and Sons.

PEARCE, J.A. and CANN, J.R., (1973). Tectonic setting of basic volcanic rocks determined using trace element analysis. EARTH PLANET SCI LETT **19:** 290.

PEARCE, J.A. and GALE, G.H., (1977). Identification of ore-deposition environment from trace-element geochemistry of associated igneous host rocks. **In** Jones, M.J., (Ed.). Volcanic processes in ore genesis. SPEC PUBL GEOL SOC LONDON **7:** 14.

PEARCE, J.A. and NORRY, M.J., (1979). Petrogenetic implications of Ti, Zr, Y and Nb variations in volcanic rocks. CONTRIB MINERAL PETROL **69:** 33.

PEARCE, T.H., GORMAN, B.E. and BIRKETT, T.C., (1977). The relationship between major element chemistry and tectonic environment of basic and intermediate volcanic rocks. EARTH PLANET SCI LETT **36:** 121.

PEARCE, J.A., HARRIS, N.J., and TINDLE, A., (1984). Trace element discrimination diagrams for the tectonic interpretation of granite rocks. J PETROL 25: 956.

PEARCE, T.H., (1971). Short distance fluvial rounding of volcanic detritus. J SEDIMENT PETROL **41:** 1069.

PECCERILLO, A. and TAYLOR, S.R., (1976b). Geochemistry of Eocene calc-alkaline volcanic rocks from the Kastamonu area, northern Turkey. CONTRIB MINERAL PETROL **58:** 63.

PETTIJOHN, F.J., (1975). Sedimentary Rocks. New York. Harper Row.

PETTIJOHN, F.J., POTTER, P.E. and SIEVER, R., (1972). Sand and Sandstone. Springer, New York.

PHILLIPS. W.J., (1956). The metasomatic rocks associated with the Criffel-Dalbeatie granodiorite. GEOL MAG **92:** 1.

PHILLIPS, W.J., FUGE, R., and PHILLIPS, N., (1981). Convection and crystallization in the Criffell-Dalbeatie pluton. J GEOL SOC LONDON **138:** 351.

PHILPOTTS, J.A., MARTIN, W., and SCHNETZLER, C.C. (1971). Geochemical aspects of some Japanese lavas. EARTH PLANET SCI LETT **12** : 89.

PITCHER, W.S., (1983). Granite type and tectonic environment. **In** : Hsu, K. (Ed.) Mountain Building Process. Academic Press, London.

PITTMAN, E.D., and LUMSDEN, D.N., (1968). Relationship between chlorite coatings on quartz grains and porosity, Spiro Sand, Oklahoma. J SEDIMENT PETROL **38:** 668.

PLYMATE, T.G. and SUTTNER, L.J., (1983). Evaluation of optical and X-ray techniques for detecting source-rock controlled variation in detrital potassium feldspars. J SEDIMENT PETROL **53:** 509.

POLDERVAART, A., (1955). Zircon in rocks. I : Sedimentary Rocks. AM J SCI **253:** 433

POLDERVAART, A., (1956). Zircons in rocks. II : Igneous rocks. AM J SCI **254:** 521.

RAHMANI, R.A., (1973). Grain surface etching features of some heavy minerals. J SEDIMENT PETROL **43:** 882.

READ, H.H., (1961). Aspects of the Caledonian magmatism in Britain. LIVERPOOL MANCHESTER GEOL J **2:** 653.

READ, W.A., and JOHNSON, S.R.H., (1967). The sedimentology of sandstone formations within Stirling, Scotland. SCOTT J GEOL **3:** 242.

REICHMANN, W.J., (1961). Use and abuse of statistics. Methuen, London.

REYNOLDS, D.L., (1942). The albite schists of Antrim and their petrogenetic relationship to the Caledonian orogenesis. PROC R IRISH ACAD **48B:** 43.

REYNOLDS, R.C., (1963). Potassium-rubidium ratios and polymorphism in illites and microclines from the clay size fractions of Proterozoic carbonate rocks. GEOCHIM COSMOCHIM ACTA **27:** 1097.

ROGERS, J.J.W. and ADAMS, J.A.S., (1969). Uranium, Thorium. **In** Wedepohl, K.H., (Ed.). Handbook of Geochemistry II. Springer-Verlag, Berlin.

ROGERS, J.J.W. and NOVITSKY-EVANS, J.M., (1977). The Clarno Formation of central Oregon, U.S.A. - volcanism on a thin continental margin. EARTH PLANET SCI LETT **34:** 114.

ROGERS, J.J.W. and RAGLAND, P.C., (1980). Trace elements in continental margin magmatism : Part 1. Trace elements in the Clarno Formation of central Oregon and the nature of the continental margin on which eruption occurred. BULL GEOL AM **91:** 1217.

SAXENA, S.K., (1966). Evolution of zircons in sedimentary and metamorphic rocks. SEDIMENTOLOGY **6:** 1.

SCHUMM, S.A. and STEPHENS, M.A., (1973). A mechanism for rounding and size reduction of coarse sediments in river. GEOLOGY **1:** 37.

SHAND, S.J., (1947). Eruptive Rocks. Allan and Unwin, London.

SHERLOCK, R.L., (1947). The Permo-Triassic Formations. A World Review, London. Hutchinson.

SHOLKOVITZ, E.R., (1976). Flocculation of dissolved organic and inorganic matter during the mixing of river water and sea water. GEOCHIM COSMOCHIM ACTA **40:** 831.

SIMON, J.B. and BLUCK, B.J., (1982). Palaeodrainage of the southern margin of the Caledonian Mountain chain in the northern British Isles. TRANS R SOC EDINBURGH **73:** 11.

SIMPSON, G.S., (1976). Evidence of overgrowths on, and solution of, detrital garnets. J SEDIMENT PETROL **46:** 689.

SMITHSON, F., (1941). The alteration of detrital minerals in the Mesozoic rocks of Yorkshire. GEOL MAG **78:** 97.

STABLEIN, N.K. and DAPPLES, E.C., (1977). Feldspars in the Tunnel City Group (Cambrian), Western Wisconsin. J SEDIMENT PETROL **47:** 1512.

STALDER, P.J., (1975). Cementation of Pliocene - Quaternary fluviatile clastic deposits in and along the Oman Mountains, GEOL EN MIJNBOUW **54:** 148.

STEPHENS, W.E. and HALLIDAY, A.N., (1984). Geochemical contrasts between late Caledonian granitoid plutons of northern, central and southern Scotland. TRANS R SOC EDINBRUGH **75:** 259.

STRECKEISEN, A., (1976a) To each plutonic rock its proper name. EARTH SCI REV **12:** 1.

STRECKEISEN, A., (1976b). Classification of the common igneous rocks by means of their chemical composition. NEVES JAHRB MINERAL MONATSCH **1976:** 1.

SUTTNER, L.J. and BASU, A., (1977). Structural state of detrital alkali feldspars. SEDIMENTOLOGY **24:** 63.

TAIT, A.M., (1973). Sedimentation of the Craigmaddie Sandstone Formation, Western Midland Valley, Scotland. Unpublished PhD thesis, University of Glasgow.

TAMMEMAGI, H.Y. and SMITH, N.L., (1975). A radiogeolic study of the granites of SW England. J GEOL SOC LONDON **131:** 415.

TAUBENECK, W.H., (1957). Zircons in the metamorphic aureole of the Bald Mountain batholith, Elkhorn Mountains, northwestern Oregon. BULL GEOL SOC AM **68:** 1083.

TAYLOR, R.P. and FRYER, B.J., (1981). REE geochemistry as an aid to interpreting hydrothermal ore deposits. **In** Problems of mineralization associated with acid magmatism. Conference Report. J GEOL SOC LONDON **138:** 211.

TEXTORIS, D.A., (1971). Grain size measurement in thin section. **In** Carver, R.E., (Ed.). Procedures in Sedimentary Petrology . Wiley : 95.

THIRLWALL, M.F., (1981). Implications for Caledonian plate tectonic models of chemical data from volcanic rocks of the British Old Red Sandstone. J GEOL SOC LONDON **138:** 123.

THIRLWALL, M.F., (1983). Isotopic geochemistry and origin of calc-alkaline lavas from Caledonian continental margin volcanic arc. J VOLCANOL GEOTHERM RES **18:** 589.

TILLEY, C.E., (1925). A preliminary survey of metamorphic zones in the southern Highlands of Scotland. QUART J GEOL SOC LONDON **81:** 100.

TODD, T.W., (1963). Post-depositional history of Tensleep Sandstone (Pennsylvanian), Big Horn Basin, Wyoming. BULL AM ASSOC PETROL GEOL **47:** 599.

TRELOAR, P.J., (1978). The stratigraphy, geochemistry and metamorphism of the rocks of the Recess area, Connemara, Eire. Unpubished PhD thesis, University of Glasgow.

TRENDALL, A., (1961). Origin of albite porphyroblasts. GEOL MAG **98:** 263.

TRENDALL, A., (1962). Origin of albite porphyroblasts. GEOL MAG **99:**94.

TROTTER, F.M., (1953). Reddened beds of Carboniferous age in northwestern England and their origin. PROC YORKSHIRE GEOL SOC **29:** 1220.

TURNEAURE, F.S., (1960). A comparative study of major ore deposits of Central Bolivia. Part I. ECON GEOL **55:** 217.

TURNER, P. and WHITAKER, J.H.McD., (1976). Petrology and provenance of Late Silurian fluviatile sandstones from the Ringeike Group of Norway. SEDIMENT GEOL **16:** 45.

UPTON, B.G.J, ASPEN, P., and HUNTER, R.H., (1984). Xenoliths and their implications for the deep geology of the Midland Valley of Scotland and adjacent regions. TRANS R SOC EDINBURGH EARTH SCI **75:** 65.

VAN BREEMEN, O and BLUCK, B.J., (1981). Episodic granite plutonism in the Scottish Caledonides. NATURE **291:** 113.

VAN HOUTEN, F.B. (1968). Iron oxides in red beds. BULL GEOL SOC AM **79:** 399.

VIKRE, P.G. (1981). Silver mineralization in the Rochester district, Pershing County, Nevada. ECON GEOL **76:** 580.

VISHER, G.S., (1969). Grain size distributions and depositional processes. J SEDIMENT PETROL **39:** 1074.

WALKER, T.R., (1967) Formation of red beds in modern and ancient deserts. BULL GEOL SOC AM **78:** 353.

WALKER, T.R., (1974). Formation of red beds in moist tropical climate: A hypothesis. BULL GEOL SOC AM **85:** 633.

WALKER, T.R., (1976). Diagenetic origin of continental red beds. **In** Falke, R., (Ed.) The Continental Permian in Central, West and South Europe. Dordrecht, Holland. 240.

WALKER, T.R., RIBBE, P.H. and HONEA, R.M., (1967). Geochemistry of hornblende alteration in Pliocene red beds, Baja California, Mexico. BULL GEOL SOC AM **78:** 1055.

WALKER, T.R., WAUGH, B. and CRONE, A.J., (1978). Diagenesis of first-cycle desert alluvium of Cenozoic age, southwestern United States and northwestern Mexico. BULL GEOL SOC AM **89:**19.

WARNER, N.M., (1965) Cementation as a clue to structure, drainage patterns, permeability, and other factors. J SEDIMENT PETROL **35:** 797.

WATKINS, K.P., (1983) Petrogenesis of Dalradian albite porphyroblast schists. J GEOL SOC LONDON **140:** 601.

WATKINS, K.P., (1984) The structure of the Balquiddar-Crianlarich region of the Scottish Dalradian and its relation to the Barrovian garnet isograd surface. SCOTT J GEOL **20:** 53.

WATKINS, K.P. (1985) Geothermometry and geobarometry of inverted metamorphic zones in the west central Scottish Dalradian. J GEOL SOC LONDON **142:** 157.

WATSON, J., (1985). Northern Scotland as an Atlantic - North Sea divide. J GEOL SOC LONDON **142:** 221.

WEDEPOHL, K.H., (Ed.) (1978). Handbook of Geochemistry II/1-5. Springer-Verlag, Berlin.

WHITE, A.J.R. and CHAPPELL, B.W., (1977). Ultrametamorphism and granitoid genesis. TECTONOPHYSICS **43:** 7.

WILSON, A.C., (1971). Lower Devonian sedimentation in the north-west Midland Valley of Scotland. Unpublished PhD thesis, University of Glasgow.

WILSON, A.C., (1980). The Devonian sedimentation and tectonism of a rapidly subsiding, semi-arid fluvial basin in the Midland Valley of Scotland. SCOTT J GEOL **16:** 291.

WILSON, G.V. and FLETT, J.S., (1921). Special reports on the mineral resources of Scotland. MEM GEOL SURV SCOTLAND **17.**

WINCHESTER, J A. and FLOYD, P.A., (1977). Geochemical discrimination of different magma series and their differentiation products using immobile elements. CHEM GEOL **20:** 325.

WOODWARD, H.H., (1972) Syngenetic sanidine beds from Middle Ordovician St Peter sandstone, Wisconsin. J GEOL **80:** 323.

WRIGHT, M.D., (1964). Cementation and compaction of the Millstone Grit of the Central Pennines, England. J SEDIMENT PETROL **34:** 756.

WRIGHT, T.L., (1968). X-ray and optical study of alkali feldspar: II. an X-ray method for method for determining the composition and structural state from measurement of 20 values for three reflections. AM MINERAL **53:** 88.

WRIGHT, T.L. and STEWART. D.B., (1968). X-ray and optical study of alkali feldspar: I. Determination of composition and structural state from refined unit cell parameters and 2V. AM MINERAL **53:** 38.

WYATT, M, (1954). Zircons as provenance indicators. AM MINERAL **39:** 983.

WYBORN, D, OWEN, M., COMPSTON, W. and McDOUGALL, L, (1982). The Laidlaw Volcanics : a late Silurian point on the geological time scale. EARTH PLANET SCI LETT **59:** 90.

YOUNG, S.W., (1976). Petrographic textures of detrital polycrystalline quartz as an aid to interpreting crystalline source rocks. J SEDIMENT PETROL **46:** 595.